SHH SIGNALLING IN ACUTE PULMONARY CELL INJURY AND CHRONIC FIBROSIS

Paul Michael Fitch

A thesis submitted for the degree of Doctor of Philosophy

University of Edinburgh

2005

For my parents, family and my supervisors

TABLE OF CONTENTS

TABLE OF FIGURES

ACKNOWLEDGEMENTS

I would like to thank Professor Sarah E. M. Howie and Dr William A. H. Wallace for their supervision, help and advice during my thesis. Many thanks to all in the Immunobiology group past and present, especially to Su Haley for her help with laser micro-dissection studies and Dr Sharon Ahmad for instruction on mouse techniques.

I would also like to thank my family and friends for their support and encouragement during my thesis.

LIST OF ABBREVIATIONS

4-1BBL	Type II transmembrane glycoprotein with TNF homology
AM	Alveolar macrophage
APC	Antigen presenting cell
ARDS	Acute Respiratory Distress Syndrome
ATCC	American tissue culture collection
BALF	Bronchoalveolar lavage fluid
BALT	Bronchus associated lymphoid tissue
BCA	Bicinchoninic acid
BOOP	Bronchiolitis obliterans organising pneumonia
BSA	Bovine serum albumin
BMP	Bone morphogenic protein
CD	Cluster of differentiation
cDNA	Complementary DNA
CFA	Cryptogenic fibrosing alveoilitis
cpm	Counts per minute
CMT	C57Bl/crf-a^t mouse tumour
^oC	Degrees Centigrade
DAB	Diaminobenzidine tetrahydrochloride
DC	Dendritic cell
DepC	Diethylpyrocarbonate
Dhh	Desert hedgehog
Disp	Dispatched
DMEM	Dulbecco's minimum essential medium
DMSO	Dimethyl sulfoxide
DNA	Deoxyribonucleic acid
ECACC	European collection of cell cultures
ECM	Extracellular matrix
EDTA	Ethylene diamine tetraacetic acid
EIA	Enzyme immunoassay
ELISA	Enzyme linked immunosorbent assay
EXT	Exostoses gene family
FACS	Fluorescence activated cell sorting

FAM	6-Carboxy-fluoroscein
FCS	Foetal calf serum
FGF	Fibroblast growth factor
FITC	Fluorescein isothiocyanate
g	Gravitational force
g	Gram
GAPDH	Glyceraldehyde-3-phosphate dehydrogenase
Gli	Glioma-associated oncogene homolog
GM-CSF	Granulocyte macrophage colony stimulating factor
H_2O_2	Hydrogen Peroxide
H&E	Haemotoxylin and eosin
Hh	Hedgehog
Hip	Hedgehog interacting protein
HIPIF	Hapten immune pulmonary interstitial fibrosis
HNF3β	Hepatocyte nuclear factor 3β
Hrs	Hours
HRCT	High resolution computed tomography
HSPG	Heparan sulphate proteoglycan
iBALT	Inducible BALT
ICAM-1	Intercellular adhesion molecule 1
Ig	Immunoglobulin
Ihh	Indian hedgehog
IIP	Idiopathic interstitial pneumonia
IL	Interleukin
IL-1ra	Interleukin-1 receptor antagonist
IFN-γ	Interferon-γ
ILD	Interstitial lung Disease
IPF	Idiopathic pulmonary fibrosis
kb	Kilobases
kDa	Kilodaltons
KGF	Keratinocyte growth factor
KO	Knockout
LAL	Limulus amebocyte lysate test
LAR	Luciferase assay reagent

LB	Luria-Bertani
LPS	Lipopolysaccharide
LRP	LDL receptor related protein
MCP-1	Monocyte chemoattractant protein
mg	Milligram
MHC	Major histocompatibility complex
MIP	Macrophage inflammatory protein
ml	Millilitre
MMP	Matrix metalloproteinase
Mn-SOD	Manganese superoxide dismutase
mRNA	Messenger RNA
N-	N-terminus
ng	Nanogram
nm	Nanometre
NO	Nitric oxide
NPC-1	Niemann pick type C 1
NSIP	Non specific interstitial pneumonia
OCT	Trade mark cryopreservative compound (Sakura)
PAF	Platelet activating factor
PALM	Positioning and ablation with laser microbeam
PBS	Phosphate buffered saline
PCR	Polymerase chain reaction
pg	Picogram
PGE_2	Prostaglandin E_2
PMN	Polymorphonuclear cell
PMSF	Phenylmethylsulphonylfluoride
Ptc	Patched
RLT	Cell lysis buffer supplied with Qiagen RNA kits
RNA	Ribonucleic acid
RND	Resistance nodulation division
RT	Room temperature
RT-PCR	Reverse transcription PCR
Shh	Sonic hedgehog
Smo	Smoothened

SPC	Surfactant protein C
Strep-HRP	Streptavidin horseradish peroxidase
Su(Fu)	Suppressor of fused
Tag	DNA Polymerase enzyme isolated from *Thermus aquaticus*
TAMRA	6-Carboxy-tetramethyl rhodamine
TCR	T cell receptor
TE	Tris base & EDTA buffer
TGF-β	Transforming growth factor β
Th	Helper T cell
Th1	T helper 1
Th2	T helper 2
TIMP's	Tissue inhibitors of metalloproteinases
TLR	Toll-Like receptor
Tm	Annealing temperature
TNF	Tumour necrosis factor
TNBS	2,4,6-Trinitrobenzene sulfonic acid
Ttv	Tout velu
UIP	Usual interstitial pneumonia
UV	Ultraviolet radiation
μCi	Microcurie
μg	Microgram
μl	Microlitre
μm	Micron
VEGF	Vascular endiothelial growth factor

ABSTRACT

This thesis addresses the hypothesis that the sonic hedgehog (Shh) signalling pathway is up regulated in response to cellular injury and that this signal acts as a potential pro-fibrogenic signal in pulmonary inflammation. *In vitro* studies utilised human (A549) and mouse (CMT) type II like epithelial cell lines in an analysis of epithelial response to injury. An immediate up regulation and release of soluble Shh in response to hydrogen peroxide exposure was identified in mouse epithelium, utilising both RT-PCR and a novel Shh ELISA developed here. Subsequent up-regulation and release of GM-CSF was shown to be Shh independent. Human epithelial cells demonstrated a similar release of Shh, suggesting a common pathway in both species. In contrast GM-CSF was not up regulated in human cells, but IL-8 up regulation did occur. The relevance of these studies to *in vivo* signalling was ascertained through use of the FITC instillation mouse model of inflammatory fibrosis.

Previous work by our group has illustrated epithelial up-regulation of Shh in areas of inflammatory fibrotic disease in the FITC model, and in biopsies from patients with idiopathic pulmonary fibrosis. Transoral intratracheal delivery of FITC on two occasions six weeks apart reproduced previous histological findings made in the lab using a surgical intratracheal FITC instillation. However, use of improved immunohistochemical (IHC) techniques would suggest that, unlike human disease, Shh expression in the FITC mouse model is not solely restricted to epithelium in areas of inflammation or fibrosis. To determine the Shh responder cell populations in human disease and determine the validity of the IHC findings in the FITC model, a laser micro-dissection technique was developed. Viable mRNA for sequences including the Shh receptor patched (Ptc), and downstream signalling component smoothened (Smo) have been recovered from archival formalin fixed human biopsy material, sufficient for RT-PCR and agarose gel electrophoresis visualisation. mRNA analysis of material derived from fibrotic areas of a single standard section of archival human lung biopsy has now been performed.

Observations correlating levels of FITC specific IgG1 antibody and disease severity in FITC treated animals suggest an immuno-modulatory role for T lymphocyte dependent, Th2 type antibodies in disease progression. In support of this iBALT has also been identified in diseased lung and T-lymphocyte depletion results in disease amelioration.

Taken together these findings suggest that Shh is an indicator of acute cellular injury, but that the principal component of FITC induced fibrotic disease progression is immune mediated and that this does not depend on Shh up regulation.

CHAPTER 1 GENERAL INTRODUCTION

1.1 INTRODUCTION

Previous work in our group[1] had identified expression of the developmental signalling ligand, Sonic Hedgehog (Shh) in the adult lung. Shh is a molecule crucial for the correct branching morphogenesis and differentiation of the embryonic lung. Shh expression was shown to be increased in inflamed and fibrotic areas of chronic pulmonary fibrotic disease, primarily in the epithelium, where expression of its receptor, Patched (Ptc), had also been identified, although not always in the same epithelial cell populations[1].

Ptc was also identified on pulmonary fibroblasts and infiltrating cells and this lead to a hypothesis that Shh might be involved in epithelial mesenchymal signalling in lung remodelling, such as that which occurs in chronic fibrotic lung disease, given Shh's potent epithelial mitogenic function and putative role in developmental fibroblast function. Further to this, novel observations made in this lab concerning a post-embryonic function of Shh in the peripheral immune system, would suggest that Shh expression in diseased areas might have some immune modulatory function[2, 3].

This introduction begins with a description of the Shh signalling pathway and its involvement in pulmonary development. This is followed by a brief description of pulmonary biology and human interstitial fibrotic lung diseases, and mouse models of these conditions, concluding with a discussion of the hypothesis, aims and objectives of this thesis.

1.2 THE SONIC HEDGEHOG SIGNALLING PATHWAY

Despite its inherent complexity, development relies heavily on a restricted number of signalling pathways, which remain largely conserved from *Drosophila* to vertebrates. One such pathway is the hedgehog signalling pathway. First identified as a segment polarity gene in drosophila, three vertebrate homologues of hedgehog have now been identified, *Shh*, Desert Hedgehog

(*Dhh*) and Indian Hedgehog (*Ihh*)[4]. Unless specified this thesis will deal entirely with those features of Shh signalling identified in vertebrate studies.

Whilst Dhh and Ihh have been shown to have more restricted roles, Shh signalling has been identified in a wide variety of systems, from midline, neural tube and muscle precursor patterning, to polarising activity in limb development, lung morphogenesis and radial patterning in the mouse intestine (reviewed extensively by McMahon and colleagues[5, 6]). The Shh protein like the Ihh and Dhh variants is highly conserved from mouse to man, where human Shh has 92.4% homology with the mouse homologue[7]. Knockout and overexpression studies have shown that murine Shh shares almost all known functionality with human Shh, shown through the discovery of allelic variants, cell line and primary cell studies.

The production of the hedgehog protein is as unusual as it is complex and has attracted substantial study, having been recently reviewed by Sukegawa and colleagues[8], it will be discussed only briefly here, and can be found summarised in Figure 1.1 at the end of this section.

The Hh glycoprotein is produced as a 45-46kDa precursor. The C-terminus of this precursor possesses no signalling function but acts to auto catalytically cleave and cholesterol modify the N-terminus, generating a 19kDa hydrophobic protein with a C-terminal cholesterol moiety[9-13].

Cholesterol modification was originally thought to be a requirement for a subsequent palmitoylation step[14], however, recent studies would suggest that the Hh can be generated with either or both modifications, as singly palmitolyated or cholesterol modified Shh has now been identified in separate tissues[15]. Studies by Feng and colleagues[15] following on earlier studies[16-18], would suggest that these modifications have both synergistic and antagonist functions in adapting Shh signalling activity. Thus, tissue restriction of these modified forms of Shh may represent tissue specific adaptive changes to the function of the Shh signalling pathway.

Paradoxically, given the hydrophobic nature of these modifications, Shh has been established as both a soluble and cell surface signal. Current investigation would suggest that solubility is achieved by concealing hydrophobic moieties within multimer micelles at the cell surface prior to release, in a process requiring the 12 span membrane protein Dispatched (Disp)[19 20 21]. Whilst cholesterol modification alone has been shown to be sufficient for multimerization and membrane tethered modes of signalling, palmitoylation facilitates multimerization but not membrane tethering[15]. This is notable given that multimerization is necessary for Shh differentiation inducing activity in neural explant studies, where palmitolylation increases, but cholesterol reduces this function[15, 18]. This would suggest that functional variation occurs with the mode of delivery of Shh signal, be it cell contact or as a soluble multimer and that further to this, by varying the modification type, Shh producing cells can alter the function of that multimer on contact with responder cell populations[15, 20].

A further level of control of the Shh signalling pathway occurs through modulation of the concentration gradient by hedgehog interacting protein (Hip) and by heparan sulphate proteoglycans (HSPG)[22].

Hip is up regulated in response to Hh and interacts with and sequesters all three hedgehogs with affinity comparable to Ptc, regardless of modification state as it lacks a sterol sensing domain[22]. In *Drosophila*, the Tout velu *(Ttv)* gene product[23] is essential for the movement of cholesterol modified Hh. The vertebrate homologs of Ttv, the exostoses gene family *(EXT)* encode GAG transferases involved in HSPG synthesis[24 25]. This would suggest that the activity of the *Ttv* gene product and its vertebrate homolog, might be the generation of a proteoglycan that mediates the transfer of Hh between cells, or its presentation to Ptc[23, 26, 27], although this remains a contentious issue[28] and studies have been largely restricted to *Drosophila*.

The manner in which the Shh signal is delivered to the 12 span receptor, Ptc[29 30], has been a point of much conjecture, given conflicting reports concerning

intracellular and membrane localisation of Ptc[31, 32], and the identification of 2 Ptc isoforms and a third receptor megalin[33].

The identification of megalin (gp330/LRP-2) a member of the low-density lipoprotein (LDL) receptor family, as a Shh binding receptor, was interesting as it is expressed exclusively in epithelial cells of the embryo and the adult, where its primary function is the endocytosis of a wide range of ligands[34]. A number of authors now suggest that megalin could act to deliver Shh internally to Ptc, or that megalin might mediate the movement or clearance of Shh across epithelial barriers[35], although these questions remain unanswered.

No direct signalling function has as yet been ascertained for megalin, although interestingly, given the previously ascribed function of HSPG in Shh movement, the uptake of other megalin family ligands such as hepatic lipase and circumsporozoite protein, is absolutely dependent on HSPG binding previous to LRP interaction[36 37]. Thus, rather than mediating Ptc uptake of Shh as some authors have suggested, the necessity for *Ttv* function in *Drosophila* may lie in its interaction with megalin. Were this found to be true for *EXT* / Megalin interaction in vertebrates it would present an excellent means of delineating megalin function at epithelial sites.

Although there have only been two conclusively established signalling receptors identified for Ptc, the pathway retains an inordinate level of complexity, not through differences in affinity, as both Ptc receptors, Ptc1 and Ptc2 are bound by all Hh family members with similar affinity[38], but through spatial localisation of ligand and receptor sub types, and use of cell type restricted pathways downstream of Shh signalling function, in combination with the control exerted at the level of ligand generation as discussed previously.

Ptc1 and 2 appear to have distinct expression profiles, and recent data would suggest a restriction to hedgehog sub types, where Ptc2 has a greater importance in Dhh signalling than Shh or Ihh signalling[38]. Another point of variation arises from the method of the delivery of the Shh signal as discussed previously. Although some authors have attributed this variation to differing

affinity of Ptc for modified variants of Shh. A consensus interpretation would now suggest that in some cells Ptc occurs in lipid rafts, and that it is the effect that cholesterol and palmitoyl modification has on the ability of Shh to incorporate into these rafts that is responsible for the observed variation in function with differentially modified and delivered Shh signal[15 39-42].

Ptc is classically described as occurring in a receptor complex in which Ptc is the membranous ligand-binding subunit and Smoothened (Smo), a G protein-coupled receptor-like molecule[43], is the intracellular signalling component[44] where Ptc acts as a direct[45] negative regulator of Smo. This inhibition is removed by Ptc-Shh interaction, allowing Smo to transduce the Shh signal into the cell.

Some studies however, would suggest that Ptc, rather than being found on the cell membrane, like most classical receptors, is instead found primarily in intracellular vesicular structures resembling endosomes, with barely detectable amounts found in the membrane[46]. In contrast, the internal signalling component of the pathway, Smo, is found predominantly localised to the membrane[47]. This has led some to hypothesise that Ptc may chaperone Smo, compartmentalising it, rather than directly inhibiting its function[27].

Given the identification of megalin as a receptor, it is also possible that Ptc need not be delivered to the membrane, but might have Shh shuttled to it in a cell sub-compartment, either actively by megalin, or via passive internalisation of membrane raft incorporated Shh. In such a situation Ptc might be viewed as a channel localising cell Shh to discrete endosomes.

Others have further developed this hypothesis, suggesting that Ptc can function as a channel. Inactivating mutations in Ptc are similar to those that abolish transport activity in bacterial protein transporters and Ptc has a high degree of homology with the bacterial proton-driven molecular transporters of the RND family and their eukaryotic members such as NPC-1[47, 48]. Therefore, some publications have suggested that rather than act as a direct receptor, Ptc might actually function as an entry point for Smo modulators, such as those identified

by the Beachy lab[49] and others[50 51]. In such a situation, Shh-Ptc binding might be envisioned as *preventing* the entry of Smo antagonists, or *facilitating* the entry of agonists. This raises the possibility of small molecule treatment of Shh associated conditions such as basal cell carcinomas and Parkinson's disease.

Thus the current model of Smo signalling, although contentious is one of a catalytic, rather than stoichiometric system of Ptc mediated control, with active and inactive Smo conformations selected by binding of ant/agonists at independent sites generating negative co-operativity. Phosphorylation of Smo is another area of conjecture, which would appear to differ in its necessity for pathway activation between species.

Smo influences gene expression through the Gli family of zinc finger transcription factors, of which there are three, Gli1-3. These molecules have high homology in their five zinc finger domains but only limited homology outside this region. The Gli are inhibited in the absence of Smo signal, via sequestration in the cytoplasm by suppressor of fused Su(fu), which also targets them for proteosomal destruction. Further roles for Su(fu) include nuclear recruitment of the histone deacetylase associated molecule Sap18 when bound to Gli, preventing Gli mediated transcription. Su(fu) inactivation is postulated to occur through Smo mediated phosphorylation.

Gli2 and 3 are expressed in the absence of a Shh signal. Gli2 possess an N-terminal repressor domain, inhibiting C-terminal transcriptional activator function and Gli3 is autoproteolytically cleaved into a repressor molecule. Functionality of these domains appear to vary with cell type, resulting in a confused literature, however a general consensus would suggest that in the absence of Shh signal, Gli2 possesses weak activator function and Gli3 a repressor function [52 53].

Shh signalling results in the removal of the repressor domain of Gli2 and the inhibition of Gli3 autoproteolysis. Active Gli2 would appear to be the primary transcription factor involved in Shh signalling as although it up regulates *Gli1* which has been shown to share some *Gli2* functionality, *Gli1* but not *Gli2* is dispensable for lung development[54].

Other potential intracellular signalling mechanisms and transcriptional mediators have been suggested, including the Forkhead gene family, *Foxf1*, but recent studies would suggest that Shh responsive genes are restricted to those with functional Gli binding sites[55, 56].

Shh signalling can induce expression of a variety of signalling proteins and transcription factors in development, but has only been *directly* linked with regulation of *Ptc* and *Gli1* expression in all systems, and *HNF3β* in cells of the central nervous system[29, 57 58]. However, work with Shh responsive cell lines would suggest that a number of factors involved in cell growth and apoptosis may also be modulated by Shh signalling[59]. Surprisingly, Smo, despite being increased in responder cells, is not a gene upstream of the Gli, instead it would appear that Smo has increased stability in active responder cells[50].

The majority of the putative downstream effector functions for the Shh pathway were elucidated from developmental observations, made through over expression and knockout studies of pathway members, and through immunohistochemical and *in situ* analysis of sequential activation with development. The specific role of Shh in lung development is discussed in the subsequent section, both as an extension to the studies described here, and to demonstrate its potential as a signalling molecule in the adult lung.

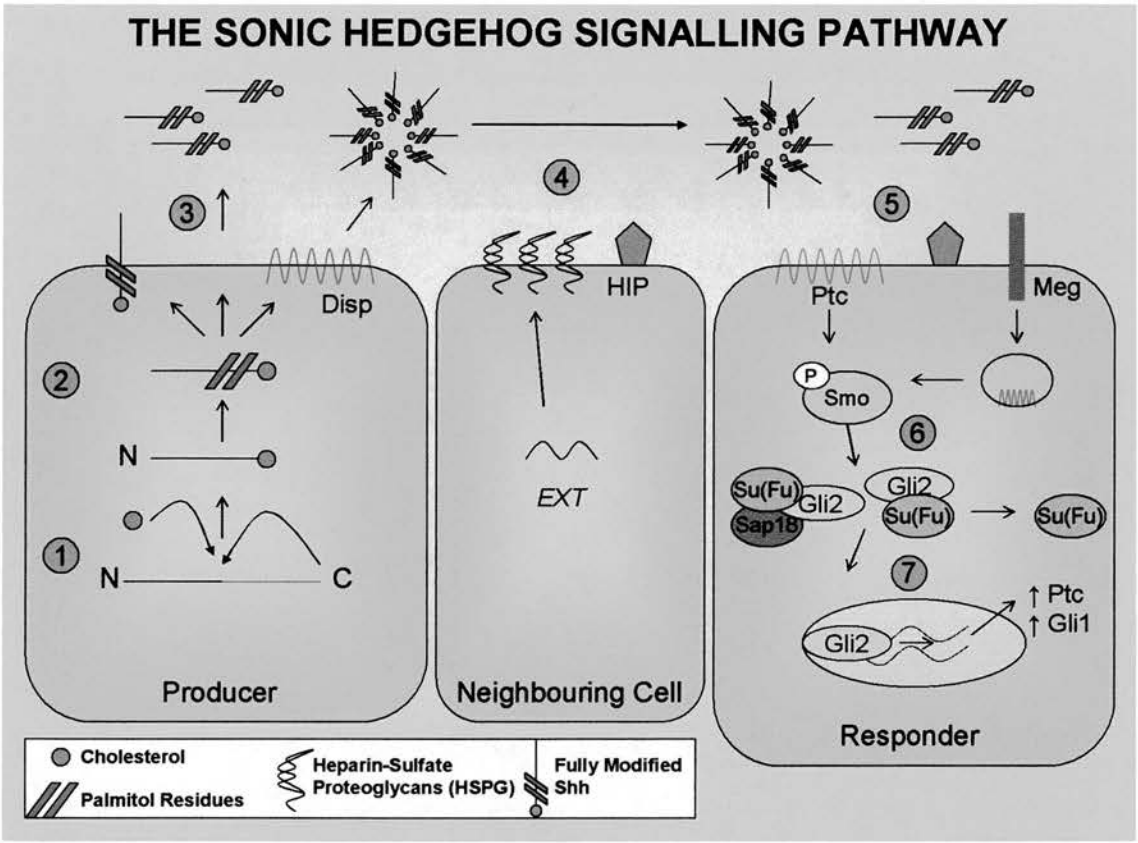

Figure 1.1: The Shh Signalling Pathway

(1) Autocatalytic addition of a cholesterol moiety to the C-terminus of the Shh protein, can be followed by a palmitoylation step (2). (3) Membrane association results in signalling either as a cell contact entity, or via secretion, in a process absolutely requiring Disp. Soluble signals occur as a multimer. (4) Neighbouring and responder cell populations restrict this signal gradient via non signalling Ptc expression or expression of Hip, whilst its sustenance is thought to involve HSPG associated gene products [EXT gene products]. (5) Shh Ptc binding results in Smo activation via removal of Ptc inhibition, occurring through either Ptc mediated chaperoning of Smo to agonist containing vesicles or entry/exit of antag/agonists. Megalin may also deliver Shh to Ptc microvesicles. (6) The exact manner and location of Smo/Gli interaction is poorly characterised, but in *Drosophila* homologues, this involves multiple de/phosphorylation steps. (7) Smo allows activation of Gli responsive genes by activating Gli2 and inactivating Su(Fu), facilitating the dissociation of the histone deacetylation associated protein Sap-18, and nuclear localisation of Gli2 for the up regulation of downstream genes.

1.3 SONIC HEDGEHOG IN LUNG DEVELOPMENT

Lung development initiates with an evagination of two ventral buds of foregut endothelium into the surrounding mesoderm. This is followed by a series of lateral branching steps, establishing the lobation of the lung. During this initial

branching step the intruding buds of proliferating cells differentiate into tubules of progenitor pulmonary epithelial cells. Reiterated budding and branching of these tubules results in the formation of the full respiratory tree. (recently reviewed by Cardoso[60]).

Branching and budding occurs as a result of a complex network of interacting signalling pathways, of which the Shh signalling pathway is one. Shh is expressed along the length of the epithelium of these tubules, with greatest expression gradating from the proliferating tips. The target cells for the Shh signal are most likely the mesenchymal cells into which the tubules tips intrude. These mesenchymal cells express Ptc1, Hip1 and all three Gli members with up regulated Ptc1 expression restricted to cells underlying those areas of greatest epithelial Shh expression[61, 62].

Shh mutagenesis studies have been the most instructive techniques for the elucidation of Shh function, and have lead Bellusci, Lebeche and colleagues to put forward the following model of Shh function[61, 63].

Areas of mesenchymal Fibroblast Growth Factor 10 (FGF-10) expression act as an epithelial chemo-attractant. Progressive growth of tubules to this source is halted by FGF-10 mediated up-regulation of Bone Morphogenic Protein 4 (BMP-4) expression in the tubule tips and by concomitant mesenchymal Transforming Growth Factor β (TGF-β) expression. Shh expressed in the tubule tips represses FGF-10 expression, removing the chemoattractant stimuli. This results in the formation of a cleft and reduced Shh expression. Low FGF-10 levels are maintained by residual Shh and local TGF-β production, which also leads to matrix deposition. Branching then occurs via lateral outgrowths of epithelium from the clefted tubule to new sources of FGF-10, forming new, high Shh expression, tubule tips.

1.4 SONIC HEDGEHOG AND IMMUNITY

The Shh signalling components, Shh, Ptc, Smo and Gli1-3, are expressed in murine foetal and adult thymus. Cells entering the thymus are pluripotent bone marrow derived progenitors which become progressively more lineage restricted through their passage in the thymus, facilitated by specific retention or destruction signals. These signals are generated through the ability of each cell to recognise thymic epithelial signals during a series of defined maturation steps, and ignorance of self. These cells become Thymic lymphocytes (T-cells), capable of orchestrating immunity against antigenic compounds via a specialised T Cell Receptor (TCR) receptor, genetically rearranged during maturation to generate a full repertoire of antigen affinities, where individual cells express only one variant.

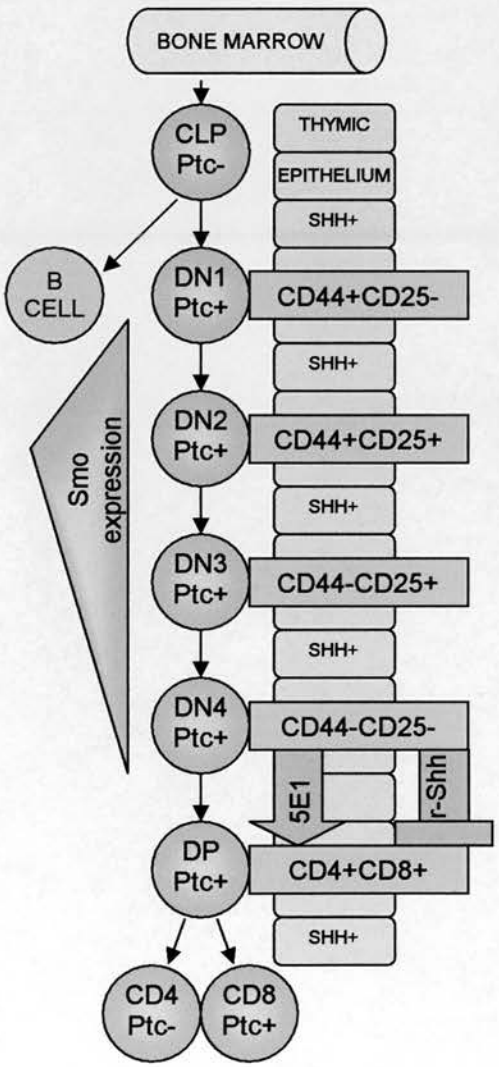

Figure 1.2: T-Lymphocyte Development
Commited Lymphocyte Progenitor (CLP) cells are generated in the bone marrow. Here they can generate new B lymphocytes or they can circulate to the thymus to generate cells of the T cell lineage. Upon first contact with the thymic epithelium CLP cells are refered to as Double Negative (DN) cells in reference to the absence of CD4 or CD8 protein expression. Signalling interactions with the thymic epithelium leads to a complex set of TCR rearrangements, marked by differing expression of CD44 and CD25 on the surface of the DN cells, which along with other signals selects those DN cells suitable to transcend each developmental stage (1-4). Exogenous Shh has been shown to prevent the transition from a DN to a Double Positive cell (DP) which marks a commitment to a thymocyte lineage. This observation has been confirmed with the Shh neutralising antibody 5E1 which enhances progression through this stage of T-lymphocyte differentiation.

Shh expression was found restricted to thymic epithelium and Smo expression to cells committed to the T-cell lineage. Outram et al, referencing neutralising antibody and exogenous r-Shh studies suggest that these Smo positive thymocytes are maintained in a non-proliferative state by an epithelial derived Shh signal, facilitating T-Cell Receptor (TCR) β gene rearrangement at the DN3 stage, necessary for the generation of a full repertoire of TCRβ expressing T-lymphocytes[64]. Further to this these authors suggest Shh signalling may be involved in the expression of CD44 (cellular adhesion) and CD25 (activation marker) in these precursors at the DN2 stage.

1.5 PULMONARY STRUCTURE AND FUNCTION

1.5.1 THE UPPER RESPIRATORY TRACT

The upper respiratory tract acts as a conduit for gas exchange, warming and humidifying air on its passage from the mouth and nose through the trachea and bronchi, then into the bronchioles, terminal bronchioles and acini of the lower respiratory tract. Potentially injurious, reactive or infective agents are also removed from inspired air, during this transition, preventing their entry into the delicate epithelial structures of the gas exchange surfaces.

The upper airway surfaces have a primarily defensive function, stratified with multifunctional cells of connective, nervous, secretory and immunological function, making gas exchange impractical. Reflexes such as glottic closure and coughing prevent the entry of larger particulates into the airways, whilst smaller items, driven by turbulent airflow of the bifurcating bronchi and bronchioles, become lodged in the thick mucus lining of the airways.

The mucus lining is produced by the mucus glands of the upper airway and contains opsonising IgA antibodies transcytosed with secretory component by the underlying bronchial epithelium and anti-microbial and proteinase inhibitors produced by specialised non-ciliated epithelial cells called Clara cells[65]. Unlike the predominant ciliated bronchial epithelial cell, whose primary function is to sweep mucus from the lung, the Clara cell is multifunctional, performing secretory and immunological functions. These

cells can be identified by expression of Clara cell protein 10 (CC10)[66], whilst a subclass of Clara cell termed a variant Clara cell (vCC)[67, 68], can be identified by low CyP450 expression[67-69], and are found associated in neuroepithelial bodies with pulmonary neuroepithelial cells[70]. These bodies have putative neural synapse connections and are believed to represent a neurologically controlled secretory cell population. Further to this, vCC have now been identified as a repopulating cell for the epithelium in mouse, similar in function to progenitors identified in the mucus ducts of the upper airways[71]. Whether vCC cells represent a transient amplifying cell, with limited proliferative capacity or a pluripotent stem cell remains to be clarified. The main repopulating cell of the airways is the non-cilliated basal cell which underlies the stratified cell layer at the basement membrane[72]. Basal cells have the capacity to replace almost all epithelial and some subepithelial cell types in the lung. Interestingly, these cells have recently been identified as expressors of Shh which, given the prominent signalling role of Shh in the branching morphogenesis of the lung epithelium, might suggest a role for Shh in epithelial repopulation in the adult lung[73, 74].

1.5.2 THE LOWER RESPIRATORY TRACT

This is not an absolute transition, but can be marked by reduced airway associated smooth muscle and the loss of the overlying sticky mucus layer, leaving an underlying thin surfactant rich serous layer, to continue into the terminal bronchioles [75].

The epithelium also reduces in thickness, now largely composed of ciliated and Clara cells in the bronchioles with occasional vCC/neuroepithelial clusters, underlain by thin fibroblastic projections and an ECM rich interstitial layer. Entry into the specialised gas exchange surfaces of the terminal bronchioles and acini mark another transition. These surfaces are populated by two types of epithelial cell, the flat type I epithelium specialised for gas exchange, and the cuboidal secretory Type II cell, which has putative progenitor function for Type I cells. In mice, type II cells predominate (~90%), whilst humans have equal proportions of type I & II cells, although type I have the greatest (~95%) surface area.

1.6 MAINTENANCE OF EPITHELIAL INTEGRITY

The surface of the lung is approximately the size of a singles tennis court through which the entire blood volume travels every minute, separated from the external environment by just two cell layers at the gas exchange surfaces. These surfaces continually interact with or are affected by particulates and potentially pathogenic organisms and whilst numerous defensive mechanisms provide substantial protection, inevitably sometimes these defence mechanisms fail. Epithelial surfaces then become injured, and denudement of the respiratory surfaces occurs. Rapid reestablishment of the integrity of the epithelial surface is absolutely essential to prevent the establishment of infection, excessive transudation of profibrotic plasma proteins into the airspaces and the initiation of a potentially harmfully inflammatory cell recruitment process. The mechanisms involved in this process are a point of much debate, but undoubtedly differ with location in the lung.

At the bronchi and bronchiole surfaces, within 20 minutes of columnar epithelial cell removal, basal cells become flattened and cover the basement membrane, this is then superseded by a rapid μm/min migration of overlying epithelium, restoring normal architecture. The prompt recovery of these surfaces following epithelial shedding and lack of associated inflammation would suggest that this is a normal response to injury and infection, similar to that observed in the digestive tract. This would serve to rapidly remove infected or damaged epithelial cells with the mucus prior to establishment of infection or neoplastic growth[76].

The alveolar surface, lacking stratified layers, brings the external milieu into close contact with the circulation, requiring prompt repair to prevent systemic infection. Necrotic shedding or apoptotic clearance of type I/II cells results in exposure of the underlying basal lamina, consisting of lamin, collagens and other connective molecules. This matrix acts as a reservoir for epithelial proliferative factors such as Keratinocyte Growth Factor (KGF) and FGF-10, and accumulates transudated plasma derived growth factors. In response to these molecules and a loss of contact inhibition type II epithelial cells are

thought to differentiate into rapidly proliferating *Repair cells / Intermediate cells*, which migrate across the surface of the basal lamina, differentiating towards type I cells, secreting anti-microbial compounds and proinflammatory cytokines such as IL-1 as they do so. This occurs in balance with epithelial expression of IL-1ra, a IL-1 receptor antagonist, in order to prevent erroneous inflammation and immune infiltration[75-77] and results in the restoration of normal lung architecture.

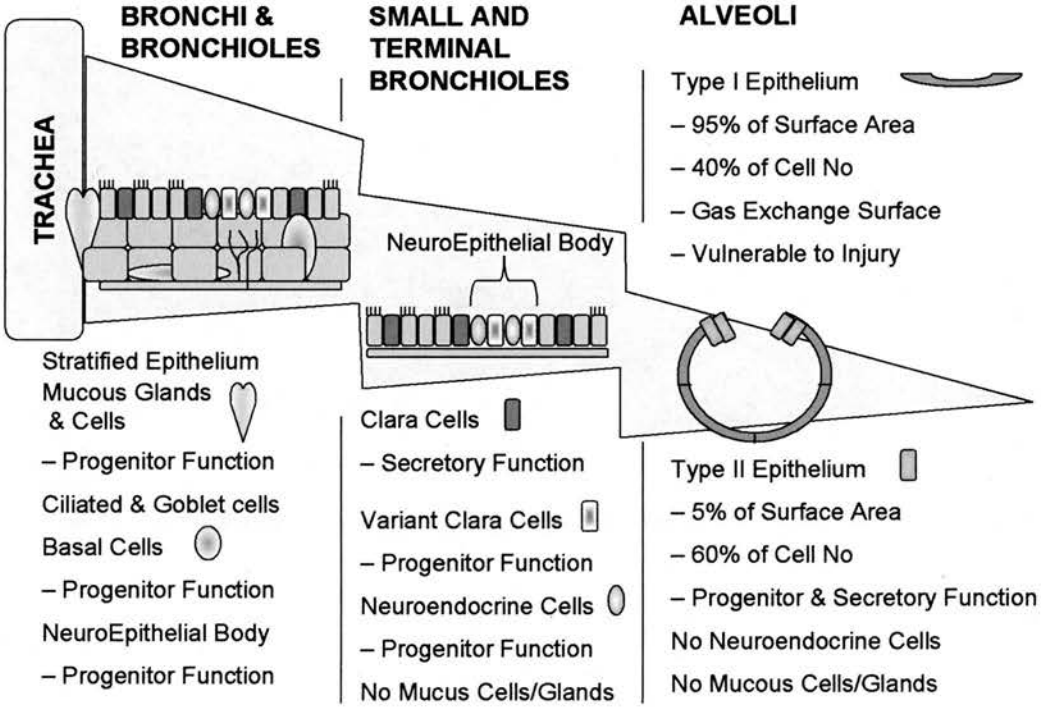

Figure 1.3: Epithelial Cell Subset Localisation and Function

1.7 LUNG RESPONSES TO INFECTION AND INJURY

The lung is continually exposed to injurious and potentially pathogenic particulates. This requires a predominantly anti-inflammatory environment at the pulmonary surfaces, to enable engulfment and removal of particulates by alveolar macrophages, prior to the stimulation of inflammatory cell infiltration and innate reactivity, which can be potentially damaging to the pulmonary system. Indeed many functional proteins and carbohydrates in the lung milieu have dual anti-inflammatory roles[65].

Whilst conventional investigation would decree that immunological intervention is required to remove persistent infective agents or particulates from the respiratory surface, a growing body of evidence would now suggest that stromal and epithelial cells in combination with alveolar macrophage derived signals have both the signalling and functional capability to deal with potentially pathogenic events in isolation from circulating effectors.

Alveolar macrophages (AM) act as the sentinels of the respiratory surface, phagocytosing particulate and opsonised debris from the epithelial surfaces. In contrast to the immune antigen processing and presentation function of interstitial macrophage, AM engulf and inactivate particulates, but possesses only limited presentation capabilities, and are largely anti-inflammatory in phenotype[78].

In response to a threshold concentration of bacterial contaminants e.g. Lipopolysaccharide (LPS), AM can reverse this phenotype producing a number of pro-inflammatory cellular signals including in humans Platelet Activating Factor (PAF), Tumour Necrosis Factor α (TNFα), Interleukins 1 and 8 (IL-1) (IL-8) and Granulocyte Macrophage Colony Stimulating Factor (GM-CSF)[79]. Responses in mice are similar, but IL-8 is replaced by Macrophage Inflammatory Protein 2 (MIP-2) as the cytokine characteristic of a pro-inflammatory macrophage.

PAF, released by activated AM and particulate injured epithelium[80] can up-regulate mucin production in the larger airways and increase cilia activity, removing contaminating material from the lungs. More specifically, PAF can up-regulate hydrogen peroxide (H_2O_2) production by epithelial cells, generating harmful hydroxyl molecules analogous to the respiratory burst function of the neutrophil, which serves to kill bacterial contaminants in the mucus. Concomitantly, signals such as TNFα increase Manganese Superoxide Dismutase (Mn-SOD) (anti-oxidant) production by epithelial cells, limiting injury from exogenous and endogenous oxidants.

Epithelial cells can also signal in an autocrine and secretory fashion in the complete absence of AM; exposure to particulates has been shown to

directly activate epithelial cell production of TNFα, IL-1β and IL-6, accompanied by Type II cell specific changes in Surfactant Protein C (SPC) and the 10KDa Clara Cell Specific Protein CC10[81]. In the event of damage or infection surpassing these functions, TNFα and IL-1β can act directly locally in a paracrine fashion, but are also implicated in the up regulation of local secondary mediators.

TNFα and IL-1β are functionally very similar and are collectively referred to as the early response cytokines. Produced by epithelium and immune cell populations such as macrophages, their primary function is the initiation of local inflammation and endothelial activation. Activation results in the up regulation of a number of cell adhesion molecules on the luminal surfaces of the endothelial cells lining the blood vessels, such as Intercellular Cellular Adhesion Molecule 1 (ICAM-1), E-Selectin and P-Selectin, facilitating the margination and transmigration of inflammatory cells from the blood into the lung architecture.

Cells entering the lung do so under the direction of signalling gradients of molecules called chemokines. IL-8 is one such molecule, expressed by AM, and by endothelium in response to early response genes. This recruits neutrophils, basophils and T-lymphocytes to the respiratory surface. Once within the interstitial layers, cells migrating on endothelial derived gradients require further directional cues. Apical MCP-1 (Monocyte Chemoattractant Protein-1) expression and up regulated adhesional receptor expression by TNFα /IL-1β stimulated epithelial cells forms one such gradient, which is amplified in an autocrine fashion through epithelial activation by MCP-1[82].

Early response genes continue to participate in inflammation with the arrival of inflammatory cells. They increase the phagocytic and respiratory burst functions of macrophages and neutrophils and prime for increased cytokine secretion upon activation. A prime example of a cytokine induced in activated AM and epithelial cells is granulocyte macrophage colony stimulating factor (GM-CSF). This promotes neutrophil and monocyte survival and differentiation in the interstitial spaces. It also removes the AM mediated maturation inhibition of dendritic cells, facilitating their progression to the

lymph nodes to stimulate adaptive immunity[79, 83]. Lymphocyte activity is also facilitated by a GM-CSF mediated reduction in AM lymphocytostatic activity at the site of injury or infection[84, 85].

1.8 ADAPTIVE IMMUNITY AT THE MUCOSAL SURFACE

The development of immunity to a specific pathogenic or particulate antigen is a highly complex series of events and will be addressed here only briefly and at a level necessary for explanation of immunological features at the pulmonary surface, and the potential for the involvement of Shh. Whilst the majority of immunological features addressed here were elucidated in mouse and tissues other than the lung, subsequent investigation has illustrated similar processes in the human lung. The major point of variation is that given the interaction of the lung with the external milieu, it is comparatively difficult to mount an adaptive immune response to respiratory stimuli, attributable to a largely anti-inflammatory cytokine environment, present to prevent immunity against inocuous antigens and the development of allergy. More advanced coverage of these topics can be found in texts such as Janeway et al, Immunobiology[86]. Material from this section can be found summarised in Figure 1.4 and Figure 1.5.

Individual naïve T lymphocytes leaving the thymus after Shh facilitated TCR gene rearrangement posses a highly specific TCR and broadly conform to two subsets, those expressing the CD4 co-receptor and those expressing the CD8 co-receptor. Both co receptors mediate their intracellular signalling through co-localisation with the TCR signal transducing CD3 molecule (not shown in Figure 1.4, for reasons of clarity). Activation of these cells into effector populations occurs in the lymph nodes and spleen in a process summarised in Figure 1.4 and below. Dendritic cells are the main activator of naïve T-cells, due in part to an enhanced co-stimulatory function, although activated macrophages can also serve this function in the right microenvironment.

1.8.1 CD4 CELL ACTIVATION

Recognition of Major Histocompatibility Complex II (MHC II) : antigen results in a physical TCR : CD4 association, inducing conformational activation of adhesion receptors, through CD3 mediated TCR signalling. This facilitates binding of the costimulatory ligand CD80 or CD86 expressed on APC, by CD28 receptor on the bound T-cell. Termed signal one, these events induce IL-2 secretion as an autocrine proliferative factor by the bound T cell and induces CD154 ligand up-regulation. CD154 (CD40L) is bound by the receptor CD40 on the APC and may lead to further activating signals from the APC and constitutes signal two.

1.8.2 CD8 CELL ACTIVATION

Recognition of MHC I: antigen results in a physical TCR : CD8 association, inducing conformational activation of adhesional receptors, through CD3 mediated TCR signalling. This facilitates binding of the costimulatory ligand CD80 or CD86 expressed on APC, by the CD28 receptor on the bound T-cell. However, in order to avoid stimulation of anti-self reactivity, given that MHC I present all internal peptides, CD8 cells require increased costimulatory levels compared to CD4 cells. Dendritic cells typically present signal one with sufficient CD86 for effective co-stimulation. However, other APC will require another stimulus, either CD4 mediated CD40 stimulation, or recognition of a conserved pathogen pattern, e.g. LPS or double stranded RNA, by Toll like receptors in order to supply sufficient co-stimulation. CD4 binding to the same APC further aids this response through local IL-2 secretion. Recent studies suggest that such supplemental activation of APC may increase expression of the 4-1BB ligand (also refered to as (CD137L), which serves as a secondary signal to the CD8 cell to enable activation[87].

1.8.3 EFFECTOR CELL FUNCTION

CD8+ cells recognise intracellular antigens, such as virus proteins, presented on MHC I molecules common to almost all cells; inducing death upon recognition, either directly or through the recruitment of complement proteins. In contrast, $CD4^+$ cells recognise exogenous antigens such as bacterial

fragments, presented on MHC II molecules, restricted to antigen presenting cells such as dendritic cells and macrophages. CD4 antigen specific binding of these cells results in their activation, both as secretors of cytokines, and in the case of macrophage, increased phagocytic surveillance.

Activated CD4+ T-cells can be classified for the purposes of this introduction into two functional sub-types, Th1 and Th2, differentiated according to APC derived cytokine signals at the time of antigen presentation. There are similar sub-type classifications in CD8+ cells and APC[86]. Th1 are classically defined as inflammatory, they secrete IFN-γ and express CD40 to activate cells such as macrophages. Th2 cells are specialised for humoral immunity through B-lymphocyte activation via CD28 and CD154 expression, and the production of the B-cell growth factors IL-4, IL-5, IL-9 and IL-13. This is discussed in greater detail within the legend of Figure 1.5.

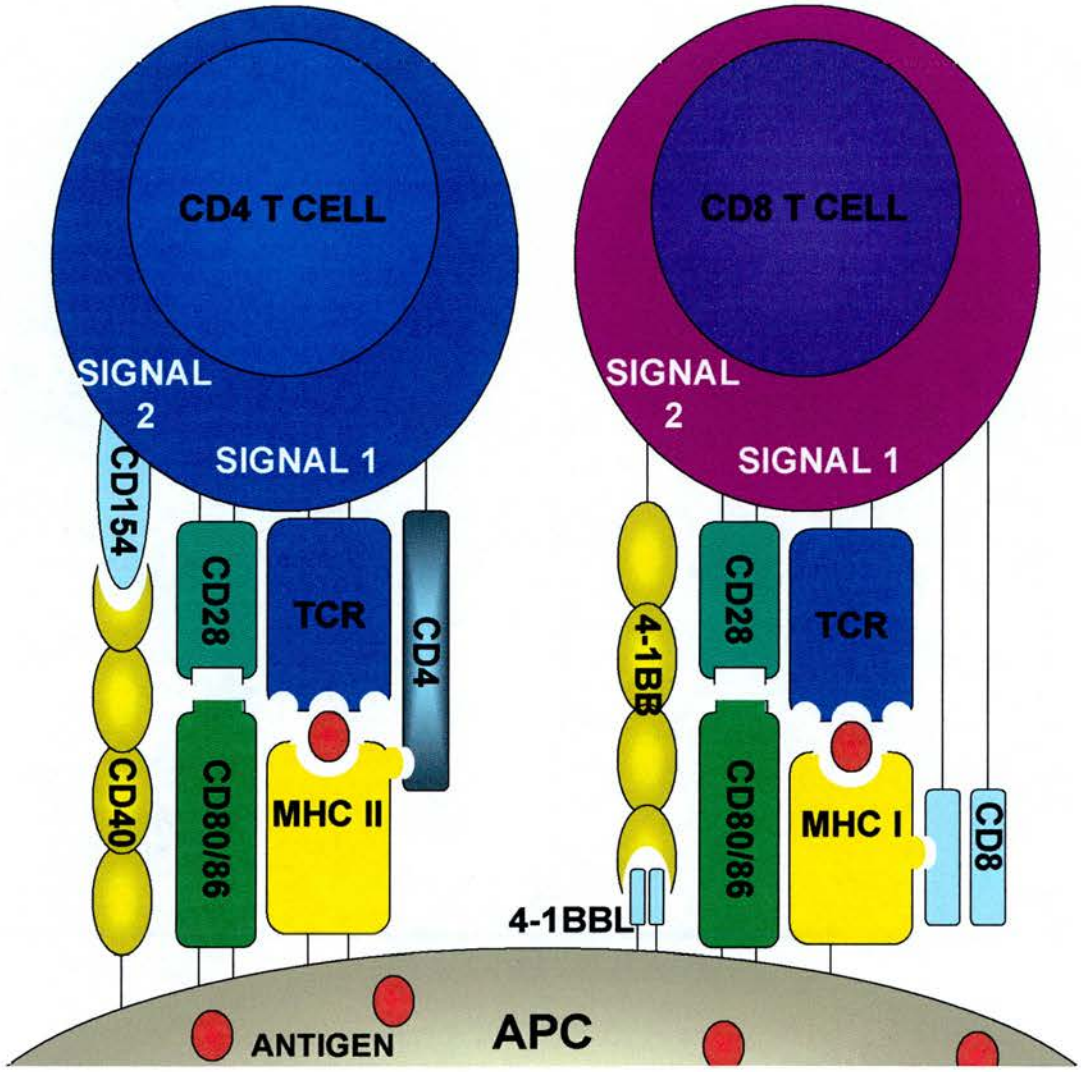

Figure 1.4: T Cell Activation
$CD4^+$ T cell recognition of antigen presented on the MHCII of APC, via TCR : CD4 interaction facilitates CD28 : CD80/86 interaction which constitutes signal one. This results in the secretion of the autocrine activator IL-2 by the $CD4^+$ T cell, leading to the upregulation of CD154 and the further activation of APC costimulatory expression. $CD8^+$ T cell recognition of antigen on MHC I occurs via a TCR: CD8 interaction, facilitating the interaction of CD28 : CD80/86. However, full activation of the $CD8^+$ T-cell requires total activation of the APC, which depending on the type of APC may require exogenous IL-2 or signalling through other pathogen recognition systems. A fully activated APC will present 4-1BBL to the $CD8^+$, facilitating its activation via 4-1BB binding.

Figure 1.5: The Generation of Adaptive Immunity

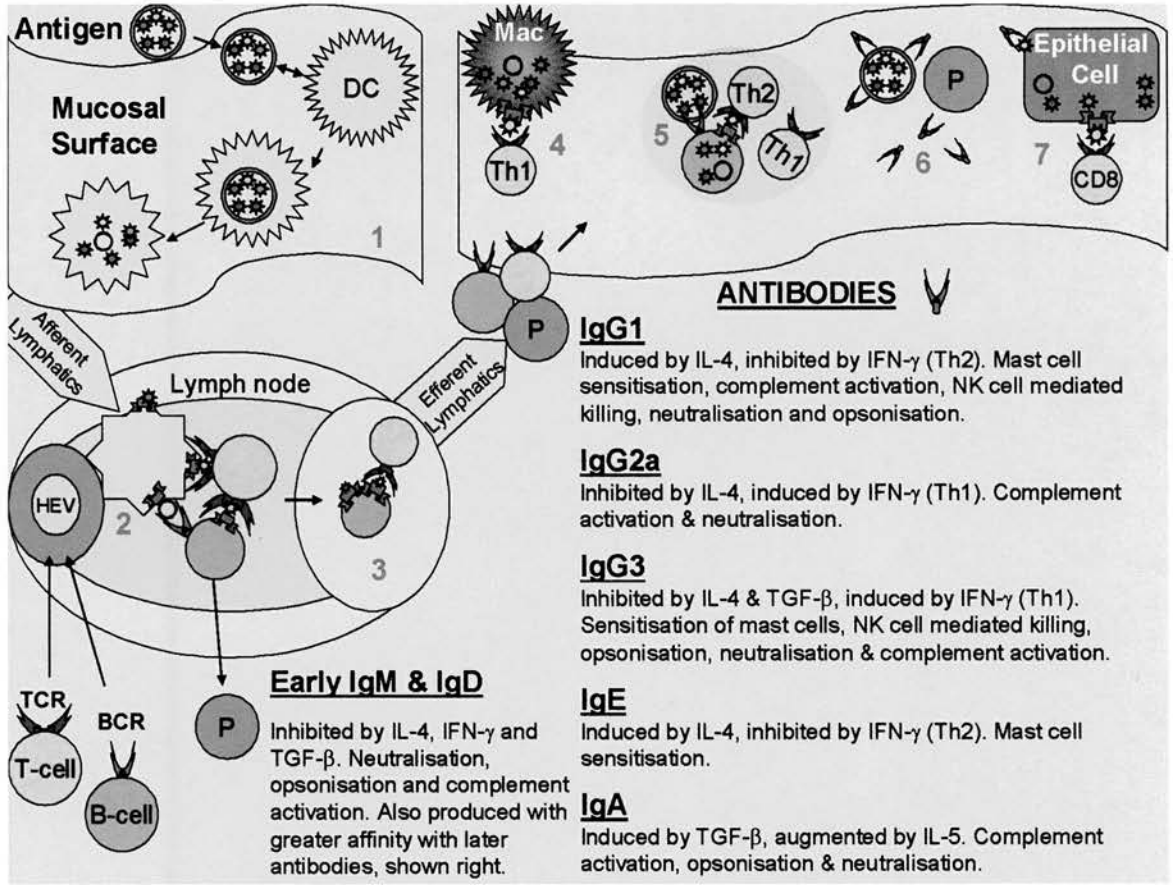

(1) Immature DC collect antigen and in response to *in situ* cytokines and conserved antigenic sequences, mature, a process resulting in their migration, via the lymphatics to the T-cell area of the lymph nodes and spleen (not shown here). (2) Naïve T and B cells circulate through the lymph node via the high endothelial venule. These cells up regulate adhesional receptors when their antigen receptors recognize material presented on the surface of the mature DC. T-cell activation can occur in the absence of B-cells whilst B-cell activation requires the presence of T-cell CD154 costimulation[88]. B-cells undergo early rapid division and may leave the lymph node as specialist antibody secreting B cells termed plasma cells (P), producing early IgM and IgD. (3) The majority of B and T cells migrate to the medullary chords of the node where proliferation occurs, accompanied by B-cell / plasma cell isotype switching in response to T-cell cytokine stimuli. These cells exit via the lymphatics to the mucosal surface. (4) Th1 T-cells provide cytokine stimuli to activate macrophage expressing antigen on MHCII. (5) Th2 cells produce cytokines which provide proliferative signals for B-cells. These interactions can be observed as mononuclear clusters in chronic Th2 pulmonary inflammation, termed inducible bronchus associated lymphoid tissue (iBALT)[89]. (6) Plasma cells secrete antibody which can neutralize / opsonise, particularly IgA, which is actively translocated across epithelial layers into the overlying apical mucus layer. (7) Binding of antibody to antigen expressed on infected cells can induce complement protein deposition and cell death. Antigen expression on MHCI facilitates CD8 mediated lysis.

1.8.4 SHH IN ADAPTIVE IMMUNITY

Shh and Ptc have been identified in both resting and activated murine and human peripheral CD4+ T lymphocytes, human macrophages, CD8 T lymphocytes and secondary lymphoid tissue. Work by Lowrey and colleagues demonstrated that contrary to its role in development, endogenously produced Shh *maintains* normal mouse T lymphocyte proliferation and survival, and that exogenous Shh can *enhance* this response[2]. Work by Stewart and colleagues with human T lymphocytes has shown enhanced expression of the activation antigens CD25 and CD69 with exogenous Shh, along with increased production of IL-2, IL-10 and IFN-γ[3].

More recent work by Lowrey and colleagues would suggest that Shh can compensate for CD28 in *in vitro* T lymphocyte activation (J.Lowrey, personal communication). These studies would suggest that Shh expression in the adult may maintain and enhance immunological responses, this may have particular relevance at the respiratory surface which will be discussed later.

1.9 IMMUNE AND NON-IMMUNE ASSOCIATED LUNG FIBROSIS

In the event of lung injury or chronic disease exaggerated repair responses can occur, termed remodelling. This response is typically found associated with an inflammatory cell infiltrate and results in permanent disruption of normal lung architecture, with features such as scarring and fibrosis, smooth muscle hyperplasia and "bronchiolisation" of the respiratory surfaces. Remodelling is a characteristic feature of chronic fibrotic lung disorders and of mouse fibrotic models.

The classical approach to the delineation of fibrotic progression has been to identify the initiating inflammatory insult, and the polarisation (Th1/Th2) of the immune response. However, a number of studies would now suggest that whilst an injurious event may be a catalyst, the involvement of an

inflammatory infiltrate is not an absolute requirement for fibrotic progression in a number of pulmonary fibrotic conditions[90 91].

Instead, fibrosis can be regarded as a series of progressively less reversible remodelling steps, the end stage of which is irreversible scaring, resulting from the deposistion of excess ECM by pulmonary fibroblasts, either through up regulated deposition of collagen (one of the main components of the ECM) or increased fibroblast numbers. Equally changes in the ratio of collagen degrading Matrix MetalloProteinases (MMP's) and their inhibitors (TIMP's), can lead to ECM accumulation, but is usually dependent on a collagen switch to a less degradable type, before becoming irreversible scarring.

The extent to which infiltrate is required to facilitate fibrotic progression differs with disease phenotype. Diseases or conditions associated with inflammatory infiltration, are typically Th2 polarised in cytokine profile, with the exception of gramuloma associated diseases such as sarcoidosis[92].

Th2 polarisation is more fibrogenic than Th1, as it includes cytokines with potent ECM modulating activity such as IL-4 and IL-13. Profibrotic effects can be direct, such as increased collagen production in pulmonary fibroblasts in response to IL-13[93], or indirect, via alterations in the balance of collagen degrading MMPs and TIMPs[94]. Th2 cytokines can also activate secondary signals, such as the release of TGF-β2, GM-CSF or IL-8 from IL-4 or IL-13 stimulated epithelial cells[93 95]

However, Th2 polarity alone cannot be the cause of fibrosis, as not all Th2 lung conditions result in fibrosis. A more plausible explanation may lay in a deregulated response or disruption of normal signalling balance in susceptible individuals. Indeed, recent studies have shown increased expression of high affinity receptors for IL-13 and IL-4 in fibrosis patients[96-98] where polymorphisms in ligand have shown little correlation[99]. Equally, IL-6, an anti-proliferative signal for normal human fibroblasts, is actually mitogenic for fibroblasts from fibrosis patients[100-102].

Equally, the susceptibility of an individual to the development of fibrosis, may rely on their response to, or ability to generate, secondary, epithelially derived signals, such as GM-CSF.

GM-CSF up regulates prostaglandin E_2 (PGE_2) in fibroblasts, an anti-fibrogenic lipid. PGE_2 acts by inhibiting proliferation and collagen synthesis and by up regulating collagen degrading mechanisms[103]. Thus, GM-CSF is anti-fibrotic, which could lead to a delay in wound healing. However, GM-CSF has also been shown to possess a proliferative function with type II epithelium[104] and a proliferative function with (anti-inflammatory) AM. Thus it is likely that GM-CSF facilitates rapid repair of denuded sites preventing the establishment of fibrotic plaques as a result of extended denudation.

However, it may be the ability to switch off these secondary signals, which could affect fibrosis susceptibility. Protracted production of IL-8, an initiating factor in the recruitment of inflammatory infiltrate, could lead to fibrosis in inflammation associated fibrotic conditions, whilst over expression studies with GM-CSF have illustrated that continued GM-CSF expression leads to TGF-β1 mediated myofibroblast accumulation[105], a scarring associated fibroblast subtype, and reversion of the anti-inflammatory phenotype of AM[106], potentially increasing local inflammatory activity and associated fibrosis.

To further discuss fibrotic remodelling and related mouse models, it is first necessary to review some associated medical terminology.

1.10 LUNG FIBROSIS

The heterogeneous nature of the fibroblast population and the multitude of defensive and remodelling mechanisms operating in the lung, combined with individual susceptibility factors, mean that fibrotic lung conditions are frequently classified by histology and clinical diagnosis, rather than exclusively by causative agent, as the response of the individual to that agent will dictate the success of any subsequent treatment.

As representative examples of the different pathologies discussed in this thesis, two types of fibrosis are considered here. Bronchiolitis Obliterans Organising Pneumonia (BOOP), an example of an airway obstructive fibrosis resulting from inflammatory signalling, and Idiopathic Pulmonary Fibrosis (IPF), an example of interstitial lung disease, resulting from fibrosis inducing signalling pathways.

Information given here is derived from indicated references and materials obtained from postgraduate courses attended at the European Respiratory Society Annual Meeting 2003, and American Thoracic Society Annual Meeting 2004 (See Section 7.5).

1.10.1 BRONCHIOLITIS OBLITERANS ORGANISING PNEUMONIA

First described as a distinct entity in 1985 by G.R. Epler M.D[107, 108] (www.epler.com), BOOP most commonly occurs between the ages of 40 and 60, although it can occur at any age. Clinically these patients present with symptoms including fever, mild cough and breathlessness and in some patients, there is an associated decrease in vital and diffusing capacities with influenza like symptoms. Radiologically, patchy opacities can be observed in the lung, which biopsy reveals as connective tissue masses within the lumens of terminal and respiratory bronchioles, continuing into the alveolar spaces (Figure 1.6). Within these fibrotic masses, which frequently exhibit abundant capillarization, are invaginating or free floating polyps of mononuclear inflammatory cells. The surrounding airways appear inflamed and exhibit features of atelectasis, but the architecture is not irreversibly disrupted. Within these areas reactive proliferating type II epithelial cell populations can be identified along with increased numbers of macrophages. Distal to this occlusion obstructive pneumonia may develop, characterised by foamy, lipid laden macrophages.

Preliminary IHC investigation undertaken during the course of this investigation identified Shh and Gli expression in the type II epithelial cells in

these areas, with foci of nuclear localised Gli1 indicating active signalling in individual cells (Figure 1.6).

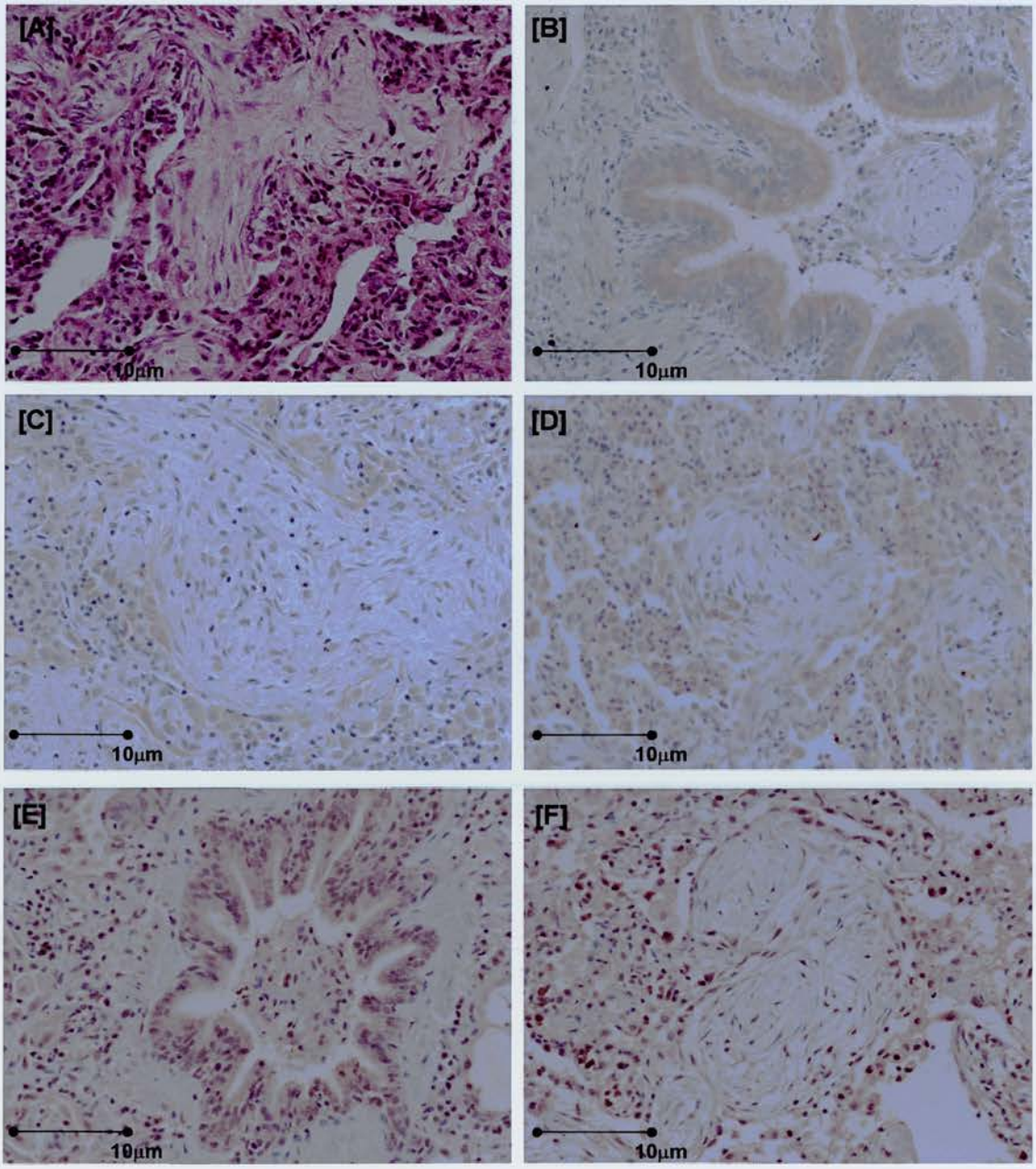

Figure 1.6: Shh Signalling in BOOP Biopsies
[A] H&E, [B] Shh, [C] Shh, [D] Ptc [E] Gli1 [F] Gli1
[A] The lighter central material in this H&E stain is fibrotic. [B] Shh IHC is specific for bronchial epithelium and Type II like cells associated with fibrotic foci [C]. [D] Fibrotic foci are also found associated with Ptc positive cells. [E] The occurrence of Gli expression in Shh positive bronchial cells suggests some autocrine signalling capability. [F] Gli1 expression and nuclear localisation in areas of fibrosis would indicate an active Shh signalling pathway in these regions.

The cause of BOOP, when known, is used to sub classify these conditions, as are distinctive pathological features without those covered in the central definition of BOOP given above.

Idiopathic BOOP is corticosteroid responsive, where 65-80% of patients are completely cured following treatment. A subset exhibit stabilisation, whilst others exhibit complete resolution of disease without therapeutic intervention at all. Whether these variations represent patient variation or a differing disease process is a matter of continuing discussion. But, crucially, with correct treatment this disorder, worldwide has only a 5% mortality rate, which is in stark contrast to that of IPF.

1.10.2 IDIOPATHIC PULMONARY FIBROSIS

IPF is contained within the Interstitial Lung Disease (ILD) classification, which encompasses a wide range of end stage inflammatory and fibrotic disorders, and has recently undergone dramatic reclassification in order to address more recent diagnostic advances and problematic geographical variation in terminology [109]. ILD is classified into those conditions of known aetiology, such as asbestosis, and those conditions of unknown aetiology, now referred to as idiopathic interstitial pneumonias (IIP). The most common and progressive of these conditions is Idiopathic Pulmonary Fibrosis (IPF), previously known as cryptogenic fibrosing alveolitis, in which Stewart et al identified epithelial expression of Shh[1].

IPF affects more males than females, usually over 50 years of age, with 75% of patients being current or former smokers. It carries a grave prognosis of survival, typically 4-5 years post diagnosis. Some familial clustering has been observed, suggesting some genetic predisposition, although, there is as yet no specific evidence of a disease associated gene abnormality. Clinical diagnosis of IPF requires the exclusion of identifiable cause, exertional dyspnoea, non-productive cough and lower respiratory crackles with chest auscultatation. Confirmation of disease requires a Usual Interstitial Pneumonia (UIP) pattern of disease in HRCT or wedge biopsy. Absence of

this pattern results in a diagnosis of non specific interstitial pneumoniae (NSIP), which carries a better prognosis, as unlike IPF, this is corticosteroid responsive.

UIP pathology is patchy and heterogeneous in progression, characterised by remodelling lung where "honeycombing" is the defining feature. This describes an area of fibrotic lung where the lung architecture has collapsed to reveal macroscopically visible spaces. Cellular infiltrates may also occur, typically dominated by lymphocyte and monocyte populations with granulocytes. The occurrence of eosinophils in this infiltrate may be associated with a reduced prognosis of survival. A pathological hallmark of UIP is the presence of discrete areas of fibroblastic proliferation, termed fibroblastic foci, usually underlying hyperproliferative type II epithelial cells.

Stewart et al identified membrane and cytoplasmic Shh expression in areas of remodelling hyperplastic epithelium in this condition (Figure 1.7[A-D]). The presence of epithelial and mesenchymal expression of Ptc, in both diseased and non diseased areas, suggested that a recapitulation of this developmental signalling pathway might be involved in the remodelling process, such as that performed by TGF-β.

TGF-β, a developmental signalling molecule, with both pro and anti fibrotic function in the adult lung, exhibited a marked up regulation in UIP, but not bronchiectasis, despite fields of similar disease morphology (Figure 1.7 [J-L]).

Differences in Shh expression were also observed between UIP and bronchiectasis. Bronchietasis biopsies exhibited an epithelial, perinuclear dot Shh expression pattern in diseased areas, not observed in UIP. This would suggest that an element of the Shh expression process may be disease specific[1](Figure 1.7 [F]).

Indeed, whilst bronchiectasis is thought to originate with airway damage, where subsequent chronic infection causes enlargement and dilation of the

airways, UIP is believed to have an immunological basis in its progression, linked in some way with aberrant epithelial mesenchymal interaction[110]. Thus, it maybe, that this difference in expression pattern, is attributable to a differing mechanism of disease progression.

Previous work by Wallace et al in this laboratory, identified circulating antibodies to a 70-90KD protein in IPF patient serum, which were not observed in normal controls[111, 112]. This protein was later localised to type II cells, suggesting an autoantigen[111, 112]. Experiments *in vivo* with a polyclonal antibody raised against the epithelial antigen and a human type II epithelial cell line showed up regulated tenascin and TGF-β production[113]. Where tenascin is an extracellular matrix protein associated with active scar formation, well characterised with TGF-β, as being present in the lungs of patients with IPF[114-116], up regulated in areas of active fibroplasias or fibroblastic foci[114, 115].

Thus it could be hypothesised that the autoantibodies observed in IPF maybe directly involved in the Shh up regulation, or indirectly through protracted TGF-β and tenascin expression and that regulation of Shh in bronchietasis differs, due to an absence of this auto-antibody.

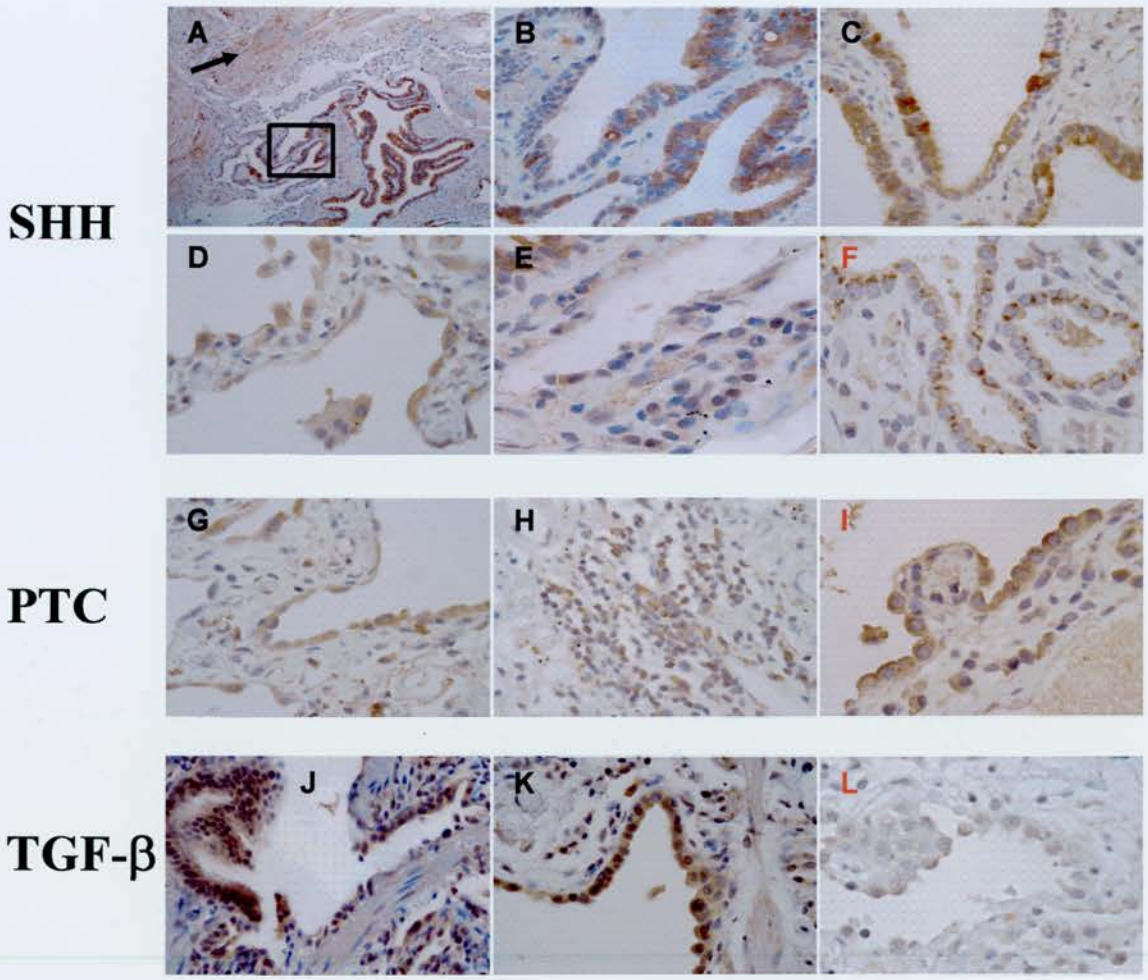

Figure 1.7: UIP Biopsy IHC Analysis
Photos taken from the thesis and publication[1] of Dr G.A Stewart. Photo's from UIP biopsy are denoted in black, bronchiectasis cases in red. [A] x100 image of strong Shh staining restricted to specific areas of lung observed in large cuboidal epithelial cells, positive staining hypertrophic muscle arrowed. The boxed area in [A] is shown in [B] at x400 where metaplastic epithelial cells are strong Shh expressors, similarly shown in a x600 magnification image in [C]. [D] A x600 image of type II epithelial cells stained positively for Shh. [E] A x600 image of Shh expression in infiltrating cells. [F] A x600 image of Shh staining in bronchiectasis illustrates a differing staining pattern. [G] A x600 image of Ptc staining in type II cells and in [H] infiltrating cells. [I] A x600 image of bronchiectasis showing a similar pattern of Ptc staining. TGF-β staining was positive in epithelial cells both at airway junctures [J] and normal epithelial surfaces [K] x600, but is relatively weak in bronchiectasis biopsies [L]x600.

1.11 ANIMAL MODELS OF PULMONARY INFLAMMATION AND FIBROSIS

Despite the vast array of animal models for human lung fibrosis currently in use, there is still no definitive model which recapitulates all the features of human lung fibrosis. In fact, given the inherent variation in human physiopathology with lung fibrosis, it is perhaps unreasonable to expect that this would be the case. The difficultly arises from the fact that in humans most fibrotic conditions develop as a consequence of months, perhaps years of aberrant extracellular matrix deposition. Thus whilst the more acute fibrotic responses of rodents to particulates such as asbestos and silica have been shown to be broadly similar to those induced in humans, and fibrotic models can be established by adenoviral transfer and *in vivo* overexpression of pro-fibrotic agents, it has been more difficult to establish models of chronic fibrosis.

Part of the difficultly lies in the fact that, like humans, strains of mice vary in their response to different pulmonary stimuli, the most frequently made comparison being that of the tendency for the C57Bl6 strain to mount Th1 mediated responses, making them relatively fibrosis resistant, versus the Th2 polarisation of the Balb-c strain, making them relatively susceptible to the development of fibrosis and allergy. Thus even withstanding the species comparison there is variation in model systems according to the mouse strain utilised.

An excellent review by Chua *et al.* has recently been published concerning the use of animal models and the inherent problems in their development[117]. Subsequent sections make reference to three commonly used animal models, the 2,4,6-trinitrobenzene sulfonic acid (TNBS) hapten model, the bleomycin model and the FITC model.

1.11.1 THE TNBS HAPTEN MODEL

The particular model of Hapten Immune Pulmonary Interstitial Fibrosis (HIPIF) described here was initially characterised in hamsters, but was subsequently developed into a mouse model. Pulmonary fibrosis is induced by epicutaneous application of a water soluble form of the hapten TNBS (3% solution) to the abdomens of Balb-c mice (100μl/mouse). This is followed five days later by an intratracheal challenge with 50μl of a 1%TNBS solution.

Haptens are non immunogenic but because of their chemical reactivity, covalently bind to proteins and lipids disrupting function and making new modified molecules which appear as antigenic to the immune system. Thus whilst ensuing immune responses are primarily against the hapten component, autoimmune elements in the immune response also perpetuate at the point of initial sensitisation.

The intratracheal delivery results in a focal recall response against hapten conjugates and leads to an autoimmune mediated fibrosis with features similar to those observed in human IPF[118]. The immune response is antigen specific, requires both CD4 and CD8 T cells and the development of fibrosis in these animals is completely dependent on the presence of alveolar macrophages[119].

The advantages of this model are that it is highly reproducible and the induced immune response has been well characterised through a number of complex adoptive transfer experiments[120]. The disadvantages are that it has primarily been used as a means to demonstrate the role of APC in autoimmunity and tolerance, thus the induced pathology has not been as well characterised as for other models.

1.11.2 THE BLEOMYCIN MODEL OF LUNG INJURY

Bleomycin is used as a cytotoxic agent in the treatment of human cancer, but was soon found to have toxicity in the pulmonary system and acted dose dependently as an inducer of lung fibrosis. This activity has been utilised in

the establishment of a number of rodent injury models. These are the most commonly used models of fibrotic lung injury. Induction of disease likely arises from the ability of bleomycin to bind DNA/iron and its subsequent involvement in free radical formation and lipid peroxidation, but as yet, the central cause has yet to be explained.

Method of delivery differs with animal species and like the FITC model, discussed below, a number of modifications have occurred to the technique across publications and labs. The lab of Galen Toews, Ann Arbor, Michigan, as an example inject a single 30μl injection of 0.025U of bleomycin (in saline) into the surgically exposed tracheae of a mouse anaesthetised by sodium pentobarbital[121]..

Following instillation, rapid type I epithelial cell necrosis occurs, leading to denudement and transudation of inflammatory factors and thickening of the respiratory surfaces (acute alveolitis), an inflammatory infiltrate becomes prominent and inflammation spreads interstitially and is maintained for 12 days post instillation. During this period fibroblasts are activated and proliferate, resulting in a two fold increase in lung collagen content by three weeks post challenge. Subsequent loss of elasticity in the lung through fibroblastic growth leads to a high rate of fatality in these mice.

Some studies would suggest that this fibrotic progression in this model is Th1 mediated, and that TGF-β and TNF-α play crucial roles. However recent work using CCR2 knockouts (the MCP-1 (CCL-2) receptor) would suggest that GM-CSF in combination with low TNFα can protect against fibrosis development, likely through up regulation of the anti-fibrotic protein PGE_2 [103, 122].

1.11.3 THE FITC MODEL OF PULMONARY INFLAMMATION AND FIBROSIS

The fluorescein isothiocyanate (FITC) hapten instillation model was first characterised in our lab by S Roberts[123]. FITC was surgically instilled intratracheally under halothane anaesthetic and mice sacrificed up to 5

months later. This technique was later modified by Dr Gareth Stewart, to use avertin anaesthetic instead of Halothane, and a transoral method of instillation of FITC was selected. This method was then further modified by Dr Sharon Ahmed to incorporate a 2 step delivery of FITC separated by a 6 week period.

FITC is a fluorescent compound which readily forms non-specific covalent attachments within the protein matrices of the interstitium. FITC can be identified here over 5 months post instillation, bound to putative slow turnover proteins, where circulating FITC specific IgG antibodies can still be detected (Roberts et al unpublished observations). In terms of pathology, epithelial cell remodelling and mononuclear cell infiltration in areas of persistent FITC deposition have been described, superseded by the formation of fibrotic plaques and honeycombing, reminiscent of a UIP phenotype. The specifics of this model will be discussed in greater detail in Chapter 3.

Using this model Gareth Stewart et al identified Ptc expression in bronchial & alveolar epithelial cells and AM. There was no difference in expression between FITC and PBS treated mice, although Ptc was also found on the mononuclear infiltrate localised around areas of FITC deposition in FITC treated mice.

When compared with PBS treated mice, and areas lacking FITC, foci of FITC deposition showed up regulated Shh expression at 7 days post instillation, through to 5 months in bronchial and alveolar epithelial cells (Figure 1.8).

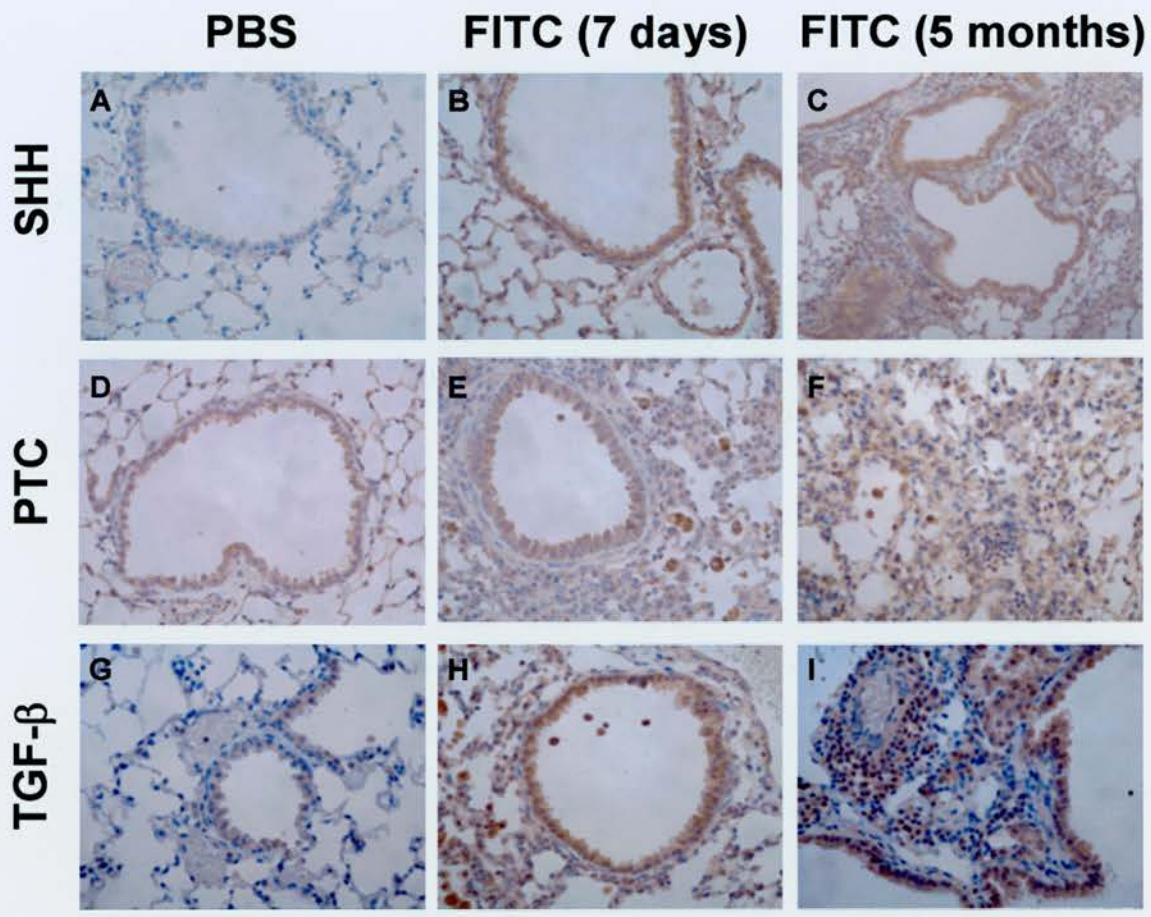

Figure 1.8: IHC of the FITC Model from a Paper by Dr GA Stewart[1]
Representative Shh (A-C), Ptc (D-F) and TGF-β (G-I) IHC on mouse sections after a single surgical intratracheal delivery of PBS or FITC. Time points for 7 days and 5 months post instillation are shown.

1.12 A ROLE FOR DEVELOPMENTAL GENES IN ADULT DISEASE?

Given the complex network of signals that occur in development, it is possible that Shh upregulation in lung disease results inconsequentially from protracted expression of other recapitulated developmental signalling molecules such as TGF-β. However, recent studies have elucidated a plethora of post embryonic functions for the hedgehog signalling pathway, suggesting that Shh may have a crucial role in post embryonic systems. Research has centred largely on the role of Shh in the brain, where it has been described as having inductive, proliferative, neurotrophic and neuroprotective activities, being involved in neurological disorders such as

Multiple Sclerosis and Parkinson's disease[124]. Other areas of research include the role of Shh signalling in the development of basal cell carcinomas, (reviewed by [125]), disorders of the digestive system, and its role in cell cycle progression in activated peripheral T-cells[2].

1.12.1 SHH AS A STEM CELL MODULATOR

A number of studies have highlighted the potential for Shh signalling as a differentiation modulator, but only the recent publications of Watkins et al have conclusively investigated this at the post embryonic pulmonary surface[73]. Watkins and colleagues depleted Clara cells from mouse airways via their sensitivity to naphthalene injury, leaving the naphthalene resistant vCC population. This resulted in a transient peak in Shh and Gli expression 3 days post depletion that coincided with the reestablishment of a complete epithelial barrier. It was suggested that Shh signalling might be involved in this repopulation step, since this peak preceded an increase in the number of pulmonary neuroepithelial cells - a cell type identified as a potential epithelial progenitor[67, 68]

Epithelial coverage is already completed by the peak of Shh expression, thus a causative role in epithelial proliferation is unlikely, and this is confirmed in our studies where we observe bronchiolar Shh expression restricted to areas of complete epithelial coverage. It is interesting that coverage normally occurs in the absence of differentiation, which typically occurs following re-establishment of epithelial integrity. Given the necessity for confluence for Shh signalling in some cell Shh bioassays[59, 126] it is interesting to speculate that perhaps Shh is a differentiation and proliferation modulation signal. Hypothetically this could occur as follows:

Loss of cell contact induces proliferation and Shh production by stem cell populations, but these cells only become responsive to their own Shh signal once an intact epithelial barrier had been re-established.

Whether such a signal would act to induce differentiation in these cells or maintain their stem cell phenotype would be difficult to determine. Reasoning for such speculation arises through the well characterised progenitor modulating role of Hh in a range of post embryonic systems including T lymphocyte development[64] and haematopoiesis[127].

The work by Bhardwaj in haematopoiesis was notable for it clearly defined the downstream effector of Shh function as BMP-4, where Shh addition to an enriched population of human CD34+Lin-CD38- progenitor cells resulted in increased self renewal, albeit in combination with many other growth factors.

The use of BMP-4 in this process was notable given innovative *in vivo* studies from the lab of Brigid Hogan and colleagues which have demonstrated a potential progenitor cell modulating function for BMPs in epithelium; cells exposed to high levels of BMP-4 retained undifferentiated characteristics[128, 129]. In light of these studies, were Shh to modulate pulmonary epithelial progenitor function through the BMPs, it would likely be in conjunction with a number of other signals, such as FGF-10, perhaps in a recapitulation of the process of cell fate designation which occurs in the embryonic lung[128].

An example of Hh mediated progenitor cell modulation in injury comes indirectly from several sources[130, 131]. Pepinsky et al demonstrated that Shh administration can accelerate nerve recovery following sciatic nerve crush injury[130]. A possible explanation for this response comes from studies by Bambakidos et al, using a rat demyelination model[131]. These authors observed increased proliferation of nestin+ve stem cell like progenitors in areas of chemical demyelination following direct Shh administration. This suggests that exogenous Shh at a site of injury induces proliferation in stem cell populations, although the specificity of this progenitor proliferation was not addressed in this study.

1.12.2 SHH AS A MODULATOR OF FIBROSIS

The recapitulation of developmental genes such as Shh in remodelling and fibrotic processes is not without precedent; certainly TGF-β and Tenascin have been shown to have prominent roles in both development and fibrosis[132, 133]. However, the localisation of Shh expression, and therefore its involvement in pulmonary disease remains undetermined as whilst Watkins et al have demonstrated bronchiolar epithelial expression of the Shh signalling components in mouse[73], our lab has demonstrated both bronchiolar and alveolar expression of Shh in mouse and human, where alveolar Shh expression was restricted to the type II like cells of inflamed remodelling areas[1].

Interestingly, a murine model of allergen induced inflammation, despite greater inflammation than the FITC model, showed no Shh up regulation[1, 123]. This was highly suggestive of Shh expression as a fibrosis associated factor.

Shh and FGF are commonly associated signalling molecules and are co expressed in a number of systems both pre- and post-natally[134-137] and hedgehog signalling has been linked with collagen fibre induction in the neural system[138]. Shh also has substantial cell cycle modulating capabilities[139, 140] and participates in well characterised proliferative mesenchymal interactions in the developing lung. Thus the localisation of Shh to areas of fibrosis in IPF may present a causal relationship with fibrosis in the IPF patient.

However, the up regulation of Shh at sites of epithelial injury comes amongst a plethora of other modulating signals and could therefore represent a downstream marker of a much larger process initiated by the underlying mesenchymal/fibroblastic cells, which play a crucial role in epithelial maintenance.

Mesenchymal cells produce specific epithelial growth factors such as KGF and FGF-10. These are up regulated in response to injurious stimuli, resulting in increased epithelial proliferation and rapid reestablishment of an intact

epithelial layer, (for a review see Ware et al[141]). Studies using FGF-10, FGFR2b and Shh knockout mice have recently confirmed Shh to be downstream of FGF-10 signalling[142]. Thus Shh expression on epithelium at sites of fibroblastic proliferation, such as that observed in IPF, may be a consequence of this repair process rather than an instigator of repair. In this situation Shh could be considered a regulatory factor, given its ability to down regulate FGF-10[134].

Alternatively expression at the alveolar surfaces of IPF patients and in the FITC instillation mouse model, might relate to a specific element of the disease process. Although without known cause, IPF progression is believed to have an immunological basis, linked in some way with aberrant epithelial mesenchymal signalling[110] One hypothesis might be that Shh expression might modulate the cross talk between disease process and T-cells, perhaps involved in the stimulation of auto antibody generation against epithelial antigens observed in these patients. Similar hypotheses could be drawn from the observations made in the fibrotic FITC mouse model of IPF pathology[123]. Fibrosis and inflammation are believed to be induced in this model through the persistence of the intratracheally instilled irritant FITC, which lodges in the interstitium and binds resident proteins. The observation that antibodies are then raised to FITC would suggest that anti-self antibodies are also raised in this model, given the ability of FITC to covalently attach itself to host proteins, effectively making normal lung proteins part of an antigenic molecule..

1.12.3 SHH AS AN INDICATOR OF INJURY

Shh would appear to share many of its effects with KGF and FGF-10[139], most notably, stimulation of increased cellular resistance to injury and death[143, 144]. Shh exhibits this effect in a number of cell types[139, 145, 146], but it has yet to be established at the pulmonary interface. Perhaps the best example of this activity is in Parkinson's disease, where exogenous administration of Shh in both a marmoset and mouse model of the disease results in improved locomotion and function[147, 148]. Tsuboi and colleagues[148], citing work by Miao et al[146], have suggested that this is likely due to Shh acting as a

neuroprotective agent against dopaminogenic neuron cell death, which is central to disease progression.

Indeed current research would show that Shh can induce the anti-apoptotic protein Bcl-2 in keratinocytes and T-lymphocytes[2], and that its presence prevents the apoptosis of neuroepithelial cells[145]. Therefore in a pulmonary situation of injury, such as exposure to environment oxidants, Shh release, along with KGF and FGF-10, may serve to temporarily increase surrounding epithelial cell resilience, and prevent complete denudation of an epithelial surface and the risk of secondary infection.

Sustaining viability of injured cells carries with it the increased probability of populating the epithelium with cells which have incurred genetic damage. Indeed, this may help to explain the higher incidence of small and non-small cell lung cancers following epithelial trauma, and the preponderance for the involvement of Shh signalling in these carcinomas[68].

Up regulation of Hh signalling following injury, can be found in a number of model systems. Pola et al [149, 150] have demonstrated the up regulation of Shh and Ptc1 expression in a rodent hind limb ischemia model. Furthermore, the same group demonstrated that the administration of Shh induced robust neovascularisation, enhanced blood flow, and the up regulation of the angiogenic factors, vascular endothelial growth factor (VEGF) and the angiopoietins, Ang1 and Ang2[149],although any direct association is a matter of conjecture [151, 152]. The findings from other groups have been broadly in keeping with those of Pola et al (2001) demonstrating that Shh is capable of inducing VEGF expression[151] and angiogenesis[152].

Such angiogenic modulation could have important implications at the respiratory surfaces of IPF patients, where we have observed Shh expression in association with areas of fibrosis.[1]. Shh expression here may represent an attempt by the lung to revascularise and remodel the fibrotic architecture. Although current studies would suggest that Shh expression is not substantially greater in BOOP, where, given the neovascularisation of

vacuous fibrotic deposits, greater Shh expression might be expected, were angiogenesis a function of pulmonary Shh. Interestingly, VEGF itself is found up regulated with epithelial injury, thus Shh mediated VEGF up regulation might have other functions at the respiratory surface.[46]

1.13 AIMS, OBJECTIVES AND HYPOTHESES

In summary of the discussion contained with this introduction, the hypotheses raised prior to this body of work are listed below:

- Shh expression is an indicator of acute or chronic epithelial cell injury.

- Shh upregulation initiates defensive functions independent of systemic immunity, i.e. the activation of epithelial cytokine production, maintenance of stem cell function and effects on alveolar macrophage and fibroblast function.

- Shh expression in UIP and the FITC lung model indicates an active association of Shh signalling with the development of fibroblastic foci

- Disease progression in the FITC instillation mouse model is potentiated by Th2 anti-FITC antibody

The main objective of this thesis is therefore to address these hypotheses either directly, or through the establishment of techniques to facilitate their analysis. Subsequent Chapters of this thesis aim to address these hypotheses. Chapter 3 details investigations performed using a modified FITC mouse model, where an increased dose of FITC is transorally intratracheally delivered twice, six weeks apart. Studies using this model are compared with previous findings and approaches made at addressing the immunobiology behind disease progression; via antibody analysis, primary cell extraction studies and use of new IHC protocols.Chapter 4 details *in vitro* studies using epithelial cell lines as an approach to delineate the response of epithelium to

injury and exogenous Shh, and includes the development of a novel method for the quantitative detection of soluble Shh. Chapter 5 details the development of laser capture microdissection protocols for the confirmation of active Shh signalling at the genetic level in mouse FITC and human UIP sections, with an intention to identify putitative producer and responder populations in confirmation of IHC observations.

.

CHAPTER 2 MATERIALS AND METHODS

2.1 TISSUE CULTURE

2.1.1 GENERAL CELL CULTURE

All subsequent references to Foetal Calf Serum (FCS) (Labtech International, Rigmer, Sussex) refer to FCS heat inactivated at 56°C for thirty to forty five minutes in a water bath to inactivate complement. All cell lines were checked for LPS and mycoplasma contamination using the limulus amebocyte lysate coamatic assay (Quadratech Ltd, Surrey, UK) and Mycoplasma PCR ELISA (Roche Diagnostics Ltd, Surrey, UK) kits respectively, as per manufacturers instructions. Initial cell line culture established a cell bank storage system for these lines by culturing large numbers of cells then freezing in 50% FCS : 50% culture media containing 20% DMSO (Sigma-Aldrich Ltd, Poole, Dorset, UK), where cells were first suspended in FCS, then the DMSO containing fraction added with vigorous swirling to generate an even DMSO distribution, prior to aliquoting and freezing. All tissue culture was performed in class II safety cabinets using relevant plastics produced by Costar (Corning-Costar, Schiphol-Rijk, Netherlands)

CELL LINES

Cell lines listed below are adherent and were passaged via trypsinisation following two washes with serum free media, with the exception of the CCL-226 line which was also split via cell scraper removal. All lines were split sub-confluence in a ratio necessary to facilitate passage every 3-4 days. Relevant details are defined at the end of each cell line section as approximates of *trypsin volume per medium (75cm^2) flask / average time for sufficient lifting / split ratio*.

A549 (European Collection of Cell Cultures (ECACC)):

The A549 human pulmonary type II epithelial cell line is of lung carcinoma origin[153], it has been well characterised as a type II epithelial cell and is frequently used in expression and response investigations of human epithelium[113, 143, 154, 155]. The A549 cell line was cultured in RPMI 1640 (Sigma-Aldrich), supplemented with 2mM L-glutamine (Invitrogen Life Technologies, Paisley), 100U/ml penicillin / streptomycin (Invitrogen). Initial culture following

defrost also used a supplement of 10% FCS, this was reduced following 2 successful passages to 5% as the rapid proliferation produced in 10% was not suitable for many of the desired experiments. Of note, A549 continue to grow to healthy confluence in <2.5% FCS. *(4mls/7mins/1:9)*

CMT (ECACC):

The CMT mouse pulmonary type II like cell line, abbreviated to CMT in this work, was derived from a C57BL/6 lung carcinoma[156](ECACC) and although less utilised in the literature than A549, was derived from well characterised source material. Tumour structure was described as of alveolar patterning, with predominant type II like cells exhibiting pre-secretory pulmonary surfactant machinery. These cells were separated from fibroblast outgrowths in culture by repeated trypsinisation until a uniform phenotype was observed. The luminal borders of these cells are coated in microvilli, resembling brush cells, whilst shorter variants resemble respiratory ciliated cells. Thus it is likely that this cell line represents a mixed bronchiolar/alveolar epithelial subtype that could represent either two separate populations, or an interchangeable phenotype.

The CMT cell line was cultured in Waymouths media (Invitrogen) supplemented with 2mM L-glutamine, 100U/ml penicillin/streptomycin. As with A549, initial culture post defrost was performed with a 10% supplement of FCS reduced to 5% with two successive passages. Of note, despite references to the contrary[156], 2.5% FCS is sufficient to maintain CMT cells and a little proliferation and monolayers will continue in serum free media, but prolonged exposure to these conditions through passage leads to a halt in proliferation. *(8mls/15mins/1:10)*

CCL-226 / C3H/10T1/2 (American Tissue Culture Collection (ATCC)):

The C3H/10T1/2 line consists of embryonic mouse fibroblast cells which were cultured for use in the establishment of a bioassay system. Owing to difficulties in the development of the bioassay these cells were cultured in a variety of different media including RPMI-1640 and DMEM (Sigma-Aldrich) supplemented with 10% FCS or 10% charcoal stripped FCS (Labtech), 2mM L-glutamine and 0.0007% βMercaptoethanol (Sigma-Aldrich). Of note, if allowed to reach

sustained confluence, proliferative capacity may be lost and permanent morphological cell phenotype changes can occur. These cells were found to proliferate best in the absence of the standard 100U/ml penicillin/streptomycin supplements. *(various/5mins/1:10).*

CCL-206 (ATCC):

This is a fibroblast cell line derived from the lung of a normal new born ddY mouse[157, 158]. This cell line has been frequently used as an example of a lung fibroblast cell[159, 160], but there is a paucity of data relating to the original method of its isolation[158]. The CCL-206 cell line was cultured in DMEM supplemented with 2mM L-glutamine and 10% FCS. Of note, these cells exhibited reduced proliferation and appeared less healthy when cultured with standard 100U/ml penicillin / streptomycin supplements. *(5mls/5mins/1:8)*.

NIH-3T3 (ECACC):

This is a fibroblast like cell line derived from embryonic NIH swiss mouse cells used as a vehicle for plasmid bioassay and reporter vectors and cultured in DMEM supplemented with 2mM L-glutamine and 10% FCS. Of note these cells could be grown normally in penicillin/streptomycin supplemented media, but were not for reasons of increased transfection efficiency. *(5mls/5mins/1:6).*

NS-1 (SHH) (Developmental Studies Hybridoma Cell Bank, USA):

This hybridoma cell line, designated NS-1 was derived from the fusion of NS1 myeloma cells with cells taken from the spleen of a female Balb-c mouse immunised four times with baculovirus expressed rat Shh[161]. The line was cultured in RPMI supplemented with 100U/ml penicillin / streptomycin and 2mM glutamine, plus 10% FCS and βMercaptoethanol. This hybridoma produces 5E1, an anti-Shh antibody which is of isotype IgG1 and is specific for chick, rat and mouse.

2.2 CELL ASSAYS

2.2.1 MTT

MethylThiazolyldiphenyl-Tetrazolium bromide (MTT) stock was prepared by dissolving a 100mg pot of MTT powder (Sigma-Aldrich) in 20mls of sterile room temperature PBS (Sigma-Aldrich). Upon solution, this is passed through a 2μm syringe filter (Sartorius, Goettingen, Germany) and stored at 4°C in a foil wrapped universal. Of note, is that this solution is light sensitive and exhibits a drop in signal if stored for greater than 10-14 days and is not stable when frozen.

MTT is a yellow solution, converted into an insoluble purple substrate by intracellular mitochondrial enzyme activity, which can be read using visible wavelengths in a standard plate reader. This conversion reduces cellular function and is thus toxic at certain concentrations and duration of exposure. To account for this, MTT was titred into cell culture, to determine optimum concentration and time of exposure. Leaching of blue into the media demonstrated reduced membrane integrity and was taken as the upper limit of use, and the Optical Density (OD) of detection used as the lower determinant. The duration of exposure was selected from the most consistent data within this range i.e. CMT cells were co-cultured with MTT for 3 hours, whilst, A549 were co-cultured for only 45 minutes. However, the general protocol is described below, any derivations from this are recorded in relevant figure legends.

Cells were washed with serum free media / PBS, aspirated and replaced with serum positive media to a volume of 450μl in a 24 well plate, followed by 50μl of MTT stock per well. Cells were then incubated for a cell specific duration, then the medium discarded. The PBS wash step of the remaining MTT monolayer, which is commonly included in most protocols was excluded due to a loss of cells through lifting. Aspiration of remaining media with a yellow Gilson tip, was found to reduce residual media carryover to less than that obtained with a PBS wash step. The monolayer was then left to dry completely in a sterile hood. Once dry, 350μl of DMSO was added to each well, and the plate gently rocked to ensure the complete solution of the blue MTT precipitate. 100μl of this

solution was then transferred to a 96 well plate and read at 490nm/ref 630nm in a 96 well plate reader (see Section 2.7).

2.2.2 MTS AND LDH ASSAYS

Due to limitations in the use of MTT related to the loss of cells through lifting during the course of the assay, another approach was taken, utilising a Promega (Promega, Southampton, UK) cell titre assay. This uses a compound called 3-(4,5-dimethylthiazol-2-yl)-5-(3-carboxymethoxyphenyl)-2-(4-sulfophenyl)-2H tetrazolium (MTS). A variant of the MTT compound, working along the sample principles, but where the product is soluble, allowing *in situ* measurements, without the need for media removal or a DMSO solubilisation step. Of note, although this kit does draw attention to the need for media colouration controls. Studies here suggest that reproducibility can only be achieved using phenol red free media, not available for all cell lines.

Cell necrosis was recorded as per manufacturers instructions using the Tox7 LDH toxicology kit (Sigma-Aldrich).

2.3 SHH CULTURE REAGENTS

2.3.1 RECOMBINANT SHH PROTEIN

Recombinant Shh amino-terminal peptide (r-Shh) (R&D Systems, Abingdon, UK) was obtained as a bulk stock to avoid batch variation such as endotoxin contamination. The peptide is supplied in a PBS solution containing 50μg BSA per 1μg peptide, this was aliquoted and stored at -20°C. The peptide is derived from a DNA sequence of mouse origin expressed in *E. Coli* and has a predicted molecular mass of 20kDa and purity of greater than 97%. Using the LAL method the manufacturer estimates endotoxin levels to be below 1.0 Endotoxin Units per mg of protein, where the test has a maximum sensitivity of 0.001 Endotoxin Units. r-Shh activity is measured by alkaline phosphatase induction in C3H10T1/2 cells, the ED of which is typically 0.6-3mg/ml. This peptide has been shown to induce Shh specific responses in human, mouse, rat and chick systems.

2.3.2 5E1 ISOLATION AND PURIFICATION

The 5E1 antibody is produced by a hybridoma cell line derived from the fusion of the NS1 myeloma line with cells taken from the spleen of a female Balb-c mouse immunised four times with baculovirus expressed Rat Shh[161]. 5E1 is a mouse IgG1 antibody which has been shown to have functional neutralising function with chick, rat and mouse Shh protein. Mapping studies with human protein have shown that it binds to the same residues as the receptor Ptc[161, 162]

5E1 was purified from NS1 hybridoma line via the following method. Supernatants were taken from the NS-1 hybridoma cell line when slightly yellow and centrifuged several times to remove debris. Supernatant was then concentrated via dialysis (Medicell International Ltd, London UK) on poly-ethylene glycol, then purified using Hi-Trap (Amersham Pharmacia Biotech) columns according to the manufacturers instructions.

Briefly, the column was filled and flushed with 20mM phosphate buffer, supernatant loaded (following pH adjustment to pH.7.2), column washed with further phosphate buffer, then eluted with 0.1 M glycine-HCL, pH 2.7. Eluted samples were then tested for protein concentration with the BCA protein quantification kit and stored aliquoted in PBS at -20°C.

2.3.3 CYCLOPAMINE

Cyclopamine (Toronto Research Chemicals, Ontario, Canada) a Smo inhibitor was initially stored aliquoted at 1mM in DMSO, but primarily in limulus amebocyte tested : (endotoxin free) (LAL) water.

2.4 SONIC BIOASSAY

Two approaches, novel to this lab, were taken to determine the biological activity of Shh. The first was a differentiation induction assay using the C3H/10T1/2 cell line with Alkaline Phosphatase activity (ALP) used as a read out. The second utilised the NIH-3T3 line for transient transfections with a luminescent construct responsive to Gli activity. Neither of these methods

reached final stage use, still being under development at the time of submission. Thus the protocols described below are those which were found to be the most successful, but where they are likely to require substantial optimisation. Variations in protocol are discussed at greater length in Chapter 3.

2.4.1 C3H/10T1/2

C3H/10T1/2 cells were plated at 50000 cells per well in 100μl of media with charcoal stripped serum (Luke Eckersley, Manchester University, UK, personal correspondence) in a 96 well plate, left five hours to adhere, then supplemented with 100μl of either r-Shh peptide (Sigma-Aldrich) diluted in medium or CMT cell line supernatant, where Shh has been shown to induce ALP activity in these cells.

Use of charcoal stripped media was suggested as a means of removing factors, (lipid residues) from sera, which might interfere with Shh signalling, as previous studies I had conducted, and those of Luke Eckersley had shown only marginal differentiation of cells with r-Shh in normal serum containing media.

This cell density was selected to give around 60% confluence at the moment of r-Shh exposure, reaching full confluence one day previous to the culmination of the assay, 5 days later. Prolonged confluence of this cell line has been shown to induce differentiation, thus further incubation of these cells would have been counterproductive.

Medium was removed after 5 days and the cells washed, first in PBS, then 20mM Tris/0.15M NaCl (Sigma-Aldrich). Cells were then lysed through a 1 hour, 37°C incubation with 1M Diethanolamine/0.5mM $MgCl_2$, p.H.9.5 (Sigma-Aldrich). ALP activity in this lysate was then visualised using a 2mg/ml P-Nitrophenyl phosphate (Sigma-Aldrich) solution for various times greater than 30 minutes and stopped with 25μl of 3M NaOH per 100μl reaction solution, and read at 405nm. Cell lysates had their protein content quantified via bicinchonic acid assay (BCA) kit (Pierce/Perbio, Northumberland, UK), and data presented,

per minute, per mg protein. A Calf Alkaline Phosphatase (CAP) was used to confirm substrate viability. See Figure 2.1.

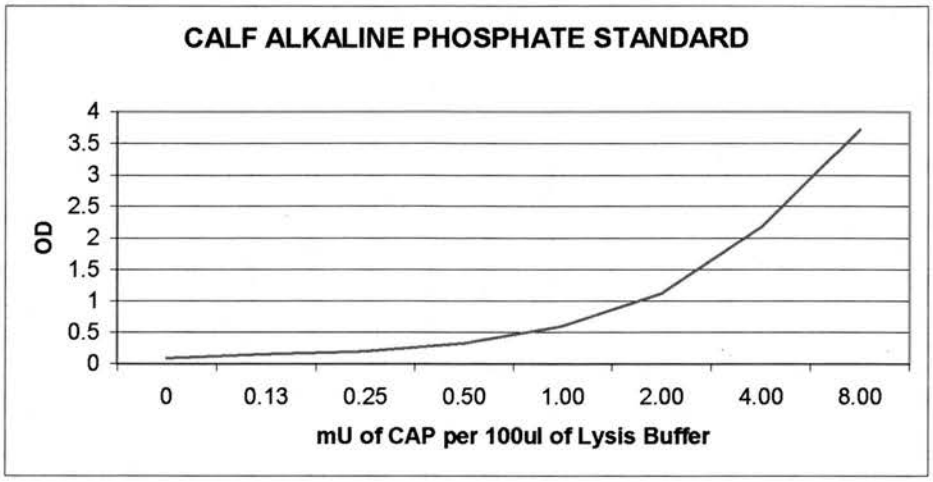

Figure 2.1: Calf Alkaline Phosphatase Standard Control Curve

2.4.2 GLI LUCIFERASE REPORTOR CONSTRUCT

This assay utilised two plasmid constructs, the Gli reporter plasmid: kindly donated by Beachy et al (John Hopkins, School of Medicine, Baltimore) and the pRL-TK control plasmid from Promega, www.promega.com E2241 / EMBL Accession no AF025846.

The Gli plasmid was shipped as a glycerol stock and consisted of an 8 fold repeat of the Gli binding site inserted between *Sac1* and *Nhe1* cut sites in a pGL3-basic plasmid which contains lactamase for Amp resistance selection and firefly luciferase www.promega.com. See Figure 2.2

The pRL-TK control plasmid contains a Renilla luciferase under the control of the Herpes Simplex Thymidine Kinase. This is used as both a transfection and expression normalising control for the Gli plasmid. The plasmid can be used at as low as 20:1 ratio, i.e. 1μg Gli reporter to 50ng Renilla control.

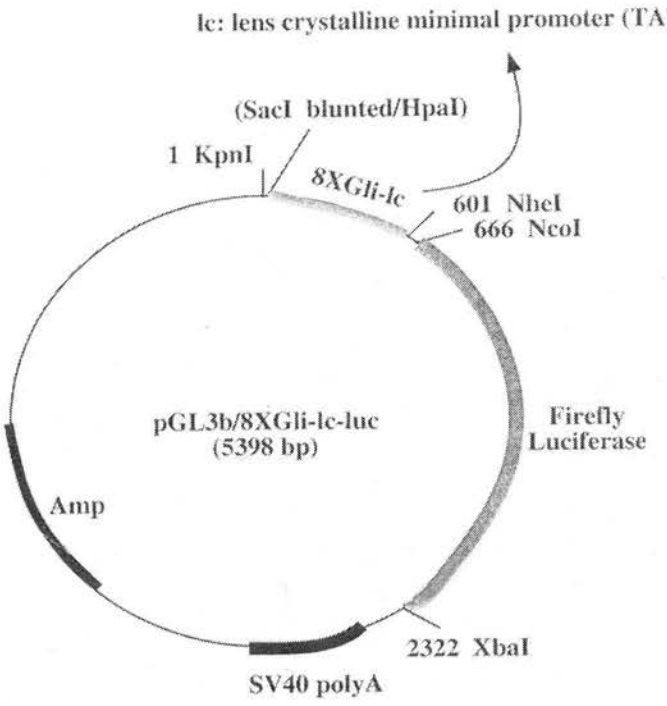

The parent vector pGL3basic is from Promega.
Information on pGL3b is available through their website.

Figure 2.2: Plasmid Map of Gli Construct

PLASMID SELECTION

The Gli reporter plasmid was amplified using *E. coli* cells grown in ampicillin conditions. Briefly, Agar was prepared from 2.5g yeast, 50g tryptone, 5g NaCl, 7.5g agar, 500mls water containing 1 NaOH, pellet, autoclaved on the same day. This was microwave heated, cooled slightly and supplemented with ampicillin to 100μg/ml, mixed and poured into plates, left to set for 1hr then stored overnight in the fridge, then placed upside down in an incubator to remove condensation and to warm the agar. To an aliquot of 200μl competent cells (XL1 blues), 0.5μl of plasmid was added (personal communication Beachy et al), incubated on ice for 1hr, heat-shocked at 42°C for 30 seconds, then incubated on ice for 2 minutes. 250μl of room temperature Luria Bertanti (LB) broth was then added and placed at 37°C on its side in a shaker for 1hr. 100μl was then spread per plate and left for 24hrs in an incubator to cultivate.

Colonies were then picked using a yellow tip to generate starter cultures. The tip was dropped into 5mls of LB broth in a 50ml falcon tube taken from a stock

prepared with 10 capsules (Sigma-Aldrich) in 500ml dH_2O, autoclaved, & ampicillin added to 100μg/ml. The tip was left in the tube, lid loosely closed and placed in a 37°C incubator shaker overnight.

PLASMID ISOLATION AND VALIDATION

The plasmid was isolated and purified from 1.5ml aliquots of the starter cultures by using the Promega Wizard plasmid DNA purification system, as per manufacturer's instructions, and quantified using a UV visible spectrophotometer Ultra-Spec2000 (Amersham Pharmacia Biotech, Little Chalfort, UK).

Restriction digests were then performed to confirm plasmid isolation in each starter prep isolate by using 1μl 10xbuffer, 1μl Nco1, 1μl Kpn1, 0.1μl BSA, 1.9μl H_2O and 5μl of plasmid (total 1μg), and visualised with orange G loading buffer (BDH, Poole, UK) on a 2% agarose gel (Cambrex, Rockland, USA). The desired insert was 28 + 4bp of overhang + 3bp to kpn1 and 63bp to Nco1: total 98bp. The actual insert was taken from a publication by Sasaki et al[52, 58] and is shown below:

TCGACAAGCAGGGAACACCCAAGTAGAAGCTC
GTTCGTCCCTTGTGGGTTCATCTTCGAGAGCT

For long term storage a glycerol stock of the starter culture containing the greatest plasmid expression was prepared by adding 300μl of autoclaved glycerol to 1ml of culture, if repeated, the glycerol would be better made to 30% and added as an equal volume for greater ease of use. Glycerol stocks were maintained at -70°C.

PLASMID AMPLIFICATION

The high expressing starter culture was then diluted 1/500 into LB broth and cultivated for 24hrs at 37°C with vigorous shaking. The cells were then isolated by centrifugation at 6000g and re-suspended in buffer P1 of the endofree plasmid maxi kit (Qiagen, Sussex, UK), and isolation proceeded according to

manufacturers instructions. The sample was eluted in Tris EDTA (TE) buffer to a concentration of 3.4mg/ml and aliquoted in 4μl aliquots at -20°C.

DUAL LUCIFERASE ASSAY

This method was still under optimisation at the time of thesis submission, thus the method described is only an example of those tried, which varied with cell density, concentrations of lipofectamine and reporter and control plasmids. The duration, volume and concentration of samples added for analysis and culture media used was also varied. Lipofectamine time and concentration were determined by titration (see Chapter 3).

CELL TRANSFECTION

NIH-3T3 cells were plated at $2x10^5$ cells per ml/$1x10^5$ per well in 24 well plates, 24 hours before transfection. Immediately prior to transfection, solutions A and B were prepared:

Solution A: For each transfection, 2 μg of total DNA* was diluted into 100 μl of serum-free medium (without penicillin/streptomycin (Invitrogen)) (*100ng Renilla luciferase (stock 20μg) for every 2μg of firefly luciferase).

Solution B: For each transfection, 5μl of lipofectamine (1mg/ml) (Invitrogen) reagent was diluted into 100 μl serum-free medium (without penicillin/streptomycin (Invitrogen).

The two solutions were combined, mixed gently and incubated at room temperature for 30 minutes to generate lipid-DNA complexes. 0.8 mls of serum-free D-MEM without penicillin / streptomycin was then added to yield a 1ml final volume. This solution was mixed gently and 250μl added to each well of NIH-3T3 cells previously washed and aspirated with 2 ml of serum-free D-MEM without penicillin / streptomycin. A minimum of two wells of non-transfected control cells were maintained.

Cells were incubated with this solution for 5h at 37°C in a 5% CO_2 incubator. This was then supplemented with 250μl of D-MEM without penicillin /

streptomycin containing 20% calf serum, without removing the transfection mixture. (Results with protocols using complete aspiration and replacement of transfection mix, did not differ). Cells were incubated overnight and media replaced with penicillin / streptomycin positive media prior to the addition of test solutions.

APPLICATION OF THE BIOASSAY

Supernatants and r-Shh control solutions were administered at various times post transfection, but most recently 24hrs after transfection. No difference was observed in response with time of delivery.

Both Cyclopamine, a Smo inhibitor, and 5e1 an antibody capable of blocking Shh binding, were incubated with solutions as specific negative controls. Shh solutions with Cyclopamine were incubated together for 5-30 minutes prior to addition, as were 5e1 Shh combinations. (Cyclopamine was stored aliquoted at 1mM in DMSO or limulus amebocyte lysate tested : (endotoxin free) (LAL) water).

Passive lysis buffer from the Stop and Glow Dual Luciferase Kit (Promega) was prepared by adding one volume to 4 volumes of distilled water. Media was then removed from wells by gently washing in PBS. This must be completely aspirated prior to the addition of the small 150μl volume of passive lysis solution to avoid dilution. The wells were then placed on a rocker for various lengths of time ranging from 20 minutes - 1hour, where duration of lysis was found not to affect luminescent readings.

The lysate material was then transferred to an Eppendorf tube (Eppendorf, Hamburg, Germany), if protein quantification was required this sample was centrifuged at maximum speed (approx 13,000g) in a refrigerated centrifuge for 30 seconds to clear the lysate and allow isolation of the protein containing supernatant. If protein quantification was not required then no centrifugation was performed. In this condition the luciferases are stable for at least 6 hours at room temp, up to 16 hrs on ice and can be stored at -20°C short term or -70°C long term.

From this point forward the stop and glow kit protocol (Promega) was followed: briefly 20μl of each cell lysate sample was transferred to the wells of a 96 well cellstar plate (Greiner-bioone ltd, Gloucestershire, UK), 100μl of Luciferase Assay Reagent II (LAR II) added, mixed and read on a luminometer (Fluoroskan Spectrometer / Luminometer (Labsystems, Cambs, UK)) with a 2 second pre-read delay followed by a 10-second measurement period (extended to minute long measurement periods in some studies, but with no effect). 100μl of Stop and Glow reagent was then administered, the plate shaken briefly and read, again with a 2 second pre-read delay followed by a 10-second measurement period (also extended to minute long measurement periods in some studies but with no effect).

As a control for cellular luminescent noise non-transfected controls were also lysed and read 3-4 times following both the LAR II and stop and glow additions. Recent studies using a single purpose luminometer would suggest that the dual luminometer / fluorometer used here, does not have the required sensitivity for this assay. Future protocol optimisation with single purpose hardware may improve detection with this assay.

2.5 ANIMAL TECHNIQUES

All mice used in this thesis were female Balb-c mice (B&K Universal, Hull, UK), maintained in the MFAA animal facility at The University of Edinburgh Medical School. All animal work was carried out with Home Office and local ethical committee approval.

Avertin (Tribromoethanol anaesthetic) was used from a pre-prepared frozen stock of ; 2.5g 2,2,2-tribromoethanol (Sigma-Aldrich), 5ml 2 methyl-2-butanol tertiary amyl alcohol; (Sigma-Aldrich); made up to 200ml with dH_2O. FITC solutions were prepared by suspending FITC powder (Sigma-Aldrich) at 3mg/ml in sterile PBS with vigorous shaking.

2.5.1 INTRATRACHEAL ADMINISTRATION

Following a two week acclimatisation period, mice were anaesthetised with 0.3ml of Avertin given intraperitoneally. Each mouse was placed in a support where the upper incisors were placed across a steel wire support, maintaining the head at a 45° angle to horizontal, facing the researcher. A weighted string was then looped around the bottom teeth to hold the mouth open, the tongue pulled forward using curved forceps and the trachea visualised using a cold fibre-optic light. A pipette was then used to dispense 50μl of a 3mg/ml FITC solution (in PBS) or sterile PBS alone into the end of a blunted 25-gauge needle, to which a 1ml syringe was then attached. The needle was then inserted into the trachea of the mouse, and the syringe carefully depressed, delivering the liquid into the lung. The mouse was then removed from the support and laid on its side. Mice were monitored on a regular basis during their recovery from the anaesthetic, where complete recovery generally occurred within a couple of hours. Of the 120 mice used in this thesis only 4 failed to survive to their appropriate time points, 3 of unknown cause, 1 from suspected tracheal trauma.

2.5.2 LUNG EXTRACTION

The specifics of the lung extraction protocol differed according to the end application of the tissue. The method used for the preparation of mouse lung tissue for immunohistochemical analysis is described here. Derivations from this protocol for specific applications are described subsequently.

Mice were dispatched using a lethal intraperitoneal injection of 0.5ml pentabarbitone (Sagatal) (Merial Animal Health, UK). The peritoneal cavity and neck were then exposed and a set of watchman scissors used to expose, stretch and lift the trachea, which was then transected laterally using a fresh scalpel. A blue needle covered in a 1 inch stretch of flexible tubing was then inserted into the trachea for approx 2cm, and tied off mid cartilage ring via fine suture.

0.5ml of saline was then inserted into the lungs and withdrawn for cytokines, followed by a 0.8ml volume which was also inserted and removed for cellular

material, pooled with the centrifugated component of the initial wash. The right ventricle of the heart was then cut and a fine bore tube from a tapped tank of PBS inserted under approximately 0.25 metres of header pressure. The swollen atrium was then cut and clearing of the lungs facilitated by expanding them with air via the tracheal intubation. The lungs were then excised and expanded with formalin via the tracheal tube.

2.5.3 EPITHELIAL CELL ISOLATION PROTOCOL

This protocol has been used by others in the laboratory where studies have shown that the majority of epithelial cells isolated are Clara Cells. The recipes for the solutions used in this protocol are listed below.

Lungs were extracted as described previously (Section 2.5.2), but were expanded with 0.8ml trypsin (Sigma-Aldrich) which is rapidly withdrawn. The heart and lymph nodes were left attached to avoid the possibility of piercing the lung during their removal. The lungs were then suspended in contact with 37^{0}C 0.15M NaCl (Sigma-Aldrich) and reloaded with a syringe of trypsin solution under natural gravitational pressure alone and left for 15 minutes, topping up trypsin if required. The lung was then transferred to a Petri dish, where connective tissues, heart and lymph nodes were removed and the remaining lung parenchyma chopped into 1-2mm cubes using curved scissors in 1ml FCS. The material was then transferred via wide bore transfer pipette to a tube and supplemented with dissociation solution, approx 4ml/lung and gently swirled for 4 minutes. This solution was then pushed through 30μm gauze covered syringes and a final volume of 4mls centrifuged at 32xg for 6 minutes at 10^{o}C, this was then removed and re-suspended in dissociation solution and re-centrifuged. The pellet was then re-suspended in 3ml of attachment medium and placed in a small Petri dish at 37^{o}C 5% CO_2 for 1.5hrs, where cytospin morphology would indicate that this extract is rich in alveolar macrophage, fibroblasts and epithelial cells.

Following this attachment step, contaminating alveolar macrophage and fibroblasts remained attached to the Petri dish and epithelial Clara cells could be isolated as clumped balls of cells by gently rocking the dish. Epithelial cells

were then counted (approximately) and transferred, via centrifugation to further culture in a culture medium at $1x10^5$ cells per ml, 100μl per well in a 96 well plate.

The solutions used in this protocol were prepared as follows:

DISSOCIATION SOLUTION

12.5mg DNase (Roche Diagnostics, Mannheim, Germany) (protects cell's) in 50mls of PBS without calcium or magnesium, containing 500μg gentamycin (Sigma-Aldrich) (inhibits 50s ribosomal unit of bacteria and mycoplasma) and 800μg tylosine (Sigma-Aldrich) (acts against mycoplasma and Gram +ve bacteria), filter sterilised, kept at RT and used fresh for each experiment.

TRYPSIN SOLUTION

65mg crystalline trypsin (type I) (Sigma-Aldrich) (endopeptidase) into 26mls PBS with calcium and magnesium. Time was allowed for the reaction to proceed prior to filter sterilisation, used fresh at 37°C.

ATTACHMENT MEDIUM

RPMI-1640, 2mM L-glutamine, 100U/ml penicillin/streptomycin, 60μg/ml gentamycin.

CULTURE MEDIUM

RPMI-1640, 2mM L-glutamine, 100U/ml penicillin/streptomycin, 60μg/ml gentamycin and 2% Ultraser G (Ciphergen biosystems/Biosepra, Cal, US).

2.5.4 FIBROBLAST ISOLATION

As above, but the larger material retained from the gauze step was used for cell isolation. Pieces were laid in approximately 7mls of medium in small ($25cm^3$ growth area) filter top flasks pre-coated overnight at 4°C with type 1 collagen (Sigma-Aldrich) at $5\mu g/cm^2$. A range of media were trialled including primary rat fibroblast medium (Cell Applications, CA, US) and DMEM with and without FCS and/or collagen coating [see Chapter 4 for the most advantageous conditions].

Media were replaced 3 times in two hours after plating, then twice in the subsequent 24hrs, then once every 48hrs. Of note not more than five fragments could be placed in any one flask, as this resulted in significant necrotic death. Outgrowing fibroblasts were trypsinated after 10-12 days.

2.5.5 T-LYMPHOCYTE DEPLETIONS

All depletions were performed by Steve Roberts et al prior to the initiation of the work detailed in this thesis, only the block processing and immunohistochemical staining procedures were conducted through the work here, but for reference depletions were conducted as follows:

24hrs prior to FITC instillation according to the model one method (one surgical instillation of 2mg/ml FITC in a 50μl volume of PBS, under halothane anaesthesia), mice were given 40μg of the relative depleting antibody (listed below), resulting in a greater than 50% depletion by 7 days as ascertained by flow cytometry of both spleen and lymph node. The antibodies shown below were grown from ECACC cell line stocks.

Cell Line Name	Isotype	Reactivity	Principal Cell Type
YTS154.7.7.10	IgG2b	Anti-Thy-1, Mouse	T-lymphocytes
YTS169.4.2.1	IgG2b	Anti-Lyt-2, Mouse	CD8 T-Lymphocytes
YTS191.1.1.2	IgG2b	Anti-L3T4, Mouse	CD4 T-Lymphocytes
85060405	IgG2b	Anti-Phytochrome	Control Antibody

2.5.6 ALVEOLAR MACROPHAGE

BALf and AM were extracted in the manner described in Section 2.5.2. However, in order to maximise AM recovery, where *in vitro* studies were required in addition to cytospins, 5 separate washes of 0.8ml of saline previously warmed to 37°C were used, where lungs were gently massaged with blunt forceps. Isolates were pooled and kept on ice at all times to reduce cellular activity and macrophage loss through adherence to the bijou. Saline and saline + 0.2% BSA (Sigma-Aldrich) were used, but found not to affect AM recovery. AM extracts were centrifuged at 300xg for 10minutes at 4°C and the

resulting pellet re-suspended in F10 medium containing 20% FCS with cells at $7.5x10^4$ cells per ml, 150μl per well of a 96 well plate. Cell densities and media FCS content were identified here by individual titre, where they were shown to yield the greatest survival possible with a cell number high enough to yield cytokine data in supernatants but low enough to facilitate the greatest number of replicates per mouse.

Plated AM were left for 1-2 hours then media removed including contaminating red blood cells, and replaced with medium containing 10% FCS. LPS (Sigma-Aldrich) from *E. coli* 055:B5 used in activation studies was vigorously vortexed prior to use and prepared in media immediately prior to addition or 10 minutes before, when using Polymyxin (Sigma-Aldrich) treated medium. Polymyxin was prepared as a 50mg/ml stock as per manufacturers instructions, and used by adding 1μl to 5mls media or 1μl to LPS or Shh prior to its dilution to 5mls, yielding a final concentration of 10μg/ml, which has been shown by others to give a 60-70% inhibition of LPS reactivity[163].

2.6 COLLAGEN ASSAY

Based upon information derived from personal communication with the producers of the Biocolour™ collagen estimation kit (Biocolor Ltd, Newtownabbey NI) and a number of references, the following protocol was devised and optimised.

Lungs were removed as described previously, but the BALf was collected in, and lungs transported with, PBS containing a proteinase inhibitor cocktail (Roche). Lung tissue was cut into small pieces in a Petri dish and excess liquid pressed out and material weighed in a bijou. Material was then transferred to (1ml per 100mg) 0.5M glacial acetic acid (Sigma-Aldrich) containing (1ml in 100ml) peptidase inhibitor (Sigma-Aldrich).This material was then briefly vortexed, then left rotating at 4°C for 24hrs. Material was then centrifuged at maximum speed (approx 800g) in a refrigerated centrifuge for 5 minutes, and 150μl of supernatant transferred to Eppendorf tubes. To this supernatant

aliquot, 1ml of dye reagent was added. This was inverted twice, then tubes loaded into 50ml tubes and placed on a roller at room temperature for 35 minutes. Samples were then removed from the 50ml tube and centrifuged at maximum speed (approx 10,000g) for 12 minutes in an ultrafuge. These were then inverted on paper towel to remove supernatant and excess liquid from inside the tube using cotton buds. To these tubes 1ml of Alkaline reagent was then added, the tube capped and vortexed repeatedly. This was left to stand for 5 minutes prior to reading in a spectrometer or plate reader at 540nm, then calibrated to a linear collagen standard curve.

24hr lysates were also assessed for total protein content using the BCA protein assay as per manufacturers instructions, and collagen results given as a value of total protein.

2.7 ELISAS & CYTOMETRIC BEAD ARRAYS

2.7.1 SHH ELISA

In this novel ELISA, further discussed in Chapter 3, Shh levels in plate bound cell supernatants and BALf were quantified through the use of two antibodies, the 5E1 antibody mentioned previously and a biotinylated goat anti-mouse IgG antibody (R&D). The latter had been preabsorbed with human IgG and rat serum.

In this assay samples were bound to high binding Enzyme ImmunoAssay (EIA) plates (Corning-Costar) with a 1:1 dilution in carbonate-bicarbonate buffer (Sigma-Aldrich). These were measured against an 8 point standard curve of r-Shh (R&D Labsystems), which was made in one part culture medium, one part carbonate-bicarbonate (Sigma-Aldrich), with a top standard of 200ng/ml. All standards and samples were loaded in 50μl volumes per well and incubated overnight at 4°C.

Unless stipulated, all subsequent steps are separated by wash steps (full well volumes x5) using 0.005% Tween 20 (Sigma-Aldrich) in PBS (Oxoid, Hamps,

UK), where the final wash step was banged out on a flat surface covered in absorbent towelling. Recipes for diluting fluid and block buffer are given below:

BUFFERS

Diluting Fluid:(0.1%BSA, 0.05%Tween-20 (Sigma-Aldrich) (pH7.2-7.4 & 0.2μm filtered (Corning-Costar)

Block Buffer: (1%BSA (Sigma-Aldrich), 5% Sucrose (Sigma-Aldrich), 0.05% Azide (Sigma-Aldrich))

Plates were washed, then blocked for 2 hours at room temperature with 300μl per well of block buffer. Plates were then washed again and 5E1 added at 640ng/ml in diluting fluid, also 50μl per well and incubated at room temperature for 2hrs. Plates were then washed, and a 50μl volume of biotinylated goat anti-mouse IgG antibody added to each well, at 250ng/ml in diluting fluid. This was also incubated for 2hrs at room temperature. The biotinylation signal was developed and visualised using a streptavidin/substrate system whereby, following a wash step, 50μl of streptavidin (R&D) (diluted 1 in 200 in diluting fluid) was delivered to each well for 20 minutes at room temperature, followed by washing and 50μl of 3,3,5 tetramethylbenzidine (TMB) (Sigma-Aldrich) or substrate A&B (R&D) for 25 minutes or appropriate timing at room temperature. This process was stopped (without a wash step), with the addition of 25μl of 2N H_2SO_4 (Sigma-Aldrich).

All ELISA data were recorded on Dynex or Anthos 2001 plate readers (Dynex technologies, Sussex, UK / Anthos Labtech Instruments, Wals, Austria), using Revelation / Stingray software respectively at a wavelength of 450nm, with a subtracted reference at 560nm or 650nm.

2.7.2 SERUM ELISAS

ELISAs for FITC specific serum antibodies were developed from a template of concentrations used in a DerP1 specific ELISA. All volumes are 50μl with the

exception of blocking (300μl) and stop solution (25μl). Wash steps were performed between steps, as for the Shh ELISA with PBS/0.05%Tween20.

BUFFERS

Diluting Fluids: 1%BSA in PBS for IgG ELISAs, PBS-Tween for IgE ELISAs. Streptavidin dilutions were always performed in PBS, plate coating always performed in 0.05M carbonate buffer (Sigma-Aldrich).

Blocking Buffers: 3% BSA in PBS for IgG ELISAs, 5% BSA in carbonate buffer for IgE ELISAs.

IgG_1 SPECIFIC

High binding EIA plates were bound overnight at 4°C with 125ng/ml FITC/BSA(Sigma-Aldrich), 50μl per well. This was washed and blocked for 1hr at 37°C. Blocking buffer was washed off and 50μl samples volumes added per well from 1:3 serial dilutions of samples performed in a separate non-binding flexi plate. Samples were incubated for 1hr at 37°C. Plates were then washed and a 1 in 8000 dilution of biotinylated rat anti-mouse IgG1(Serotec-MCA336B) administered for 1hr at room temperature. Following a wash step the ELISA was developed and visualised using a 1hr room temperature 1 in 200 streptavidin addition, and a 25 minute room temperature TMB incubation, stopped with $2NH_2SO_4$ for 450/560nm quantification.

IgG_2 SPECIFIC

High binding EIA plates were bound at 4°C overnight with 125ng/ml FITC/BSA (Sigma-Aldrich). These were washed and blocked for 2hr at 37°C. Block was then thrown without a wash step and 1:3 serial dilutions of samples administered as described above. Samples were incubated for 1hr at 37°C. Washing was followed by addition of a 1 in 1000 dilution of biotinylated rat anti-mouse IgG2a (PharMingen, San Diego, CA) administered for 1hr at 37°C. This ELISA was then developed and visualised as for the IgG1 ELISA.

TOTAL IGE

High binding EIA plates were bound at 4°C overnight with 2μg/ml mouse anti-IgE [clone 35-74] (PharMingen). This was thrown out and blocking buffer administered for a 2hr incubation at 37°C without an intervening wash step.

Plates were then washed and serially diluted samples administered as described for IgG ELISAs. These were quantified against an 8 point standard curve of purified mouse IgE [Clone 27-74] (PharMingen) with a top standard of 500ng/ml. Samples and standards were incubated for 1hr at 37°C, prior to washing and administration of 2μg/ml biotinylated mouse anti-IgE [clone R35-118] (PharMingen) detection for 1hr at 37°C. This ELISA was developed and visualised using a 1hr Room temperature incubation of a 1 in 200 dilution of Streptavidin, a wash step, followed by a 5 minute room temperature TMB step, stopped with $2NH_2SO_4$ for 450/560nm quantification.

FITC SPECIFIC IgE

Samples were IgG depleted using fast flow protein G (Amersham) once for 30 minutes at room temperature and for a second time overnight at 4°C to ensure complete depletion. Beads were used at the maximum concentration possible where an 85μl pellet of beads was resuspended to 100μl. This was added 1:1 to a 1:4 dilution of sample. Beads were recycled using 5-10 centrifuged washes in 0.1M glycine buffer (pH2.5-3) followed by 5-10 centrifuged washes in 20mM sodium phosphate as per manufacturer's instructions.

High binding EIA plates were bound at 4°C overnight with 125ng/ml FITC/BSA (Sigma-Aldrich), with a control plate coated with 4μg/ml Der P1. This solution was then thrown and block administered and incubated for 2hr at 37°C, without the intervening wash step. Serially diluted samples were then administered as discussed previously, and incubated overnight at 4°C. Control samples included a depleted DerP1 exposed allergic mouse sera as a positive control.

Following a wash step, 50μl per well of 4μg/ml biotinylated mouse anti-IgE [clone R35-118] (PharMingen) was administered and incubated for 1hr at 37°C. This was developed and visualised using a 1hr room temperature incubation of

a 1 in 200 dilution of streptavidin, and TMB stopped with $2NH_2SO_4$ at a suitable time interval for 450/560nm quantification. In the case of samples analysed here, DerP1 controls came up rapidly within minutes whilst preservation of FITC IgE plate up to 1hr post addition of substrate did not result in any detectable signal.

2.7.3 DUOSET KITS

Duoset ELISAs for GM-CSF, TNF-α and TGF-β (R&D) were performed as per manufacturers instructions, but with all volumes halved from 100μl to 50μl except, block buffer. Samples were added as 1:1 dilutions. Both total and active TGF-β were analysed with the specified ELISA.

2.7.4 CYTOMETRIC BEAD ARRAYS

Two kits were used in the work contained in this thesis, namely the mouse and the human inflammation kits (BD Biosciences/PharMingen). The human kit contained antibodies to IL-8, IL-1β, IL-6, IL-10, TNF-α & IL-12p70. The mouse kit contained antibodies for TNF-α, IL-12p70, IFN-γ, MCP-1, IL-10, IL-6. Kits were prepared as per manufacturers instructions and run on a Becton Dickinson FACS Caliber flow cytometer, with the exception that all volumes were halved and bead to mastermix calculations performed as a division of total volume by total number of beads rather than suggested set volume of each bead. This reduced excess bead wastage maximizing the number of samples run per kit.

2.8 IMMUNOHISTOCHEMISTRY

Mouse lungs were fixed in buffered neutral formalin for 48hrs prior to processing and embedding in paraffin wax. Blocks were stored at lab temperature out of direct light. Sections for immunohistochemistry were cut at 3μm thickness on a microtome and floated at 42°C prior to mounting on superfrost slides (BDH, Poole, UK). Slides were incubated overnight at 37°C, then stored at room temperature away from direct light.

Protocols varied with antibody utilised. The common core protocol is described below and variations from this are described under specific antibody headings.

Formalin fixed paraffin embedded sections were prepared for immunohistochemistry by dewaxing in xylene (Genta Medical, York, UK), where slides were submerged for 2x5minutes, followed by 1 minute submersions in 100%, 70% & 50% methylated spirit (Genta Medical) for serial rehydration to water. From here slides underwent antigen retrieval with antigen unmasking solution (Vector, CA, USA) where 5mls is added to 500mls of water in a plastic container, slides are then submerged and microwaved on full power for 3x5 minutes. Slides were then cooled for 20 minutes in flowing tap water. This was then followed by a peroxidase blocking step, where slides were incubated in a 2% H_2O_2 solution (Sigma-Aldrich) for 15 minutes, then washed in PBS for 2 minutes.

Slides were then loaded into sequenza coverplate clips (Thermo Shandon, Cheshire, UK), which allow use of small 125µl volumes to cover sections through utilisation of capillary action across the surface of the slide. Reagent deliveries to these clips were separated by two to three full PBS washes.

Once the sequenza was loaded, slides were biotin and avertin blocked using a Vector kit. Three drops of each (approx 125µl) were applied for 15 minute room temperature incubations, separated by PBS wash steps. This was then followed by the specific primary and secondary antibodies, where secondaries where biotinylated. Bound secondary was visualised with RTU Vectorstain (Vector) for 30 minutes at room temperature, followed by use of the diaminobenzidine (DAB) chromogen development systems (Dako Cytomation, CA, USA), where 1 drop of concentrate was added per ml of supplied buffer and administered to sequenza for 5 minutes at room temperature. Slides were then counter stained in haematoxylin (Shandon/Thermo) for 5 seconds (to stain the nucleus) and rinsed in tap water for 5 minutes. This was followed by submergence in Scot's tap water (Sodium bicarbonate 17.5g, magnesium sulphate 100g (Sigma-Aldrich), five litres of water) for 1 minute. Slides were then rinsed in tap water

and dehydrated through three alcohols and three xylenes, 1 minute each, prior to cover slip addition with DPX mountant.

Cell culture immunohistochemistry was performed in NUNC culture cover slides (Nalge Europe Ltd, Hereford, UK), or on superfrost slide cytospins fixed in 90% dry acetone, 10% methanol (Fisher Chemicals, Leistershire, UK). Cytospins were loaded directly into sequenzas. Coverslide cultures were not amenable to sequenza, so immunohistochemical analysis was performed in wells using various volumes per well, most frequently 250μl.

2.8.1 SHH & PTC

Goat polyclonal anti Shh (N-19) & Ptc (C-20) antibodies were supplied by Santa Cruz (Delaware, CA, USA) (Stock 200μg/ml). N19 was raised against an N-terminal Shh peptide of human origin which was identical to the corresponding region of the mouse sequence. The antibody has been shown to detect mouse, rat and human Shh protein. C-20 was raised against a carboxy terminal Ptc peptide of human origin which differed from the corresponding mouse sequence by one amino acid. This antibody has been shown to detect mouse, rat and human Ptc protein. Positive binding was detected through the use of a biotinyated rabbit anti-goat secondary (Dako Cytomation) raised against goat serum antibodies (primarily IgG) and preabsorbed with human serum. Relevant cross reactants as determined by ELISA (Dako technical, personal communication) include: human immunoglobulins <1%, FCS <2%, mouse and rat immunoglobulins 25%.

Slides had non specific antibody binding blocked with protein block (Dako Cytomation Glostrup, Denmark) for 10 minutes. Primary antibodies were added in a 1 in 30 dilution in Antibody Diluent (DAKO Cytomation) (with the exception of blocking studies and Nunc coverslide applications(see Chapter 3)). These were incubated in sequenza overnight at 4°C. Following a 30 minute period of room temperature acclimatisation, slides underwent a 30 minute incubation with a biotinyated rabbit anti-goat secondary at a 1:400 dilution in Dako Diluent. Specificity was checked via pre-incubation studies with commercial blocking

peptides consisting of the relevant peptide immunogen as described above (100μg/ml) (Appendix Figure 7.2).

2.8.2 FITC

Rabbit Polyclonal anti-FITC antibody (Dako Cytomation) was stored at -70°C in a 1:1 dilution in normal goat serum, this was utilised at a final dilution of 1 in 250 in Dako diluent. Antibody incubation was limited to 30 minutes at room temperature followed by administration of a biotinylated goat anti rabbit secondary (Dako Cytomation) diluted 1:300 in Dako Diluent for 30 minutes at RT. Specificity is illustrated by negativity on PBS instilled and normal lungs and positive binding on FITC instilled lungs.

2.8.3 CC10

The antibody used in CC10 IHC is derived from a rabbit immunised against urine protein 1 from pooled urine (tubular proteinuria). This protein has significant homology with rabbit uteroglobin and with human Clara cell protein. Slides had non specific antibody binding blocked with protein block for 10 minutes. Rabbit polyclonal anti-CC10 antibody (Dako Cytomation) was used at 1:300 in Dako diluent for 2hrs at RT. This was followed by a RT 30 minute detection step with biotinylated goat anti-rabbit secondary detection (Dako Cytomation) diluted 1:300 in Dako Diluent.

2.8.4 GLI

Gli1 staining was performed on human lung sections using an IgG polyclonal rabbit anti-Gli1 preparation from Abcam. This antibody was raised against synthetic peptide corresponding to the carboxy-terminal region of mouse Gli1. This antibody has shown to be reactive with both human and mouse protein and activation of the protein is marked through a transition from cytoplasmic to nuclear staining. Positive binding was detected with a biotinylated goat anti rabbit antibody (Dako) derived from goats immunised with rabbit serum immunoglobulins. The antibody reacts with all known classes of rabbit immunoglobulin. Human cross reaction is minimal. Specificity has been illustrated with mouse tissues through the staining of Gli1 knockout tissues, and

positivity in mouse and human through staining of glioma, a pathology associated with upregulated Gli1 expression.

Slides had non specific antibody binding blocked with protein block for 10 minutes. The Gli antibody was added in a 1 in 400 dilution in Antibody Diluent These were incubated in sequenza overnight at 4°C. Following a 30 minute period of room temperature acclimatisation, slides underwent a 30 minute incubation with a biotinyated goat anti-rabbit secondary at a 1 in 300 dilution in Dako Diluent.

2.8.5 SPECIALIST STAINS

Standard Haemotoxylin and Eosin (H&E) staining for nucleus and cytoplasm visualisation was performed by dehydrating sections as described previously, followed by submergence for 1 minute in haemotoxylin (Shandon/Thermo). This was followed by 5 minutes in running tap water then 1 minute in Scot's tap water, followed by another 5 minute tap water step. Slides were then submerged in acidified Eosin (Solmedia, Romford, UK) for 30 seconds, followed by rapid dehydration through an alcohol series to xylene and DPX mountant. This staining regime results in sections where individual cells have their nucleus stained dark purple and the cytoplasm pale pink and is commonly used to differentiate cell types by nuclear shape and overall morphology .

The Picrosirius stain also utilised in this thesis illustrates areas of collagen deposition in pink. For the purposes of work in this thesis this stain was also combined with fast green which stains cellular cytoplasm green, but is hence forth refered to inclusively as picrosirius stain.

The silver trichrome staining method also employed in this thesis stains nuclei red and connective tissue green. The advantage of the trichrome method is that it is qualitatively more sensitive to low level increases in connective tissue deposition, however cytoplasmic and connective tissue staining can become easily confused in areas of collapsed lung architecture. In these situations the distinct and bright pink staining of collagen in the Picrosirius stain allows immediate recognition of areas of fibrosis and the intensity of staining can be

proportional to the extent of fibrosis such that, in some solid tissue systems, this stain has been used with computerised microscope systems to quantify levels of fibrosis.

Trichrome and Picrosirius stains were performed in the Pathology Dept, R&D lab, Royal Infirmary of Edinburgh. Others such as Giemsa and Methyl green are discussed in Section 2.12.4.

2.9 SCORING TECHNIQUES

2.9.1 ASHCROFT

Based on the scoring system devised by Ashcroft et al in 1988[164], this system apportions numerical scores to randomly selected microscope fields. Ashcroft et al proposed the following scale of damage to apply to over 50% of the tissue within a field **excluding** main airways, blood vessels and inflammatory exudate in air spaces. The original study examined human disease biopsies at x10 magnification. To adjust for the difference in size between human and murine acini we use x40 magnification. This method has been used by several other groups to assess murine lung fibrosis[165, 166].

To allow for differences between FITC+ve and FITC-ve areas of the lung sections stained with anti-FITC antibody were used for scoring. A field was considered FITC+ve if over half the tissue within the field stained and negative if less than half the field stained.

As proposed by Ashcroft et al the damage was assessed by assigning fields to an odd number on their scale and only using even numbers if it was difficult to decide between two odd numbers (Table 2.1).

Grade of fibrosis	Histological features
0	normal lung
1	minimal fibrous thickening of alveolar or bronchiolar walls
2	
3	moderate thickening of walls without obvious damage to lung architecture
4	
5	increased fibrosis with definite damage to lung structures and formation of fibrous bands or small fibrous masses
6	
7	Severe distortion of structure and large fibrous areas: honeycomb lung is placed in this category
8	Total fibrous obliteration of field

Table 2.1: Ashcroft Scoring Criteria

36 FITC+ve and 36 FITC-ve fields were assessed as this was in the middle of the range of field numbers proposed by Ashcroft et al and also covered nearly the entirety of the biopsy when proceeeding from one outside edge in non-overlapping rows across the section. Some areas where there was poor or over inflation [usually at lobe margins] were ignored. The sections were assessed on a multi-header microscope and a consensus number was reached between two observers for each field. The median score for fibrosis was determined for both FITC+ve and FITC-ve areas and the group mean established. An example of each score category is given in Figure 2.3.

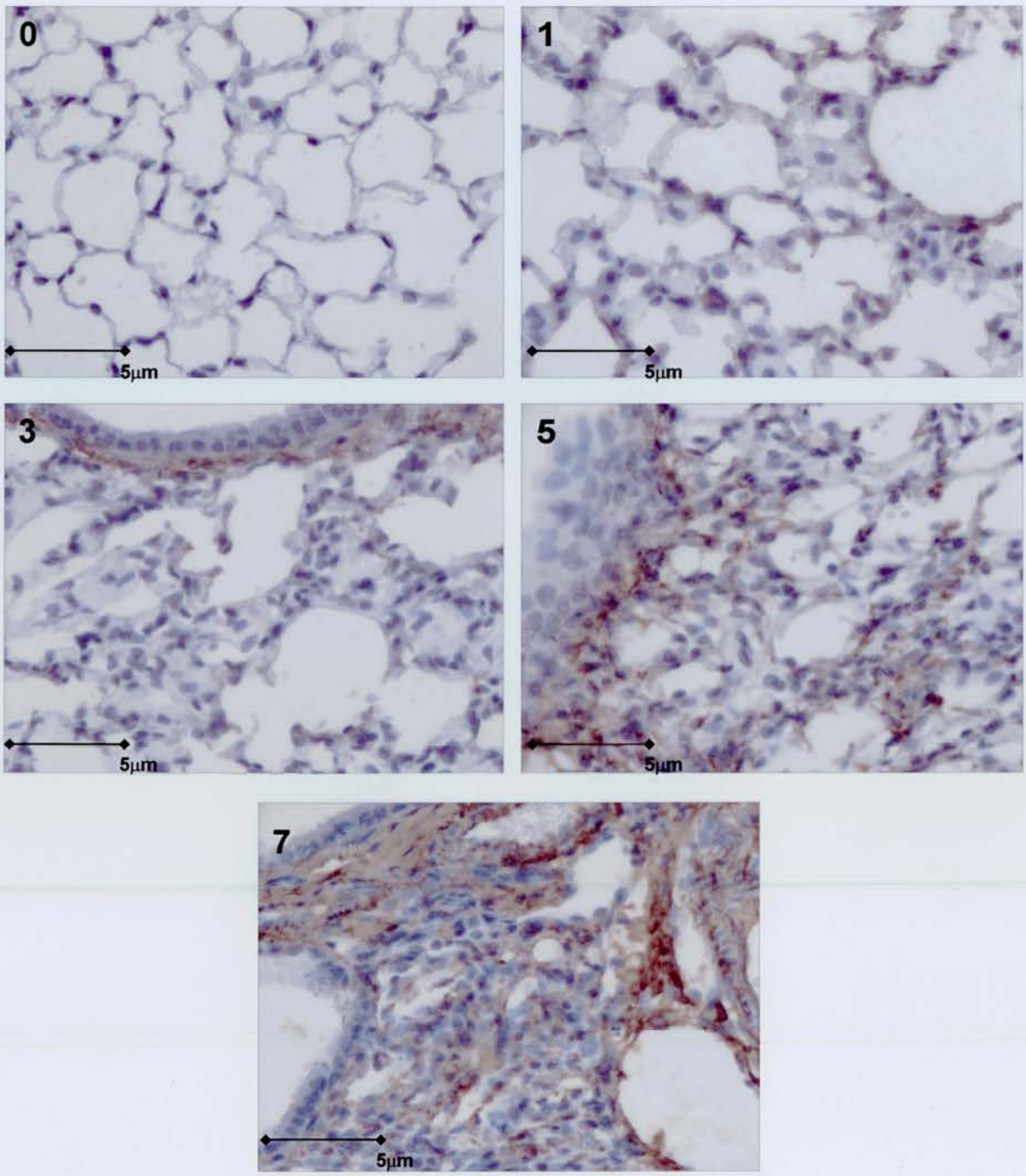

Figure 2.3: Ashcroft Scoring Illustrations
The score for each representative field is displayed in the corner of each photograph.

2.9.2 INFLAMMATORY INFILTRATE

Scoring peripheral lung inflammation was done on an H&E section at x200 magnification scoring 10 consecutive fields where the lungs were correctly inflated and where the field contained a complete transection of at least one bronchiole less than half a field width in diameter and blood vessel as well as an alveolar airway. The lungs were all perfused and lavaged before fixation thus no comment can be made on the infiltrate in alveolar airspaces. Inflammation was scored in:

- The perivascular compartment as:
  - 1= no infiltration, 2= <20, 3= <100 and 4= >100 cells around blood vessel walls
- The bronchiolar epithelium as:
  - 1= no infiltration, 2= <5, 3= <10 and 4= >10 cells in the bronchiolar epithelium
- The peri-bronchiolar alveolar tissue* as:
  - 1 = no infiltration, 2= <20, 3= <100 and 4= >100 cells in the peri-bronchiolar alveolar tissue
- The alveolar walls as:
  - 1= no infiltration, 2= focal cellular expansion of the alveolar walls by 2-3 cells, 3= by 4-5 cells, 4= >5 cells

* Peri-bronchiolar alveolar tissue was defined as sub-bronchiolar tissue, beneath basement membrane and smooth muscle, not immediately adjacent to a blood vessel, i.e. cells have moved away from the perivascular compartment presumably along a chemoattractant gradient.

The worst score in each compartment per field was used to set the score for that field. For each field a combined score was given which equalled the sum of all the scores on the field, this was averaged for the 10 fields per section.

2.10 PROTEIN EXTRACTIONS

Protein extraction methods were varied according to tissue type and final use of the extract. i.e. a variety of extraction buffers were used for cell line lysates for westerns, but only a few of these proved to be compatible with the BCA protein assay kit.

For cell line and brain protein extractions (embryonic and adult) the following Sigma-Aldrich components were prepared on ice:

Tris HCL pH 7.5 1M	5ml
Sucrose (Final Conc 0.32M)	10.9g
EDTA 0.5M pH 8 (Final Conc 1mM)	0.2ml
10x Proteinase inhibitor cocktail	1ml
PMSF	10μl

with water to 100mls

Cellular material in this lysis buffer (approx 10^6 cells in 200μl) was sonicated on ice for 1 minute in 5 second bursts. Brain tissue was first homogenised in a 1ml glass homogeniser (Uniform, Jensons, UK) on ice with an average of 50 strokes per 1ml

For protein extraction from lungs inflated with OCT™ (Sakura Finetek Europe, Zoeterwoude, Netherlands) and snap frozen in liquid nitrogen (See Section 2.12.2), the following was used:

0.1% Triton-X (Sigma-Aldrich)	10μl
0.1mM Sodium Orthovanadate (Na_2VO_4) (Sigma-Aldrich)	5μl
Proteinase Tablet (Roche Diagnostics)	x1

with water to 10mls

2.11 RNA EXTRACTIONS

With the exception of trials of using trizol (Invitrogen) extraction (as per manufactures instructions) RNA isolations were performed using Qiagen kits (Qiagen Ltd, Sussex, UK), both mini (for cell line and tissue extractions) and micro (for laser microdissection) as per manufacturers instructions. Qiagen's Qishredders were also used throughout for mini kit isolations, although recent studies would suggest that they are an unnecessary step for cell culture isolates. Low concentration studies would also suggest that the Qiashredder columns reduce final RNA yield (data not shown).

Culture well lysates were prepared by adding RLT (including 2-βmercaptoethanol (Sigma-Aldrich)) to PBS washed cells, removing to an Eppendorf tube, and freezing at -70°C. Volumes used were dependent on cell number, but on average 110μl per 24 well plate well. This allowed for the pooling of three wells to approximately 330μl, thus when an equal volume of 70% alcohol is added the total volume does not exceed that of 700μl, the maximum loading volume of the Qiagen columns. All procedures used the option of on column DNA digestion. Minikit elution's were performed in 30μl-40μl, micro in 14μl.

Isolation of RNA from whole tissue was varied according to tissue type and condition. RNA extractions from adult and embryonic brain were performed in glass micro-homogenisers in RLT prior to extraction via Qiagen mini kits as per manufactures instructions. Larger fresh tissue such as lung was processed using Trizol, whilst formalin fixed material, for use as a control in laser microdissection was processed using RLT.

2.11.1 RLT TISSUE EXTRACTION

Formalin fixed human lung tissue was used in a preliminary attempt to develop a real time standard curve. RNA was extracted in two ways, freeze shattering and physical abrasive separation. Material was first processed as normal to

remove formalin, then removed prior to wax embedding and either frozen at -70°C or used immediately, see below.

FREEZING

Frozen formalin fixed materials were transferred to a metal strainer, and submerged in liquid nitrogen, these were then crushed with a compression gun (Biospec Products Inc, Bartlesville, OK, USA) (pre-cooled with isopropanol on dry ice) into small pieces, which were transferred to RLT for overnight incubation with proteinase K as for microdissected material (See Section 2.12.5).

PHYSICAL DISSOCIATION

Material transferred directly to a metal strainer following processing was chopped into small pieces and pushed through in 4mls of RLT with the end of a syringe. Material transferred to a cell culture sieve was pushed through, then material was frozen for storage or immediately incubated overnight with proteinase K as with microdissected material.

2.12 LASER CAPTURE/CATAPULT METHODS

The techniques used in the preparation, isolation, processing and analysis of section material have all been optimised and developed in this thesis. Protocols described here represent the most recent ones used, a more extensive discussion ascertaining to their development can be found in Chapter 5.

2.12.1 MATERIALS

WATER

RNase free water was generated by adding 1ml of Diethyl Pyrocarbonate (DepC) enzyme (Sigma-Aldrich) to 100mls of distilled water, and incubated overnight in a non-pressurised container, protected from light. This was then autoclaved to inactivate the enzyme and sterilise the water.

Scot's tap water was prepared using 250mls of RNase free water with 0.875g of Sodium bicarbonate and 5g of $MgSO_4$.

GLASSWARE

All glassware was baked in foil at 220°C for 40 minutes, whilst more perishable items were washed in RNase removing solutions (Ambion, Huntington, Cambs, UK & Sigma-Aldrich) and rinsed in nuclease free water.

DISSECTION SLIDE PREPARATION

Superfrost slides were used in Laser Capture Microdissection (LCM) studies and are supplied RNase free. Laser Pressure Catapult (LPC) studies used membrane coated microscope slides (PALM, Bernried, Germany) which were prepared as follows:

Slides were sprayed with a complete coverage of RNase zap (Ambion) and were transferred to a plastic sealed holder (5 per box). Two further sprays were then applied, and the box sealed and inverted several times. This was then washed out with RNase free water, several times. Slides were then dried for 30 minutes at 37°C in a sealed silica gel (BDH) container, then exposed to UV at (254nm) for 30 minutes. This kills any enzyme activity on the slide and makes the membrane adhesive, ready for section floating and mounting as described previously, but with RNase free water.

2.12.2 FROZEN LUNG SECTIONS

Lungs were removed as described previously, but final inflation was performed with an optimised ratio of 1:1 of OCT & Saline. These were then transferred to a foil cup and under maintained pressure / inflation, the cup was filled with OCT. This was then placed directly into liquid nitrogen.

Lungs were cut at 10μm on a cryostat (Bright, Huntingdon, UK) either onto -20°C superfrost slides for visualisation, or placed directly into Eppendorf tubes for RNA extraction. Frozen mounted sections, were air dried for 20 seconds prior to fixation in -20°C 70% ethanol for 5 minutes. These were then removed and air dried for up to 30 minutes. Slides were then taken to Dep-C treated

water for 30 seconds then fresh Dep-C treated water for a further 30 seconds to remove OCT prior to staining.

2.12.3 FORMALIN FIXED LUNG SECTIONS

Mouse lungs were fixed in buffered neutral formalin for 48hrs prior to processing and embedding in paraffin wax. Blocks were stored at lab temperature out of direct light. Formalin sections were cut at various thicknesses using a microtome sprayed with RNase away and rinsed with RNase free water. Blocks were cooled on RNase free ice prior to cutting.

SLIDE MOUNTING

Sections were floated on 42°C RNase free water for 1-2 minutes prior to slide mounting. For LCM studies, slides were mounted as standard and stored in a silica gel box at various temperatures (see Chapter 5) for 1Hr-overnight prior to dewaxing (see 2.12.4).

For LPC studies the section was mounted onto the membrane slide and incubated overnight at 37°C in a silica gel box, prior to dewaxing (see 2.12.4)

2.12.4 STAINING METHODS

Preparatory steps for staining differed according to type of dissection, material and stain. Frozen sections could be stained directly following OCT removal with water, whilst embedded material required dewax/rehydration.

LCM was conducted using sections mounted on normal superfrost slides, which were dewaxed for 2x5minutes in xylene then approximately 1 minute in each of the descending alcohols of 100%, 95% 75% and 50% then to water for 2 minutes, optional staining then dehydration through alcohols to a 10-15 minute xylene incubation.

LPC membrane slides were found to undergo significant degradation with prolonged xylene exposure, thus dewax steps were restricted through the course of the work presented here to 2x2minutes with agitation. Recent studies

(data not included in this thesis) have shown that Histoclear™ (National Diagnostics, Hull, UK) is an excellent alternative to xylene, dewaxing without lifting. Rehydrating alcohol steps were as above, but performed in Falcon tubes. These slides were not dehydrated previous to catapulting owing to the solubility of the Giemsa stain in alcohols.

METHYL GREEN (Dako)

Slides were submerged for 2-5 minutes, rinsed in nuclease free water then air dried at RT in an RNase free box with silica gel.

H&E (Sigma-Aldrich)

Slides were submerged for 3 minutes in Mayers haematoxylin (Sigma) followed by 3 minutes in RNase free Scot's tap water. Slides were transferred to eosin (pre-acidified with glacial acetic acid 250μl to 50mls) for 1 minute, then quickly run through increasing ethanols. Slides were then air dried at room temperature in an RNase free box with silica gel for LPC, or via submergence in a xylene series for LCM.

GIEMSA (BDH)

Slides were covered for 1-2 minutes and staining checked by washing slide in DepC water and looking under microscope. If over stained, slides were de-stained in alcohol. Water was then used to rinse slides, which were then air dried and transferred to a silica gel box

2.12.5 LASER MICRODISSECTION DIGESTION BUFFERS

A number of different buffers were used for the digestion of frozen and formalin sections and dissected material. The three main ones trialled are detailed below:

- PALM buffer (All Sigma-Aldrich)
    - 0.5M EDTA pH 8.0 20μl
    - 1M Tris pH 8.0 200μl
    - Igepal CA 50μl

— RLT buffer (Qiagen)

  - +/- βmercaptoethanol 10μl/ml as per manufacturers instructions

— Cells to cDNAII lysis buffer (Ambion)

The above recipes correspond to frozen digests, for formalin fixed samples PALM and RLT buffers were supplemented with 10μl of proteinase K and incubation times varied from 10 minutes to 5 days, see Chapter 5.

Digestions performed using the Ambion cells to cDNA II kit and paraffin block kits (Ambion) were done as per manufacturers instructions. A failure to produce viable RNA resulted in supplementation of lysis buffer (which already contains proteinase K (personal correspondence)) with 2-3 times more proteinase K. Incubation times were also varied from 10 minutes to 4hrs. These kits are effectively very similar in methodology, differing only in that the paraffin block kit contains xylene and alcohol reagents. These kits differ from conventional methods in that RNA is not purified and that the reverse transcription is performed on crude lysate (via Murine Moloney Leukaemia Virus enzyme). PCR is then conducted with 10xSuper Taq (Enzyme Technologies Ltd, Cambridge, UK) as per manufactures instructions. The kits are supplied with oligonucleotides and random decomers. The majority of studies used decomers as they gave the greatest electrophoresis band intensity from low concentration cell line control RNA samples.

2.12.6 PROCESSING OF PARAFFIN EMBEDDED BIOPSY MATERIAL

WHOLE SECTIONS

Cut section material was stored in 1.5ml Eppendorf tubes at room temperature in darkened conditions. Prolonged storage has been shown to have no effect on viability for up to six weeks of storage. Further storage duration has not been analysed.

Material was centrifuged for 2 minutes in an ultrafuge at maximum speed to pellet and 1 ml of fresh xylene added to each tube. Samples were inverted to

mix and left at room temperature for 10 minutes. This was then spun for 1 minute in an ultrafuge at maximum speed. The supernatant was then carefully pipetted off and 1ml of molecular grade 100% ethanol added (Sigma-Aldrich). This was inverted to mix, then spun in an ultrafuge for 1 minute on maximum speed. The supernatant was again pipetted off and this was repeated for 70% and 50% ethanol additions, completing with 1ml of DepC water, which was ultrafuged for 3 minutes on maximum speed. This supernatant was then carefully pipetted off and another 1ml added and centrifugation repeated prior to the addition of 150μl of RLT (containing 2-βmercaptoethanol, 295 μl DepC water and 10 μl proteinase K) to each tube. The Tube was then shaken to ensure complete submergence of material and incubated overnight in a shaking incubator at 55°C. Following this period the sample was either frozen at -70°C or applied to the Qiagen RNeasy Microkit as per manufacturers instructions. Notably, use of the Qiashredders here was found to reduce yield, thus these were excluded, where normal cell lysate and tissue extractions included them.

LASER DISSECTED MATERIAL

For laser capture, twice autoclaved RNase free 'safelock' 1.5ml Eppendorf tubes were prepared containing 150μl RLT+2 βmercaptoethanol, 295 μl DepC water and 5 μl proteinase K, into which the membrane cap (see Chapter 5) was pressed, and the tube forcefully inverted and placed upside down in a 55°C shaker overnight, processed as for whole sections with Qiagen RNeasy microkit.

For laser catapulting, 80μl of RLT (without 2-βmercaptoethanol) was placed in the lid of a standard RNase free 0.5ml Eppendorf tube. Once all material had been catapulted into this, 0.8μl of 2-βmercaptoethanol was added per lid, the lid closed and pulse centrifuged briefly in an ultrafuge at maximum speed. To this tube a solution of (70μl RLT+2-mercaptoethanol, 295 μl DepC water) and 10 μl of proteinase K was added, inverted forcibly with gentle vortexing, pulse centrifuged to force the material into the base of the Eppendorf tube and placed to incubate at 55°C overnight. The 450μl of RNA containing extract was then purified and isolated using the Qiagen RNeasy microkit.

2.13 REVERSE TRANSCRIPTION AND PCR

Initial studies into frozen microdissection utilized the specialist Promega access RT-PCR kit as per manufacturers instructions, as did β–Actin check PCR for genomic contamination. However conditions were found to be inflexible for new primers and random hexomers were required, (see Chapter 5). Thus real time RT-PCR reagents and gold Taq were utilized in the majority of studies.

2.13.1 REALTIME RT-STEP

RNA extractions were run through a standard *β-Actin* PCR to check for genomic contamination. In those reactions when low yield RNA sequences were investigated, RNA checks were also used with mastermixes used for cDNA PCR to allow for potential variation in stability of any contaminating DNA. e.g. checks were performed with *β-Actin*, but other genomic sequences might be more stable or other primers might be more effective. However, at no point was contamination identified in any of the low yield isolates from microcolumns, when on column digestion was performed, with either *β-Actin* or any of the other genes of interest used here.

RNA was quantified on a visible UV spectrophotometer, and diluted to 100ng/μl. This was then reverse transcribed using the real time reverse transcription reagents supplied by Applied Biosystems according to the manufacturers instructions. Hexomers were used as these pick up total RNA, necessary if 18s was to be utilised as a housekeeping gene. An example of a reaction mix is given in Table 2.2.

	REAL TIME RT (μL)
Taq Buffer	2
$MgCl_2$	4.4
dNTPs	4
Random Hexomers	1
RNase Inhibitors	0.4
Multiscribe	0.5
Nuclease Free Water	3.7
RNA	4

Table 2.2: Real Time Reverse Transcription Mastermix
The above was made up in 0.2ml tubes and run for: 25°C: 10mins; 48°C: 40mins; 95°C: 5mins, 4°C hold step. In those reactions where RNA concentrations were lower than 100ng/μl, or below detection, as in the case of some laser microdissection studies, volumes up to a maximum of 7.7μl were applied to the mix through substitution of water.

Real time RT mixes were then diluted to 100μl via the addition of 80μl of nuclease free water and stored as 15μl aliquots. This was then used in the subsequent reaction.

For laser micro-dissection, this dilution was not performed. To investigate the effect of excess reagent carryover resulting from this adaptation, on PCR function, preliminary experiments assessed PCR reactions using a known concentration of RNA diluted in concentrated reagent mastermix or normal mastermix. Bands were found to be brighter in undiluted mastermix reactions, suggesting that carryover of RT reagents increased PCR function. This was trialled on two primer sets.

2.13.2 REAL TIME PCR

	REAL TIME PCR (μL)
PCR MM	12.5
18s Primer Probe	1.25
Nuclease Free Water	1.75
*Primer Probe Stock	7
RNA	2.5
*Primer Probe Stock	
Nuclease Free Water	1620
Probe	300
Primers	90 of each

Table 2.3: Real Time PCR Mastermix
For those reactions where low yield cDNA was expected from the reverse transcription step, such as laser microdissection, volumes up to 4.25μl were loaded through substitution for water.

2.13.3 STANDARD PCR

Whist some primer sets could be used at a range of temperatures and mastermixes, such as the *β-Actin* sets, without any apparent affect on yield or stringency, others had very strict requirements. An example of an optimisation titration is displayed in Table 2.4.

Tube	RB	[1]dNTPs	[2]Mg	[3]Primers	cDNA	[4]BSA	H_20	[5]Taq
				Shh	+ve			
1	1.8	0.4	5	1	2	1	6.8	2
2			5	1	2	-	7.8	2
3			3	1	2	1	8.8	2
4			3	1	2	-	9.8	2
5		0.2	5	1	2	1	7	2
6			5	1	2	-	8	2
7			3	1	2	1	9	2
8			3	1	2	-	10	2
				β-Actin				
9		0.4	5	1	1	-	8.8	2
10		0.4	5	1	-	-	9.8	2

Table 2.4: Titration of Primer Conditions
Volumes given as μl, final total tube volume 20μl RB refers to reaction buffer. [1]dNTPs from a 10mmol mix prepared from 1/10 dilution of 100mM base stock. [2]$MgCl_2$ from a 25mM stock. [3]Primers taken from a mastermix of 20μl Fwd, and 20 μl Rev primers at 50pmol, plus 10 μl H_2O. [4]BSA at 0.2% in water. [5]Gold Taq Polymerase (5units/μl) was used at 0.25units of enzyme/reaction taken from a freshly prepared mastermix: e.g.: 20 samples, requires 20+2 for excess - equals 22 x 0.25 = 5.5 units of enzyme = 5.5/5 = 1.1 μl enzyme + 4.4 μl 10xReaction Buffer + 38.5 μl H_2O; as 2 μl per sample x 22 = 44μl).

0.2ml tubes from Table 2.4 were loaded into a graduated (horizontally graduated) PCR block set to a range of approximately 10-15°C across the average annealing temperature supplied by the primer manufacturer or primer design software. 6 copies of tubes 1-10 were prepared where 1-8 were loaded in every other column of the block and copies of 9-10 loaded between as positive controls.

Appropriate conditions were selected via narrowing of each range in subsequent trials. DNA positive controls for check gel PCR were tail tip DNA from routine genotyping undertaken in the lab. Positives for laser micro PCR were cell line cDNA. These were generated by removing media from 70-80%

confluent 75cm^2 growth area flask (medium flask), washed thrice with 10mls PBS, and RNA extracted in 4mls RLT, aliquoted in 100µl aliquots and frozen at -70°C. These were then incubated overnight with proteinase K along with microdissected material.

Agarose gels for electrophoresis were visualised using a visible UV transilluminator and Grabbit software (version 2.55) where OD values were analysed using Gel Blot pro v.3.30 software (UVP Ltd, Cambridge, UK).

The subsequent pages include tables of the RT primers and real time primers and probe used in this thesis.

2.14 STATISTICAL ANALYSIS

Individual data sets were analysed with a paired T test and groups via a repeated measures ANOVA and Student T-test using the INSTAT software package (www.graphpad.com). P values are displayed as follows: * $p<0.05$ ** $p<0.01$ *** $p<0.001$

Gene Name	Type of Gene	Forward Primer	Reverse Primer	Product (bp)	Accession No / Ref
Human					
Shh	Shh pathway	ACTGGGTGTACTACGAGTCCAAGG	AAAGTGAGGAAGTCGCTGTAGAGC	211	[127]
Ptc	Shh pathway	TCCTCGTGTGCGCTGTCTTCCTTC	CGTCAGAAAGGCCAAAGCAACGTGA	202	[127]
Smo	Shh pathway	CTGGTACGAGGACGTGGAGG	AGGGTGAAGAGCGTGCAGAG	140	[167]
Gli1	Shh pathway	ACTGAAGACCTCTCCAGC	GCTGACAGTATAGGCAGA	244	[127]
Gli2	Shh pathway	TGGCCGCTTCAGATGACAGATGTTG	CGTTAGCCGAATGTCAGCCGTGAAG	200	[168]
β-Actin	Control	CCACCAACTGGGACGACATG	GTCTCAAACATGATCTGGGTCATC	153	NM001101*
Mouse					
Shh	Shh pathway	TTAAATGCCTTGGCCATCTC	CCACGGAGTTCTCTGCTTTC	261	NM009170
Shh	Shh pathway	AGGGGGTTTGGAAAGAGG	GGATTCATAGTAGACCCAGTCG	450	[64]
Ptc	Shh pathway	ATCGGAGTGGAGTTCACC	CTGCTGTGCTTCGTATTGCC	466	[64]
Smo	Shh pathway	CATCAAGTTCAACAGTTCAGGC	ATAGGTGAGGACCACGAACCACACTACTCC	465	[64]
Gli1	Shh pathway	GAGAAGCCACACAAGTGC	AACAGTCAGTCTGCTCTCTTCC	404	[64]**
GM-CSF	Cytokine	TTTTGTGCCTGCGTAATGAG	GAGTCAGCGTTTTCAGAGGG	113	X03019
β-Actin	Control	CCACCAACTGGGACGACATG	GTCTCAAACATGATCTGGGTCATC	153	NM007393*

Table 2.5: RT Primers

Where accession numbers are supplied, primers were designed using the primer express 1.5 software and run through a simulated PCR using the Amplify 1.2 package to yield expected product sizes. **β-Actin* primers were routinely used from housekeeping stock for check gels and RT-PCR, specific for genomic and mRNA, however primer dimmers are produced in low template / high salt conditions. ** Although from a published article these primers gave 3 bands of 221bp, 404bp and 743bp, plus minor bands, these were all removed with increased stringency. A BLAST pubmed search would suggest primer binding would also occur with newly published predicted sequences *Gli2*, although this would not produce a PCR product, it could interfere with any semi-quantification assay.

Gene Name	Type of Gene	Forward Primer	Reverse Primer	Probe	Amplicon (bp)	Accession Number
Shh	Shh pathway	TGACCCCTTTAGCCTACAAGCA	TTTTTGTGATCTTCCCTTCATATCTG	TTTATTCCCAACGTAGCCGAGAAGACCC	92	NM_009170
Shh	Shh pathway	GAGCAGACCGGCTGATGACT	AGAGATGGCCAAGGCATTTAACT	TGTCTTTGCACCTCTG	61	NM_009170
Ptc	Shh pathway	CTCCAAGTGTCGTCCGGTTT	TGTACTCCGAGTCGGAGGAATC	CGTGCCTCCTGGTCACACGAACAA	77	NM_008957
Gli1	Shh pathway	GGCTGTCGGAAGTCCTATTCAC	CAACCTTCTTGCTCACACATGTAAG	CGCACCTTCGGTCGCACACG	97	NM_010296
GAPDH	Endogenous control	GACGGCCGCATCTTCTTGT	CACACCGACCTTCACCATTTT	CAGTGCCAGCCTCGTCCCGTAGA	67	NM_001303
CC10	Epithelial marker	CCTTTCAACCCTGGCTCAGA	GAGGGTATCCACCAGTCTCTTCA	CTGCAAAATGCGGGCACCCAG	68	NM_011681

Table 2.6: Mouse Real Time Primers

Mouse real time RT-PCR primers were prepared as were human ones, by adhering to the guidelines supplied by Applied Biosystems. Primers have a Tm 58°C-60°C, 20-80% GC, a maximum of 2/5 G or C at 3' end and of a length of 9-40 bases. The probe must have a Tm 1.0°C higher than primer Tm, not more G`s than C`s and a 20-80% GC content with no G on the 5' end with no contiguous G`s. probes were also designed to be between 9-40 bases. Total amplicons are designed to be between 50-150bp in length with the 3' end of the primer as close to the probe as possible without overlapping.

Gene Name	Type of Gene	Forward Primer	Reverse Primer	Probe	Amplicon (bp)	Accession Number
Shh	Shh pathway	TAAGGACAAGTTGAACGCTTTG G	TCGGTCACCCGCAGTTTCAC	CATCTCGGTGATGAACCAGTGG CCA	74	NM_000193
Ptc	Shh pathway	TGCAAACCGGCAGCCGCGATAA G	TTAATGATGCCATCTGCATCCA	ATCGACATCAGCCAGTTGACTAA ACAGCGTC	86	NM_000264
Smo	Shh pathway	CTCCTTCTCCTGTTCCATTTCAG T	GGTCCTCATCAACAAAAAGGAA AC	CAGTTTCAGCGGTGCCAACCTC TTTG	80	NM_005631
Gli1	Shh pathway	GGGCACCATCCATTTCTACAGT	TCAGTCTGCTTTCCTCCCTGAT	AGCCCAAGAGGGAGCGGGAAG G	77	NM_005269
Gli2	Shh pathway	CATTCGGCTAACGAGGGATTAC	CCAAATGCTCCCTACCATCTTT	TTGGCCAAAACCTTTCAAAGGAT ATGCA	76	NM_005269
Gli3	Shh pathway	AAGTATCATTCAGAACCTTTCCC ATAG	TAGGGAGGTCAGCAAAGAACTC A	CCTCCCGCCTCACCACGCC	137	NM_000168
Megalin	Shh pathway	CCATCGACACACGGTGTATGA	CCAATCTGTCCAATAAATAGTGT	CACTGCCTCACCCTTTCGCTATT ACCATT	88	NM_004525
TGFb-1	Cytokine signalling	CCCTGCCCCTACATTTGGA	GCGCCCGGGTTATGCTGGTTGT	CACGCAGTACAGCAAGGTCCTG GCC	81	NM_000660
TGFb-2	Cytokine signalling	CTACGCCAAGGAGGTTTACAAA ATA	GGCGGGATGGCATTTTC	ACATGCCGCCCTTCTTCCCCTC	68	NM_003238
TGFb-3	Cytokine signalling	GGCTGAGATGGAGGTTTCCTT	CCAAACCCACACTTCTTTACCA	GAACATTTCTTTCTTGCTGGCTC T	85	NM_003239
BMP4	Embryonic TGF-b	CCCGCAGCCTAGCAAGAGT	CCAGACTGAAGCCGGTAAAGA	CCGTCATTCCGGACTACATGCG G	68	NM_001202
Tenascin	Fibrogenesis	CTGCTCCCAAGCAATGCTGAA	CTTCCAGCGCCTGAGCCTTATC ACCAT	AGACACGACCTCTGGCCTCTAC ACCATTTATC	89	NM_002160
MMP7	Matrix metalloprotease	TGGTAGCAGTCTAGGGATTAACT TCCT	CATAGGTTGGATACATCACTGCA TTA	TGCTGCAACTCATGAACTTGGC CATT	112	NM_002423
GAPDH	Endogenous control	AAGGACTCATGACCACAGTCCA T	CCATCACGCCACAGTTTCC	CCATCACTGCCACCCAGAAGAC TGTG	84	NM_002046

Table 2.7: Human Real Time Primers

CHAPTER 3 HYDROGEN PEROXIDE INDUCED EPITHELIAL CELL INJURY UP REGULATES SHH RELEASE

3.1 INTRODUCTION

The function of the epithelial surface gradates from a largely defensive and structural role in the upper airways, to a predominantly gas exchange function at the alveolar surface. Whilst upper airway defence mechanisms such as mucus production and IgA translocation have been well characterised, it is only comparatively recently that the endogenous defence mechanisms of the lower airways have attracted substantial attention. These bronchiolar and alveolar responses can be stimulated and regulated either by direct stimuli from the apical milieu, or by secondary signals, such as those delivered by the AM, underlying connective tissues or cells of the immune system. Epithelial responses can include the secretion of cytokines and chemokines with both local and systemic effects, as well as changes in proliferation and subsequent differentiation. These responses can occasionally become deleterious, such as in asthma and allergic rhinitis, where epithelial activation can worsen hyper-responsive reactions to non-pathogenic interactions. Thus an understanding of the mechanisms involved in these responses is essential in understanding the response of the pulmonary surface to infectious and deleterious insults, and subsequently, its response to the delivery of ameliorative or curative treatments.

The pulmonary epithelium of the lower airways constitutes a collection of cell types with vastly differing morphological and functional properties. The majority have some secretory function, although the cuboidal type II and Clara epithelial cells are considered to have the most significant effect on the lung milieu (see Chapter 1). In areas of bronchiole - alveolar injury these cells are often observed as spreading and proliferating cells termed "repair" or "intermediate" cells, which are thought to be prominent secretors of cytokines. These can act as immune modulators, affecting sub epithelial macrophage, DC, T-cells and AM, whilst also having a range of affects on structural cells such as the fibroblasts, myofibroblasts and smooth muscle cells which constitute the subepithelial connective structures. Epithelial signals such as IL-6 and FGFs can induce proliferation in fibroblasts and lead to their up regulated production of components of the extracellular matrix,

aiding wound repair and preventing transudation of plasma factors which may be detrimental to the restoration of normal lung physiology following a period of epithelial denudement.

As discussed in Chapter 1, work of this lab had identified alveolar epithelial cell expression of Shh in areas of disease in UIP & in the FITC model of lung fibrosis[1]. Shh expression was observed to be greatest in cuboidal and metaplastic epithelial cells in areas of inflamed or fibrotic lung, and up regulated in areas of bronchiolisation in human disease. This expression pattern matched that observed for many immunologically relevant factors secreted by proliferating epithelial repair cells in mouse and human lung.

3.1.1 HYPOTHESIS

This chapter will address the hypotheses that

- The up regulation in epithelial Shh expression is a response to injury
- That this injury also affects other epithelial cell functions.
- Up regulated Shh affects epithelial and fibroblast function.

3.1.2 EXPERIMENTAL METHODOLOGY

The response of epithelial cells to injury was initially investigated using a reductionist *in vitro* approach. Type II like epithelial cell lines were utilised, where the A549 cell line was utilised for human studies, and for mouse studies, the CMT-64 cell line. In addition to this a mouse pulmonary fibroblast line was also used CCL-206, described here using the ATTCC nomenclature, but also referred to as MLg, in the literature[160].

EPITHELIAL CELL ASSAYS

Epithelial cell injury assays were developed to investigate the proliferative and secretory responses of epithelial cell lines to injurious stimuli. As the nature of the injurious stimulus in human ILD is unknown it was decided to

investigate responses to a known damaging agent, H_2O_2, and to the hapten FITC, which induces fibrosis in the mouse lung. As discussed in Chapter 1, the epithelium has the capacity to modulate and initiate immune responses through a wide range of cytokines and chemokines. The work of this Chapter focused on the inflammatory/anti-inflammatory mediators and conserved developmental signalling molecules produced.

ROLE OF SHH SIGNALLING IN EPITHELIAL / FIBROBLAST FUNCTION

It is only comparatively recently that Shh has been identified as an active signalling molecule in post embryonic organisms. Elucidation of its up regulation in the epithelium of fibrosed lung[1], coupled with its potentiation of immune responses[2, 3, 169], would suggest that Shh expression may be a novel signal in post embryonic lung cell function.

Previous *in vitro* investigations into Shh function have been hampered by a lack of suitable investigative tools, particularly for the measurement of soluble Shh signal. Only a very limited number of antibodies were available, no ELISA could be commercially obtained, and bioassay applications were notoriously variable. This necessitated the development of quantitative methods of measuring soluble Shh protein levels for the analysis of cell line supernatants. Two approaches were taken, a bioassay system and a novel ELISA based system which I developed. These were used to measure whether the exposure of epithelial cells to injurious stimuli affected their production and / or release of soluble Shh.

The results reported here will first address the development of the cell line injury assays and subsequent cytokine analysis, followed by detailed coverage of the steps taken in the development of the analytical tools for measuring Shh release, and their application to these *in vitro* studies.

3.1.3 AIMS OF CHAPTER

- Establish an *in vitro* damaging assay system
- Identify epithelial cytokine response to *in vitro* injurious stimuli
- Develop a quantitative method of detecting Shh
- Investigate the postulated link between Shh and injurious stimuli
- Determine whether Shh exposure alters fibroblast activity

3.2 RESULTS

3.2.1 EPITHELIAL INJURY ASSAY DEVELOPMENT

ESTABLISHMENT OF OPTIMAL CELL DENSITIES

Preliminary attempts at developing cell line injury assays used 96 well culture plates, but within these excessive lifting of cell monolayers was observed during media replacement. This was overcome via use of 24 well plates, where wells were sufficiently small to minimise the number of cells required for the relevant number of replicates and the amount of reagents required, but large enough to ensure the maintenance of a robust cell layer during media replacement. Thus all subsequent injury experiments were performed in 24 well plates.

In order to facilitate consistent and healthy cell growth in injury assays, A549 and CMT were serially plated from a top concentration of $1x10^6$ cells/ml and the optimum plating density that would allow continuous proliferation throughout the duration of the assay determined. This was assessed with the MTT assay system (see Chapter 2). In this assay, mitochondrial enzyme mediated conversion of a pale yellow substrate into an insoluble purple compound, yields a colourimetric signal proportional to viable cell number.

From these studies (Figure 3.1) the optimal plating cell densities for both cell lines were identified as $2.5x10^5$ per ml, plated as 500μl per well. This gave the maximum number of cells per well for the generation of detectable cytokine levels in 500μl of media, without affecting proliferation over a 72/96hr time course.

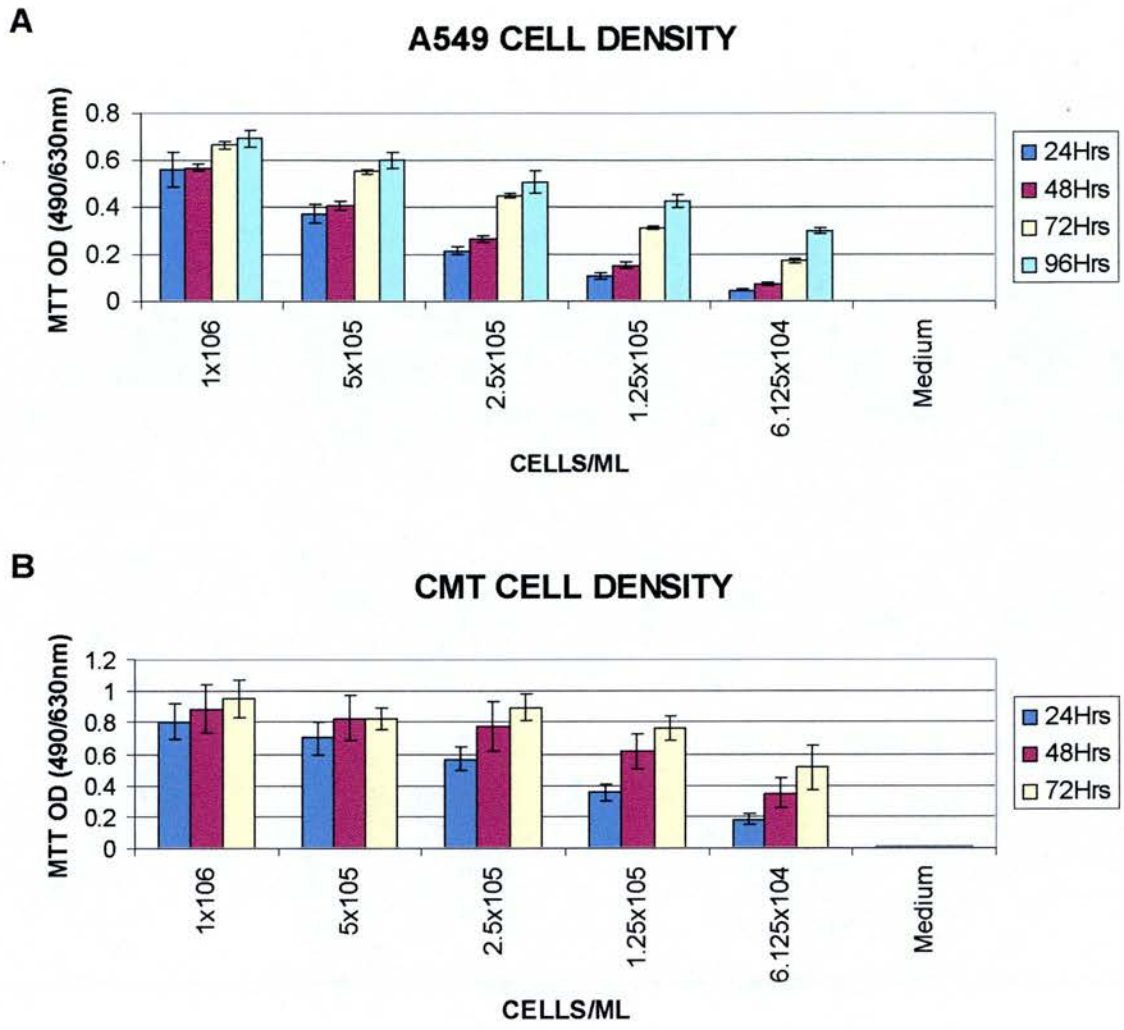

Figure 3.1: A549 and CMT Cell Density Titration
Error bars denote standard error of 3 separate experiments using cells not more than 3 passages apart. Cells plated in 500µl volumes, media unchanged through time course.

FITC EXPOSURE

Initial experiments using FITC powder in media had serious limitations. Despite apparently being in solution, once administered to cells, FITC formed clustered aggregates on the surface of cells which were impossible to remove without injuriously forceful wash steps. The continued presence of FITC caused sustained injury and reduced viability of the cells, as measured by MTT (data not shown), and inhibited the colourimetric and fluorometric analysis of cell supernatants.

FITC retention as aggregates was avoided by pre-solubilisation of FITC in DMSO, prior to its addition to serum free media. Whilst this did slightly reduce the affects of FITC on the epithelium, it allowed efficient removal of the compound and reduced variability. The effect of FITC on CMT cells was ascertained via titration starting at a high of 1mg/ml in serum free media, and MTT values recorded up to 48hrs post exposure.

Administration of FITC in a DMSO carrier solution to CMT cells results in complete loss of the MTT signal at 1000μg/ml, where DMSO alone had no effect. A 250μg/ml solution reduced the increase in the MTT signal over 24-48hrs, when compared to cells alone, whilst 125μg/ml exposure had only a marginal affect on cells. This would suggest that whilst FITC can affect the number of viable CMT cells, persistent affects on viable cell number occur only within a limited range, from almost complete loss of viability with 500μg/ml to almost no affect with 125μg/ml (Figure 3.2[A]).

Analysis of supernatants taken from FITC/DMSO exposed CMT cells did not yield any substantial difference in cytokine production compared to non exposed cells, as discussed below. This may indicate that although FITC has inherent toxicity, it does not stimulate epithelial cytokine secretion. Although possible, such a finding is highly at odds with experience *in vivo*, where FITC administration is found associated with an acute subepithelial inflammatory infiltrate. What is perhaps more likely is that FITC stimulates pathways not analysed here or that the solubilisation step necessary for *in vitro* application has altered the response of epithelial cells to FITC exposure.

H_2O_2 EXPOSURE

H_2O_2 was always used from a fresh sterile bottle and was titred into serum free medium from a high of 40mM, prior to addition to cells. H_2O_2 addition was performed with both A549 and CMT cultures (Figure 3.2[B]&[C]).

H_2O_2 exposure in CMT cell cultures resulted in a titration profile similar to FITC, but with broader inhibition of temporal increase in MTT signal (Figure 3.2[B]), which continued with further titration (data not shown). Cells exposed to concentrations of H_2O_2 between 10mM and 2.5mM illustrated a

stabilisation of viable cell number, suggesting either a loss of proliferative capacity or persistent cell death equal to that of proliferation. Concentrations of H_2O_2 capable of inducing complete loss of MTT signal were used for reasons discussed in Section 3.2.7.

H_2O_2 exposure in A549 reduced the MTT signal up to 72hr after addition, and this was not a consequence of symbiotic reliance on cell number, as shown by the cell density titre in Figure 3.1. Contrary to the stabilisation of the MTT signal observed in CMT cells with H_2O_2 exposure, A549 exhibited an active reduction in the MTT signal over the same time period, suggesting a non recoverable reduction in cell proliferative capacity or an elevated rate of cell death following H_2O_2 exposure. (Figure 3.2[C]).

3.2.2 H_2O_2 EXPOSURE AFFECTS EPITHELIAL CELL CYTOKINE PRODUCTION

In the mouse CMT cell line, of those cytokines analysed by CBA and ELISA (TNF-α, TGF-β, GM-CSF, IL-12p70, IFN-γ, MCP-1, IL-10, IL-6) only GM-CSF and MCP-1 demonstrated any consistent expression. In the human A549 cell line, of those cytokines analysed by CBA and ELISA (GM-CSF, IL-8, IL-1b, IL-6, IL-10, TNF, IL-12p70), only IL-8 demonstrated any consistent expression.

CMT CELLS EXPRESS GM-CSF AND MCP-1

Constitutive production of GM-CSF by CMT cells was below the standard curve of the GM-CSF Duoset ELISA (R&D). However, its detection in CMT cell supernatants was significantly increased by exposure to H_2O_2 (n=6), but not by FITC/DMSO (n=3 data not shown) (Figure 3.3). Both agents resulted in a reduction in viable cell number, thus it was concluded that upregulation was an agent specific response. Whether the FITC or H_2O_2 is representative of a normal GM-CSF response to injury would require trials with a greater variety of agents.

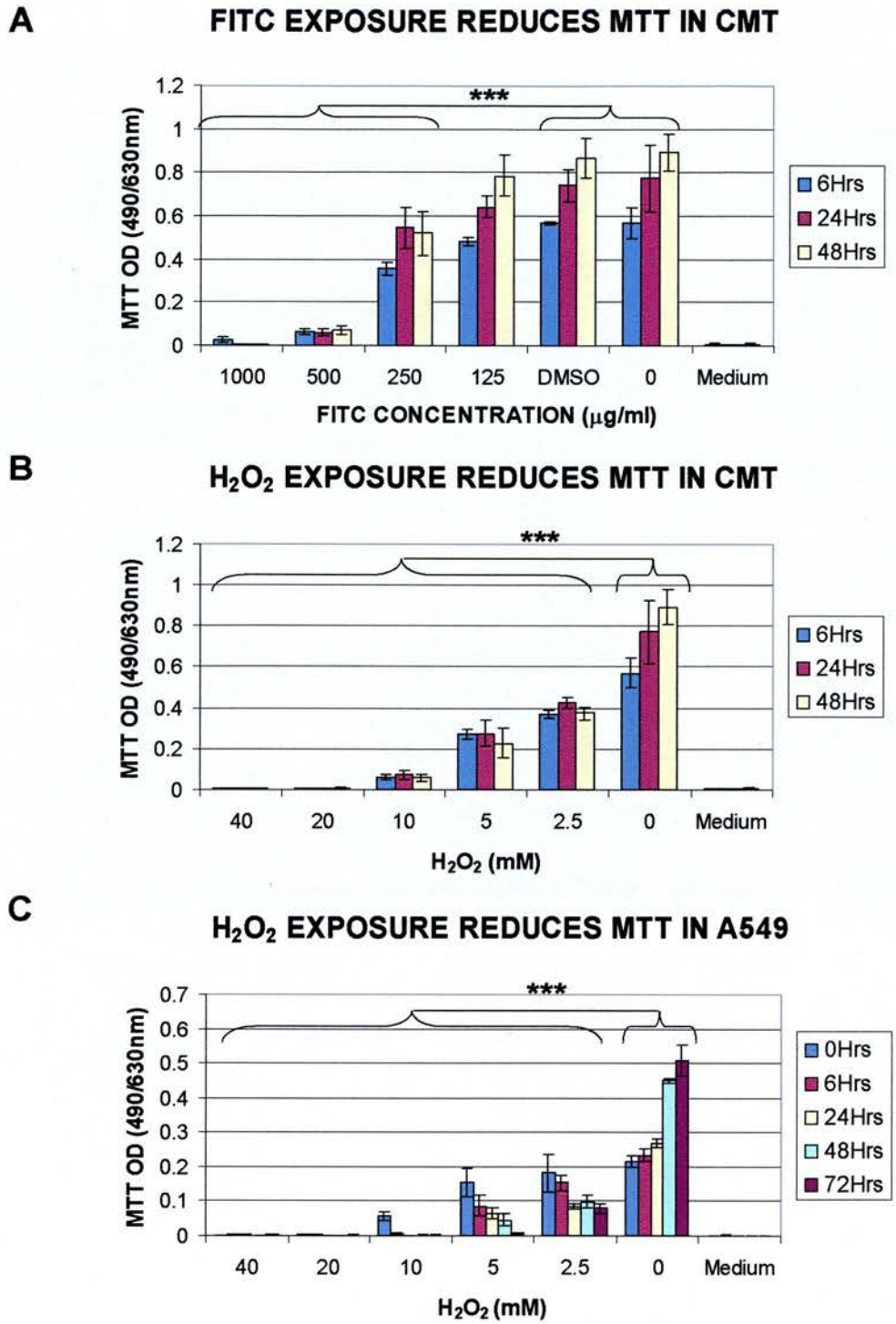

Figure 3.2: FITC & H_2O_2 Reduce MTT

Cells plated at $1.25x10^5$ per well, 24 hours prior to a 1.5 hr damage step. n refers to number of experiments incorporating duplicate wells. [A] FITC powder dissolved in 500µl DMSO added to >15ml serum free media; n=3. [B] H_2O_2 in serum free media; n=6. MTT assay performed over 3hrs [C] A549, n=3. MTT performed for 45mins. All medium wells treated with highest concentration of injurious compound to control for any possible FITC or H_2O_2 carryover affect. All error bars denote Standard Error. Statistical analysis *p<0.05, **p<0.01, ***p<0.001 by parametric tests.

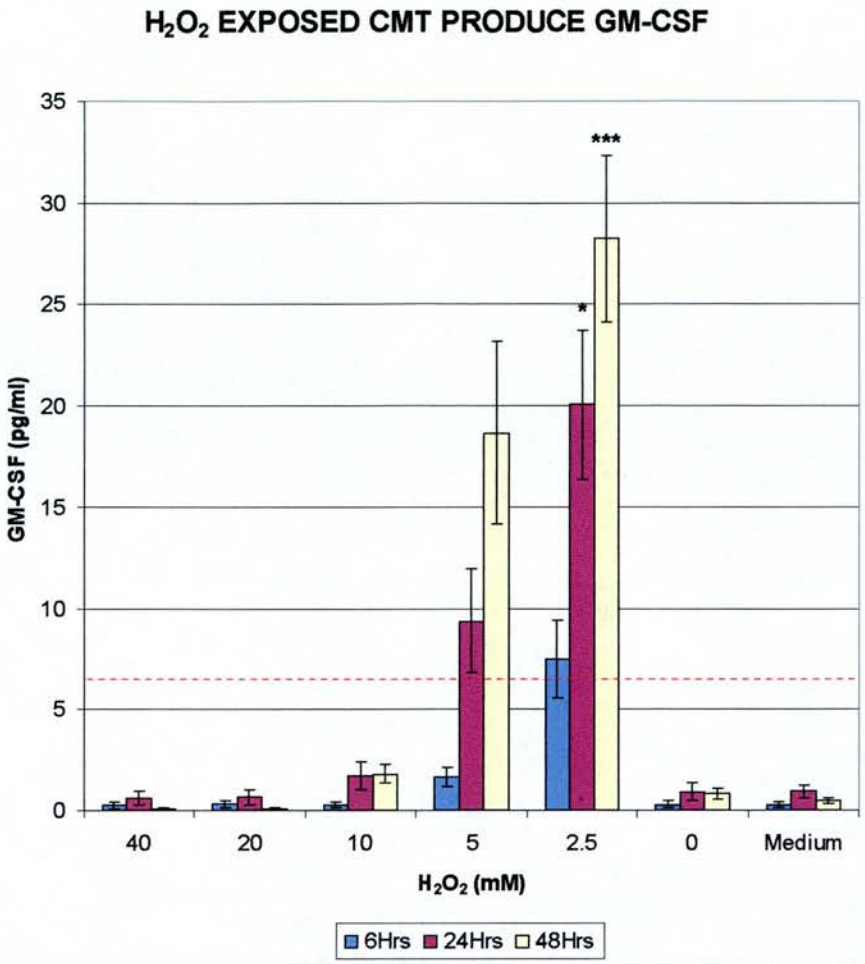

Figure 3.3: H_2O_2 Exposed CMT Release More GM-CSF
Exposure to 2.5mM of H_2O_2 for 1.5hrs resulted in a 14 fold increase in GM-CSF detected by ELISA (low standard 7.8pg/ml shown by red line) 48 hours after damage. Legends refer to time after agent removal. Cells were plated 24hrs previously at $1.25x10^5$ cells per well. n=6. Error bars denote Standard Error. Statistical analysis *p<0.05, **p<0.01, ***p<0.001 by parametric tests, refer to values vs. 6Hrs.

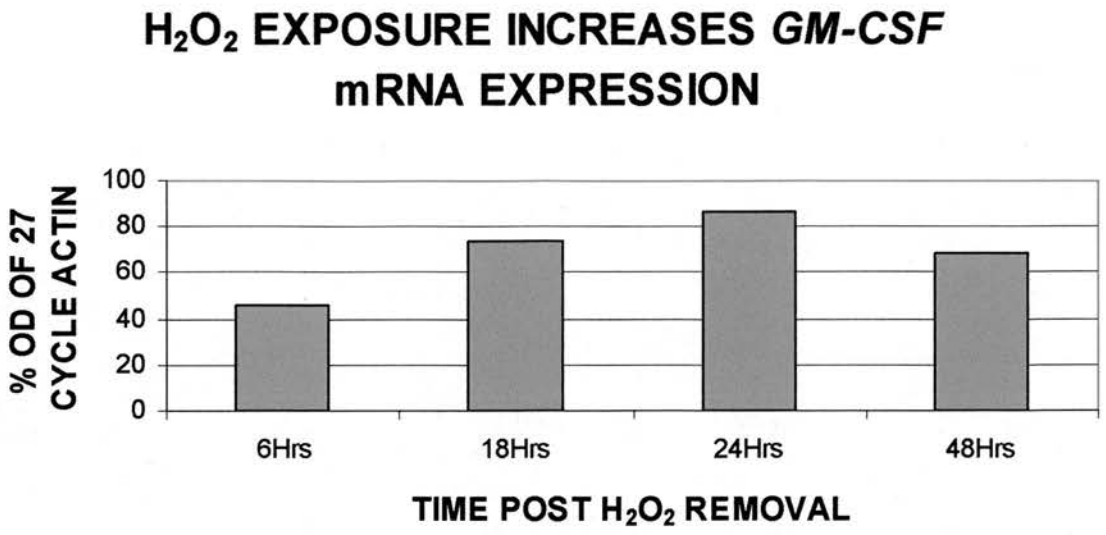

Figure 3.4: *GM-CSF* mRNA Increases Following H_2O_2
RNA extracted from CMT exposed to 5mM of H_2O_2 for 1.5hrs in serum-free media as described previously. 2% agarose gel OD values and relative band size were analysed following 27cycle (β–*Actin*) and 35 cycle (*GM-CSF*) PCR from a common mastermix following PCR with annealing temperature of 60°C. Data here are representative of three repeats.

True up regulation of GM-CSF over release of stored cytokine was confirmed by semi-quantitative RT-PCR for *GM-CSF* compared to *β-Actin.* Untreated CMT cells had mRNA levels below the level of detection. Following H_2O_2 exposure, mRNA levels increased to a maximal expression of >80% of *β-Actin*, 24hrs after the removal of H_2O_2 and 24hrs prior to the peak in protein expression (Figure 3.4). OD values were obtained from Gel blot pro software analysis of RT-PCR product bands in 2% agarose gels on a visible UV transilluminator. Gels were loaded with a 1:1 ratio of orange g to sample in a 10μl volume per lane.

MCP-1 secretion (data not shown) was not affected by either H_2O_2 or FITC/DMSO, but increased with time in culture to a high of 55 pg/ml at 96hrs with a plating density titration of $5x10^5$ cells per well. Values were below the limit of detection (<20pg/ml) with $3.125x10^4$ cells per well.

A549 CELLS EXPRESS IL-8, BUT NOT GM-CSF

No GM-CSF or MCP-1 were detectable in this cell line. However, IL-8 was detected. In untreated cells, expression of IL-8 correlated with cell number, as shown in a cell density titre (Figure 3.5).

However, supernatants taken from A549 cells exposed to H_2O_2 demonstrate that H_2O_2 exposure increases constitutive levels of IL-8 production from <200pg/ml to a high of >700pg/ml Figure 3.5. This was interesting given that previous reports have suggested that A549 up-regulate IL-8 in response to AM derived IL-1β and TNF[170] and that MCP-1 is also normally up-regulated[171], which was not observed with H_2O_2 exposure. Data here, in the absence of detectable TNF, could suggest that these cells can produce IL-8, in the absence of MCP-1 as a direct response to injurious stimuli. However an analysis of IL-1β levels would be required to confirm this.

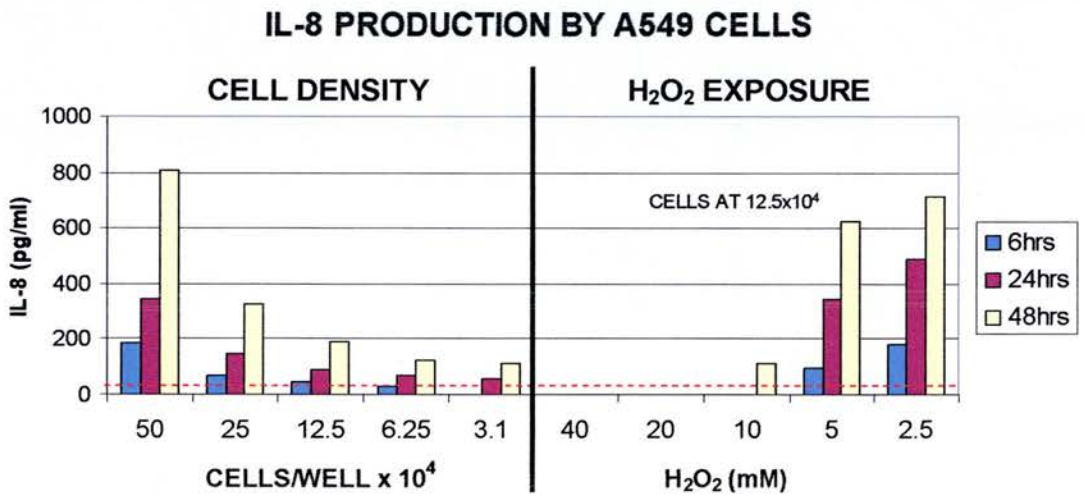

Figure 3.5: A549 IL-8 Production

Cell density titre demonstrates constitutive release relative to cell number. A549 cells were plated at $12.5x10^4$ per well for addition of H_2O_2. Representative of 2 repeats. A549 altered their IL-8 release in response to H_2O_2 exposure. Legend times refer to time after removal of H_2O_2. CBA low detection limit 20 pg/ml, shown by red line.

3.2.3 EXPRESSION OF THE SHH PATHWAY SIGNALLING COMPONENTS IN THE CMT, A549 & CCL-206 CELL LINES

In order to determine whether epithelial cell injury affected Shh signalling it was necessary to establish the presence of components of the signalling

pathway in these cells. A549, CMT and also the mouse pulmonary fibroblast cell line CCL-206 were assessed for *Shh* signalling components via RT-PCR (Figure 3.6). The expression of *Shh* and *Ptc* by A549 has previously been published by this lab[3], but owing to conflicting reports[73, 172], this was confirmed with new primer sets, along with expression of *Smo*, and *Gli1&2*.

The mouse cell lines were also analysed for *Shh* pathway components along with a mouse brain positive control. The mouse *Shh* primers were designed using the primer express software and all sequences were checked in the Amplify software package to confirm band size and check for primer dimers and secondary products. Both A549 and CMT cells exhibit all of the major pathway components, including *Shh, Ptc, Smo & Gli* (Figure 3.6). This demonstrates that these cells have the capability to both produce and respond to a Shh signal, if protein expression mirrors the mRNA profile. In contrast, the fibroblast cell line, lacked *Shh* expression and was positive only weakly for *Ptc*, but with strong *Smo* expression, demonstrating a potential responder profile to a Shh signal. Negative *Gli1* signal in these cells (where *Gli1* is induced via signalling through *Gli2*) confirms an absence of Shh in this monoculture.

Cell lysates were taken at 70% confluence as this represents the average confluence of the cells in tissue culture plates during injury assays. This is crucial as expression profiles might be expected to change within a confluent monolayer.

The mouse primers presented a number of optimisation problems, which deserves some discussion here,. notably, the *Gli1* primer, which was taken from a published paper by Outram et al[64]. When these primers were processed through the Amplify software, three bands of 221, 404 & 743bp were generated. Thus optimisation problems were attributable to the original sequence rather than the mastermix conditions used. Whether the optimised band at 404bp represents the strongest possible product has not been ascertained. Subsequent analysis of recently published mRNA sequences during the preparation of this thesis, has shown that this primer set also has high affinity with *Gli2* when run through a pubmed BLAST search. However,

artificial PCR in the Amplify package would suggest that this does not yield a product. Thus these primers can be considered *Gli1* specific. Subsequent attempts at generating new primer sequences for this mRNA sequence comes too late for inclusion in this thesis.

Mouse *Shh* RT products were unpredictable in quality and quantity and particularly susceptible to freeze thaw degradation. Best results were obtained with fresh RNA and cDNA. Prolonged storage on ice during PCR preparation was also found to be detrimental to efficient amplification. Similar problems were experienced in real time primer-probe design and would suggest that some element of secondary folding or short half life interferes with effective detection of this transcript.

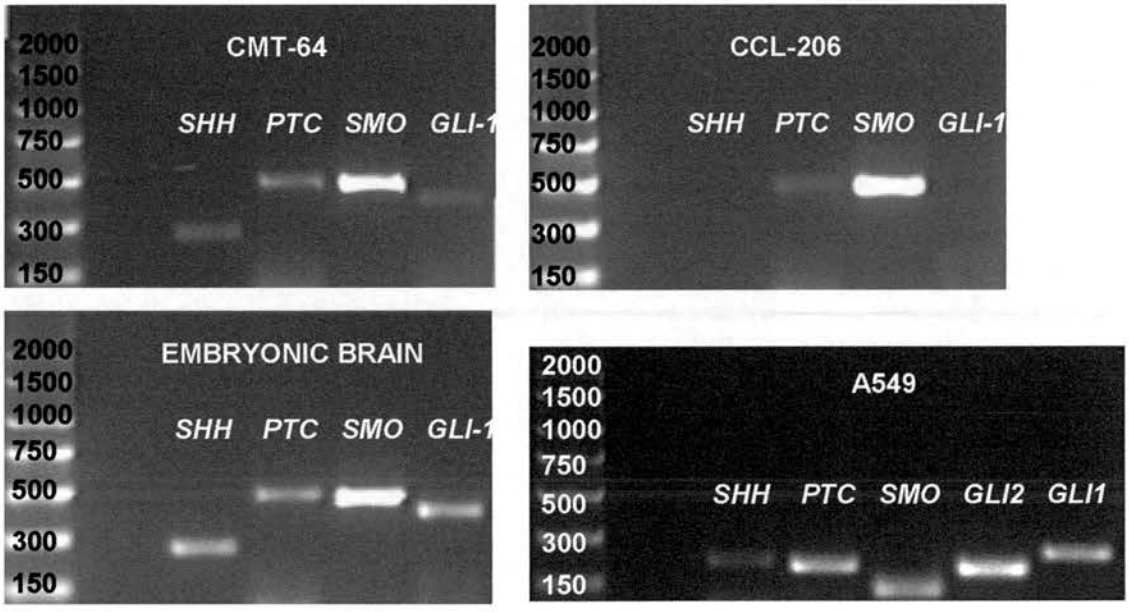

Figure 3.6: mRNA of Shh Signalling Components in Cell lines
RNA isolated from cell lines at 70% confluence in vented flasks. Mouse primer product sizes and references are as follows: *Shh* 261bp, designed with Primer 3 Express primer design software, *Ptc* 466bp, *Smo* 465bp & *Gli1* 404bp[64]. Embryonic mouse (Balb-c) brain tissue was homogenised prior to normal RNA isolation. A549 product sizes and primer references are as follows: *Shh* 211bp [127], *Ptc* 202bp [127], *Smo* 140bp[167], *Gli2* 200bp[168], *Gli1* 244bp [127].

3.2.4 IMMUNOHISTOCHEMICAL DETECTION OF SHH AND PTC IN CELL LINES

Immunohistochemical analysis was utilised to confirm translation into protein in the CMT cell. CMT cells were also exposed to FITC and H_2O_2 to see if

exposure altered the localisation of Shh or Ptc in these cells. CMT cells were fixed 1 day after exposure to H_2O_2 or FITC for 45 minutes or 1.5hr in Nalgene chamber-slides. Immunohistochemistry was performed using the Santa Cruz antibodies for Shh (N19) and Ptc (C20) at a 1 in 30 dilution (Figure 3.7). Shh appears membranous after a 45 minute exposure to FITC [A] & H_2O_2 [B], and staining was almost completely lost after 1.5hr, whilst Ptc remains relatively unchanged. Negative controls in this study were omission of the primary antibody on cells not exposed to either FITC or H_2O_2.

The specificity of this immunohistochemistry was checked by pre-incubation of primary detection antibody with commercially available blocking peptide. This required a reduction in primary concentration to a dilution of between 1 in 60 & 1 in 80. Use of the C20 (Ptc) blocking peptide, completely blocked immunohistochemical detection (Figure 3.8), showing signal specificity. However, use of the N19 blocking peptide in my hands, results in increased signal, where blocking peptide alone was negative. Use of neat blocking peptide with a 1 in 80 dilution of N19 further increased immunohistochemical signal (data not shown). Thus Shh staining could not be validated with the blocking peptide, although there are a number of possible explanations for this. If the blocking peptide was significantly similar to the Shh peptide itself it is plausible that the N19 antibody containing bound peptide might bind to Ptc, Hip or indeed Megalin and the postulated HSPG modulators of Shh. Equally, the N19 may have greater affinity for the native peptide, thus displacing the blocking peptide.

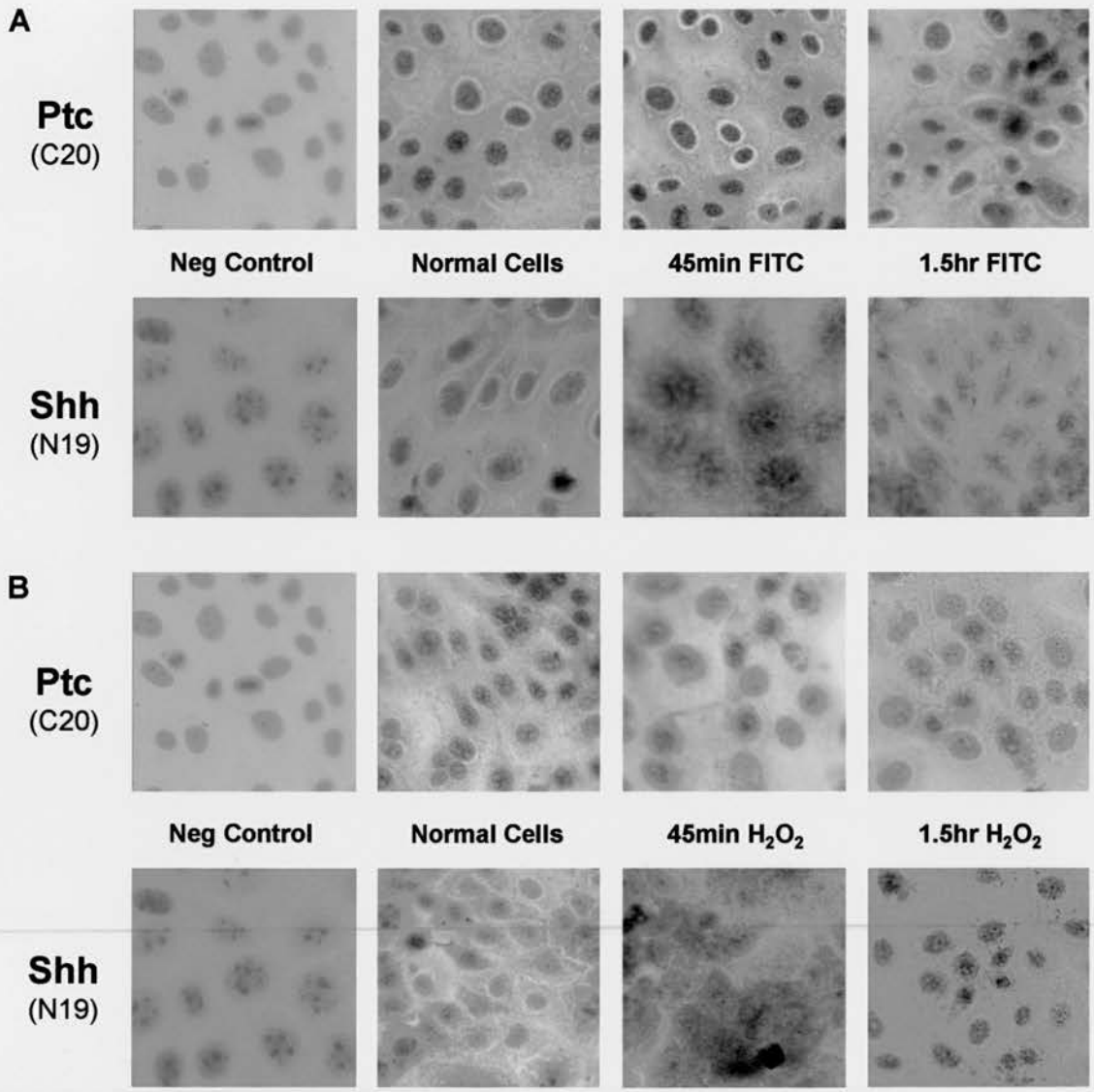

Figure 3.7: CMT Immunohistochemistry For Shh & Ptc
CMT cells grown on Nalgene chamber slides for 24 hours, exposed to damaging agent, washed and left 24hrs prior to fixing. [A] FITC exposure (250μg/ml), [B] H_2O_2 exposure (5mM). Ptc staining with C-20, Shh staining with N19, using a 1:40 dilution of stock (200μg/ml) in Dako diluent. Times and reagents as sequenza protocol (Section 2.8.1), 250μl of each reagent per well. Negative controls are primary antibody exclusions.

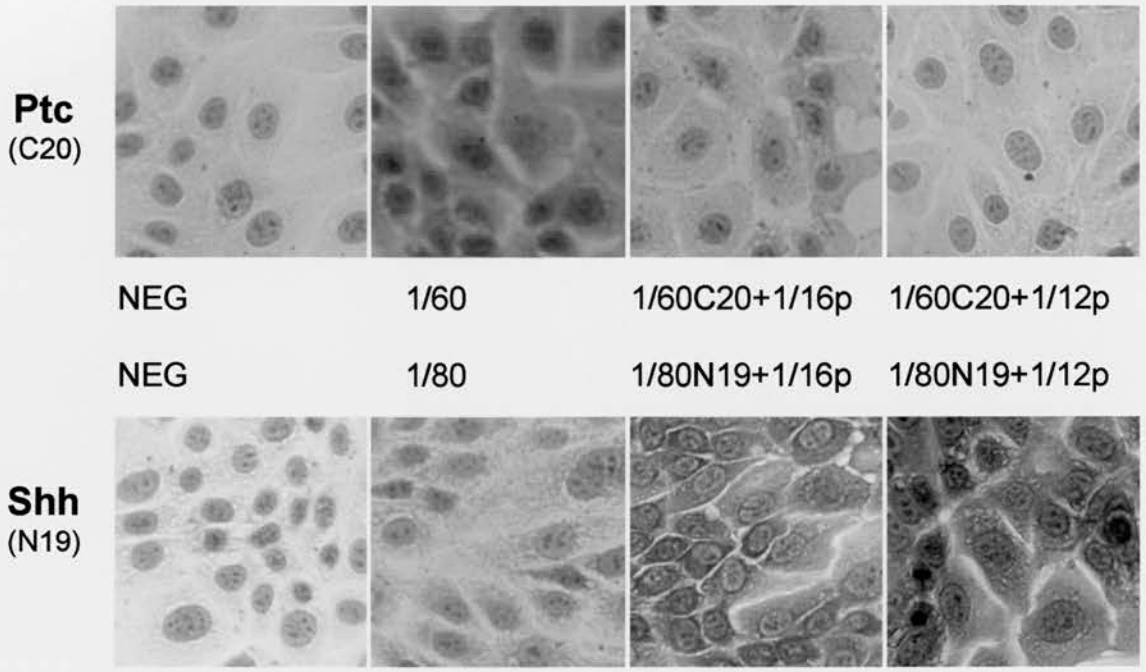

Figure 3.8: CMT Immunohistochemistry with Blocking Peptides
CMT epithelial cells on Nalgene coverslides at x200 magnification. Neg controls are omission of primary. Ab and peptide concentrations given as dilutions of 200μg/ml stock. Ptc antibody blocks, Shh antibody does not.

3.2.5 SHH ELISA

The aim of the work described in this section was to develop a Shh specific ELISA system. The initial focus was to develop a method whereby Shh containing samples coated onto a 96 well plate could be detected and quantified with the addition of Shh specific antibodies, aka a "one way" ELISA. Following this it was hoped to increase the sensitivity and specificity of the one way ELISA system, via the pre coating of the wells with a different Shh specific antibody, prior to sample addition, aka a "sandwich" ELISA system.

ONE WAY ELISA

One way ELISA`s involved coating of high binding EIA plates with a sample to be tested, followed by a protein rich blocking step, to prevent subsequent non-specific binding. One of two available anti-Shh antibodies were then added as a "primary detection", either the mouse monoclonal anti-Shh antibody (5E1), or the goat polyclonal anti-Shh antibody (N19). Bound anti-Shh antibody was then detected via the addition of biotinylated antibody

raised against the relevant species of the primary antibody, termed a secondary detection step.

Biotinylated antibody binding was then quantified using a Streptavidin/substrate development system as used by most commercial ELISA systems, e.g. R&D, whereby a colourimetric signal quantifies bound biotinylated antibody.

Initial experiments characterised relative binding capabilities of the secondary detection antibodies when added to plate bound primary antibodies as a chequerboard of 10 fold dilutions of biotinylated anti-goat/mouse secondary, added to 10 fold dilutions of plate bound N-19 or 5E1 (data not shown).

This identified that the anti-mouse and anti-goat antibodies had similar sensitivity for plate bound Shh specific antibody, and that dilutions in the range 500-100ng/ml of anti mouse/goat antibody were likely to be the most suitable.

In order to analyse the relative sensitivity of the N19 and 5E1, a high binding ELISA plate was then coated with 10, 1 and 0.1ng/ml of r-Shh peptide, blocked, then detected with the N19 and 5E1 antibodies at 1000, 300 and 100ng/ml, using a low concentration of secondary detection antibody (100ng/ml) to avoid competitive exclusion (Figure 3.9[A&B]). These studies illustrated that both antibodies had similar detection profiles, thus both warranted further investigation.

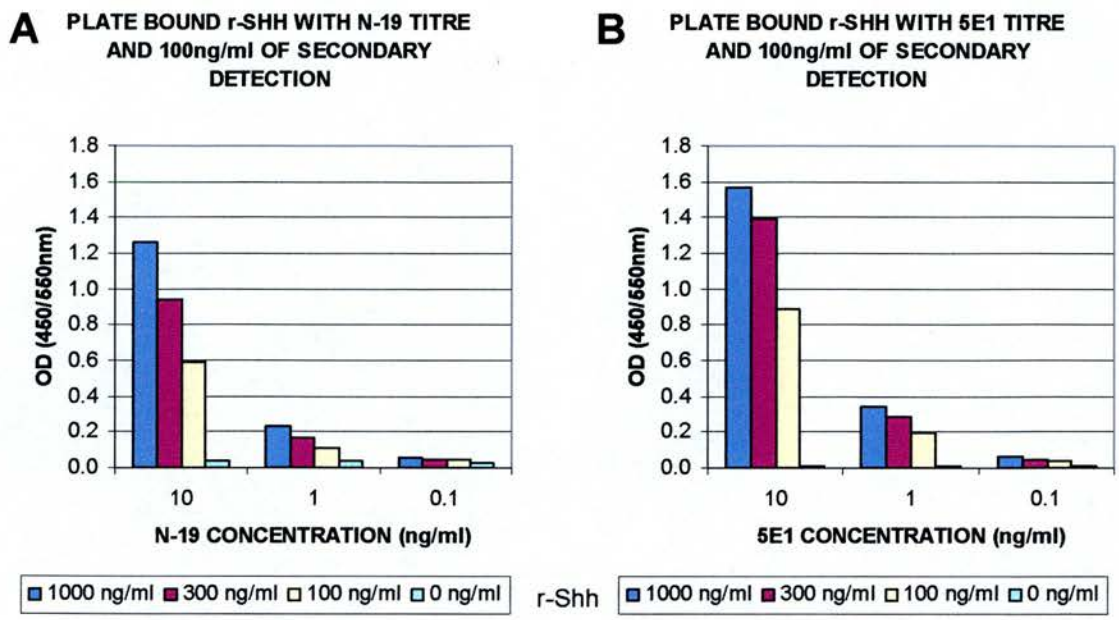

Figure 3.9: Primary & Secondary Antibody Titres
[A & B] 50µl volumes of r-Shh peptide in bicarbonate buffer were incubated overnight at 4°C in 96 well high binding EIA plates (see legend), prior to non-specific protein blocking and primary detection (X-axis). Both assays used 100ng/ml of relevant biotinylated secondary detection. Development of streptavidin activity with colourimetric substrate was extended from the standard 20 minutes to 40 minutes to facilitate further development and elucidation of signal. This was suitable for comparative analysis of antibody sensitivity with r-Shh, as shown here, but found to be unsuitable for the generation of an accurate standard curve with r-Shh. Data here are representative of two replicates.

In order to increase detectable colourimetric signal, without extending the duration of substrate development, the next stage of investigation utilised increased concentrations of primary antibody, titred from approximately 700ng/ml to 20ng/ml, and increased concentrations of secondary antibodies (250ng/ml and 500ng/ml) applied to plates coated with a serial dilution of r-Shh ranging from 200-0.2ng/ml. Antibody concentrations were selected on the basis of previous chequerboard titres and those used in commercial ELISA assays for other cytokines.

Both primary antibodies gave similar profiles of colourimetric development with 250ng and 500ng/ml secondary detection antibody concentrations, where approximately 160-80ng/ml of primary antibody in conjunction with 500ng/ml secondary detection gave the most sensitive r-Shh titre detection

(data not shown). However, this gave an exceptionally steep standard curve, only accurately displaying 2 values within a linear range. A more inclusive linear profile could be observed with a primary antibody concentration of 640ng/ml and a secondary antibody concentration of 250ng/ml for both primary antibodies. This was utilised in subsequent experiments where 5E1 was selected as the primary of choice for economic reasons (a producing cell line maintained in house) and for specificity considerations, given that it is a monoclonal antibody vs. the polyclonal N19.

Previous experiments had used r-Shh diluted in bicarbonate buffer to coat high binding plates overnight at 4°C. However, analytical samples will generally be supernatant media, where the high concentrations of r-Shh used in the standard curve negate substantial dilution in bicarbonate buffer. It was therefore necessary to assess the affect of coating medium on relative antibody detection. r-Shh was plated in bicarbonate buffer, bicarbonate buffer plus cell culture medium and PBS (Figure 3.10[A]).

PBS and cell culture medium did not generate comparable standard curves to bicarbonate buffer alone (Figure 3.10[A]). PBS markedly reduced r-Shh detection and use of 200ng r-Shh titres in this coating solution generated a steep standard curve with only two linear data points (data not shown). Dilution of bicarbonate buffer with medium resulted in a reduced OD signal, but with a similar linear distribution (Figure 3.10[A]). Further experiments with a titred dilution of bicarbonate buffer with medium, demonstrated a proportional reduction in signal (data not shown). Thus for subsequent ELISA experiments supernatants were plated 1:1 with carbonate buffer and the standard curve generated with carbonate buffer 1:1 with sample medium. Use of this technique generated standard curves similar to that shown in Figure 3.10[B]. This system was hence forth defined as the 5E1 ELISA system.

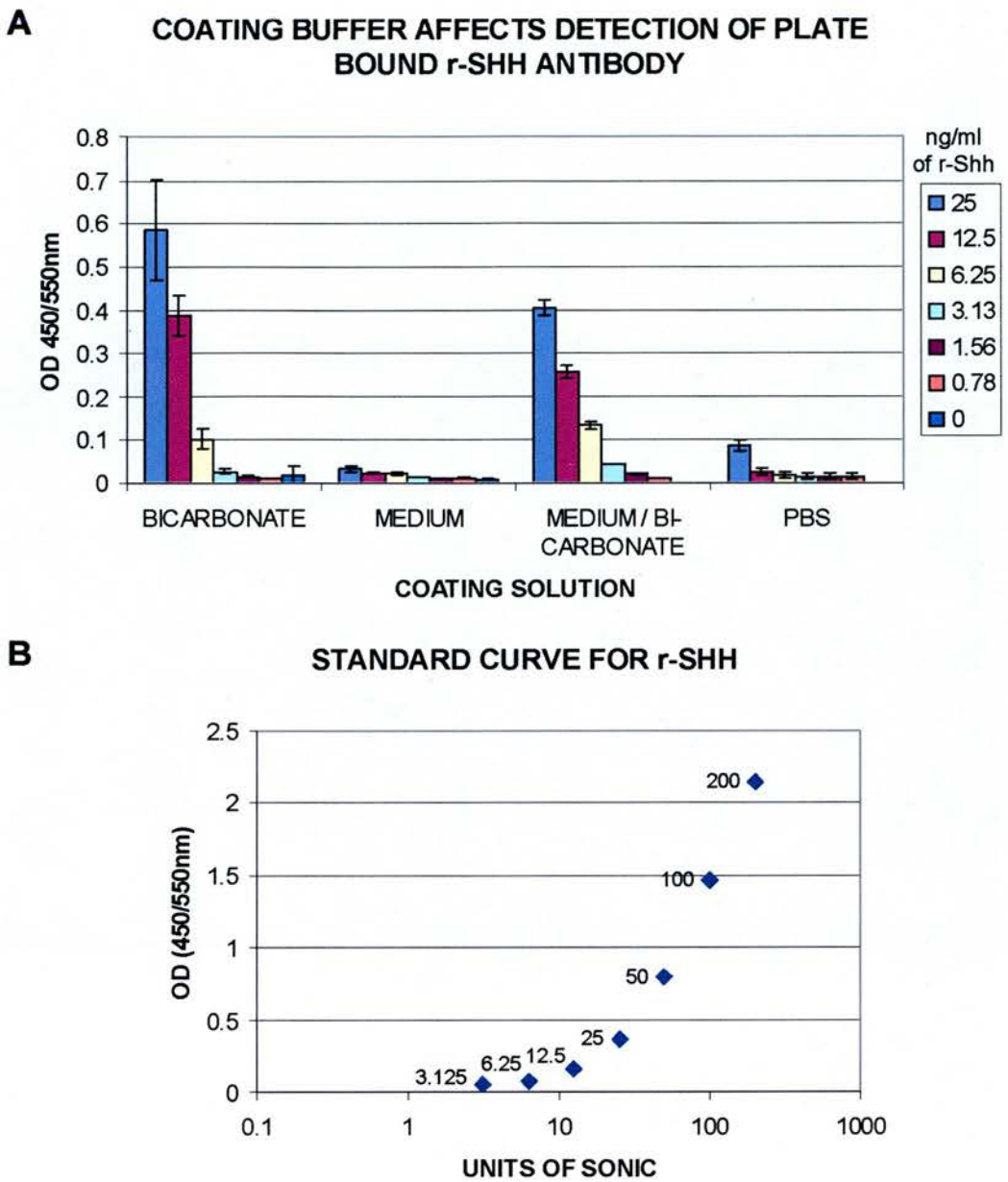

Figure 3.10 Coating Buffers & Standard Curves In 5E1 ELISA
[A] demonstrates the affect of different coating media on the efficiency of the 5E1 ELISA. Coating media are shown on the x-axis where bicarbonate is the standard bicarbonate buffer. Medium is Waymouths CMT media with 5% FCS (see Chapter 2). [B] shows an average standard curve obtained with the 5E1 ELISA using the protocol described in Chapter 2. The concentrations of r-Shh (ng/ml) added are given beside each data point.

ELISA plates were run with multiple controls; most commonly an appropriately diluted complete cell lysate of the cell type being analysed along with a control r-Shh peptide aliquot of 50ng/ml. This allowed for the rejection of data sets if values were too variable. Supernatants were assigned units rather than ng/ml quantities as antibody affinity for r-Shh may differ from that of native cholesterol modified and palmitoylated Shh. The

specificity of the 5E1 ELISA system was confirmed via pre-incubation of 5E1 with r-Shh peptide as shown in Figure 3.11.

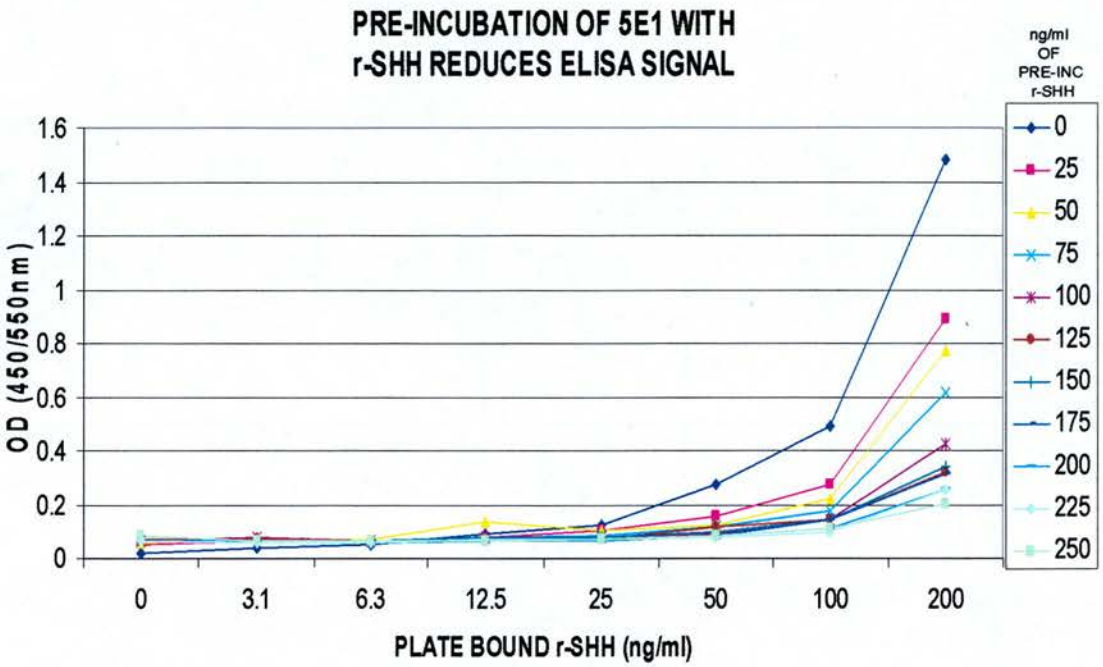

Figure 3.11: Pre-incubation Validation of ELISA

Overnight pre-incubation of 5E1 with r-Shh reduces signal in the 5E1 ELISA system. Complete blocking (<0.05) achieved with >1μg peptide (data not shown).

SANDWICH ELISA

Given that the linear range of the 5E1 ELISA system is in nanogram quantities, sandwich ELISA`s were investigated as a means of increasing sensitivity to a picogram range.

The sandwich ELISA involved pre-coating high binding EIA plate in anti-Shh antibody (N19 or 5E1) as a "capture" layer, followed by a protein rich block to prevent non-specific binding. Sample was then added, followed by the anti-Shh antibody not used in coating ("primary detection"), then the relevant biotinylated anti-Ig against that antibody ("secondary detection") for streptavidin/ substrate visualisation.

Sandwich ELISA's were attempted utilising the N19 and 5E1 antibodies in both orientations. Initial studies concentrated on plate bound monoclonal 5E1, with N19/antigoat detection, but failed to generate a specific ELISA.

This was not improved by reversing the orientation, alterations in blocking protocol, or concentrations of constituent antibodies, suggesting a non specific signal. Pre-incubation of component antibodies overnight at 4°C with goat or mouse serum did not affect non specific signal.

Due to these limitations the one way 5E1 ELISA system has been used for the work in this thesis. However, a Shh sandwich ELISA system has subsequently been marketed by R&D labsystems and has been run concurrently with the 5E1 ELISA system. R&D kits detected Shh in both embryonic and adult mouse brain homogenates titred from a concentrated stock, but at a greatly reduced level compared to the 5E1 ELISA system. Adult brain was calculated at 7000 units (ng/ml) using the 5E1 ELISA whilst the R&D kit gave a value of just 82pg/ml. Equally in the embryonic brain, the 5E1 ELISA gave a value of 141000 units (ng/ml) vs. a 3.2ng/ml value for the R&D kit. Thus it was not surprising to find that the R&D ELISA failed to detect Shh in CMT supernatants, or those of T-cell preps, where western and immunohistochemistry have previously shown the presence of Shh (J.Lowrey, personal communication). Personal communication with the supplier has confirmed that this assay system has never been validated against native Shh, as all studies were performed using a cell line transfected with recombinant protein where cholesterol and palmitoylation do not occur.

More recent attempts at generating a Shh sandwich ELISA with new N19 have yielded excellent results, with sensitivity above that of the current 5E1 ELISA system and commercial kits, but came too late for data analysis in this thesis. A standard curve using this system has been included in an Appendix to this thesis (Figure 7.1). Thus it would seem that the original cross reactivity problems found in the generation of an in house sandwich ELISA system may of lain in some component of the Santa Cruz N19 antibody, although variation in batches of r-Shh cannot be excluded.

3.2.6 SONIC HEDGEHOG BIOASSAY

The Shh protein is a heterogeneous molecule, given that it can be released with a range of differing chemical modifications, which markedly affect its signalling ability [20]. Whilst the Shh ELISA system gives an indication of the

relative concentration of Shh, it does not quantify this variation in functionality. Given that hypothetically, a cell could up-regulate Shh signalling in response to a stimulus, by just fully modifying all of the Shh released from the cell, a bioassay approach was also taken.

Initial investigations into a bioassay system concentrated on the use of the C3H10T1/2 cell line. Addition of r-Shh to cultures of C3H10T1/2 has been shown to induce differentiation into osteoblast like cells, positive for alkaline phosphatase (ALP) activity [173, 174]. Despite repeated experiments with new batches of cell line at low, medium and full confluence culture, in 6, 12 and 24 well formats and with normal and charcoal stripped serum at various concentrations, it has not been possible to repeat this observation with >1ug r-Shh. The Shh signalling blockers Cyclopamine and 5e1 had no effect on cellular MTT signal in these cells (data not shown).

Given the difficulties encountered with the C3H10T1/2 cells, a vector containing a luciferase under the control of *Gli* responsive promoters was obtained via personal communication with the lab of Beachy et al [126]. Using this system it was hoped to obtain a directly proportional readout of Shh activity, as Shh signalling involves Gli activation and up regulation, which in cells transfected with a *Gli* responsive luciferase, should result in increased luciferase expression, quantifiable on a luminometer.

Lipofectamine was used, following optimisation (Figure 3.12) to transfect permissive NIH-3T3 cells with the *Gli* reporter construct along with a control firefly luciferase construct, for use in Promega`s stop and glow dual luciferase system. This too has failed to yield the expected results, with supernatants and recombinant peptide failing to induce significant levels of luminescence. Initial studies were hampered by use of a dual fluorescence/luminescence system, which lacked sufficient sensitivity. Improved results were obtained with a single function luminometer, but results were highly variable and will require transfection and protocol system re-optimisation before yielding interpretable results. Thus at the time of submission a functional Shh bioassay had not yet been established.

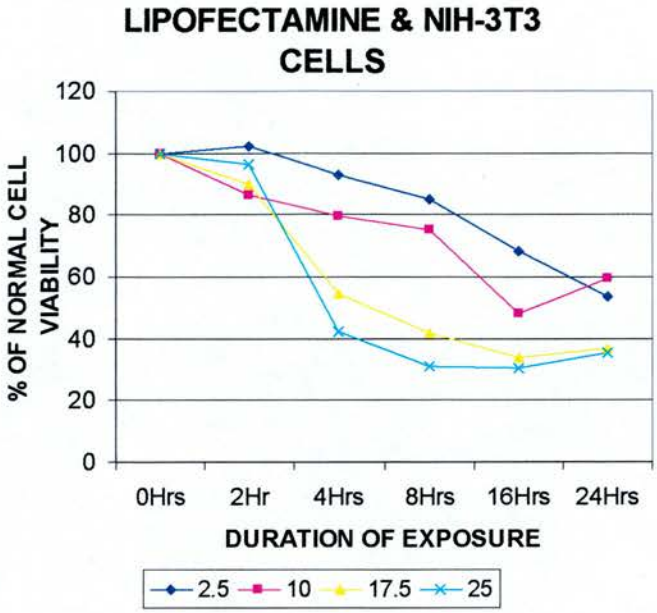

Figure 3.12: Lipofectamine Titration with NIH-3T3
NIH-3T3 cells plated at $2x10^5$ per well in 24 well plates. Viability values taken from MTT assay (1hr cell culture, 350µl DMSO, 100µl per well in 96 well plates). Legend refers to µl of lipofectamine used in transfection mix (see Chapter 2). Vectors in absence of lipofectamine did not affect cell viability. N=1.

3.2.7 SHH RELEASE BY H_2O_2 EXPOSED EPITHELIAL CELLS

Given the interesting changes in Shh immunohistochemistry following H_2O_2 and FITC exposure, the 5E1 ELISA system was used to analyse the supernatants taken from the cell injury assays for expression of soluble Shh. This was performed with both the human (A549) and Mouse (CMT) epithelial cell lines as described previously.

CMT

Shh production by CMT cells was within the lower region of the 5E1 ELISA standard curve (Figure 3.13), but would appear to be constitutive given the statistically significant increase between 6 and 48hrs without treatment, although given the small increase in this expression it is unlikely to have biological significance. Other than being proportional to cell number, Shh release was not affected by plating density (data not shown).

Exposure to FITC/DMSO for 1.5hr did not affect Shh production other than to reduce values in those wells where MTT assays would indicate a reduction in

the number of viable cells. These experiments were repeated six times (data not shown). Exposure to H_2O_2 for that same period resulted in a 25 fold increase in ELISA signal at 6hrs post exposure to 40mM H_2O_2, decreasing with time in culture, and with the concentration of H_2O_2 used (Figure 3.13). The temporal decline in Shh levels continues up to 96hrs post H_2O_2 exposure (data not shown).

No difference in *Shh* mRNA expression could be identified with semi-quantitative RT-PCR through 6-48hr post H_2O_2 exposure.

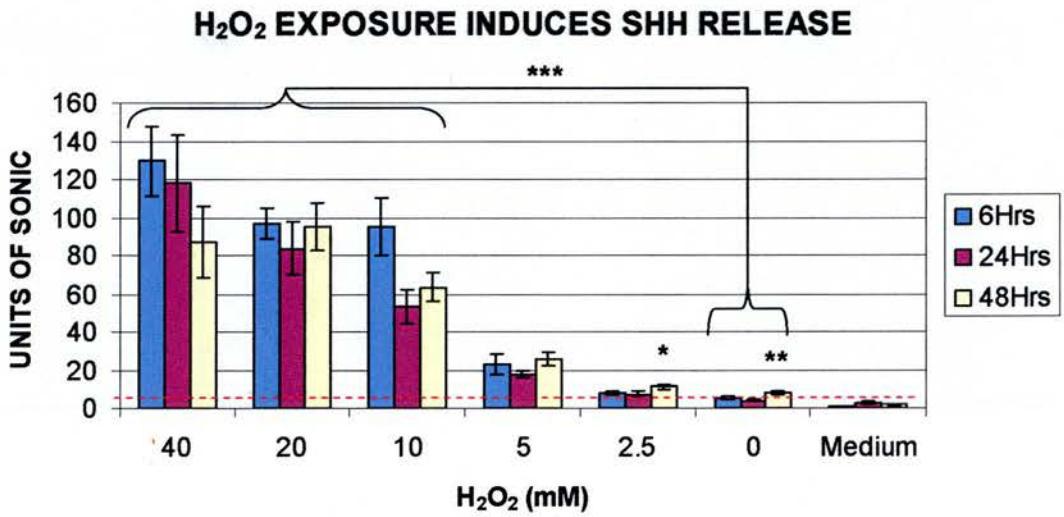

Figure 3.13: Shh Detection In CMT Supernatants
Cells plated at $2.5x10^5$ cells/ml, 500µl per well of a 24 well plate, 24hrs prior to H_2O_2 exposure for 90 minutes. Times denote time post H_2O_2 removal. 40mM H_2O_2 gave a 25 fold increase in soluble Shh at 6Hrs. Red line denotes lower range of the ELISA detection (3 units/ml). n=12. Error bars denote Standard Error. Significance of *p<0.05, **p<0.01, ***p<0.001 by parametric tests.

A549

A549 release Shh constitutively when passaged. Maximal levels were reached by 48hrs (post plating) regardless of plating density (Figure 3.14). Suggesting either release rather than active production, or a method of autocrine controlled release. Given the rapid detection of Shh following H_2O_2 exposure in CMT cells, when these experiments were performed on A549 cells, the supernatant containing H_2O_2 was collected following the 90 minute exposure period and corresponds to the 0Hr value in Figure 3.14.

A549 cells exposed to H_2O_2 show maximal Shh ELISA signal at 6hrs in the top three titrations of H_2O_2 used. Notably, exposure to 40mM and 20mM leads to increased soluble Shh within 1.5hrs of the addition of H_2O_2 (blue 0Hr bars, see below) Use of lower concentrations of H_2O_2 with A549 resulted in correlating increases in MTT and decreasing soluble Shh as observed in CMT cells.

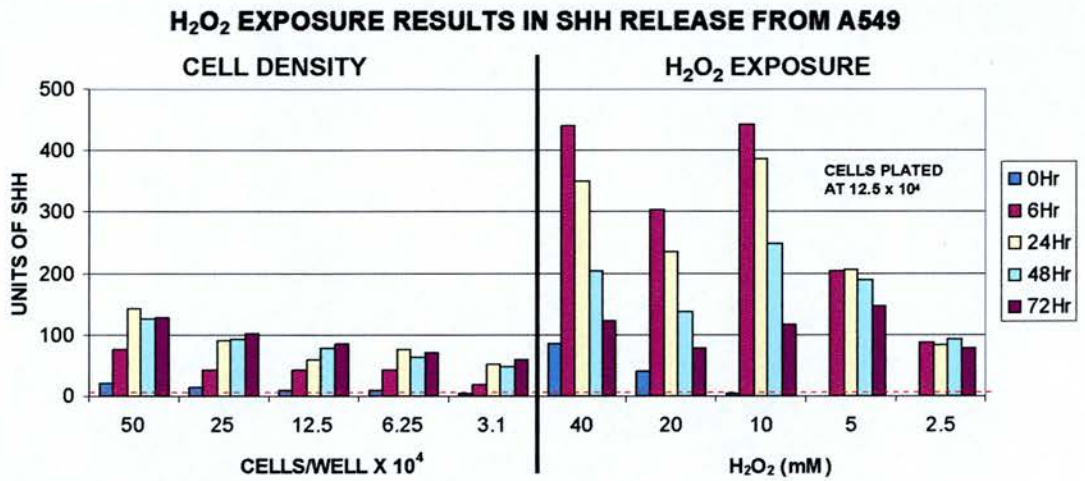

Figure 3.14: H_2O_2 Exposure Results in Increased Soluble Shh
Values have medium alone controls subtracted. H_2O_2 exposure for 1.5hrs in serum free media results in increased ELISA signal. 0Hrs represents 1.5Hr damaging solution prior to removal for wash step. Representative of three repeats. Red line denotes limit of sensitivity.

3.2.8 SHH RELEASE INCREASES WITHIN 1 HR OF EPITHELIAL H_2O_2 EXPOSURE

As peak soluble Shh levels were detected less than 6hrs post removal of H_2O_2 in CMT cells and within 90 minutes of addition in A549 cultures, shorter time point studies were undertaken with CMT cells.

CMT cell supernatants, containing the H_2O_2, were taken at intervals up to two hours after H_2O_2 addition. Both 40mM and 20mM concentrations resulted in a significant increase in Shh ELISA signal by 100 minutes post damage (Figure 3.15 [C]).

Cellular integrity and viability were measured with a commercially available Lactate dehydrogenase (LDH) kit, where colourimetric detection of LDH in

media signifies a loss of cellular retention, and therefore reduced membrane integrity.

LDH levels increase significantly, correlating with a H_2O_2 specific fall in MTT signal over the same time interval (Figure 3.15 [A] & [B]). The possible effects of injurious agents in media causing artefacts in LDH, MTT, ELISA and CBA applications were assessed by equalising the concentration in all samples following collection and application. No interference was identified, (data not shown)..

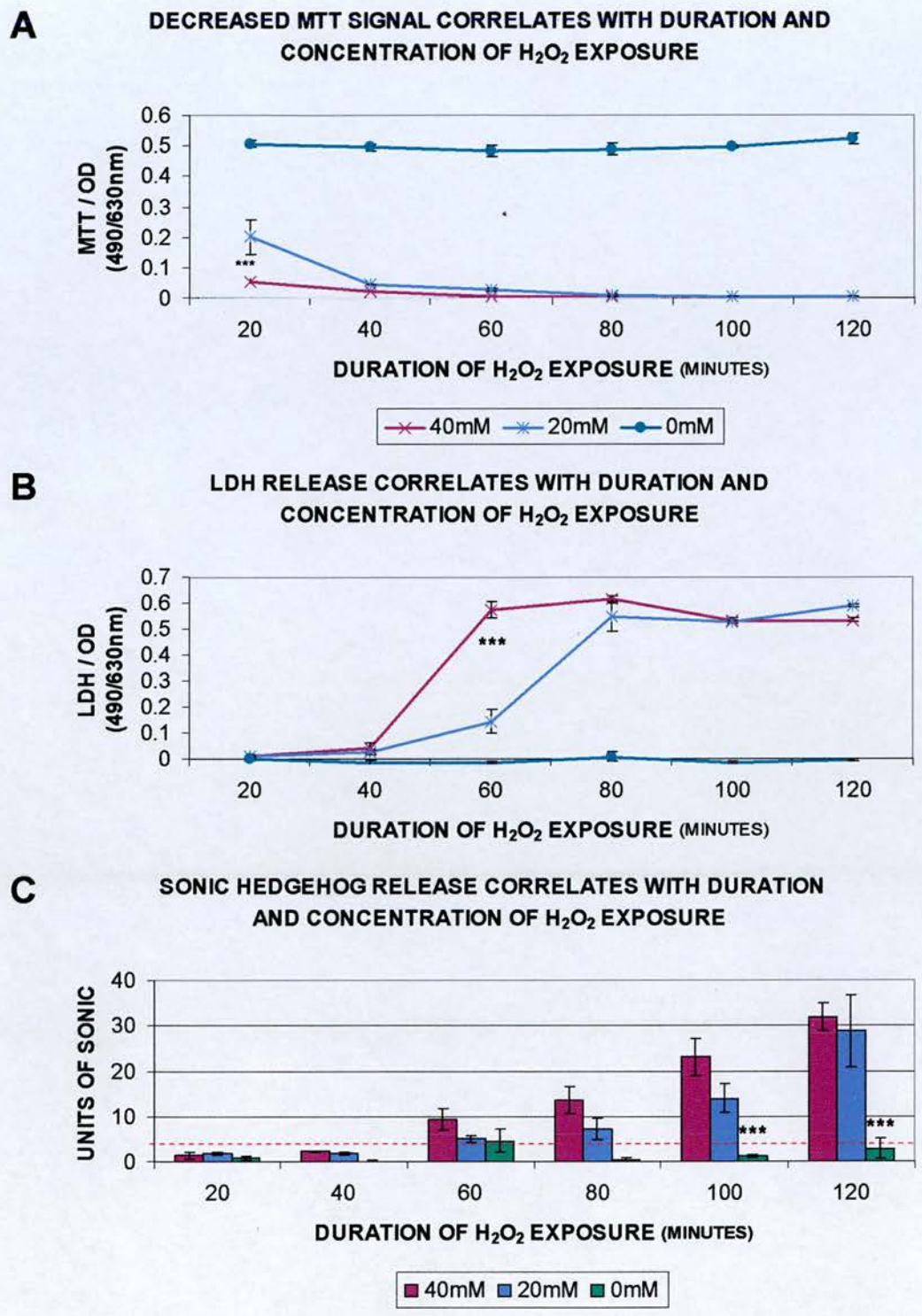

Figure 3.15: Short Term Response To H_2O_2 Exposure
[A] MTT data [B] LDH release [C] 5E1 ELISA data all n=3 with Medium Alone controls subtracted. Derived from cells not more than three passages different from long time point damage experiments. Supernatants contain H_2O_2, which does not affect MTT, LDH, Shh or Duoset ELISA detection, as determined by equalised supernatant controls (data not shown). Error bars denote Standard Error. Red line denotes limit of sensitivity. Statistical analysis *p<0.05, **p<0.01, ***p<0.001 by parametric tests.

Semi quantitative RT-PCR for *Shh* was performed in CMT cells exposed to H_2O_2 at 5mM. This reduced concentration was chosen to maximise RNA recovery from cellular material, but at a concentration where preliminary studies had confirmed an increase in soluble Shh protein to approximately 20 Shh units, 120 minutes post H_2O_2 administration. Although subsequent studies have shown that viable cellular RNA with no evidence of laddering can be obtained from non-adherent cells centrifuged from injury assay supernatants prior to sample freezing. This would suggest that RNA data may be obtainable from 40 and 20mM concentration experiments, by pooling floating and adherent cells. The occurrence of viable RNA in floating cells also has important implications for cellular viability assays as one of the assumptions of the MTT assay used here is that adherent cells are the viable population and that floating cells are non-viable. A viable floating population of cells might explain the protein release observed in Figure 3.14 in the absence of viable cells, when using the MTT assay.

Studies identified *Shh* mRNA as being highly susceptible to freeze thaw degradation and prolonged storage on ice. However two of three studies demonstrated an up regulation in mRNA in response to H_2O_2 as shown in Figure 3.16. *GM-CSF* mRNA expression was not detected during the H_2O_2 exposure period or up to 1 hour post H_2O_2 removal, thus initiation of transcription must occur between 1 hour post H_2O_2 and 6 hours (Figure 3.4).

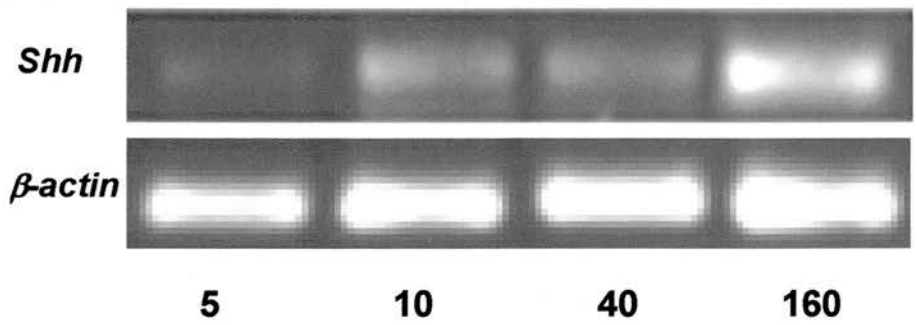

Figure 3.16: Shh mRNA Increases Following H_2O_2 Exposure
Semi quantitative RT-PCR for Shh mRNA at 35 cycles including *β-Actin* loading controls at 26 cycles. Products loaded in orange g on a 2% agarose gel. Numbers refer to minutes post addition of H_2O_2 (5mM).

3.2.9 r-SHH INCREASES IL-6 PRODUCTION IN CELL LINE FIBROBLASTS

Having identified Shh up regulation and release in response to injury, preliminary investigation was made into potential affects of this signal on other pulmonary cells. Given the expression of Shh in areas of fibrosis in human and induced mouse disease, fibroblasts were investigated as a potential responder population to the Shh signal.

A mouse fibroblast cell line CCL-206 (ECACC) was used to investigate the potential effects of r-Shh and CMT cell supernatants on proliferation and cytokine production. Addition of r-Shh to CCL-206 had no effect on proliferation when measured by MTS (a variant technique of MTT which includes viable floating cells) or tritiated thymidine, and neither did 5e1 controls (Figure 3.17). This was reciprocated with H_2O_2 exposed, 6hr CMT cell supernatants and Cyclopamine treated (5μM) controls (data not shown).

CCL-206 were found to produce MCP-1 constitutively, but did not express detectable levels of the cytokines TNF-α, IL-12p70, IFN-γ, MCP-1 and IL-10. This expression profile was not altered by r-Shh or CMT supernatants. However, IL-6 production was identified in CCL-206 exposed to the highest dose of r-Shh used, but represents only one experiment and is close to the lower level of sensitivity in CBA applications, although titration would indicate a potential trend in response (Figure 3.17[C]). This will require replication. Changes in collagen expression were not investigated.

3.2.10 THE GM-CSF AND IL-8 RESPONSES ARE NOT AUTOCRINE

Given the expression of ligand and receptor on the same cell it was hypothesised that Shh release might represent an autocrine signal involved in the up regulation of GM-CSF/IL-8 in the CMT and A549 cells respectively.

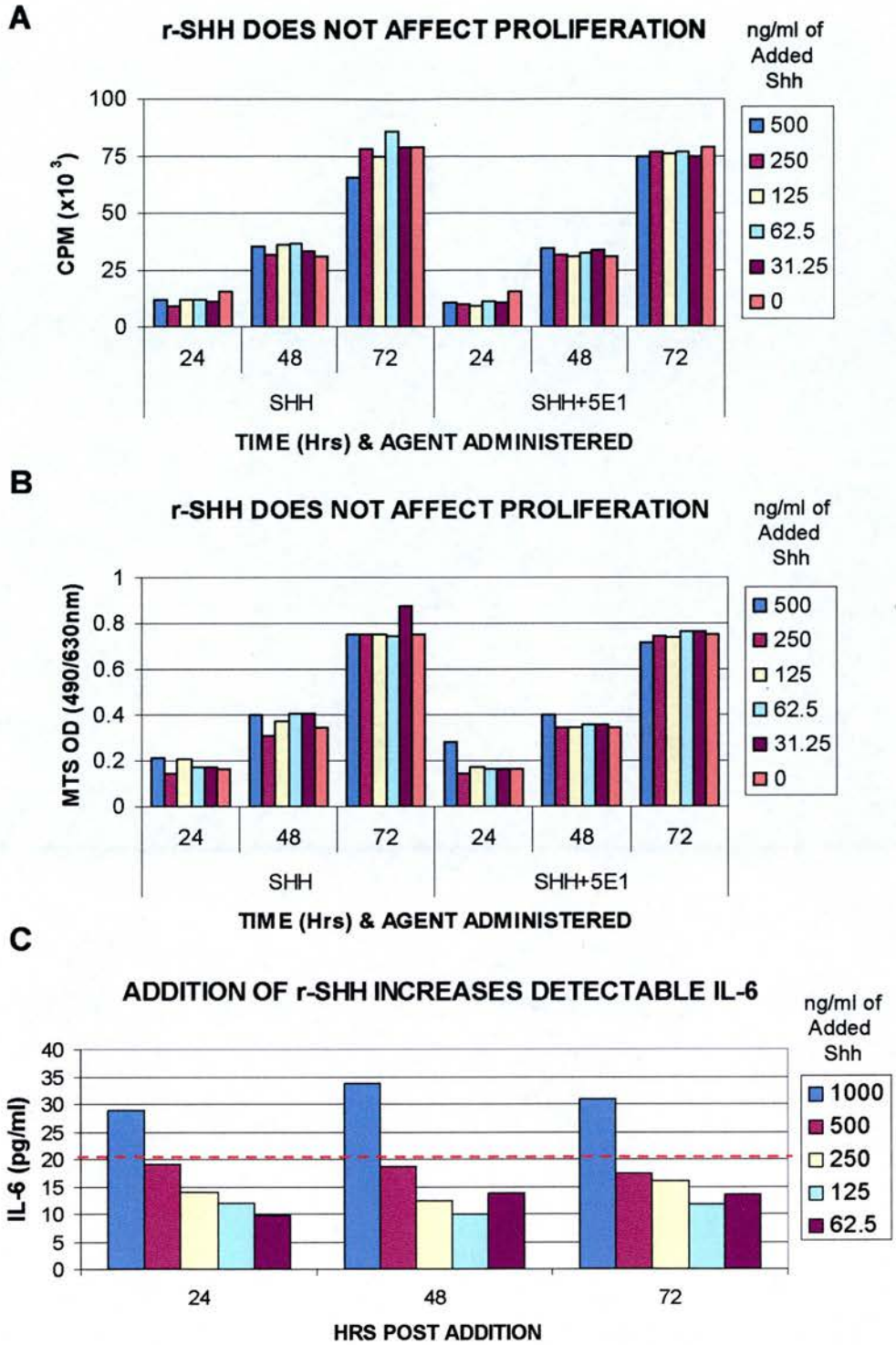

Figure 3.17: r-Shh Increases IL-6 Release from a Fibroblast Cell Line Without Affecting Proliferation

Fibroblasts plated in 500µl from $1x10^5$ cells/ml in 24 well plates, 24 hrs previous to the addition of agents to be tested. Shh pre-incubated with 5E1 for 1hr at 37°C prior to addition. [A] MTS signals (viable cell no) were not affected by Shh or 5E1 addition, representative of 2 repeats. [B] Tritiated thymidine incorporation was not affected by addition of Shh or 5E1 (n=1). [C] Addition of r-Shh resulted in increased IL-6 (n=1), red line denotes limit of CBA sensitivity.

Addition of r-Shh titrated to >1ug failed to induce any proliferation or cytokine response in either CMT cells or A549 cells, as measured by MTS and ELISA/CBA. Further to this, injury of CMT cells in the presence of Cyclopamine, a Shh inhibitor, had no affect on GM-CSF response. Addition of 6hr CMT cell supernatants to undamaged CMT cells also failed to yield any cytokine response, although proliferation was highly variable, likely a complication of differential nutrient depletion (data not shown). These experiments would suggest that Shh release was not a soluble autocrine signal for those responsive cytokines identified here.

3.3 DISCUSSION

3.3.1 INTRODUCTION

By utilising a mouse type II like epithelial cell line (CMT) an immediate up regulation and release of soluble Shh in response to H_2O_2 has been identified, with both RT-PCR and a novel Shh ELISA developed here. Release continued for between one and six hours post H_2O_2 removal, followed by an up-regulation and release of GM-CSF 24-48hrs later, which was shown to be Shh independent. Human epithelial type II cells (A549) demonstrated a similar release of Shh post H_2O_2 exposure, suggesting a common pathway in both species. In contrast GM-CSF was not up regulated in human cells, but IL-8 up regulation did occur. Preliminary investigations would suggest that cell line fibroblasts may up regulate IL-6 release in response to r-Shh, but not proliferation.

For reasons of clarity, given the broad scope of data presented in this chapter, the findings summarised above will be addressed according to the aims presented in Section 3.1.3, these were as follows:

- Establish an *in vitro* damaging assay system
- Identify epithelial cytokine response to *in vitro* injurious stimuli
- Develop a quantitative method of detecting Shh
- Investigate the postulated link between Shh and injurious stimuli
- Determine whether Shh exposure alters fibroblast activity

3.3.2 THE ESTABLISHMENT OF AN *IN VITRO* DAMAGING ASSAY SYSTEM

Establishment of the damaging assays fulfilled one of the aims of this chapter and facilitated later cytokine analysis. Whilst addition of H_2O_2 was relatively straightforward, addition of FITC *in vitro* proved problematic (Section 3.2.1), necessitating its prior suspension in DMSO; a step which may have affected the epithelial responses observed, thus limiting its comparative value with the FITC *in vivo* model. To fully characterise the response of epithelium to FITC, it may be necessary to develop a different manner of administration, perhaps

using pre-conjugated FITC. However, given that FITC normally persists in the lung, and that its persistence is in part due to its ability to conjugate itself with host proteins, use of pre-conjugated formulations, such as those with bovine serum albumin (BSA), may not be instructive. It may be that accurate, *in vivo / in vitro* relevant data can only be obtained using FITC as insoluble clumped aggregates in cell medium. This may no longer be such a complication for downstream applications as BD now produce CBA cytokine arrays with a choice of a variety of fluorescence and bead size choices, which will facilitate cytokine detection without the use of FITC conjugated beads, thus avoiding supernatant interference, although the extent of fluorescence into the red channel would also have to be compensated for.

MTT was the main assay utilised in the measurement of cellular number. This assay utilises cellular mitochondrial activity to convert a pale yellow / green substrate into an insoluble purple substrate for colourimetric analysis. When considering data derived from this assay, it is important to appreciate that it represents an accumulation of MTT over the duration of the assay; 45 minutes for A549 cells and 3 hours for CMT cells. Thus whilst high concentration H_2O_2 exposure in CMT results in a low MTT signal, there are actually viable cells remaining at the start of the assay, but these are lost into the supernatant during the period of the assay, leading to a low final MTT value. Equally, high quality un-laddered RNA can be retrieved from non adherent cells following injurious exposure. Thus it is likely that these cells could persist to release protein, where adherent MTT values would suggest the absence of viable cells. As an approach to address this problem, studies were conducted with MTS, a Promega product which produced a soluble colourimetric signal, thus giving an estimation of both adherent and non-adherent viable cell number, (see Figure 3.17 for its use in fibroblasts). However, this was unsuitable for injury assays due to the variation in phenol red colouration in medium and arising from this, the limited availability of phenol red free Waymouths medium used for the culture of CMT cells.

Another consideration when using the MTT assay is that MTT is itself inherently toxic, and although titres of concentration and duration were prepared for each cell type, injured or activated cells may be more

susceptible to its toxicity, thus artificially reducing the apparent number of viable cells following injury.

The assumption that reduced MTT signal represents a reduction in viable cell number would appear vindicated by the correlation of decreased MTT signal with increased LDH in medium (Figure 3.15). Data presented here clearly indicate that this reduction in cell viability (MTT) and loss of membrane integrity (LDH) is associated with an immediate increase in the release of Shh, preceding a subsequent increase in detectable GM-CSF (mouse) or IL-8 (human).

3.3.3 THE EPITHELIAL CYTOKINE RESPONSE TO INJURIOUS STIMULI

Unlike the increase in Shh with H_2O_2 exposure, the increases in GM-CSF (CMT cells) and IL-8 (A549 cells) were more typical up regulation responses, occurring within 6hrs of stimuli, and increasing subsequently. Up regulation has been confirmed at the genetic level for *GM-CSF* (Figure 3.4), but this has yet to be confirmed for *IL-8*. The up regulation of GM-CSF in CMT cells but not A549 cells could represent a species difference, but could also represent a variation in epithelial subtype.

GM-CSF

GM-CSF can act as a macrophage activator and AM differentiation polarisation signal[106], enhancing the removal of damaging agents and necrotic epithelium[175], whilst also maintaining an anti-inflammatory environment, via the generation of new unactivated AM. GM-CSF also stimulates DC maturation and migration to the lymph nodes, facilitating a rapid adaptive response to damaging pathogens. But it is the ability of GM-CSF to promote monocyte and polymorphonuclear cell survival that is probably the key to its function in pulmonary systems, when up-regulated in response to H_2O_2 injury.

GM-CSF may also function as an anti-fibrotic signal, as knockout mice exhibit exaggerated fibrotic disease[103]. Thus up regulation of epithelial GM-CSF in response to oxidising injury could represent an attempt by the epithelium to

limit profibrotic side effects to mediators produced by cells infiltrating the site of injury or by the epithelium itself.

IL-8

IL-8, increased in H_2O_2 exposed A549 cells, acts as a chemotactic factor recruiting neutrophils, T-cells and basophils to sites of infection, and is key to the management of infection, as discussed in Chapter 1. However, over expression can lead to chronic inflammation and fibrosis through the secondary function of mediators produced by inflammatory infiltrates, and has been postulated as the initiating factor in a number of chronic inflammatory / fibrotic disorders[176].

MCP-1

Interestingly, there was no up regulation in MCP-1 in mouse epithelium with either FITC or H_2O_2 exposure, where knockouts of the MCP-1 receptor (CCR-2) protect against pulmonary fibrosis[121, 177], and *in vivo* studies have shown strong up regulation associated with FITC models of lung inflammation / fibrosis[121, 177], suggesting that MCP-1 is crucial in pulmonary fibrosis. A possible explanation for the absence of MCP-1 effects in the studies presented here when compared to those of others [121, 177] comes from the use of whole lung homogenates in published studies, thus MCP-1 up regulation may be a feature of another pulmonary cell type, such as the fibroblasts, rather than epithelial cells, alternatively, epithelial MCP-1 up regulation may require a signal or co-factor not present in *in vitro* monocultures or carcinoma derived cell lines.

3.3.4 SHH DETECTION SYSTEMS

Immunohistochemistry on cells grown on Nalgene coverslides and exposed to FITC or H_2O_2 would suggest that Shh becomes membranous within 45 minutes in response to both stimuli, and that subsequent time points show less Shh than controls. This correlates with the observations made in H_2O_2 studies concerning the release of soluble Shh, but not FITC, where FITC was *not* found to alter soluble Shh at 6hrs post removal, (short time course studies were not performed).

There are four possible explanations for this observation.

i. Soluble Shh is released *and* up regulated in H_2O_2 injury whereas FITC induced injury only results in release, which is recycled by the epithelium itself by 6hrs post removal
ii. The presence of FITC hides or sequesters soluble Shh either directly through covalent attachment, or indirectly through up regulation of a scavenger such as Hip or HSPG's.
iii. Shh immunohistochemistry is not Shh specific
iv. Shh, induced by FITC exposure, is modified in a manner making it undetectable to either the 5E1 (ELISA) or N19 (IHC) anti-Shh antibodies.

In addressing the third explanation listed above, it is important to appreciate that Shh data presented here and discussed subsequently relies heavily on the selectivity and sensitivity of anti-Shh antibodies, as does the original premise of Shh involvement in interstitial lung disease. Thus this issue is central to the work presented in this Chapter and warrants further discussion.

Whilst standard immunohistochemistry on tissue sections has been blocked routinely in the lab by myself and others (Figure 7.2), it was not possible to block Shh staining on cell lines grown on cover-plates. This was not a feature of secondary cross reactivity as both Shh and Ptc used an anti goat secondary, where primary omission controls were negative. The blocking methodology would also appear to be correct given that Ptc staining could be blocked. Thus, the failure to block was a feature restricted to Shh staining. A reaction of blocking peptide with substrate or secondary antibody can be excluded given that blocking peptide with no primary antibody control was negative (data not shown). Some insight into this apparent failure can be drawn from the fact that staining actually increased with an increased ratio of peptide to antibody. From this data a hypothesis could be drawn that the N19 antibody blocking peptide, originating as a sequence of the Shh peptide, is bound by Ptc. Thus when N19/peptide is added it binds to Ptc, generating a positive signal. The greater the concentration of peptide the greater the Ptc binding.

Whatever the cause, the occurrence of the protein in a validated and blocked ELISA (Figure 3.11), and the identification of mRNA sequence (Figure 3.16) would suggest that wholly non specific Shh immunohistochemistry is highly unlikely, and the observations are more likely an erroneous feature of the blocking process.

A failure to replicate the observations made with the in house 5E1 ELISA system, using the commercial ELISA can be explained through a personal communication conducted with representatives of R&D, who produce the commercial Shh ELISA. They confirmed that validation was limited to recombinant Shh and that the assay had never been applied to native protein. Thus an absence of Shh signal from supernatants in this system could be a result of steric interference resulting from the modifications present in native peptide. Indeed, the 5E1 monoclonal used here is the only currently available Shh specific antibody to have had its binding specificity intensively investigated and established, where binding has been localised outside of these modification sites[162].

Certainly, comparisons between the in-house and commercial assays would suggest that whilst the commercial kit has higher recombinant sensitivity, its detection of native protein is highly restricted. Embryonic brain homogenate, required only a 1 in 5 dilution to reach the linear phase of standard curve in the commercial kit, compared with a 1 in 1000 dilution required for the 5E1 ELISA system.

Attempts to confirm ELISA data with a bioassay as a non-antibody dependent measure of Shh release and functionality were not successful. Studies here concluded that the C3H10T1/2 assay was not sensitive or robust enough for use with culture supernatants. Initial characterisation of the assay may also require a greater concentration of r-Shh than is economically practical in this lab, without in house isolation, purification and quantification of the more active native protein [126] [20]. Preliminary Gli luciferase construct experiments concluded that highly variable transient transfections were not suitable for regular use and that dual function fluorometer / luminometers did not posses sufficient sensitivity to be compatible with this assay. Other

explanations for the failure to reproduce the results observed by Taipale *et al*[126] with this peptide include loss of functionality at some point in the amplification and isolation process, which would seem unlikely given restriction digest analysis (Section 2.4.2) or loss of patched expression in the transfected cell line. Although others have shown that both C3H10T1/2 and NIH-3T3 cells posses this molecule this was never undertaken in this lab, but could be easily performed in future studies at mRNA and protein levels. Taipale *et al.* also used in house generated Shh with both cholesterol and palmitoyl modifications, thus it is possible, although unlikely, that this assay requires Shh to have these modifications. A more likely interpretation is that, similar to the C3H10T1/2 assay, the use of the fully modified, and therefore >40 fold more active protein than r-Shh may make the investigative approaches taken here with r-Shh, both uneconomical and un-physiological. If the latter explanation holds true then the failure of epithelial supernatants to induce fluorescence in this assay can only be attributed either to its absence and therefore erroneous ELISA data, the absence of modifications on this protein, or some inhibitory factor also contained within the supernatant. The solution to this conundrum will undoubtedly lie in the modification of the plasmid vector to facilitate the generation of a stable transfection in the NIH 3T3 cell line to allow procedural optimisation, perhaps with the newly commercially available modified r-Shh peptide (R&D) alongside supernatant additions with and without this peptide.

3.3.5 SHH SIGNALLING FOLLOWING INJURIOUS STIMULI

Given the prompt release of Shh, some 100 minutes post H_2O_2 exposure, and the identification of transcriptional up regulation, it is likely that increases in Shh represent a release of intracellular stores with necrotic injury (LDH release), but that those cells which survive exposure up regulate Shh expression, perhaps as a means to replace released stores, or as a means to increase release. It is possible that this up regulation is inconsequential and that soluble Shh is primarily a necrotic leakage. This does not negate its potential as a signal, indeed it could be hypothesised that this release might represent an *in vivo* danger signal, a means to preserve immune function,

through preserved T-cell function[2, 3], or act as a functional signal to neighbouring epithelial / fibroblastic cells[178].

However, such release would seem unlikely in an *in vivo* setting, due to the sentinel engulfment function of the AM. Although, there may be a limit to the level at which necrosis can be controlled in persistent inflammation and fibrosis. Certainly, necrotic cells have been identified in UIP sections[179 180], although more recent studies would suggest that apoptosis may be the dominant cell death process in UIP biopsy.[181] Such conflicting studies may be rationalised if necrosis is considered a feature of exacerbating disease, over and above persistent apoptosis in UIP.

If the observed up regulation is considered a significant finding then this could have important implications for Shh expression in human disease. If Shh is considered a marker of injurious up regulation, then its expression in regions of disease could indicate the involvement of some persistent injurious stimuli, leading to the chronic up regulation observed in UIP.[1]

The release of Shh by injured cells positions Shh, an epithelial mitogen, centrally within areas of potential epithelial denudement, thus here it could represent a normal repair mechanism, equally its interactions with the FGF`s in development, if recapitulated, could represent a means of inducing changes in the extracellular matrix or fibroblastic growth and activity to induce sealing of denuded areas preventing transudation of fibrotic growth factors from the serum into the air spaces. Such activity could place Shh as both an ameliorative and a pro-fibrotic factor in disease.

The underlying premise of this Chapter has been that by using cell lines, it is possible to avoid the injurious extraction and isolation of primary epithelial cells, facilitating a more accurate analysis of cellular response to injury in a defined population. Whilst this is undoubtebly true for inflammatory cytokines, and signals not involved in epithelial proliferation and viability; use of cell lines in the analysis of remodelling and developmental signals may be fundamentally flawed. Both cell lines shown here are derived from carcinomas, where the most common cancer associated genes in epithelium

are developmental. A549 are well characterised producers of Shh protein, an epithelial mitogen, and in that sense do not represent a normal epithelial cell, where expression has been found lacking[1]. Similarly, CMT are constitutive producers of Shh protein, where my primary cell work, (Chapter 4) and that of others would indicate that this is not the case in normal mouse epithelium[1, 73, 74]. In addition, cell lines, by their very nature, are immortal thus an analysis of proliferation following injury, whilst indicative, yields little of comparable value for *in vivo* systems.

However, given that Shh has been hypothesised as an indicator of epithelial activation and/or injury, primary isolation work is also impractical. Human primary epithelial cells are also rarely available, and primary pulmonary epithelial cell yields from mice are low, thus requiring sufficient mouse numbers to make studies such as those conducted here, restrictive both ethically and economically.

An ideal analytical tool would be a more specific advancement on the combined immunohistochemical and *in situ* RT-PCR techniques currently used for *Shh* in the gut [182]. This would address the immunohistochemistry concerns expressed here and in Chapter 4 and would confirm producer cell populations, over those which may have received protein in a Ptc, Megalin or Hip associated manner. This approach is discussed further in Chapter 5.

3.3.6 EFFECT OF SHH ON FIBROBLAST ACTIVITY

Given the hypothetical role of Shh as an indicator of injury and the localisation of Shh epithelial expression *in vivo* to epithelium in areas of fibroblastic foci in both mouse and human[1], it was postulated that Shh might modulate fibroblast function. Neither the addition of exogenous Shh, nor blockade of Shh signalling resulted in any change in fibroblast proliferation (Figure 3.17). Once again this study was limited by the use of a cell line. These studies could easily be extended to primary cell isolates, better suited to a proliferation readout. However, there can be significant variations in primary fibroblast isolate subtype, affecting both their response and proliferative rate. Thus the passage number at which the experiment is

performed could determine the fibroblast population and therefore the response obtained. A future point of analysis might be the real time analysis of procollagen expression in cell line and primary fibroblasts when treated with Shh blockers or agonists.

Interestingly, addition of r-Shh induced an up regulation in IL-6 production in these fibroblasts, albeit to just above the limit of detection of the CBA assay. However, this finding is tempered by a lack of comparable proliferative data, as the concentration which gave detectable levels of IL-6 is a titre above the upper value used in proliferative studies. Although the concentration of r-Shh used here is almost certainly un-physiological, native fully modified Shh would likely generate a similar response at a much lower, more physiological concentration.

Expression of IL-6 is particularly interesting given its anti-proliferative affect on pulmonary fibroblasts and the suggestion that it is spontaneously produced by epithelium as an autocrine growth factor, in addition to its role as an acute phase signalling molecule. Thus if Shh release is considered as an indicator of danger, it could up regulate IL-6 production in receptive fibroblasts to perpetuate this signal and as a means of preventing overzealous fibro-proliferation in the recovery from minor denudation, whilst stimulating epithelial proliferation, although given the substantial quantities of IL-6 which the epithelium is capable of synthesising in response to loss of contact inhibition, particulates and interaction with allergens such as Der P1, the affect of sub-epithelial fibroblast IL-6 production may only be marginal in this process.

3.3.7 EFFECT OF SHH ON EPITHELIAL ACTIVITY

Given the expression of ligand and receptor by the same cell it was hypothesised that Shh release might represent an autocrine signal involved in the up regulation of GM-CSF/IL-8 in the CMT and A549 lines respectively. Addition of r-Shh and 6hr supernatants, demonstrated that this was not the case, as did injury in the presence of the Shh inhibitor Cyclopamine, where no alteration in cytokine response was observed (data not shown).

A more speculative hypothesis, given Shhs role in maintaining a pluripotent haematopoietic progenitor population [127], might be that the Shh signal is there to prevent the differentiation of all type II cells into type I / repair cells,. thus maintaining the lung progenitor population. Such an explanation could be extended to the disease phenotype of up regulation observed in FITC and human lung disease by Stewart and colleagues [1]. Erroneous up regulation of the Shh pathway, either through an upstream signalling event or repetitive injurious stimuli, might result in hyper-proliferation of type II cells, which would be visualised as bronchiolisation, which is indeed a feature of human inflammatory fibrotic disease. Equally, an increase in type II cell number would increase the pool of cells capable of producing cytokine and chemokine up regulation in response to injury, which might in some way explain the hyper-responsive exacerbations observed in patients with IPF, where Stewart et al observed up regulated Shh[1].

Such a role for Shh could only be investigated through the addition of exogenous Shh to primary epithelial explants, which normally spontaneously differentiate from type II to type I.

3.4 CONCLUSIONS

The aims set out for this Chapter were achieved in that a successful *in vitro* cell injury assay was established, cytokine responses identified and analysed, a means of quantifiably measuring Shh was developed, and its release identified from injured epithelium.

The hypothesis posited at the start of this chapter was as follows:

"The up regulation in epithelial Shh expression observed in fibrotic disease is a response to injury, and that this injury also affects other epithelial cell functions. Further to this it is hypothesised that up regulated Shh affects epithelial and fibroblast function."

Data presented here suggest that soluble Shh release is indeed a response to injury and that injury also induces changes in epithelial cytokine production. However, although identifying a marginal increase in IL-6, these investigations did not conclusively characterise a function for soluble Shh. It is possible that Shh modulates responses or cells not characterised here, or that it requires the presence of an intermediate cell type to mediate its downstream effects.

3.5 FUTURE WORK

In covering the hypothesis and aims for this Chapter, the results presented here have raised a number of potentially interesting questions for further work.

3.5.1 DAMAGING ASSAYS

The issue of FITC application needs to redefined, and could be used as a clumped suspension if analytical techniques progress sufficiently to allow supernatant analysis, without the complication of fluorescent carryover.

Human experimental data here are limited to H_2O_2, and whilst FITC/DMSO and H_2O_2 are relevant *in vitro* / *in vivo* comparable reagents for mouse models of lung disease, H_2O_2 injury has only limited analytical value when compared to human conditions. Certainly the differences exhibited in data presented here would suggest that the nature of the cellular injury has important implications as to the cytokine expression profile induced in injured cells.

Another more relevant approach might be an investigation into mechanistic immunological damage at epithelial surfaces, such as the studies conducted by Wallace et al[113], where incubation of antibodies against an epithelial IPF auto-antigen with A549 cells in-vitro, resulted in reduced A549 cell number and up regulation of TGF-β and tenascin. Should Shh be identified here, using better characterised diagnostic tools it would provide a crucial link

between immunohistochemical observations in patient sections and *in vitro* mechanistic causation. Another approach might be a renewed attempt at incorporating bleomycin injury into the assays.

3.5.2 SHH ELISA AND IMMUNOHISTOCHEMISTRY

Solving the issue of r-Shh vs. native Shh will ultimately lie in the optimisation of the bioassay. This will allow the confirmation of supernatant Shh positivity in a manner not requiring antibodies, which persist in most diagnostic tests, i.e. westerns, immunohistochemistry, elispots etc.

3.5.3 SHH AS A SIGNALLING MOLECULE

Further investigation into the response of the fibroblast to r-Shh certainly merits further investigation, as IL-6 could be a key player in a number of pulmonary conditions.

Thus, in summary, the focus of future work arising from this work should be the development of a reproducible and reliable bioassay for Shh, further fibroblast studies with exogenous Shh and expansion of the compound selection in the injury assays.

CHAPTER 4: THE FLUORESCEIN ISOTHIOCYANATE (FITC) HAPTEN MODEL OF INFLAMMATORY LUNG FIBROSIS

4.1 INTRODUCTION

The initial objective of this work was to further characterise the effects of transoral intratracheal administration of the hapten fluorescein isothiocyanate (FITC) into the lungs of Balb-c mice; specifically its effects on both the immune response generated and the Shh signalling pathway.

Aspects of the FITC-mediated immune response were investigated through the development of novel ELISAs for FITC specific serum antibodies and through histological examination of archive T-lymphocyte depleted studies. The involvement of the Shh pathway in this model was assessed through Immunohistochemical analysis and primary cell studies.

Since its original conception in this lab, the FITC model has undergone substantial development from its original form and has been used to investigate both acute and chronic conditions by ourselves and others[123 1, 121]. The following sections detail these alterations, including some discussion of the findings made using the differing modifications.

4.1.1 MODEL ONE

The FITC model was first reported in 1995[123]. Initial studies utilised both HAN rats and Balb-c mice [123], later focusing on mice[1].

Mice were anaesthetised via inhalation of halothane, an incision made to expose the trachea, and FITC suspended in PBS to 3mg/ml. This was delivered intratracheally in a 50μl volume (approx 0.007mg per g body weight). Rats were anaesthetised via intraperitoneal injection of Valium™ (diazepam) and intramuscular Hypnorm™ (fentanyl/fluanison) and had 0.5ml of 1mg/ml FITC instilled intratracheally.

At three days post administration there was an increase in BALf protein levels, indicating damage to pulmonary structures facilitating exudation of serum proteins into the airspaces. This was associated with a marked

inflammatory infiltrate, predominantly of neutrophils, but also including a significant mononuclear cell population. The infiltrate penetrated both the interstitium and the alveolar spaces, with corresponding high BALf cell counts up to seven days after instillation. Alveolar oedema was also observed, along with epithelial hyperplasia; findings consistent with FITC induced acute injury.

Neutrophil infiltration resolved after this initial acute response, but interstitial mononuclear infiltration persisted up to five months post instillation, where it was found associated with focal destruction of lung architecture. These regions were patchy in distribution and exhibited features of fine honeycombing, reminiscent of that observed in UIP, and were restricted to areas of persistent FITC, where neighbouring FITC negative areas appeared to retain normal architecture[1].

The resolution of neutrophil infiltrate and protein exudation early in the acute response would suggest a mechanism other than neutrophil mediated damage or prolonged epithelial denudement be responsible for the chronic fibrotic response observed. The occurrence of serum antibodies to FITC and the continued lymphocyte infiltrate would suggest a T cell dependent immunological basis to the FITC disease process. Unpublished mouse data by Steve Roberts of this lab demonstrated a two fold increase in serum αFITC IgG titre between normal/3day and 3 weeks post instillation in FITC treated mice.

What has yet to be investigated using model one, or subsequent models, described below, is the specific disease inducing activity of FITC at the pulmonary surface, why is inflammation and fibrosis induced upon its administration and why does it persist.

A few hypotheses can be posited as to potential reasons for the pathology observed. FITC (Fluorescein isothiocyanate) is a fluorescent compound whose isothiocyanate group reacts with amino terminal and primary amines in proteins. Such a process occurring in the lung, cross linking and attaching to epithelial structures, would be expected to disrupt normal lung flexibility, and might result in the initiation of pro inflammatory and profibrotic activity.

Equally, FITC crosslinking might interfere with or inactivate normal pulmonary cellular signalling mechanisms or may act as a toxic agent inducing both acute and chronic cellular injury. Whilst these hypotheses will not be investigated directly within this Chapter it is hoped that through the study of histology and immunological responses to FITC instillation, the manner in which it induces disease may become evident.

4.1.2 MODEL TWO

The surgical technique employed in model one induced a 5-10% mortality rate within 24hrs. In accordance with the Home Office policy of replacement, reduction and refinement, Dr GA Stewart of our lab modified the model to incorporate a transoral intratracheal delivery system, which markedly reduced the mortality of the procedure (<1%)[183]. With this method, mice were anesthetised with avertin (tribromoethanol anaesthetic) at a dose of 0.2ml per 10g body weight prior to instillation of 50μl of 2mg/ml FITC via non surgical intubation with a blunted 25G needle, as described in Chapter 2.

However, no fibrosis was observed in these mice by six weeks post instillation and much of the FITC had been cleared, thus a second instillation was performed at this time point. Studies by Dr S.A Ahmad of our lab demonstrated fibrosis in 100% of FITC positive mice using this method, greatest at fourteen weeks post a second FITC instillation[184].

ACUTE EFFECTS

Just 24hrs after FITC instillation there was a marked increase in BAL neutrophils, some six fold greater than controls, decreasing to near PBS controls by 7 days post instillation. Using a novel scoring system on 10 random fields including at least one bronchiole (less than half field width in diameter), a blood vessel and an airway, Dr Ahmad also demonstrated increased infiltrate at 24hrs post instillation continuing through 7 days in the perivascular compartment, alveolar walls and peri-bronchiolar alveolar tissue, with the exception of the bronchiolar epithelial compartment itself, which decreased to near control levels by 3 days post instillation, indicating a dynamic infiltrate process[184].

During the initial seven days after instillation the FITC was observed in large/small bronchi, blood vessels and alveolar walls, with heavily stained tissue and alveolar macrophages. Alveolar thickening and infiltrate were observed by 7 days post instillation and IHC staining with a TGF-β antibody was markedly increased in FITC vs. PBS treated mice, peaking at 5 days, particularly in alveolar macrophages.

Of particular note is that both PBS and FITC intratracheal delivery induced measurable TNFα levels in BALf fluid, peaking at 24hrs post instillation, which was 2 fold greater in FITC mice than PBS mice. This provided further evidence of the acute processes initiated through FITC instillation over that induced by PBS instillation.

LONG TERM RESPONSE

FITC was observed retained in the lung up to six weeks post first instillation, although somewhat reduced in intensity. A second instillation of FITC at this time point generated a similar acute inflammatory infiltrate to that of the first, when observed 7 days post instillation, becoming predominantly mononuclear through 6 weeks post 2nd instillation, up to 14 weeks[184].

By 14 weeks post secondary instillation, FITC treated animals had developed fibrotic changes in the lung, presenting with areas of severe fibrosis with complete obliteration of alveolar architecture associated with residual FITC deposition[184].

Although there was no clear association of lymphocyte cell type with fibrotic areas, mononuclear aggregates containing T & B lymphocytes similar in composition to those observed by Wallace et al in patients with UIP, occurred with increasing intensity over 6 and 14 weeks time points, and were suggestive of a local humoral response, a feature suggested by the development of FITC specific antibodies in the single instillation model.

4.1.3 THE MICHIGAN MODEL

Colleagues at the University of Michigan School of Medicine, Ann Arbor, have also published data using the FITC instillation model. This centre uses a method similar to model one, briefly, FITC was sonicated as a 1.4 mg/ml PBS solution at 50% power for 30 seconds, later adapted to 2.1 mg/ml[121, 185]. Mice were anaesthetised with pentobarbital, a small incision made into the neck and the trachea exposed by blunt dissection. The animals were restrained at 60° angle and 50μl FITC delivered directly into the trachea through a 26g needle. This solution was vortexed vigorously prior to each instillation[121]. This group has focused on the initial innate and adaptive responses to instillation, using short recovery time points as a means of studying inflammation and acute interstitial scarring.

FITC staining remained largely peribronchial, although the authors suggest that the occurrence of alveolar wall oedema is evidence for FITC mediated affects outside its area of deposition[185]. Although possible, our experience with anti-FITC staining would suggest that oedema is also directly FITC associated and that this would be visualised with more sensitive immunohistochemistry.

Eosinophilic exudates, haemorrhage and acute inflammation were observed within the first few days of injury, with dense consolidation of PMNS and mononuclear cells by days 3-5 post instillation, persisting to the final 21 day time point. By day 21 patchy areas of increased ECM were observed, with relative increases in collagen greater in the Balb-c mouse strain when compared with the C57/BL6 strain[185]. Balb-c have a well characterised propensity to develop humoral (Th2) responses compared to primarily cellular (Th1) responses in C57/BL6[186]. This was suggestive of an immune polarisation effect on the initial scarring response, however both strains produced specific IgG antibodies against FITC, which although not instructive as to polarisation (isotypes IgG2a (Th1) and IgG1 (Th2) not supplied), would indicate that the type of response is not dissimilar in the two strains. Equally, the 21 day fibrotic response observed in these mice is identical in RAG-KO (no T/B lymphocytes) and SCID (no immune system) mouse strains suggesting that this initial scarring may occur in the absence of active

immunity, possibly involving a local up regulation in TGF-β observed following the first instillation in model 2[184].

MCP-1

Although apparently T-cell independent, the Michigan model does feature significant inflammatory infiltration, and repetition of this model in knockouts of CCR2 a chemokine receptor for MCP-1, resulted in a protection against fibrosis.[121]

MCP-1 is a chemo-attractant produced by monocytes and their derivatives, macrophages, and by endothelial, epithelial and fibroblastic cells. It may recruit CCR2 expressing cells to sites of injury, where expressors of this receptor include monocytes, macrophage, activated T-lymphocytes, B-cells, mast cells and fibroblasts. This would suggest that disruption of inflammatory recruitment, protects against fibrotic development.

However, the authors claim that protection was not linked to differences in the initial inflammatory cell response as this was similar for both wild type and knockout mice, although notably, plasma leak resolution was more rapid in CCR2-/- and later mononuclear infiltration was also reduced[121]. The authors instead, referencing studies in Acute Respiratory Distress Syndrome (ARDS)[187] suggest that MCP-1 serves an activating function in this model, increasing cytokine production.

GM-CSF

CCR2 knockouts were also found to produce markedly decreased levels of TNFα, a cytokine with well characterised pro-inflammatory and fibrotic function, and greater amounts of GM-CSF than wild type mice treated with FITC.

GM-CSF is an epithelial mitogen with the capability to influence the number and activity of alveolar macrophage and mature dendritic cells. Its up regulation here is crucial given the findings of this same group with the bleomycin model of lung injury[103, 122]. Here, GM-CSF was shown to be essential for the maintenance of PGE_2 levels, an anti-fibrotic eicosanoid.

Thus increased levels of GM-CSF in CCR2 knockouts may be responsible for reduced fibrogenesis in response to FITC, although whether this represents true protection in these mice or merely delayed progression, was not addressed in these studies[121, 121, 122].

4.1.4 REMODELLING, FIBROSIS OR REVERSIBLE INFLAMMATORY ATELECTASIS?

Remodelling is a term commonly attributed to conditions where pathologically there is evidence of lung damage or chronic progressive fibrosis. This is associated with inflammatory atelectasis and general deformation of normal lung architecture. Increasing use of this term in mouse models has been necessitated by lack of a clearly defined terminology for descriptions such as chronic and acute fibrosis, scarring and interstitial vs. sub epithelial fibrosis, as defining features often differ or are absent in mouse compared to human diagnostic criteria, and this has led to their incorrect attribution to a number of mouse lung models, where remodelling would have been a better attribution.

An example of this might be the 21 day post FITC instillation time point described by Christensen et al in the Michigan model[185]. Whilst a process which undoubtedly involves fibroblasts and increased collagen deposition is initiated in these mice, they have never been pursued to later time points (personal communication), thus it may not be accurate to define these as fibrotic, which by classical definition is an overzealous healing response to an acute or chronic event which results in permanently dysfunctional areas of lung through establishment of fibroblastic proliferation and collagen deposition.

The level of dysfunction resulting from fibrosis is perhaps the area where most variation occurs in experimental definition. Where more acute scarring might be expected to result in retention of thickened areas of epithelial mesenchymal tissue following resolution, which does not irrevocably reduce the functionality of that airway, end stage fibrosis, more typical of chronic progression, results in enlarged disorganised macrostructures, which are functionally redundant, produced by contractile restriction of surrounding

fibroblastic bundles and interstitial connective tissue deposition. Thus what some describe as acute fibrosis, such as in the 21 day Michigan model, others would define as early remodelling or more specifically, loss of structural integrity through a persistence of inflammatory infiltrate.and associated atelectasis.

Experience would suggest that much of the early airway collapse and alveolar thickening observed in FITC mice is attributable to the inflammatory infiltrate and that in the absence of a secondary instillation of FITC much of this architecture returns to normal. In our hands, fibrosis in model one only occurs as a chronic response, and in the transoral delivery method utilised in model two, fibrosis also occurs as a chronic response, following a second instillation.

4.1.5 HYPOTHESIS AND AIMS

Previous studies of Shh at the pulmonary surface utilised model one where 100% of FITC positive mice developed fibrosis following a 3mg/ml surgical instillation[1]. Subsequent transoral dual instillations used 2mg/ml of FITC, and although all FITC positive mice developed fibrosis, up to 25% of FITC instilled mice could be FITC negative by 12 weeks post second instillation[184].

The dose used in transoral dual instillations used here was increased from 2mg/ml to 3mg/ml, with the aim of increasing the proportion of mice retaining the FITC and developing fibrosis.

Given the findings discussed in the previous sections and introduction to this thesis, the first hypothesis proposed by this Chapter is that Shh is a signal found associated with areas of chronic fibrosis in the dual instillation model of FITC instillation, signalling through interactions with epithelial cells, AM and fibroblasts.

A second, broader hypothesis, is that the FITC model represents a model of acute inflammation, which primes the immune system to make an injurious and profibrotic response upon secondary instillation of FITC. A continuation

of this hypothesis was that FITC instillation induced a Lipopolysaccharide (LPS) hypersensitivity response in AM, leading to inappropriate cytokine secretion, with potential profibrotic side effects

The aims of this chapter were therefore to:

- Compare the immunohistochemical observations from the surgical model with the transoral model
- Characterise the morphological alterations and inflammatory recruitment induced by dual instillation of an increased concentration of FITC
- Screen Alveolar Macrophage isolates from FITC and PBS treated mice for differences in cytokine production in response to r-Shh and LPS
- Screen fibroblast and epithelial isolates from FITC and PBS treated mice for differences in cytokine production and responses to r-Shh
- Characterise the FITC specific antibody profile with dual instillation of FITC

4.2 RESULTS

4.2.1 INTRODUCTION TO MOUSE EXPERIMENTS

Four mouse studies were undertaken through the course of the work detailed in this Chapter, as summarised in Table 4.1. Study 1 centred on the isolation of primary cell populations for *in-vitro* culture. Alveolar macrophages were taken to investigate potential differences in LPS responsiveness between FITC and PBS treated mice, both in viability and cytokine secretion. Epithelial cell populations and fibroblasts were also analysed. Lungs were also frozen in OCT/Saline for use in studies described in Chapter 5, and for the development of an anti-FITC western on whole lung homogenates. This western will be used to identify the size of, and further analyse, those proteins to which FITC conjugates in the lung. The development of this system was underway at the time of writing, but is only in its preliminary stages and thus will not be eluded to further in this Chapter.

Study 2 also involved epithelial isolation for culture, and in this case RNA isolation, but concentrated primarily on the generation of long time course points for immunohistochemical analysis and collagen content estimation.

Findings drawn from studies 1 and 2 highlighted a number of differences between model one (single surgical halothane instillation of 2mg/ml FITC) and the current model two (two instillations, non-surgical, under avertin of 3mg/ml FITC).

This was partially addressed in Study 3 by using halothane and avertin methods of anaesthesia for FITC administration. Variations in surgical vs. non surgical were prohibited by the current animal licence. Halothane was introduced as described for model one in the previous section, and avertin as in materials and methods. No difference was observed in any of the parameters analysed (sera, histology scores, IHC, procedural mortality), thus is not discussed further in this section. Data from this study were pooled and used to address intermediate; 2 week & 6 week post first instillation and 2weeks post second instillation time points not addressed in the previous two studies. This study also involved non-terminal bleeds for a more complete

serum antibody profile. Study 4 used archival lung blocks derived from a previous model 1 experiment conducted by S Roberts in this lab, where specific T lymphocyte populations were depleted in FITC treated mice. These were analysed both as a model one comparison with the current model two, and as a means of assessing the potential role of T-lymphocytes in FITC mediated disease.

For clarity these studies are addressed in combination unless otherwise indicated. Time points are defined post the first instillation, thus 6wks refers to 6 weeks post first or only instillation, whilst 6wks + 2wks refers to 2 weeks post the second instillation, this is illustrated in the time line in Figure 4.1.

Immunohistochemical analysis is defined per time point in the subsequent sections, followed by details of quantitative counts and scores performed on section and cytospin preparations. The final material presented in this results section details some of the *in vitro* data yielded from these studies.

	No. Mice	Time Points	Instillation Method	Analysis Undertaken
Study 1	40	6wks + 6,12wks	Transoral	AM, BALf, Epithelium, Fibroblasts, IHC, Western*
Study 2	60	6wk + 6,12,18wks	Transoral	AM, BALf, Epithelium, IHC, Histology Scores, Bloods
Study 3	40	2wk, 6wk, 6wk + 2,6,12wks	Transoral	AM, BALf, IHC, Histology Scores, Bloods
Study 4	11	6wks	Surgical	Histology Scores, IHC

Table 4.1: Summary of mouse investigations
All FITC instillations were performed as described in Chapter 2. Cytokine levels in all BALf were assessed by CBA. AM culture was undertaken in Studies 1 and 2; only cytospin preparations were taken for study three. Only 6wk + 6wk data for fibroblasts are included in this chapter as 12wk cultures were found to contain fungal contamination. Terminal bleeds alone were taken from study 2, study 3 used tail and terminal bleeds. *Lungs were snap frozen in OCT/saline, see section 4.2.1 for details. IHC : Immunohistochemistry.

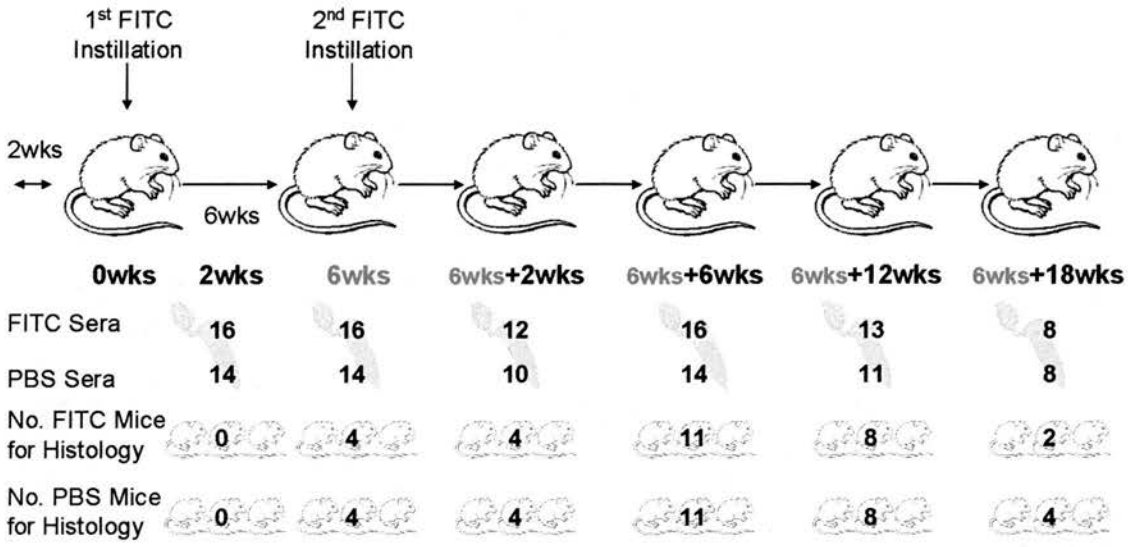

Figure 4.1: Timeline Diagram of FITC instillation Experiments
Illustration of the timeline used in studies 2 & 3 and the relative numbers of mice involved. Numbers here are used in subsequent IHC in histology studies. Study 1 is not included as these mice were primarily used for primary cell isolation, where anti-FITC IHC and H&E were only performed in representative mice per group to ascertain that FITC had been correctly instilled and mice had a similar phenotype to that expected for that time point. Mice were left for two weeks following arrival at the animal facility prior to initial FITC instillation to facilitate acclimatization. 6wks samples were taken one day prior to second FITC instillations. Only two exclusions were required, one 6wk+6wk mouse had no FITC evident in biopsy, (likely a feature of cutting location) thus was excluded from sera and histology data, and one PBS mouse at 6wk+6wk which showed histological evidence of a pneumonia. These were excluded from the numbers shown above.

4.2.2 SIX WEEKS POST FIRST FITC INSTILLATION

Mouse lung histology six weeks post the first instillation of FITC had multiple foci of mononuclear infiltrate, as observed in Figure 4.2, with both H&E [A] and trichrome [B] stains (described in Section 2.8.5). The foci can be identified by the cluster of purple nuclei observed in the top left of each image. The darker blue areas of [B], and at higher magnification in [C] illustrate areas of cellular thickening and increased connective tissue. For comparison, an area of relatively normal alveolar structure can be seen in the bottom of [E] in Figure 4.3. However, fibrosis was not observed with either trichrome or picrosirius stains (data not shown).

Mononuclear foci and cellular thickening were features restricted to areas of FITC deposition [D] where FITC was found in both large and small airways and associated with alveolar and interstitial structures. Most apical epithelial cell surfaces were FITC -ve, but strong sub-epithelial staining was observed in most small and large airways. FITC -ve areas did not appear to differ from comparable areas of PBS treated mice. Although inflammation was relatively mild in these mice at this time point, it was observed in all mice.

In contrast to previous histology from 2mg/ml transoral studies, all FITC instilled mice were FITC+ve upon Immunohistochemical examination (Figure 4.2), suggesting that either the use of 3mg/ml in these studies has been a sufficient increase to maintain a greater quantity of FITC in the lung, or that perhaps anaesthesia & delivery were more effective in these studies.

Figure 4.3, illustrates immunohistochemistry studies from this time point. Shh expression was negative in most areas, and expression did not correlate with FITC deposition or differ from that observed in localised areas of PBS mice [E], although in 1 of 4 mice Shh expression was found to be increased in an area of distorted and irregular alveolar arrangements. These could be features of poor inflation during fixation, but visible extracellular connections across these areas would suggest an irregular structure to this region prior to death, perhaps attributable to prolonged atelectasis [A,B & C]. Primary omission controls for Ptc and Shh in this region were completely negative [D].

This mouse had an apparent unilobal FITC deposition pattern, generating one highly inflamed lobe, (shown in Figure 4.3) where the vast majority of the lung was normal and FITC negative, suggesting that increased Shh in this area may have been attributable to a greater local concentration of FITC.

Although there was a marked inflammation in FITC mice including a mononuclear infiltrate, which has been shown previously to be Ptc positive[1] there was no difference in Ptc expression in FITC mice compared with PBS control mice [F]. CC10 also remained unchanged (data not shown). Therefore these data would suggest that neither Ptc or CC10 expression, or epithelial progenitor population density, is altered by FITC instillation.

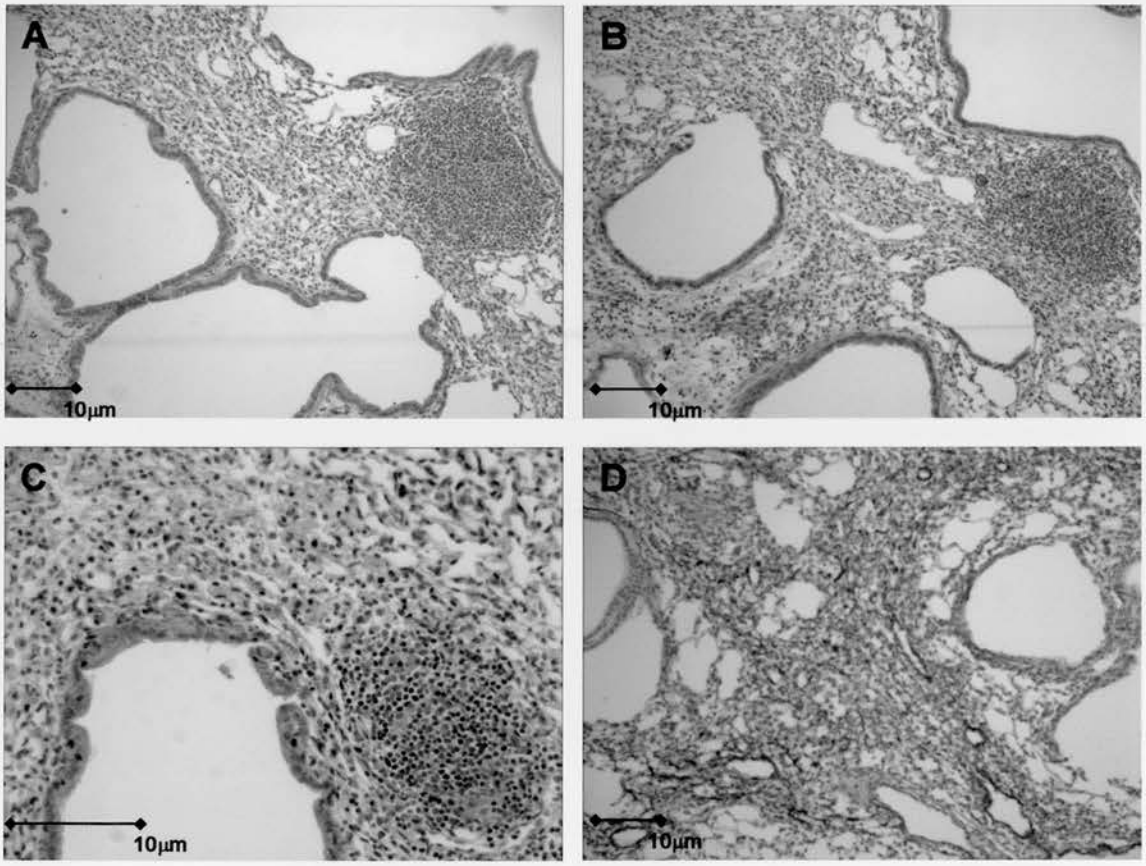

Figure 4.2: 6wk Post First FITC Instillation
[A] x100 magnification of a H&E stain of a focus of mononuclear infiltrate in an area of abnormal alveolar architecture. [B] x100 magnification of a trichrome stain of the same area shown in [A]. [C] x200 magnification of a trichrome stain illustrating alveolar thickening and mononuclear infiltrate. [D] x100 magnification the deposition profile of FITC via anti-FITC immunohistochemistry.

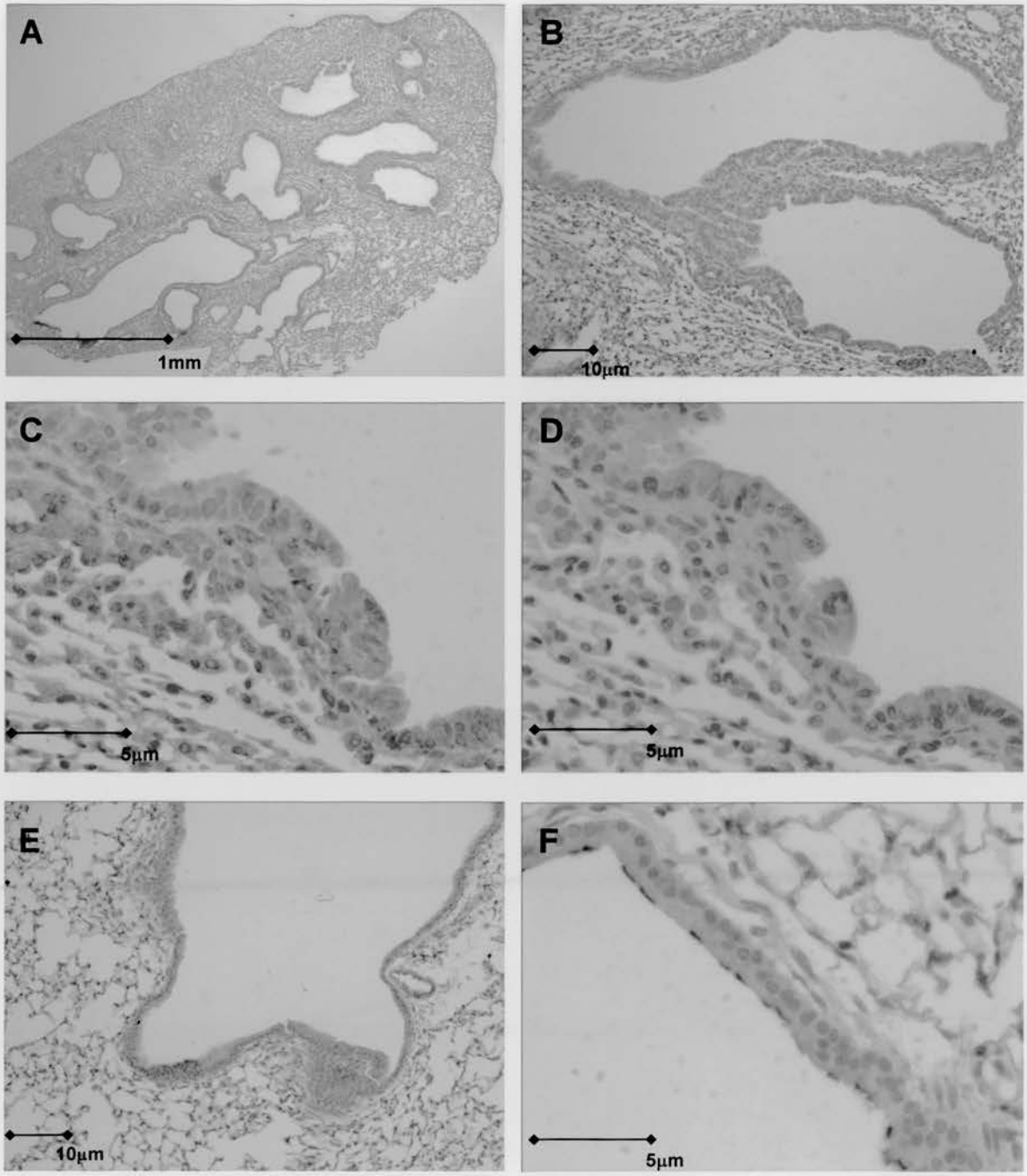

Figure 4.3: 6wks Post First FITC Instillation (2)
[A] x25 magnification of Shh expression in an abnormal area of lung which is positive for FITC. [B] x100 magnification of Shh expression around a large airway containing thickened epithelium. This is shown at x400 magnification in [C]. [D] is a x400 primary exclusion control for Shh and Ptc. [E] x100 magnification of Shh expression in PBS mouse epithelium. [F] x400 magnification image of Ptc expression in a FITC treatment mouse, where similar expression is observed in PBS control mice.

4.2.3 TWO WEEKS POST SECOND FITC INSTILLATION

Mouse histology from two weeks after the second FITC instillation (Figure 4.4) showed a similar distribution of alveolar FITC to six weeks mice, but with markedly more FITC localised in sub-epithelial areas of the larger airways [E], similar to observations made in 2mg/ml studies. This was frequently found associated with an apparent detachment of connective structures between the overlying epithelium and underlying alveolar structures. Increased FITC deposition was not associated with either increased inflammatory infiltrate or increased collagen deposition as determined by trichrome staining [B], although there appeared to be marked alveolar thickening in areas of alveolar FITC deposition as shown in the cental area of a H&E stained section in [A], where comparatively normal structures (bottom right of [A]) are retained in areas shown to be FITC –ve (data not shown). This marked epithelial thickening was not as apparent in 6 weeks mice, as reflected in the Ashcroft scores which are discussed later.

Shh and Ptc expression was similar in both PBS and FITC instillation mice [C&D], where the greatest levels of Shh expression were localised to the cuboidal epithelial cells of the larger airways [C], particularly at airway junctures/bifurcations. Ptc expression was also greatest in cuboidal epithelial cells.

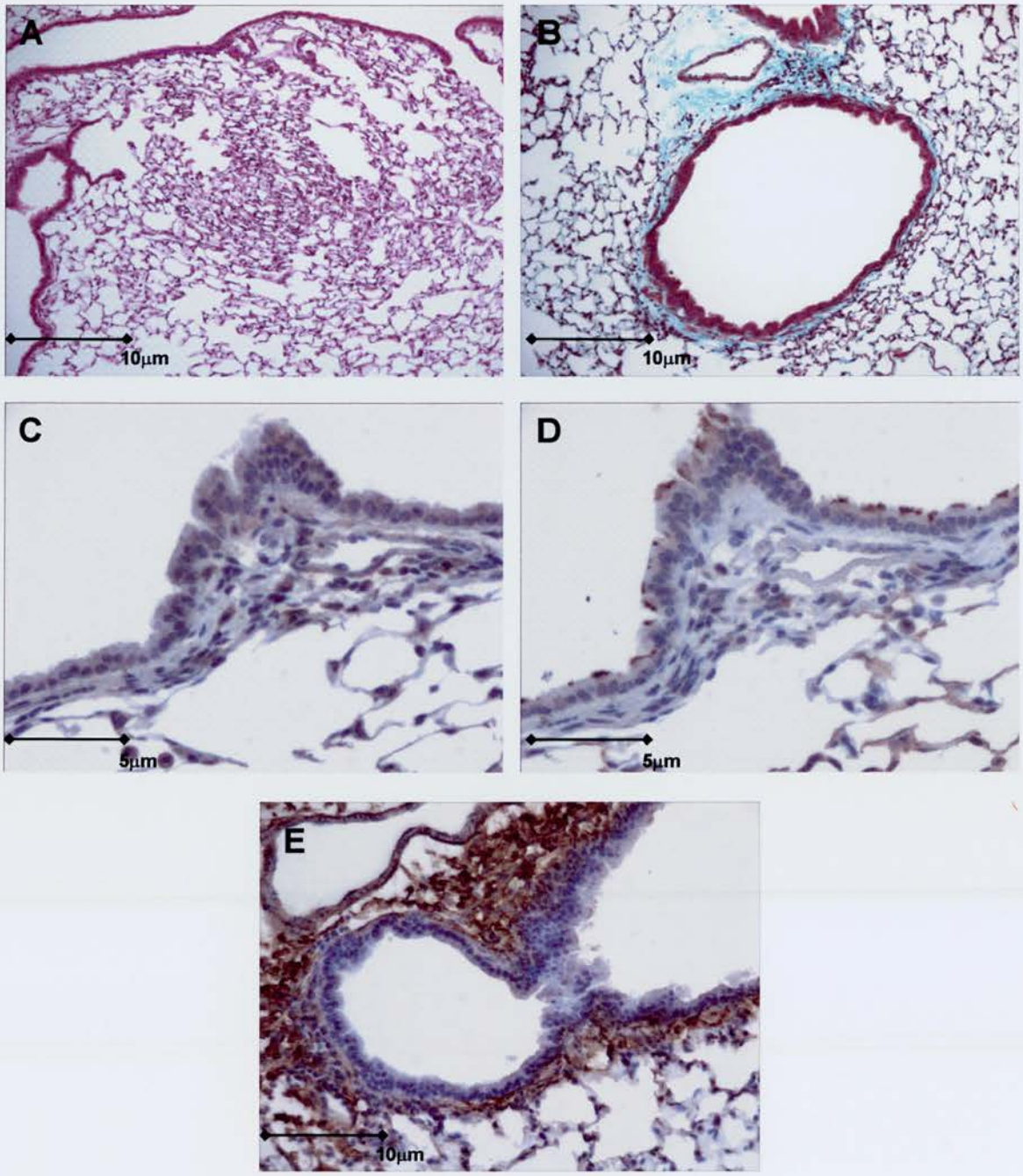

Figure 4.4: 2wks Post Second FITC Instillation
[A] x200 magnification of an H&E of an area of FITC deposition showing abnormal alveolar thickening in the absence of infiltrate. Increased collagen deposition was restricted to the larger airways at this time point as shown in a x200 magnification of a trichrome stain [B]. Shh [C] and Ptc [D] expression was restricted to the cuboidal epithelium of the large airways. Ptc expression did not differ between PBS and FITC treated mice. Shh expression in FITC treated mice exhibited marginally greater expression in some areas of FITC deposition. [E] FITC deposition occurred in clumped pattern localized to the main airways, sub-epithelial and associated with disrupted connective tissue.

4.2.4 SIX WEEKS POST SECOND FITC INSTILLATION

Mouse histology and IHC from six weeks post second instillation (Figure 4.5) were notable for a more diffuse pattern of FITC deposition, extending further into alveolar structures than previously [D], pronounced atelectasis, restricted to areas of FITC deposition [B & C], and by an increased prevalence of mononuclear foci [A, D, E & F].

Although mononuclear foci were features observed in both six week post first, and two weeks post second instillation mice, previous foci were isolated to areas of heavy FITC deposition and abnormal architecture. Their increased prevalence at this time point appeared to coincide with their appearance in areas of lesser FITC deposition. IHC conducted by Dr S.A Ahmad at this time point indicated similar foci of mononuclear cells and these were shown to be almost entirely B-cells, as defined by expression of the B220 protein, with occasional T-cells, identified by CD3 expression (See Appendix - Figure 7.3).

Mononuclear foci were frequently associated with a halo of FITC deposition [E] and increased collagen deposition. Airway collapse was associated with increased collagen staining in both trichrome stains [B&C] and weakly in picrosirius stains (not shown), but in the majority of areas, this occurred in the absence of fibrotic banding.

Shh expression did not differ between PBS and FITC mice at this time point (data not shown). However, increased interstitial staining for Ptc was observed in areas of substantial FITC deposition combined with mononuclear foci [F], suggesting that at least some of the cells contained in these foci are Ptc positive cells.

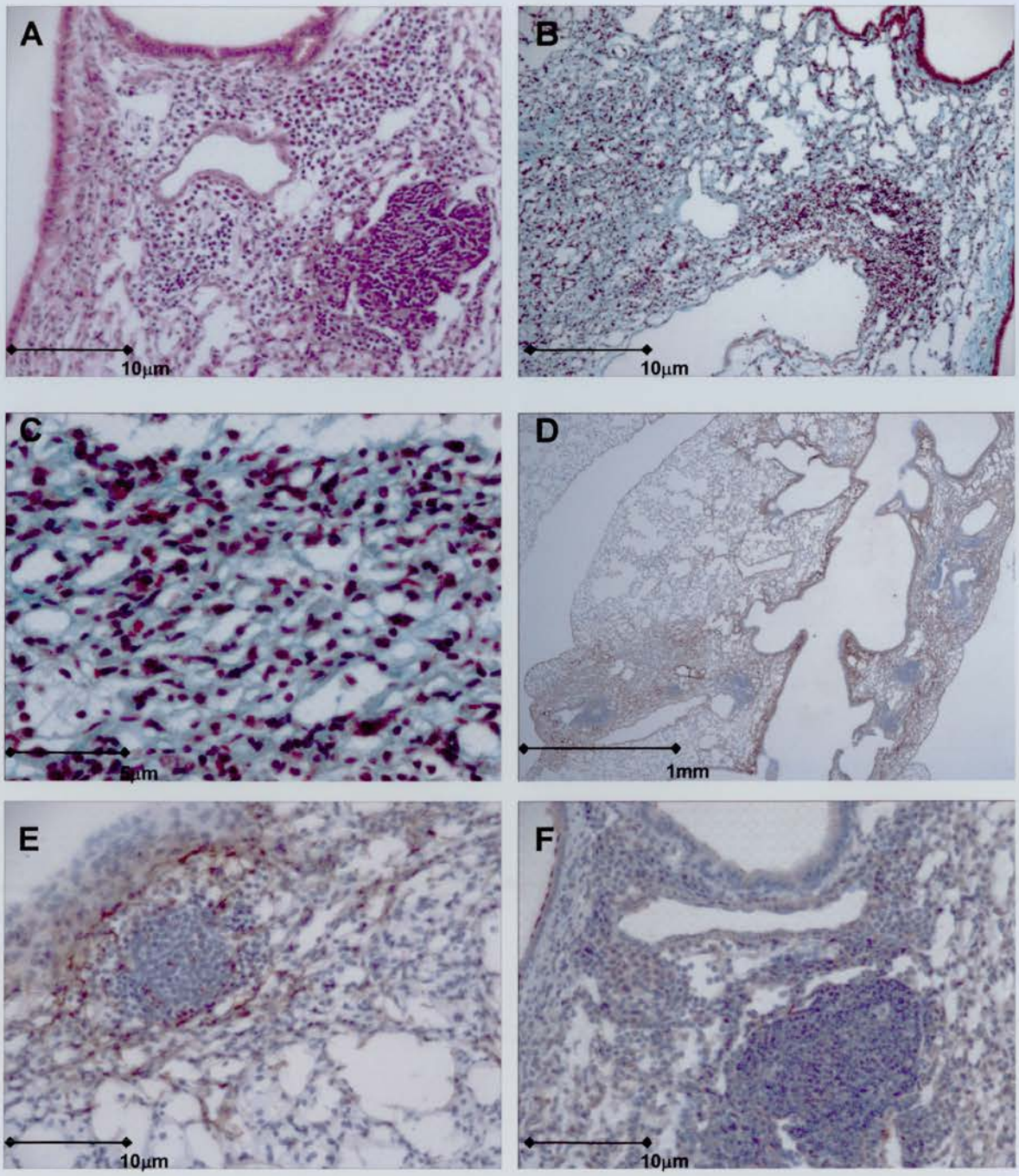

Figure 4.5: Six Weeks Post Second FITC Instillation
[A] x200 magnification of an H&E stain of a mononuclear aggregate in an area of abnormal alveolar architecture. [B] x100 & [C] x400, are trichrome stain images illustrating the loss of architecture, taken from a FITC positive area shown in [D] at x25 magnification. FITC IHC illustrated halos of FITC deposition around many of the mononuclear foci [E] which were found only in FITC positive areas. Ptc IHC [F] demonstrated increased staining in some areas of mononuclear foci, but not all

4.2.5 TWELVE WEEKS POST SECOND FITC INSTILLATION

Histological examination of lungs from mice twelve weeks post second instillation, shown in Figure 4.6. had the most pronounced pathology of all the time points examined. FITC +ve areas were associated with abnormal lung architecture almost without exception, as confirmed by Ashcroft score, discussed later. Studies with the 2mg/ml method at a 14 week time point had shown similar findings to those represented here, although not as reproducibly and with less destructive fibrosis.

Loss of lung structure is most easily visualised in [A], where large honey comb like structures can be observed. Comparing the complete loss of alveolar structure in this FITC +ve area (and in higher magnification in [B]), with a FITC -ve area to the bottom left of [A], the localised nature of this response is clear. This collapse in structure is associated with a substantial mononuclear infiltrate and increased collagen, observed both through trichrome [C & D] and picrosirius stains [E & F].

Immunohistochemical analysis shown in Figure 4.7. confirmed the localisation of FITC to areas of honeycombing [A] and iBALT [B]. Honeycombed areas appeared to contain a slightly higher proportion of CC10 positive cells [C] & [D] than in normal airway although this was a purely qualitative observation. No differences in Ptc or Shh expression could be observed in the honeycombed areas described thus far for this time point, but in a neighbouring FITC+ve area of abnormal lung architecture, there occurred an apparent co-cellular localisation of Ptc and Shh expression in individual cells, not observed at previous or later time points, or elsewhere in the section [E & F]. Thus, it is likely an isolated event or process, such as the development of a cluster of carcinoma cells, with which Shh and Ptc expression are commonly associated, and which FITC mice have been shown to have a greater susceptibility to (Roberts et al, unpublished observations).

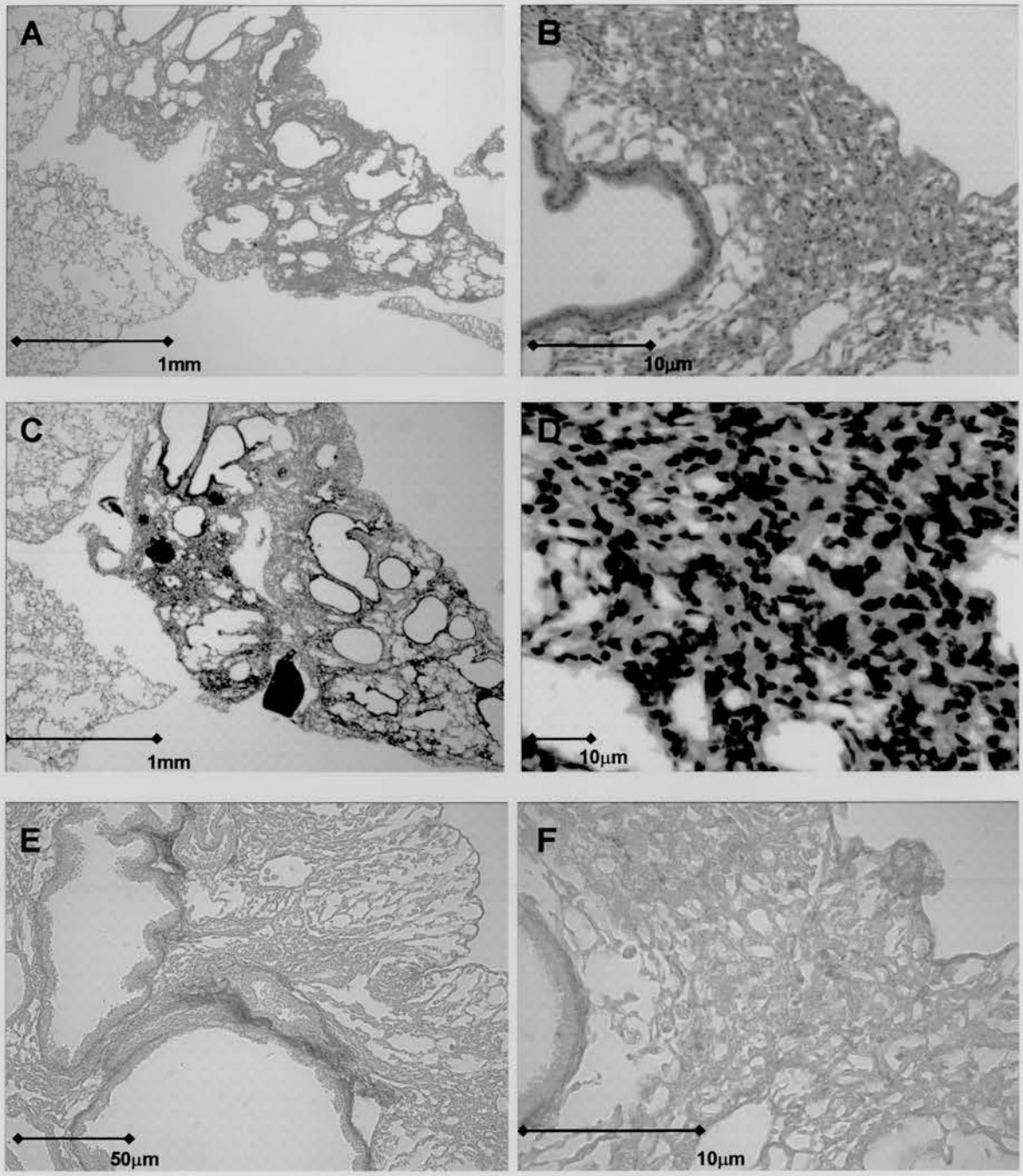

Figure 4.6: Twelve Weeks Post Second FITC Instillation
[A] x25 magnification of an H&E stain of a fibrotic, honeycombed area of mouse lung, with an area shown at x200 magnification in [B]. Panel [C] is a x25 magnification of a trichrome stain of the same area at a greater depth into the lung, this is shown at x400 magnification in panel [D]. [E] Picrosirius stain at x200 and at x400 [F], from the same area, confirm the observations drawn from the trichrome stains.

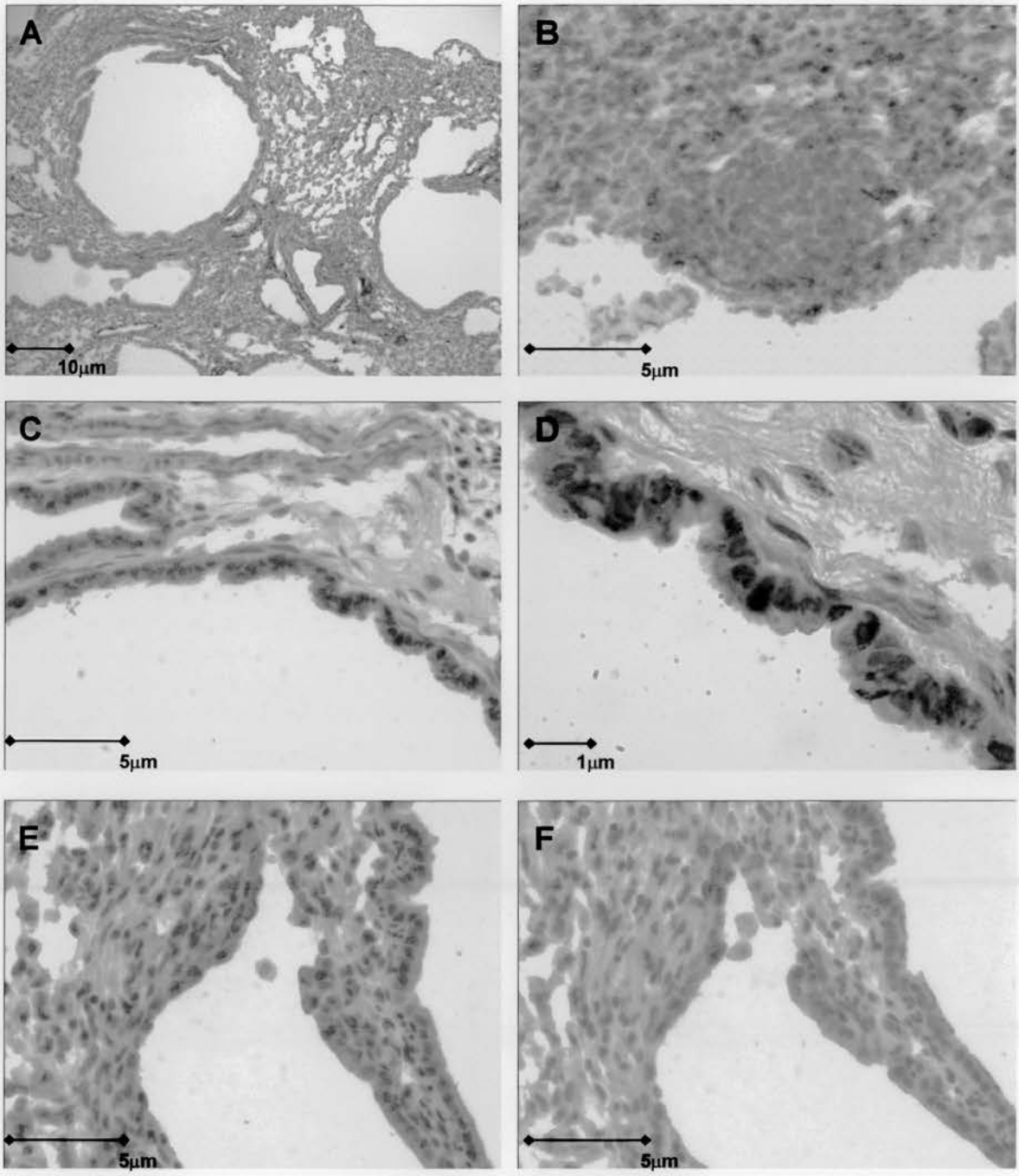

Figure 4.7: Twelve Weeks Post Second FITC Instillation (2)
[A] x100 image of FITC IHC, establishing FITC deposition central to areas of honeycombing. [B] x400 image of FITC located around a mononuclear cell foci. [C] x400 image of CC10 IHC illustrating an area of epithelial proliferation over a fibrotic focus, shown at x1000 magnification in panel [D]. Shh [E] and Ptc [F] expression in isolated cells in an area of abnormal lung at x400 magnification.

4.2.6 EIGHTEEN WEEKS POST SECOND FITC INSTILLATION

Histological examination of the lungs of mice eighteen weeks after the second FITC instillation (Figure 4.8), demonstrated FITC retention largely restricted to the sub-epithelial regions of the medium and large airways [B & C], where interstitial and alveolar retention was much reduced compared to twelve weeks mice. There was also some qualitative amelioration in inflammatory infiltrate.

FITC associated histology was highly variable ranging from completely normal to honeycomb, and whilst areas of honeycombing and atelectasis occurred less frequently in these mice than at previous time points, alveolar structures appeared thickened and disorganised, but in the absence of fibrotic deposition or inflammatory infiltration, suggesting that some epithelial mediated event must be inducing this response, or that these cells have remained activated following the removal of either FITC or a cellular infiltrate.

In these mice areas of Shh expression were marked in specific sub-epithelial cells in areas of FITC deposition [D]. It is important to note here that smooth muscle stains positively for Shh, thus it is possible that these cells represent a myofibroblast population. Equally these could represent positively staining blood cells contained within a capillary bed. However, these cells were not observed in PBS mice [F], where Shh IHC was almost completely negative, and have not been observed previously.

Ptc expression did not differ between PBS or FITC treated mice in level of expression, but gave more cellular staining in areas of FITC deposition, compared to a largely membranous profile in PBS mice.

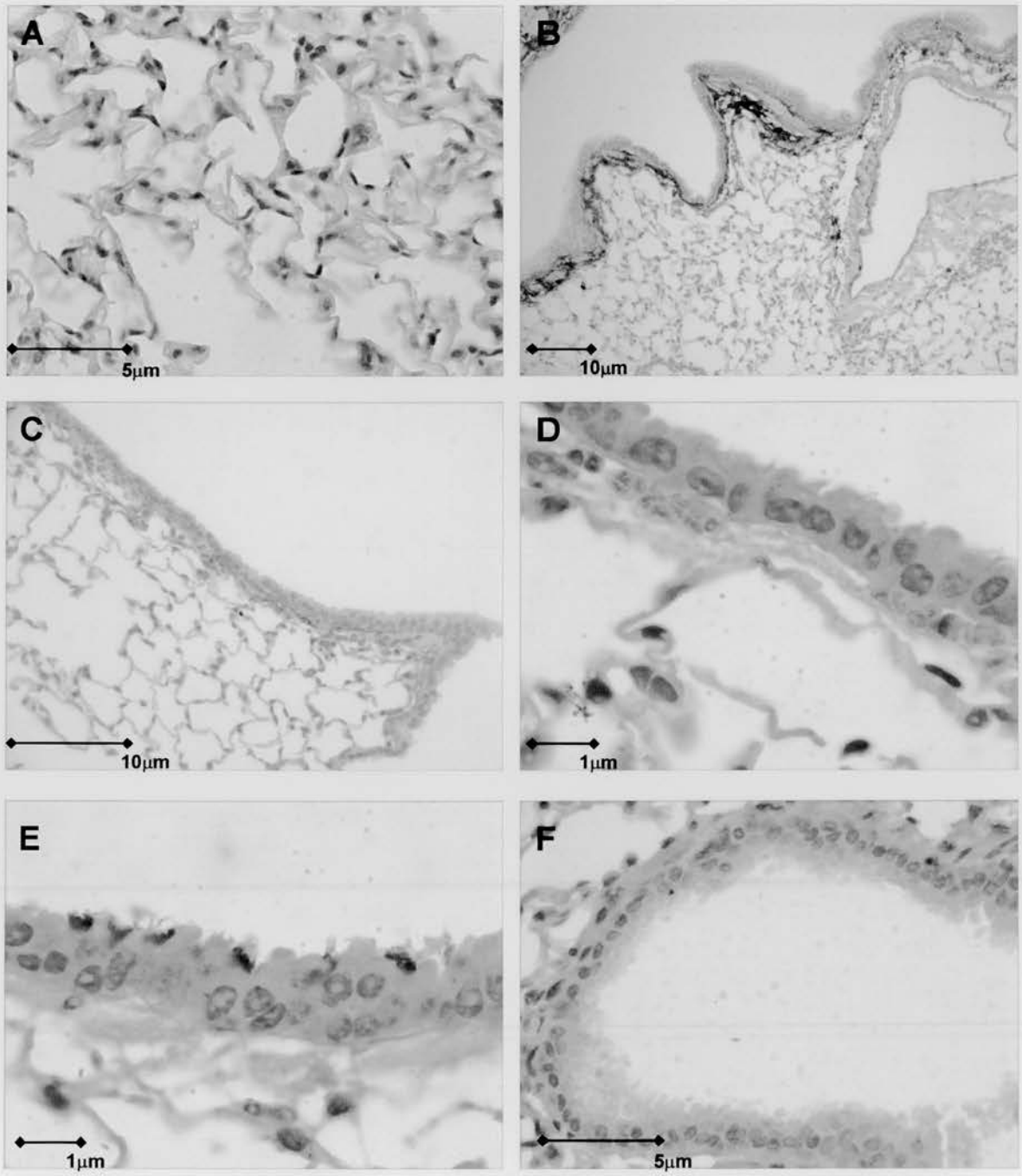

Figure 4.8: Eighteen Weeks Post Second FITC Instillation
[A] x400 magnification of a H&E stain showing a typical alveolar structure in the lungs of FITC treated mice at this time point. [B&C] show FITC IHC at x100 & x200 magnification, where FITC staining was restricted to sub-epithelial regions of large airways. In some regions such as that shown in [C] there was also Shh [D] and Ptc [E] staining observable. Whilst Ptc expression was similar in PBS mice, Shh was almost completely absent in PBS mice as shown in panel [F] at x400 magnification.

4.2.7 WHOLE LUNG COLLAGEN CONTENT DOES NOT CHANGE WITH FITC INSTILLATION

Given the qualitative differences in collagen deposition observed through trichrome and picrosirius stains, a quantitative approach was taken to confirm these observations. Lungs were taken from 3 mice per group at 12 and 18 weeks post second FITC/PBS instillation. The assay used detected soluble collagen (recently deposited material), utilising a variant of the picrosirius stain, where bound material in lysates can be isolated by centrifugation and solubilised for colourimetric measurement (see Chapter 2).

Assays for 12 week and 18 week time points were conducted on separate occasions, but with internal collagen controls and against a collagen standard curve. Samples could not be rerun on a second occasion as they were unstable following freeze thawing.

No difference was observed between PBS and FITC mice, which is perhaps not surprising given the limited collagen deposition identified by picrosirius staining and the diffuse nature of the disease. Differences between 12 and 18 week mice could be a feature of aging, but more likely represents more effective digestion of lungs at the 18 week time point (Figure 4.9).

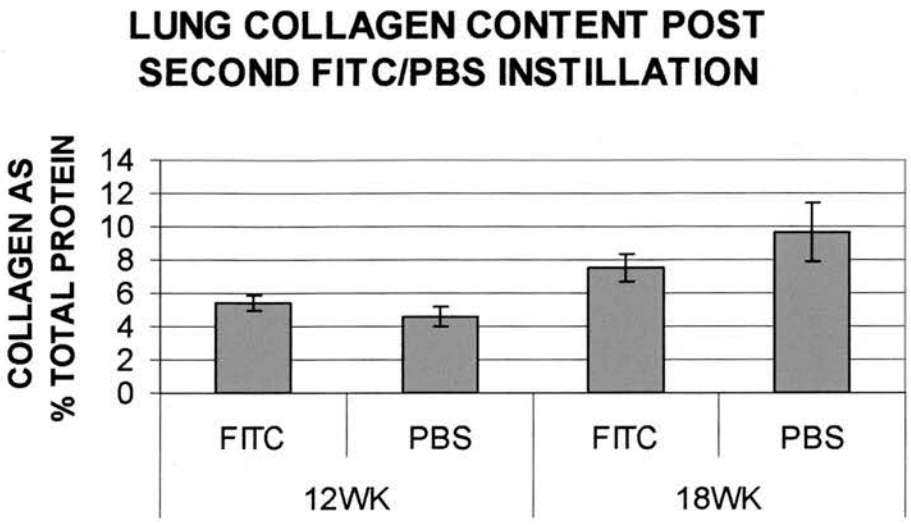

Figure 4.9: Total Lung Collagen Content is Unchanged by FITC Administration
Three lungs per group, per time point were taken, wet weight taken, and material digested acidicly according to the protocol described in Chapter 2. Collagen levels are expressed as a percentage of total protein, as estimated by BCA kit. Error bars denote standard deviation.

4.2.8 FITC EXPOSED MICE HAVE AN INCREASED ASHCROFT SCORE

Elucidation of a quantitative indicator of disease using whole lung collagen as a qualifier was likely inhibited through a dilution effect of normal pulmonary structures in what is a very patchy disease. To account for this variation, a quantitative scoring mechanism was used on anti FITC stained sections, based on a system developed by Ashcroft et al[164] detailed in Chapter 2.

Briefly, 36 fields at x400 magnification are scored according to fibrotic progression on a discrete scale of 0-7, where zero is normal and seven is a severe distortion of structure with large fibrous areas. Panels A and B in Figure 4.10 detail the score for those fields where over 50% of the area was FITC +ve. Values for FITC -ve fields can be found in panel C of the same Figure, along with those of PBS mice. No significant difference was observed between the FITC -ve areas or PBS mice, although a slight, but not significant increase was observed in group median value for FITC -ve vs. PBS at 12 weeks post second instillation, consistent with an increased score of FITC +ve areas. Most abnormal FITC -ve areas were clustered around

high scoring FITC +ve areas and may represent a non-specific bystander affect of inflammatory infiltrate.

The scores shown in panel A reflect those observations made through immunohistochemical observation, discussed previously, where evidence of active disease was most pronounced 12 weeks after the second instillation, decreasing by 18 weeks. Equally from the frequency of scores shown in panel B it can be seen that whilst at 12 weeks post second instillation, scores are skewed towards 3-7 with virtually no normal areas, at 18 weeks, normal areas return and the skewing is reduced, suggesting some remission.

However, the definition of fibrosis is that it is a permanent disruption of normal architecture. Therefore if 12 week mice are truly representative of previous histology in 18 week mice, then it must be accepted that some of the 12 week fields scored as fibrosis were in fact severe atelectasis and that this may have been responsible for the apparent fall in score.

Alternatively, given the diffuse nature of the disease and mouse to mouse variation, it may be that the sections cut from 12 or 18 week mice were not truly representative of the whole lung or group of mice. Further cutting into the blocks and increased numbers of replicate mice could address this issue. However these experiments have yet to be performed.

Figure 4.10 Ashcroft score & Frequency [Overleaf]
[A] Illustrates the average median of FITC+ fields for each group (study two and three combined). Where the number of mice is given in the base of each bar. FITC-ve fields and PBS treatment mice Ashcroft values are given in the table below [C]. Panel B shows the relative frequency of each score in each time group. Replicates are as [A].

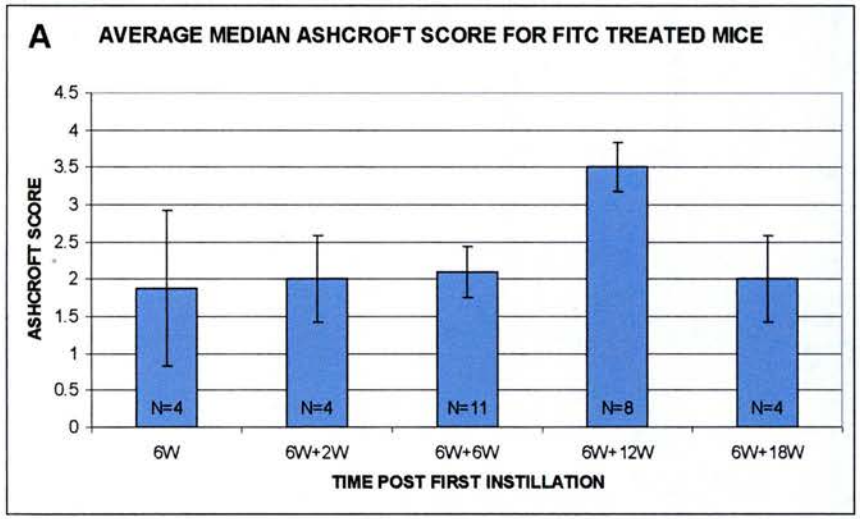

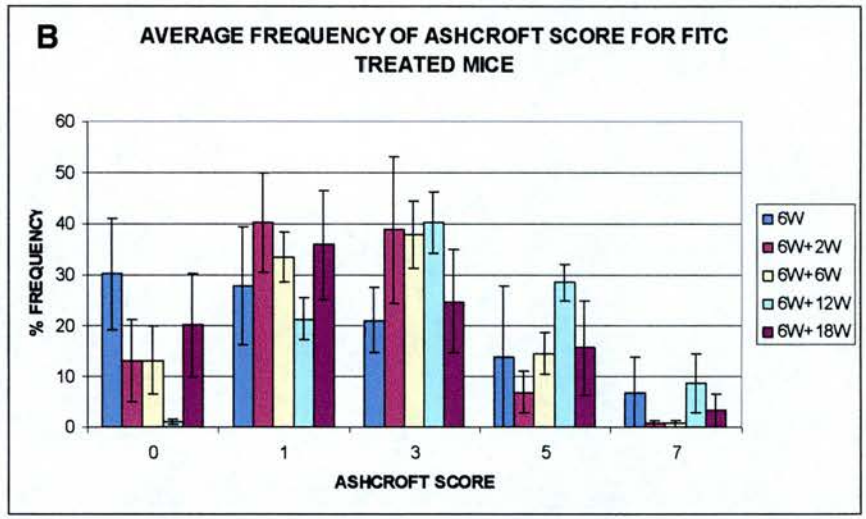

C

ASHCROFT SCORE	6W			6W+2W			6W+6W			6W+12W			6W+18W		
	FITC+	FITC-	PBS	FITC+	FITC-	PBS	FITC+	FITC-	PBS	FITC+	FITC-	PBS	FITC+	FITC-	PBS
AV MEDIAN	1.9	0.0	0.0	2.0	0.0	0.0	2.1	0.1	0.0	3.5	0.4	0.0	2.0	0.0	0.0
ST ERROR	1.05	0.00	0.00	0.58	0.00	0.00	0.34	0.09	0.00	0.33	0.18	0.00	0.58	0.00	0.00
ASHCROFT	6W			6W+2W			6W+6W			6W+12W			6W+18W		
FREQUENCY	FITC+	FITC-	PBS	FITC+	FITC-	PBS	FITC+	FITC-	PBS	FITC+	FITC-	PBS	FITC+	FITC-	PBS
0	30.14	89.58	93.75	13.19	83.33	86.81	13.26	79.29	89.90	1.04	58.33	88.89	20.14	89.58	89.58
1	27.92	10.42	6.25	40.28	16.67	12.50	33.53	19.70	9.60	21.43	37.50	10.65	35.97	9.03	8.33
3	21.11	0.00	0.00	38.89	0.00	0.69	37.91	1.01	0.51	40.28	4.17	0.46	24.86	1.39	2.08
5	13.89	0.00	0.00	6.94	0.00	0.00	14.60	0.00	0.00	28.57	0.00	0.00	15.69	0.00	0.00
7	6.94	0.00	0.00	0.69	0.00	0.00	0.70	0.00	0.00	8.68	0.00	0.00	3.33	0.00	0.00
ST ERR OF	6W			6W+2W			6W+6W			6W+12W			6W+18W		
ASHCROFT FREQ	FITC+	FITC-	PBS	FITC+	FITC-	PBS	FITC+	FITC-	PBS	FITC+	FITC-	PBS	FITC+	FITC-	PBS
0	10.80	3.47	2.63	8.21	5.78	2.08	6.72	4.21	1.60	0.51	6.58	3.04	10.23	5.36	4.59
1	11.48	3.47	2.63	9.72	5.78	1.79	4.84	4.23	1.37	3.98	5.28	3.16	10.72	4.59	4.09
3	6.43	0.00	0.00	14.30	0.00	0.69	6.60	0.56	0.51	6.10	1.74	0.46	10.05	0.80	1.33
5	13.89	0.00	0.00	4.17	0.00	0.00	4.15	0.00	0.00	3.47	0.00	0.00	9.26	0.00	0.00
7	6.94	0.00	0.00	0.69	0.00	0.00	0.70	0.00	0.00	5.83	0.00	0.00	3.33	0.00	0.00

4.2.9 FITC EXPOSED MICE HAVE FITC SPECIFIC IgG ANTIBODIES

Given the chronic occurrence of mononuclear foci and a significant mononuclear infiltrate, it appeared that the immune system could be prominently involved in disease progression. Given that previously unpublished observations by S Roberts had identified FITC specific IgG antibodies in these mice, as had others[185], bloods were taken from mice in study 2 and 3 to look for FITC specific IgG over a more inclusive and longer time course than previously, where published studies are <21days post instillation[185] and S Roberts looked in model one up to 3 weeks post instillation (Unpublished observations).

In addition to longer time points, novel ELISA's were developed to determine the subtype of the IgG antibody, revealing the polarisation of the immune response (IgG1–Th2 : IgG2a-Th1) and therefore the likely cytokines secreted by, and the effector function of, the infiltrating cell population.

IgG2a is an indicator of a cellular T-cell response, as switching to the generation of this antibody by B-cells will require stimuli from FITC specific Th1 T-cells which are involved in the activation of macrophage (see Figure 1.5). IgG1 is an indicator of a humoral response, as switching to this antibody will require Th2 T cell stimuli, a cell involved in the propagation of B-cell and therefore antibody responses.

Sera were titred out until their OD fell within 10 standard deviations of the mean of 16 negative control wells per plate, and the value of that dilution given as the end titre. The high concentrations of antibody identified, required a three fold serial titre (125μl into 250μl) such that all low and high values remained within the linear phase of detection of the plate reader. However, this titred approach means that some values may be markedly out of range of the true value, but each data set was analysed identically, thus are internally comparable.

Values are given here per study, due to different time points being taken and ELISAs were run on separate occasions for each study, thus the data are non-comparable as the ELISA does not contain a standard curve function.
FITC exposed mouse sera were found to contain substantial levels of IgG1 (Figure 4.11), which were exponentially increased over 2, 6 and 12 week time points following the second instillation of FITC. Specific IgG2a levels were undetectable. Thus of IgG1&2, IgG1 appears to be the main IgG subclass involved in this system.

Figure 4.12 includes Ashcroft scoring data along with the average titres for those particular mice and would indicate a correlative trend, however, the numbers used in these studies negate any truly reflective correlative statistical examination of this data.

Such an association is further characterized in Table 4.2, where the average IgG1 levels of individual mice for each tail and terminal bleed would appear to match their Ashcroft score, again in the absence of any correlative statistical significance due to small sample numbers.

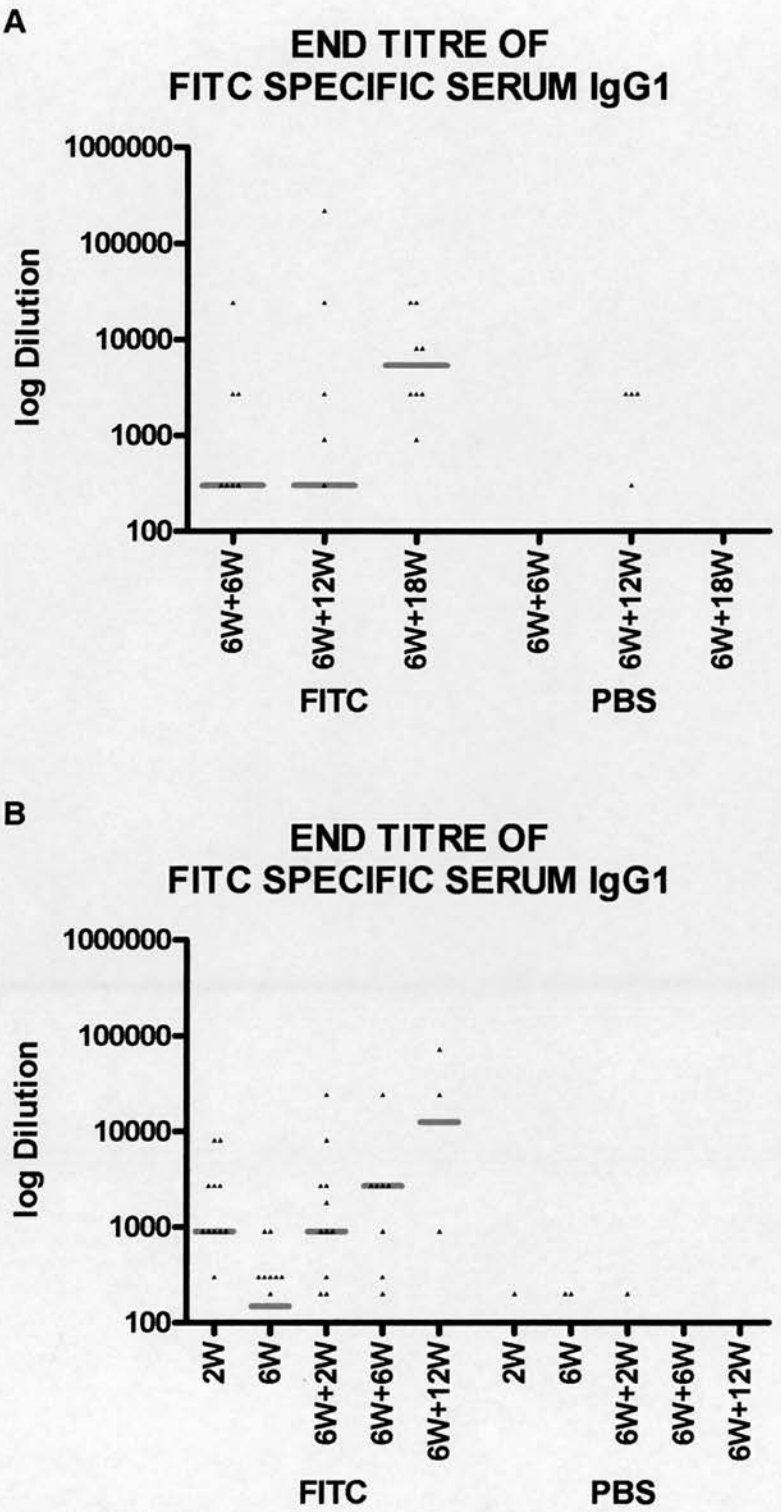

Figure 4.11: FITC Specific IgG Titres
Bars denote median values. [A] Study 2 sera had an increased IgG1 titre at 18wks vs. 6 & 12wks, 6wks n=8 mice, 12wks n=9 mice, 18wks n=8 mice. Median values for PBS mice were negative for specific IgG1 at each time point tested. 6wks included 8 mice, 12 & 18wks included 9 mice. [B] Study 3 sera had a reduced IgG1 titre 6wks post first instillation, which became boosted exponentially post second instillation. PBS were negative. Mice per time point were 2w (16), 6w (16), 6w+2w (12), 6w+6w (8), 6w+12w (4).

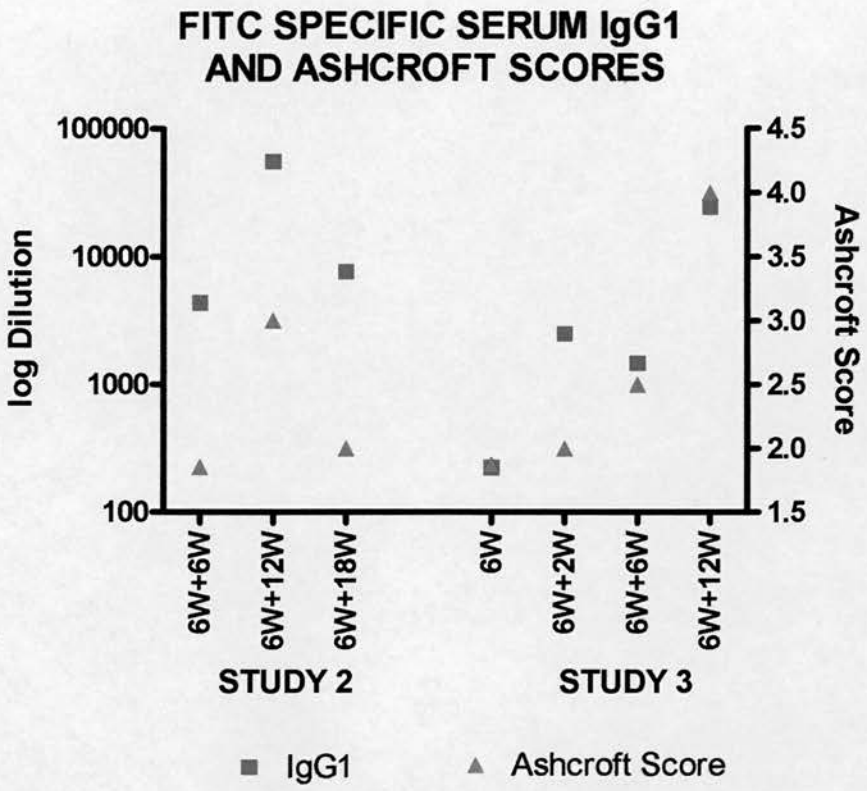

Figure 4.12: IgG2a FITC Titres & IgG1 / Ashcroft Correlation
Data represent average end titres of terminal bleed mice & their average Ashcroft score. Mice, running left to right across the x-axis are as follows: 7,4,4,4,4,4,4.

MOUSE	TIME POINT					AV IgG1 TITRE	AV ASHCROFT SCORE
	2W	6W	6W+2W	6W+6W	6W+12W		
1	100	100	2700	300		800	1.5
2	300	100	900	2700		1000	2.4
3	8100	300	1800	200		2600	2.8
4	900	100	200	2700	100	800	2.6
5	8100	900	2700	2700	24300	7740	4.3
6	2700	300	24300	24300	72900	24900	4.8
7	100	100	300	900	900	460	2.8

Table 4.2: IgG1 Ashcroft Correlation
Antibody profiles of study 3 mice until terminal bleed, combined with respective Ashcroft scores as an approach to illustrate the potential association of prior antibody profiles on observed pathology in mice at the terminal time point.

4.2.10 VARIATION IN ELISA AND ASHCROFT SCORES

Considering the sample size of 36 fields the standard error bars of Ashcroft score remain fairly substantial (Figure 4.10), illustrating variation from mouse to mouse, which may also be influenced by the depth of section cutting, which was, where possible, standardised to the first full face available. The individual mouse serum titres for IgG ELISA are also highly variable (Figure 4.11) attributable to mouse-mouse variation and the three fold titre technique employed in ELISA. Median values have been used in these studies to lessen the influence of these outlying values. For example, in a worst case scenario, the median for all the 12 weeks study 2 mice titres (n=9) is 300, where 4 of the 9 values are 100, whilst the average is 55450, due to the three fold titre utilised, generating large differences in end titre values. Variation was more commonly similar to that of 18wks mice (n=8) where the median is 5400 and the average 9225.

However, variation is most notable when comparing individual mice. Figure 4.11 details titre medians for 6wk (n=9),12wk (n=8) and 18wk (n=9) mice. When this profile is re-illustrated with only those mice for which there are Ashcroft scores, i.e. those mice not used for primary cell culture and collagen content estimation, the profile is completely different (Figure 4.12). Whilst this is undoubtedly affected by the use of average values in the latter figure, it highlights the analytical uncertainties associated with such a variable data set.

In light of this observation is the observed drop in Ashcroft score at 18 weeks post second instillation a feature of random sampling, selecting healthier mice for embedding and scoring? Closer analysis of the data contained in the previous figures would suggest no, if the serum values are taken as an indicator of Ashcroft score.

The average end titre value of all the 12wks study two mice together is 55450, which is higher than the average for those mice from this group which were taken for histology (27477). Thus, if the observed correlation holds true, then a remission in Ashcroft score would still have been expected were all

the 18wks mice taken for embedding, as the average titre of those taken for embedding (7650) is approximately the same as that of the whole group at 9225, both of which are substantially less than the 12wks data.

4.2.11 MOUSE SERUM DOES NOT CONTAIN FITC SPECIFIC IgE

Given that IgG1 is a Th2 associated antibody, it was hypothesised that these mice, due to the chronic persistence of the FITC, might also develop FITC specific IgE antibodies. These are also Th2 associated but are more characteristic of allergic diseases such as asthma and allergic bronchopulmonary aspergillosis (ABPA). ABPA, a complication commonly seen in Asthmatics, is a particularly interesting comparison given that it arises from a failure to clear epithelial associated *Aspergillus fumigatus* and patients can go on to develop end stage fibrosis[188], albeit in a bronchial rather than alveolar setting.

Bloods from study two were assessed for total IgE using a sandwich ELISA system detailed in Chapter 2, then FITC specific antibody identified using a novel ELISA system developed here. FITC specific IgE identification necessitated prior IgG antibody depletion to prevent competitive binding. When utilised in the specific ELISA, these samples were found to be completely negative.

4.2.12 BALf SHOWS NO EVIDENCE OF ALVEOLAR INFLAMMATORY INFILTRATE

BALf were taken from all mice used in this Chapter. The data in Figure 4.13 detail counts performed on those obtained from studies two and three. The airway cell populations of FITC and PBS mice did not exhibit any marked differences at early time points, although the occurrence of lymphocytes at later time points (panel D) might suggest specific infiltration. Underlying blood contamination can be dismissed, as neutrophil levels remain low in the BALf. Data from twelve weeks post the second instillation could be attributable to a condition common to the groups as it occurs in both. However, there is a significant difference between the treatment groups at 18 weeks post second

instillation. Notable as it occurs at a time when there appears to be some amelioration of disease.

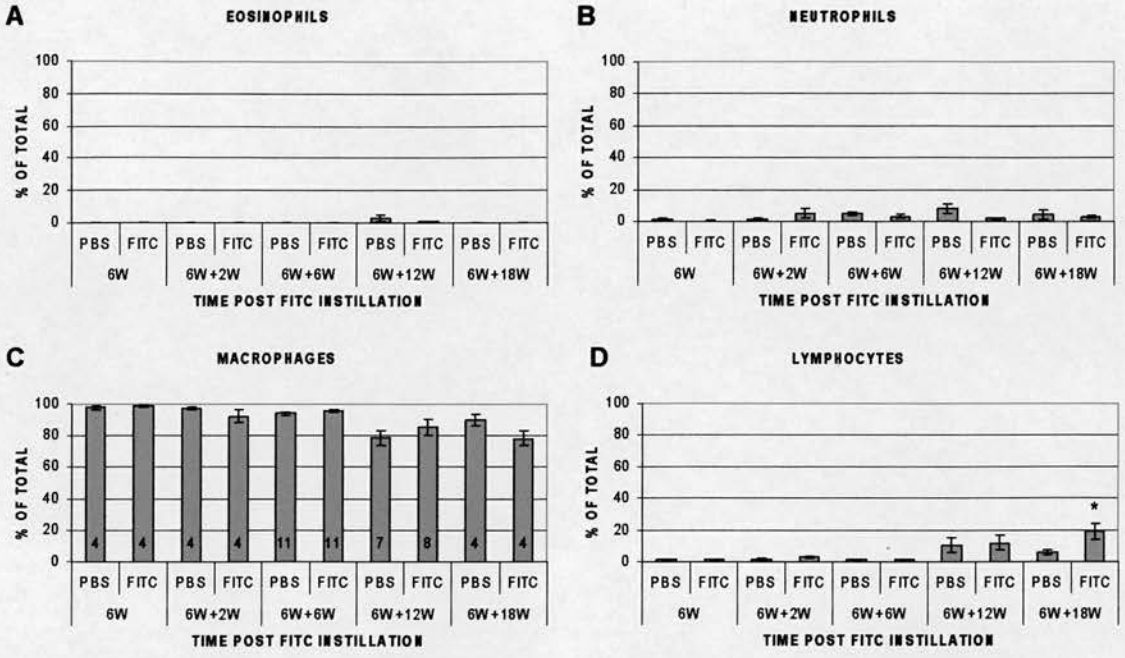

Figure 4.13: BALf Cell Populations
[A]-[D] Represent the percentage cell population of the four cell types counted. Only BALf for which there were corresponding sections were used, and the data from study 2 and 3 pooled. Replicate numbers are displayed in the base of the bars in panel [C]. Error bars denote Standard Error *=p of >0.05 with parametric tests.

4.2.13 INTERSTITIAL INFLAMMATORY INFILTRATION INCREASES IN THE TWELVE WEEKS FOLLOWING FITC INSTILLATION

Analysis of mouse histology during the treatment period identified variable numbers and size of mononuclear foci and focal areas of infiltrate mediated atelectasis. However infiltrate counts illustrated in Figure 4.14 would suggest that there is a trend for increased inflammatory infiltration over the twelve weeks following the second FITC instillation. It is important to note here that this scoring process does not discriminate between FITC positive and FITC negative areas. Thus there is likely a significant normal area dilution effect.

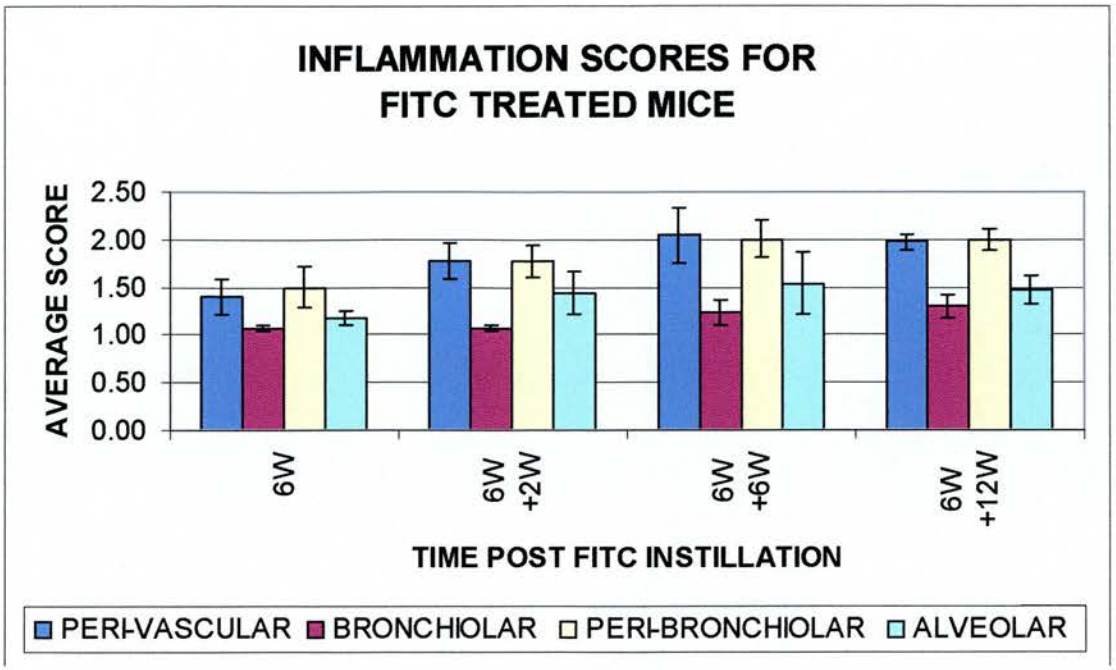

Figure 4.14: Inflammation Scores of FITC Treated Mice
Represents the relative inflammatory infiltrate identified in H&E sections of study three mice

4.2.14 MICE DEPLETED OF T-LYMPHOCTYES HAVE A REDUCED ASHCROFT SCORE

Given the prominence of lymphocytes in previous analysis, Study 4 was instigated. This utilised archival paraffin wax embedded, formalin fixed lung tissue obtained from T-cell depleted mice used in model one experiments by S Roberts. These were scored for Ashcroft and inflammatory infiltrate, the results of which are displayed in Figure 4.15.

The small replicate number negates any true analysis, but the trend would indicate that depletion of T-cells reduces atelectasis and fibrosis, as measured through the Ashcroft score, and that this affect was greatest in the CD4 T cell depleted mice (Figure 4.15[A]). Depleted mice had a greater percentage of ones, over controls, whose frequency distribution was concentrated at three (Figure 4.15[B]). Of particular note is the reduced infiltration score for CD8 and total T-cell depletion, whereas CD4 depletion retains a control level of infiltration (Figure 4.15[C]), despite a lower Ashcroft score. The pictures shown in Figure 4.16, are from total T-lymphocyte depletions, but represent features observed in all four groups

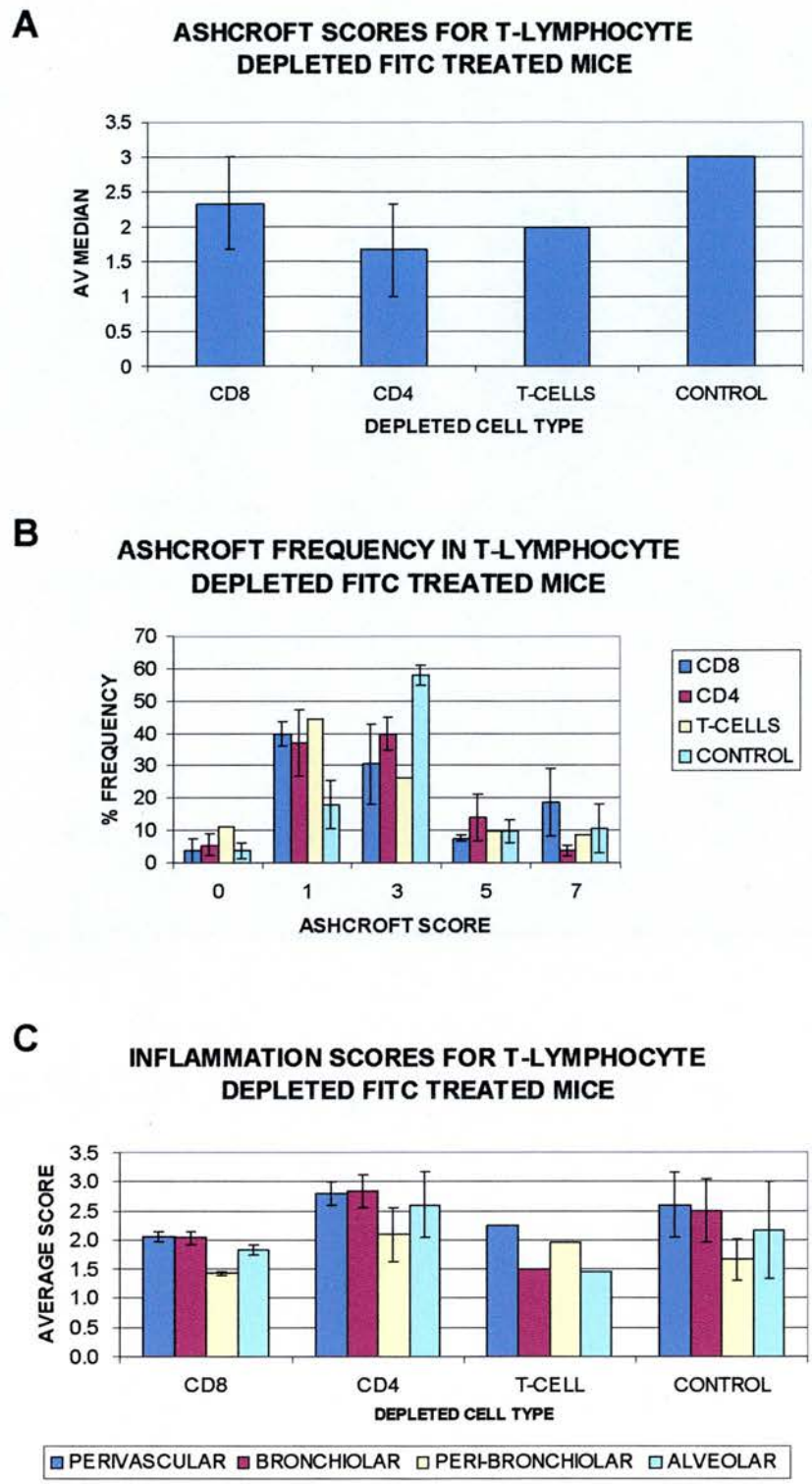

Figure 4.15: Scores for T-Lymphocyte Depleted Mice
Score data from study four, model one mice, killed 6 weeks after a FITC instillation. CD8 (n=3), CD4 (n=3), Total T-lymphocyte (n=2), control depletion (n=3). Error bars denote standard error. No error bars appear for total T cell depletion (due to number in group) or for control bar (due to absence of any variation). [A] Ashcroft scores, (there was no standard error in Ashcroft score for total T lymphocyte depletion). [B] Frequency distribution of Ashcroft score [C] Illustrates the inflammatory infiltrate scores from H&E sections with the average of each group displayed.

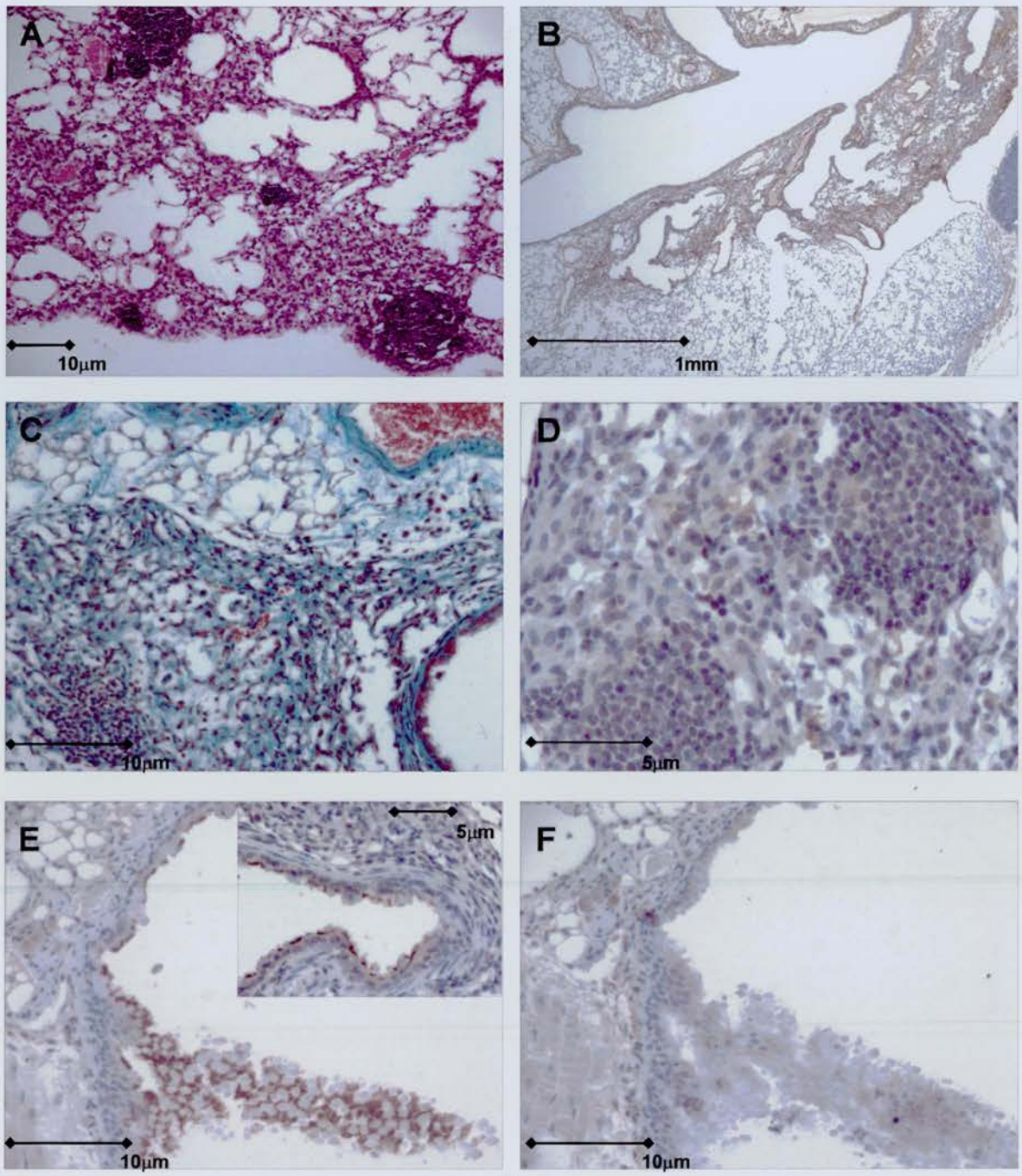

Figure 4.16: Histological Analysis of T-Lymphocyte Depleted Mice
Model one mice, killed 6 weeks after a FITC instillation, and seven days after addition of depleting antibodies. [A] x100 H&E stain showing loss of normal alveolar structure in areas of mononuclear cell foci. [B] x25 image of αFITC IHC illustrating the restriction of structural disruption and infiltrate to areas of FITC persistence, areas marked by increased collagen deposition, shown here in a trichrome stain (x200 magnification) [C]. [D] Shh expression was identified associated with foci of mononuclear infiltrate, (x400 magnification). [E] Illustrates an epithelial cross cut, such that Ptc expression can be observed as a patchwork at x200 magnification, the insert shows a normal Ptc profile at x400 magnification. [F] Shh is not expressed to the same magnitude as Ptc in the epithelial cross cut, but does appear localized, (x200).

4.2.15 EPITHELIAL CELL ISOLATES

Given that the epithelium is the first point of contact for the FITC, it was hypothesised that FITC induced its pro-inflammatory and profibrotic effects in chronic disease through an early interaction with the epithelium, altering cytokine release.

To investigate this hypothesis and the capability of these cells to generate Shh both at the genetic and protein level epithelial cell isolates were taken from 2 FITC and 2 PBS mice and pooled for culture at 12 and 18 weeks post second FITC instillation. The data in Figure 4.17 correspond to 12 weeks data, where 18 weeks data gave similar cytokine expression profiles (data not shown).

TNF-α levels were similar in each extraction, where as substantially more IL-6 and MCP-1 were obtained from PBS mouse cultures, than FITC ones. However, although cells were counted and plated according to an optimized protocol, there can not be complete certainty that the same number of *viable* cells were applied in each culture.

Equally, because no sorting was employed, contaminating fibroblastic production of these cytokines cannot be discounted, although cytospins of *pre*-differential attachment cells would indicate that cell populations were similar, consisting largely of clumped epithelial cells and contaminating macrophage with occasional lymphocytes. Studies described in Chapter 3, have shown that cell line fibroblasts produce MCP-1 and IL-6, but not TNF-α. Thus given that TNF-α levels were consistent between groups and time points (data not shown), whilst relative values for MCP-1 and IL-6 were variable, it is highly likely that fibroblast contaminants may be responsible for the differences between FITC and PBS epithelial preparations shown in Figure 4.17.

4.2.16 EPITHELIAL CELL ISOLATES PRODUCE SOLUBLE SHH

Epithelial prep supernatants were also applied to the 5E1 ELISA system discussed in Chapter 3. These supernatants demonstrated a positive signal consistent across 72 hours of culture, where media alone was negative (Figure 4.17). The FITC 48hr peak is likely an anomalous result given the standard error displayed from triplicate plating. Thus no difference was observed in soluble Shh signal. Whether this changed with stimuli was not investigated, neither was immunohistochemical analysis for reasons discussed in Chapter 3.

4.2.17 PRIMARY EPITHELIAL CELL ISOLATES CONTAIN MESSAGE FOR *SHH* AND *GM-CSF*

Epithelial cells were isolated from study 2 mice at 6, 12 and 18 weeks post second FITC instillation. RNA was isolated from all, whilst only 12 and 18wk isolates were used for culture. All three time points were positive for *GM-CSF*, and *Shh* message, where the 12 and 18wk time points are illustrated in Figure 4.18. Although non-quantitative, all samples were equally loaded and appear to lack PBS/FITC mouse differences. All samples were DNase treated and contamination checked with *β-Actin* prior to use.

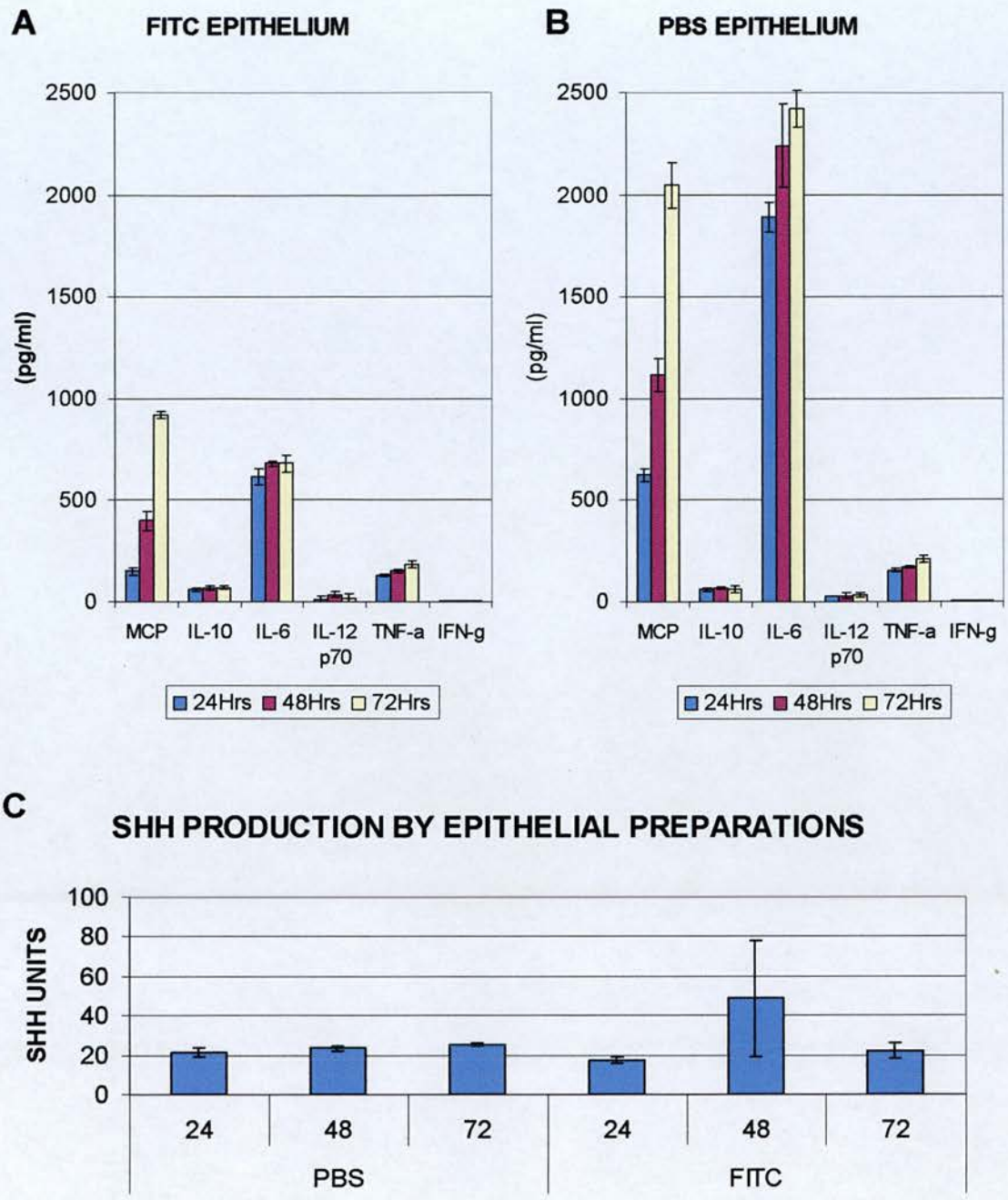

Figure 4.17: Epithelial Prep Cytokine Production
Epithelial preparations from 12wk post second instillation mice. Pooled from 2 lungs for each group. Error bars denote standard deviation. Panel A & B data derived from CBA application where detection cut off is 20pg/ml. the low end sensitivity of the Shh ELISA data shown in C is 3units/ml (samples 1:1, thus 6units/ml). Data from triplicate wells, except PBS 72hrs which is from duplicates. Cells plated at identical densities, subsequent data not adjusted for cell number as cell counts and MTT were not performed because cells were taken for RNA analysis.

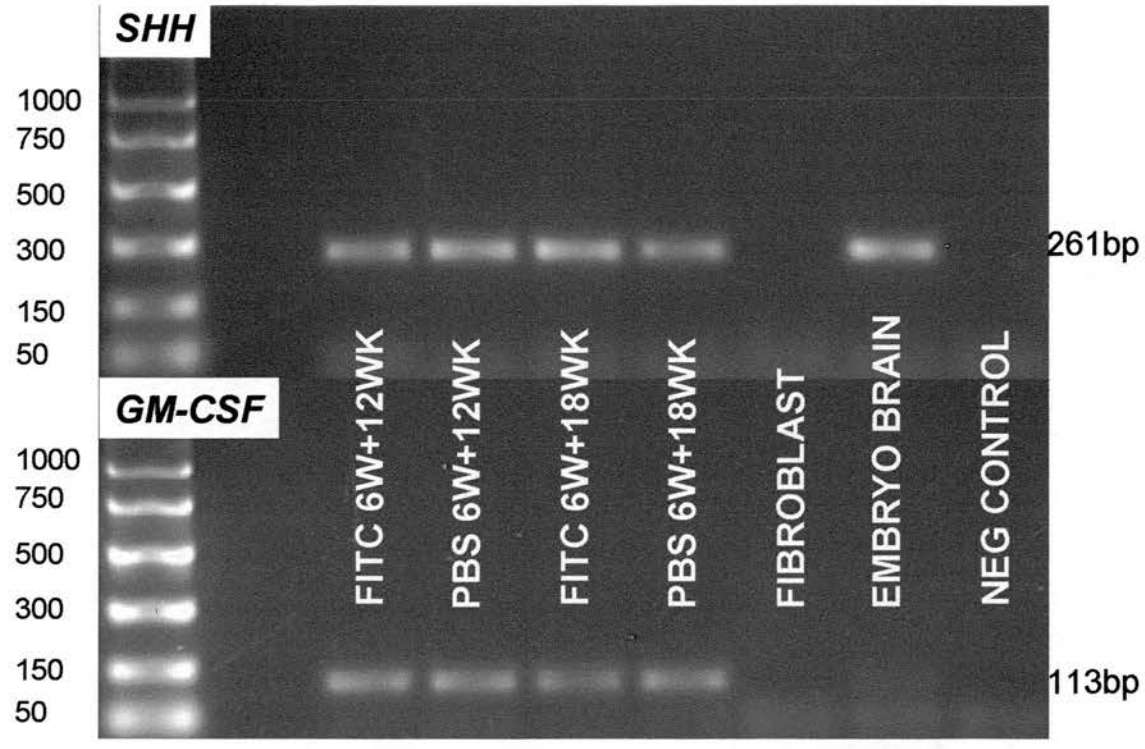

Figure 4.18: *SHH* & *GM-CSF* mRNA Profiles of Epithelial Cell Isolates

RT gels of RNA isolated from epithelial cell preparations following a differential attachment step, reverse transcribed using random hexomers and PCR processed for 35 cycles. Embryonic brain was used as a positive control for *Shh*. Cell culture activated CMT epithelial cells were used as a control for *GM-CSF* (not shown). A mouse fibroblast cell line, described in Chapter 3, was used as a negative control.

4.2.18 ALVEOLAR MACROPHAGE

To address the hypothesis that FITC induced disease was a consequence of an increased sensitivity of AM to LPS stimulation, altered cytokine secretion or response to Shh, alveolar macrophages were isolated from BALf via centrifugation for *in vitro* applications. No purification method was used as populations were generally >95% alveolar macrophages (Figure 4.13[A]).

During initial cell titrations for correct culture densities, survival was recorded via trypan exclusion and given as a percentage of cells and viable alveolar macrophage could be maintained for greater than four days in culture. During the culture there was a reduction in cellular number per well, this was not observed in wells stimulated with LPS (100ng/ml) 2hrs following plating (Figure 4.19[D&E]). This stimulation did not affect the relative trypan blue exclusion counts.

However, this technique, although relatively common, is flawed in two ways when applied to macrophage culture. Firstly, the majority of necrotic or unhealthy macrophage will be removed with supernatant extraction, thus will not feature in the percentage counts. Secondly, retained adherent unhealthy macrophage will likely be engulfed by neighbouring macrophage, hence the observed reduction in cellular number over time in the apparent absence of cell death. However if this is taken as the accepted explanation, this figure still illustrates that until 96hrs post isolation the macrophage had sufficient engulfment capability to remove necrotic or apoptotic neighbours, as floating cells were not observed in supernatants. A better measure of AM number would have been absolute cell counts or the MTS assay, which uses metabolic conversion of a colourimetric substrate to approximate cell number.

The cytokine response of AM to r-Shh and LPS was analysed using an inflammatory CBA kit. 48hrs after plating, unstimulated AM were found to produce MCP-1 (75pg/ml), IL-10 (50pg/ml) and TNF-α (100pg/ml) , but not IL-6 or IFN-γ.

LPS exposure increased the concentrations of MCP-1 (100pg/ml), IL-10 (68pg/ml) and most significantly TNF-α (608pg/ml) and induced IL-6 (50pg/ml). All concentrations remained at basal level with Polymyxin pre-incubation.

r-Shh exposure lead to marginal (<10pg/ml) increases in the above cytokines, with the exception of TNF-α, where the increase was greater (Figure 4.20). All increases were returned to basal with Polymyxin pre-incubation, suggesting that r-Shh mediated effects were attributable to the affects of LPS contamination.

Although LPS responses were higher in FITC mice BALf preparations, unstimulated and polymyxin AM cytokine production was also higher in these mice suggesting that these differences may have been attributable to the FITC preparations having higher background expression. Whether this was a

feature of preparation variability in activating the extracted cells, or a variance attributable to FITC treatment was not ascertained.

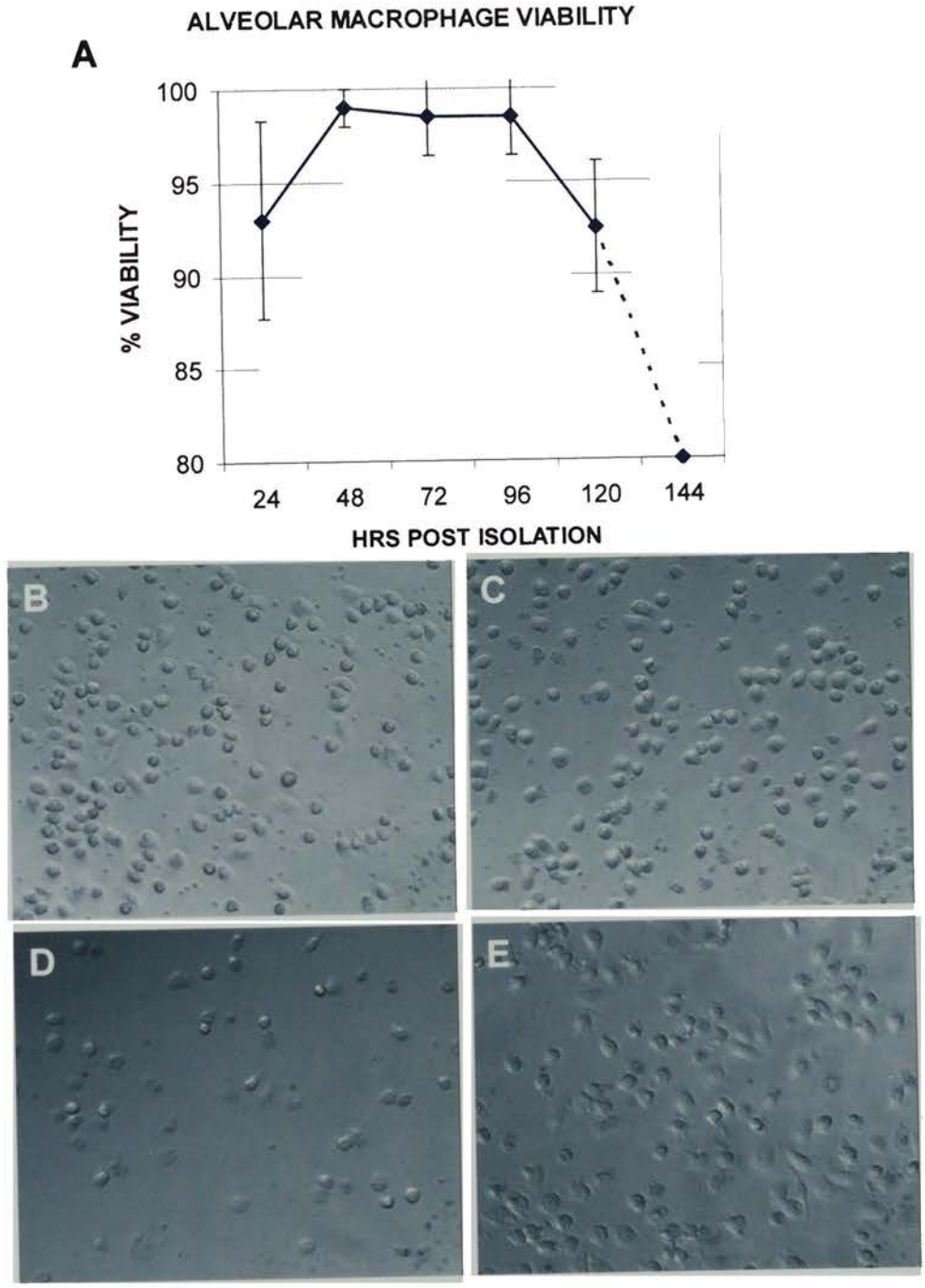

Figure 4.19: Alveolar Macrophage Isolation
[A] Cell viability ascertained via trypan blue exclusion counts of >200 cells. Photos are x200 magnification at 24 [A] 48 [B] & 72 [C] hours post isolation. Reduced cell numbers were identified at later time points in the absence of floating cells, suggesting engulfment by neighbouring macrophage. This reduction could be prevented via addition of 100ng/ml of LPS 2hrs post isolation, where [D] is a 72hrs post isolation image. LPS addition did not affect relative trypan counts. This observation was made on two separate occasions of duplicate wells.

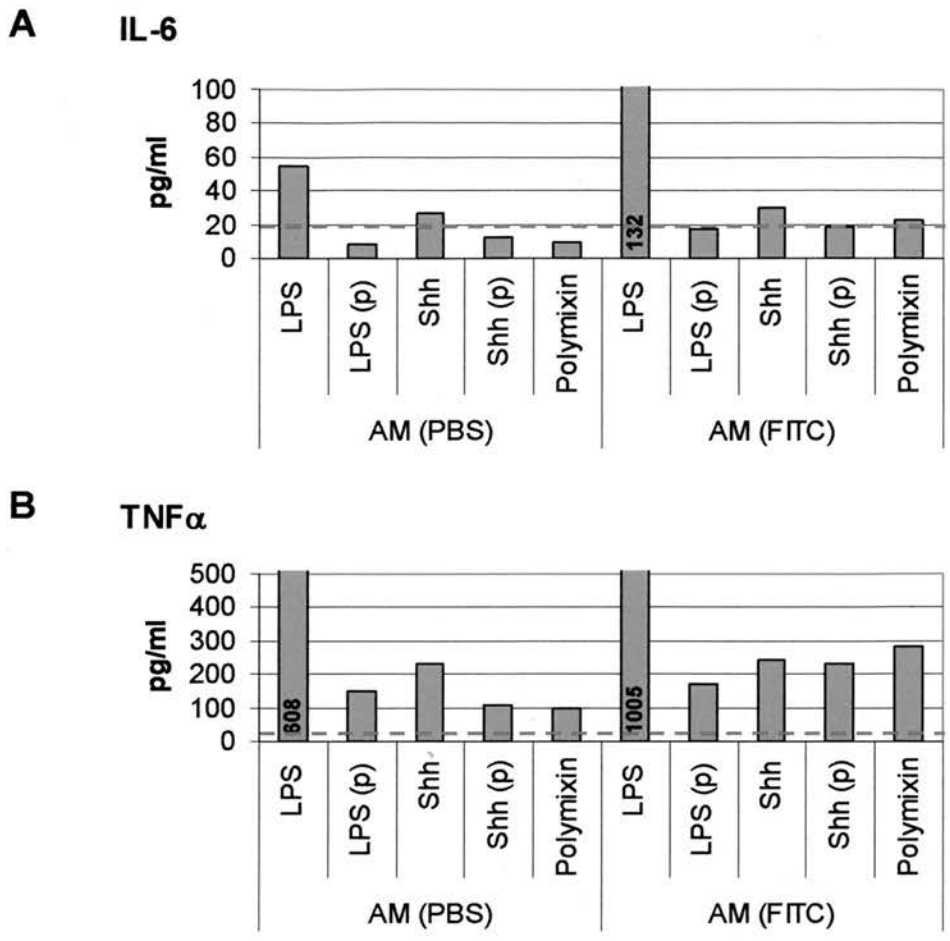

Figure 4.20: Alveolar Macrophage Cytokine Production
Data from 12wk post 2nd instillation, but representative of 18wk post 2nd instillation data. AM pooled from 2 mice, total of 4 mice from each group giving two plates of duplicate wells for each treatment. Cells at $1.5x10^4$ per well. Media removed after 2hrs, replaced with 150μl to which 150μl of prediluted agent is added, Polymyxin B (p) (10μg/ml), LPS (50ng/ml) and Shh (1μg/ml). Supernatants removed 48hrs later and duplicate wells pooled. IFN-γ below detection, MCP-1, IL-10 and IL-12p70 patterns were similar to IL-6 (data not shown). Optimal scaling has been used to the exclusion of LPS data, off scale bar values are shown in the base of each bar. Red lines refer to the lowest standard concentration used in the CBA.

4.2.19 PRIMARY FIBROBLAST ISOLATION

In order to establish whether primary fibroblasts could respond to a r-Shh signal, and therefore directly link Shh expression with a profibrotic effect, a primitive method of fibroblast isolation was devised using the fragments of lung tissue remaining following epithelial isolation. This used no method of sorting or immunohistochemical labelling, purely consisting of 2-3 passages to a point of apparent uniform morphology. Cells obtained in this manner could be maintained for a maximum of 4 passages, upon which they lost their ability to proliferate, but could be maintained as a healthy culture. The different media trialled can be seen in Figure 4.21.

4.2.20 PRIMARY FIBROBLAST PROLIFERATION IS NOT AFFECTED BY r-SHH

Primary fibroblasts were used following a second passage, where cells were considered relatively pure, as ascertained by morphological observation alone. Plating conditions and TGF-β concentrations were taken from Huaux et al [189]. Addition of r-Shh to these cells had no affect on proliferation as measured by MTT signal/cell number (Figure 4.22). TGF-β was used as a control, where fibroblasts should be responsive. TGF-β was shown to markedly reduce the MTT signal for these primary fibroblasts. This could represent cell death, but more likely illustrates an inhibition in proliferation, revealing the normal rate of cell death in these cultures. Mitomycin C could be used to confirm this hypothesis, but this has yet to be performed.

Considering the diffuse nature of the pathology induced by FITC it is perhaps not surprising that no differences could be identified from cell isolates considering the dilution effect of normal unexposed cells in each of the isolates. Cytokines were not analysed from this study, which is unfortunate given that in Chapter 3, r-Shh was shown to induce IL-6 which could be crucially linked to Shh function as IL-6 not only leads to T-lymphocyte proliferation, but also up regulates antibody production where the generation of FITC specific antibodies could be crucial for disease progression, as discussed previously.

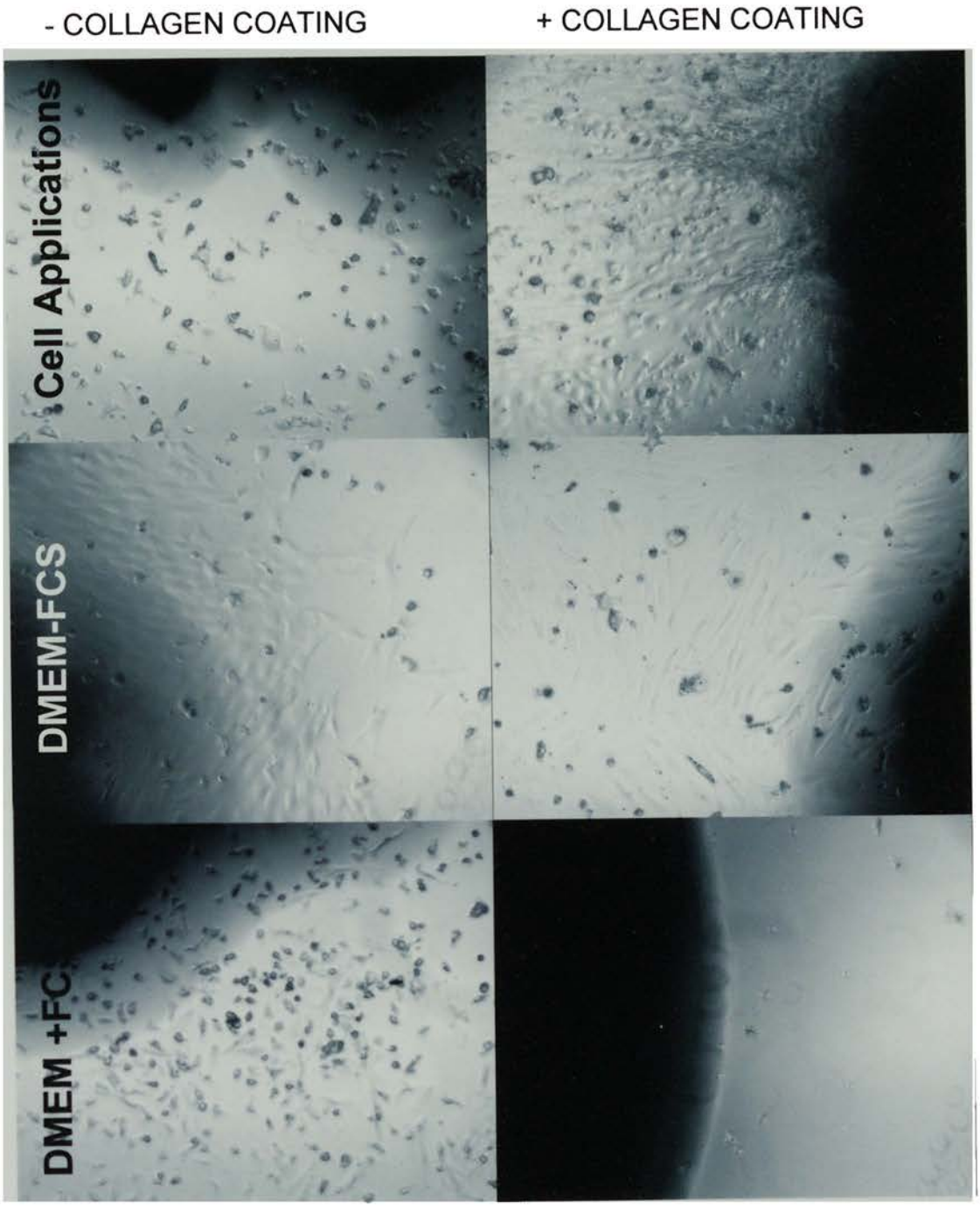

Figure 4.21: Fibroblast Isolation Protocol Development
Fibroblasts were grown out of lung fragments approx 5mm^2 (dark areas above) in differing media, with or without collagen coating of the flask (5ug/cm^2). DMEM in the absence of serum, either with and without collagen coating was identified as the best means of generating fibroblasts. Serum positive media supported non-fibroblastic proliferation in the absence of collagen. Cell applications media proliferation was similar to that observed with DMEM –FCS, but with additional non-fibroblastic proliferation.

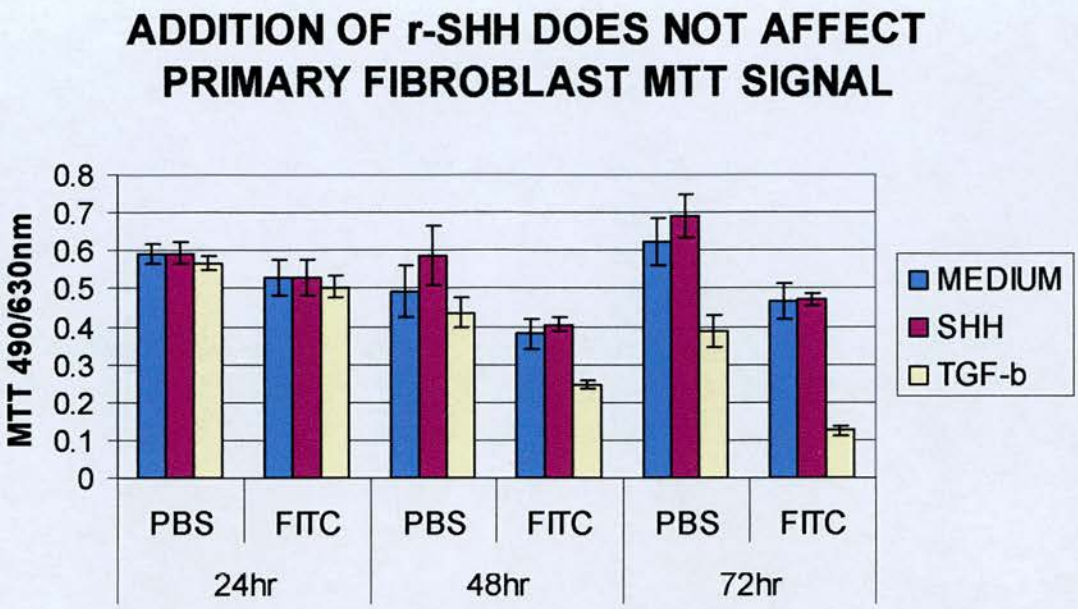

Figure 4.22: Primary Fibroblast Cell Number is Unaffected by r-Shh
Cells plated $1x10^4$ cells per well in 96 well plates. TGF-β (10ng/ml), Shh (1.5μg/ml). Cyclopamine (10mM) treated controls were no different to media and r-Shh treated wells (data not shown). Cyclopamine stock is in a DMSO carrier, DMSO controls were also no different to media controls. MTT performed from 5mg/ml in 100μl per well volumes for 3hrs prior to 200μl DMSO solubilisation.

4.3 DISCUSSION

4.3.1 INTRODUCTION

By maintaining mice for eighteen weeks after a second FITC instillation, it has been possible to illustrate a persistent mononuclear infiltrate localised to areas of FITC deposition. These regions had increased Ashcroft scores, peaking at twelve weeks post second instillation (Figure 4.10). A positive association between these scores and FITC specific IgG1 titres was observed, in the absence of specific IgG2a and IgE. Further to this, putative iBALT structures were observed restricted to regions of FITC deposition and T-lymphocyte depleted mice had a reduced Ashcroft score with FITC instillation compared with wild type. These data would suggest dual i.t. instillation of FITC into Balb-c mice results in an anti-FITC Th2 response, which is non allergic and may be involved in the fibrotic response of these mice.

The following sections will discuss these findings and their relevance to disease, concluding with an evaluation of the hypotheses posited at the start of this chapter and a brief review of future work that could address some of the issues raised in this Chapter.

4.3.2 INFLAMMATORY INFILTRATE

The association of FITC with areas of irregular epithelial-mesenchymal separation observed in these studies (Figure 4.8 [B]) indicates that some limitation in lung flexibility or cellular function has occurred, either as a direct consequence of FITC, or resulting from the inflammatory infiltrate. The occurrence of some of these irregular structures in the absence of significant infiltrate at two weeks post second instillation and persisting throughout the time course, could suggest an area of ameliorating infiltration, but given the chronic nature of this response, it is more likely that at least some component of the structural disruption induced by FITC occurs as a direct result of its interaction with pulmonary cells, not involving an inflammatory infiltrate.

Whilst FITC has the ability to covalently crosslink ECM and cell surface proteins, disrupting normal cellular interactions, studies from the lab of Toews and colleagues at the University of Michigan would suggest that FITC delivery can also directly affect cellular signalling[121, 185]. Whilst these authors concede that this cellular activation does result in the establishment of an inflammatory infiltrate, they suggest that the development of fibrosis is immune system independent[185], and that the crucial step in fibrotic progression is the CCL-2 mediated recruitment and activation of circulating fibrocytes to produce collagen 1[190]. This would suggest that the occurrence of an infiltrate in FITC instilled mice is an aside to the pro-fibrotic recruitment of fibrocytes. Notably however, these studies identified the peak of CCL-2 up regulation just 3 days after FITC instillation, returning to baseline by 7 days, where peak levels of collagen deposition were observed at 21 days, the final time point investigated. This would suggest that this early up regulation initiates later fibrotic activity.

However, these authors have never looked at later time points, where our experience would suggest that this early collagen deposition is an acute response to FITC instillation which ameliorates and that true permanent fibrotic architecture occurs chronically. Therefore whilst the initial inflammatory infiltrate may not be involved in the acute scarring response described by Toews et al, it may still play a role chronically.

4.3.3 THE ROLE OF THE EPITHELIAL CELL

As the first point of contact for FITC, the epithelium is ideally placed to orchestrate the pulmonary response. Interestingly, the dynamic apical surfaces of the stratified and small airways, composed of fast cycling protein and cell populations appeared clear of FITC by two weeks administration, whilst sub-epithelial regions, composed of slower cycling proteins remained positive throughout (Figure 4.8). This would suggest that unless some form of lineage or functional selection occurs as a result of FITC exposure, the role of the epithelium in the deposition of collagen may be primarily acute, perhaps as a source of the CCL-2 observed in the studies of Toews et al, and not involved in the chronic development of fibrosis. This of course does

not negate the possibility that these early signalling events permanently alter the epithelial signalling milieu in areas of FITC deposition. However were this the situation then areas of fibrosis might be expected where complete clearance of FITC had occurred and this was not the case.

The absolute association of FITC persistence and fibrosis, coupled with the requirement for a second instillation of FITC to induce fibrosis in the transoral model (model 2) indicates that the propensity for fibrotic disease is linked either to the persistence of the FITC in the lung, or the quantity. Ashcroft scores recorded here were higher overall than those recorded by Dr Ahmad using a dose 1mg less than that used here,and qualitatively the level of fibrosis observed was linked to the amount of FITC present in that area.

These observations would suggest that FITC does not induce a permanent change in the activity of cells where it has lodged, and that its persistence is required for fibrosis. Furthermore, if the 12 week mice are accepted as representative replicates of previous histology in 18 week mice, the qualitative loss of FITC by 18 weeks is associated with a reduction in Ashcroft score.

4.3.4 THE ANTI-FITC IMMUNE RESPONSE

If the presence of FITC is required to maintain the fibrotic response, but in the absence of direct signalling, then perhaps it is not the FITC itself, but the animals immune response to that which determines the extent of disease. Given the data presented in this thesis it is posited that whilst the acute response characterised by Toews et al can occur with or without an inflammatory infiltrate, the chronic development of fibrosis requires an immune response.

It is unlikely that fibrosis develops as a result of non-specific inflammatory infiltrate, owing to the absence of significant neutrophil numbers in a predominantly mononuclear infiltrate (Figure 4.13 & Figure 4.14), where neutrophils would be expected to predominate in responses to persistent injury, or AM induced non-specific recruitment of inflammatory cells.

Instead, the mononuclear nature of the infiltrate would indicate that, at the time points investigated here, infiltrates arose as a specific response to FITC or a FITC specific function.

The correlation of Ashcroft score with FITC specific IgG1 titre (Figure 4.11 and Figure 4.12) and the association of iBALT with areas of FITC deposition, (structures normally associated with B-lymphocyte activity and isotype switching), are highly suggestive of antibody being involved in FITC mediated inflammation and fibrosis. Furthermore, the absence of FITC specific IgG2a and IgE, suggests that the immune response is Th2, but non allergic.

Whether this immune response is ameliorative, made because of events initiated during the acute period of FITC delivery and resulting in the reduction in Ashcroft score at 18 weeks, pathologically crucial, or inconsequential to the development of disease, is a question worthy of further discussion.

The deliberating factor in the distinction between these roles is why the peak in Ashcroft score at 12 weeks and not earlier. It is possible that a persistent or maximum level of signalling must be reached associated with an inflammatory infiltrate, before fibrosis occurs, which would also explain the requirement for a second FITC instillation to act as a booster of the inflammatory response. However, not all chronic inflammatory conditions of the lung develop fibrosis, thus for the anti-FITC inflammatory response to be pro-fibrotic there must be something particular about it to initiate fibrosis.

The mononuclear infiltrate could include B & T lymphocytes and macrophage precursors, which themselves contain sub-populations. This has yet to be characterised in this work as preliminary IHC investigation with B220 (B-lymphocyte) and CD3 anti-bodies (T-lymphocyte) did not generate specific signals. However, it is likely that the increase in IgG1 observed post FITC instillation, although an indication of plasma cell number, may also be representative of FITC positive T and B lymphocyte populations represented in the infiltrate. Thus fibrosis could result from an increasingly Th2 cytokine milieu in the lung.

Alternately, fibrosis could result as a result of direct antibody function. However, unlike the well characterised association of Th2 polarisation and fibrosis, the association with antibody remains more contentious[191] .

4.3.5 FITC SPECIFIC IGG1

IgG1 is a key opsonising antibody which attached to a cell surface antigen in conjunction with complement protein 1, can initiate a complement cascade resulting in the death of the attached cell. This can occur either through membrane attack complex formation causing membrane permeabilisation, or through recognition of membrane bound IgG1 by Fc (IgG receptor) bearing cells such as macrophage, which can phagocytose the cell.

The occurrence of FITC specific antibodies could therefore be suggestive of the removal of cells to which FITC is attached, and that this process induces inflammation, maintaining the observed infiltrate, and contributing to the development of fibrosis, although eventually the removal of the FITC would reduce inflammation, through a lack of antigen.

Alternately the main pool of FITC may reside attached to ECM proteins. Were this the case large IgG complexes might be expected, with disruption of connective structures. Thus the association of FITC and areas of epithelial mesenchymal separation discussed earlier may be representative of IgG mediated ECM disruption.

However, when considering the potential relationship between FITC specific IgG1 and Ashcroft score, it is important to understand the limitations of this data set. Firstly, there are a wide array of other antibody subtypes that were not investigated here, Secondly, this system does not discount the possibility that rather than more antibody, high titres may represent greater affinity for FITC, or less competitive exclusion from another uninvestigated subtype.

Further to this, unlike common mouse model antigens such as ovalbumin or dust mite allergen, FITC has the capability to conjugate to host proteins. Thus an analysis of antibodies specific for FITC-BSA conjugates in ELISA,

does not negate the existence of antibodies specific for FITC-lung protein conjugates.

Indeed, responses against FITC-lung protein conjugates could be used as an argument for an ameliorative role for FITC specific antibody, as the perceived drop in FITC/BSA specific antibody at 18 weeks could represent a switch, or affinity maturation to anti FITC-lung protein conjugate antibodies, which are no longer specific for FITC\BSA, but which clear FITC-protein conjugates from the lung resulting in reduced FITC, and consequently less inflammation. Equally the delay in antibody peak could be explained by the gradual "purification" of these conjugates by the loss of more rapidly turned over protein conjugates, facilitating, along with affinity maturation, the breakage of T-cell mediated tolerance against the conjugated self peptide.

However, a direct link between antibody and fibrosis would appear unlikely as fibrosis would then have been expected by 2 weeks post second instillation through to twelve weeks post instillation, as this was when the greatest amounts of FITC was present with steadily increasing concentrations of antibody.

4.3.6 *IN VITRO* STUDIES

Full analysis of primary cell function in these mice was inhibited through high variance in low replicate samples, an endotoxin contaminant in the r-Shh peptide and a paucity of diseased areas limiting FITC exposed cell numbers in culture. Given the data elucidated in Chapter 3, the injurious extraction procedure will have affected epithelial cytokine production, and particularly that of Shh, thus it is difficult to draw any substantial conclusions from the data presented here, e.g. the occurrence of Shh message in epithelial isolates, does not necessarily confirm its occurrence in normal *in situ* epithelium, given its rapid up regulation with injury. True analysis of differences in mRNA and protein expression, when considering inflammatory and fibrotic processes may require another less injurious process such as laser microdissection where protein and mRNA can be extracted *in situ* from defined cell populations. This approach will be addressed in Chapter 5.

4.3.7 IMMUNOHISTOCHEMICAL ANALYSIS

Use of a newly optimised Shh and Ptc IHC procedure which takes advantage of the newly available blocking preparatory steps, has reduced what was originally a more distributed Shh signal, to an exceptionally marginal one where perhaps one or two areas of expression could be determined per section from both PBS and FITC mice. Whether this represents truly increased specificity or rather a reduced sensitivity from the previous method is a matter of conjecture. However, that the staining pattern for human tissues, which was more specific than mouse staining using the previous IHC methodology, remains the same with the new technique (Figure 4.23), would argue against a loss of sensitivity, instead suggesting that the reduction in positive staining in mouse tissues using the new technique is attributable to greater specificity.

Ptc expression was unchanged in FITC instilled vs. PBS mice and was constant in areas of normal and inflamed lung. The main area of variation was a more cellular distribution in the cuboidal epithelial cells of the smaller airways, versus a largely membranous distribution in the more mucal, larger cuboidal cells of the upper airways. Near serial sections would suggest that Ptc expression was commonly observed on CC10 positive cells, but also on CC10-ve cells, although these observations would require confocal dual stain conformation.

Regular and distinct Ptc expression on the apical surface of epithelium in the pulmonary system is highly suggestive for a role for this molecule in post embryonic systems. Although this need not be active, Ptc expression could represent a "Shh sponge", to endocytose, in the absence of signalling, free Shh, as described by Torroja and colleagues[192]. However, such a function would be largely redundant, given receptors such as megalin and Hip that could perform such a regulatory function, thus this is unlikely to be the main role of Ptc.

It is equally possible that Ptc expression occurs as a consequence of an upstream event, and that its expression is either non-functional, or related to another signalling ligand such as Ihh, Dhh or an as yet to be characterised

molecule[56]. However, data emerging from studies in the gastrointestinal tract [193-196], where Cyclopamine, a Smo inhibitor, continues to have an inhibitory effect, in the apparent absence of immuno-detectable ligand[194] and in some cases receptor [195], indicates that more sensitive methods of detecting Shh signalling may be required to discount Shh as a Ptc ligand in adult pulmonary systems. Thus, the lack of detectable Shh in this study could be attributable to a limitation in IHC technique rather than true absence of signal.

Given the findings presented in Chapter 3, it is also possible that as an indicator of injury, Shh might be a rapidly cycled protein. Thus for correct detection, more rapid fixation might be required. Certainly, methanol fixed embryonic brain tissue gave greatly improved immunohistochemistry over formalin fixed tissues (data not shown). Equally, only chronic time points were analysed in this study, where the results of Chapter 3 would indicate that greatest Shh might be expected at more acute time points.

However, what would seem more likely is that Shh expression does not play a crucial role in this disease and that the expression identified previously was largely non-specific staining. Such a view appears vindicated by current studies in the lab utilising the new Shh immunohistochemical techniques on human UIP biopsies, where Shh is still observed associated with areas of disease, as observed with the previous IHC protocol (Figure 4.23), suggesting that in this human condition, but not the FITC mouse model, Shh may have an association with disease.

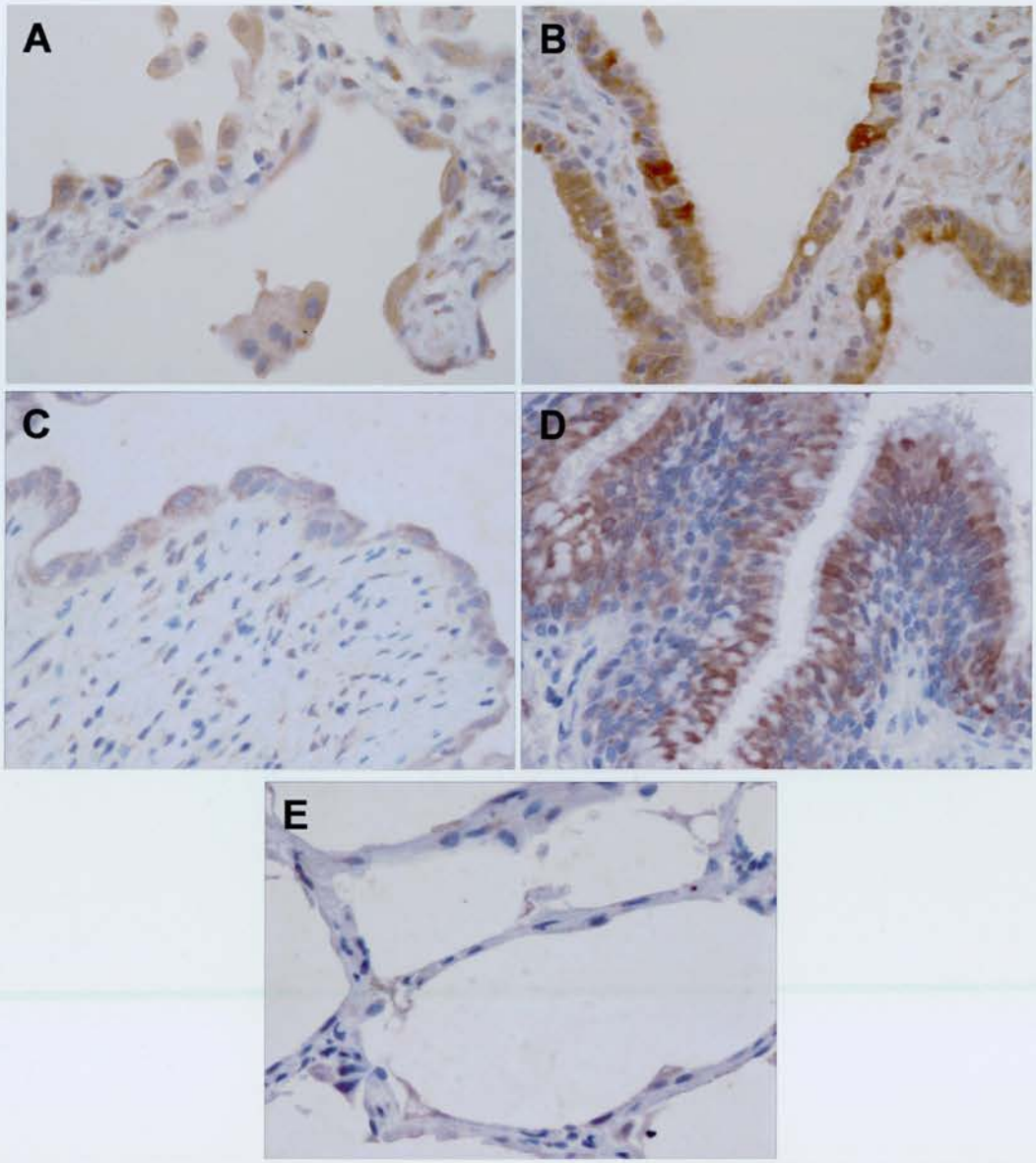

Figure 4.23: Shh Immunohistochemistry in UIP Biopsies
[A&B] Photos taken from Stewart et al[1] illustrating Shh expression in type II cells [A] and the metaplastic epithelium of bronchilarised airways [B] using the old immunohistochemical technique. [C&D] are photos of Shh visualised with new immunohistochemical techniques, where [C] are type II cells overlying a fibrotic focus and [D] are large airway epithelial cells. [E] represents Shh staining in a comparatively normal field of a UIP patient biopsy using the new methodology.

4.4 CONCLUSIONS

4.4.1 HYPOTHESIS AND AIMS

To recap the aims of this chapter were to:

- Compare the immunohistochemical observations from the surgical model with the transoral model
- Characterise the morphological alterations and inflammatory recruitment induced by dual instillation of an increased concentration of FITC
- Screen Alveolar Macrophage isolates from FITC and PBS treated mice for differences in cytokine production in response to r-Shh and LPS
- Screen fibroblast and epithelial isolates from FITC and PBS treated mice for differences in cytokine production and responses to r-Shh
- Characterise the FITC specific antibody profile with dual instillation of FITC

The aims detailed above were used to address the hypotheses that Shh is a signal found associated with areas of chronic fibrosis in the dual instillation model of FITC instillation. A secondary broader hypothesis was that the FITC model represents a model of acute inflammation, which primes the immune response to make an injurious and profibrotic immune response upon a secondary instillation of FITC. Further to this it was posited that FITC instillation might induce some endotoxin hypersensitivity in AM leading to inappropriate inflammation.

Whilst the aims detailed above were achieved through the completion of this Chapter, elements of the data collected here were preliminary. For example primary cell studies, which in retrospect, given the patchy nature of FITC induced disease, were never going to yield starkly contrasting data in PBS vs. FITC comparisons. Equally, data collected through the completion of Chapter 3 would suggest that the injurious isolation process of these cultures could mask any meaningful comparison.

Studies characterising the histological and immune characteristics of the FITC model illustrated a clear association between a Th2 polarised non allergic immune response and increased ECM deposition, specific to areas of FITC deposition, where there was no association or functional role for Shh identified. Thus to address the hypotheses posited at the start of this Chapter it would appear unlikely that Shh is associated with FITC induced disease. This of course does not negate its potential for a role in other disorders, given the prominent and regular expression of its receptor Ptc.

As to the broader hypothesis relating to immune mediated profibrotic responses, the data presented here are not conclusive. However the suggestive correlation of IgG1 (Th2) titre and disease score, along with the reduction in pathological indicators with T-lymphocyte depletion studies, and the presence of iBALT, would suggest that Th2 immunity may play a role in FITC instillation mediated disease. Whether this is ameliorative, pathological or inconsequential has yet to be determined.

4.5 FUTURE WORK

4.5.1 ANTI-FITC IMMUNE RESPONDERS

Future work should concentrate on characterising the foci of mononuclear infiltrate observed in FITC areas, specifically to identify whether they are indeed iBALT via staining for follicular DC (characteristic of these structures) and plasma cells (CD138+).

It would also be interesting to use a biotinylated anti-mouse IgG1 antibody or anti-complement antibody on sections. This may generate too much background but it would be interesting to see if it localised to areas of FITC deposition. Another approach might be to take sera from FITC or PBS mice and use as a primary antibody on mouse sections blocked with un-conjugated anti-mouse IgG. This would identify whether the sera of FITC or PBS mice contain lung or FITC specific antibodies, and the localities to which they bind.

Equally it would be interesting to take a whole lung homogenate and extract the mononuclear cells for fixed co-culture with biotinylated FITC for use in flow cytometric analysis with a cassette of lymphocyte markers, to identify whether there were FITC specific immune cell populations in the lung.

4.5.2 FITC CONJUGATES

In order to identify the compounds FITC is bound to in the lung, whole lung homogenates could be run through an anti-FITC western, isolating bands for characterisation. Another approach might be to pass whole lung homogenates through an anti-FITC antibody coated column then use the elutant both as a coating for a serum ELISA system, and as a way of isolating conjugated proteins.

4.5.3 SERUM ELISAS

To reduce serum ELISA variation, future serum ELISAs should be modified to include an anti-FITC IgG1 or 2a commercially produced control which would be run on every plate. This would be used as a standard curve or as a way to normalise the results of each plate so that sera from studies can be run on separate days, enabling combination of study data. This would also allow triplicate samples of sera to be run, as this was not possible using the current technique of running whole study samples in one batch. Use of three fold dilutions and end point titres also complicated this ELISA system, but was necessary due to the high concentration of antibody. A better approach might have been to stop the ELISA earlier or use a less sensitive substrate in combination with a standard serial titre. Alternately a nominal value could be proposed as a cut off (minus the background value. i.e. a value below 0.25+/- background OD is taken as negative). Also prior depletion of IgG1 prior to IgG2a ELISA might confirm true absence of these antibodies.

4.5.4 NEW ANALYTICAL TECHNIQUES

Data presented here highlight the limitations of looking for evidence of inflammatory mediators and potentially proliferative and differentiation inducing factors such as Shh, in primary isolates which have endured

injurious extraction procedures. Equally the pooling effect of analysing total cell isolates from a patchy disease model makes interpretation of primary cell data a very marginal process.

The newly established laser microdissection technique may present an approach that may remove such restrictions and this is addressed in the following Chapter.

CHAPTER 5: LASER MICRO-DISSECTION

5.1 INTRODUCTION

Studies discussed in the previous Chapters illustrated the limitations inherent in the analysis of injurious or inflammatory signals using both primary cell isolates and cell lines. This Chapter will describe a novel approach, taking advantage of recent technological advancements in both RNA extraction and laser dissection techniques, to analyse *in situ* mRNA expression in diseased or inflamed areas and compare them with normal structures.

5.1.1 THE LIMITATIONS OF CURRENT GENETIC ANALYTICAL TECHNIQUES

EX VIVO

The most frequently used methods for detecting and quantifying gene expression in lung are northern blotting and real time RT-PCR. However, since lung is a complex heterogeneous tissue, being composed of over 40 different cell types, use of homogenates is limited in that dominant cell types will dilute signals from minor populations. Equally, isolation of specific lung cell populations typically involves enzymatic digestion with or without physical agitation, cleaving surface proteins and disrupting cell/cell/matrix interactions. This will undoubtedly induce some manner of cellular change in the isolates. It is also difficult to obtain a specific cell population from the lung, due to a paucity of good specific markers for pulmonary structural cells.

IN SITU

In situ hybridisation (ISH) can be used to provide cell specific genetic information in tissue sections. This avoids complex isolation procedures, but only a limited number of genes can be investigated by this method. ISH is not quantitative and has a relatively low sensitivity.

IN VITRO

The most significant limitation of *in vitro* based systems is that genetic information derived from immortalised cell lines or primary cell line isolates may not accurately reflect the molecular events taking place in the tissue milieu from which they were originally derived and often, events observed at

the pulmonary interface are reactions initiated, propagated or controlled by signals or cells derived from other locations in the body; features absent from mono and co-cultures.

5.1.2 LASER MICRO-DISSECTION TECHNIQUES

Recent advances in laser microscope technology, and low yield RNA molecular procedures, have facilitated development of a new *in situ / ex vivo* technique, namely laser micro-dissection. This began as a means of ablating non specific material prior to whole section digestion and RNA isolation a process which was highly time consuming and with limited application. However, this has now advanced to specific single cell *collection*, allowing for the accurate procurement of specific cell populations from heterogeneous organ systems.

This methodology has facilitated the genetic analysis of purified lung cell populations derived from their native tissue environment, and has been successfully used in the analysis of a number of human conditions, particularly Loss of Heterozygosity and mRNA profiling in cancers[197].

There are two distinct laser micro-dissection techniques, namely Laser Capture Micro-dissection (LCM), and Laser Pressure Catapult (LPC) micro-dissection, also known as Laser Microbeam Micro-dissection (LMM). These are summarised below and in Figure 5.1 & Figure 5.2:

LASER CAPTURE MICRO-DISSECTION

Laser capture micro-dissection was developed at the National Cancer Institute of the National Institute of Health, Bethesda (USA) and this system is now available exclusively from Arcturus (Rayne, UK). In this system a low energy infrared laser pulse is fired through an area of interest in a dehydrated tissue section. This strikes and melts an overlying thermoplastic (Ethylene Vinyl Acetate) membrane mounted on an optically clear cap. This causes the membrane to form a composite with the underlying tissue. Thus when the membrane cap is lifted it takes with it those areas which have been selectively attached (Figure 5.2). The advantage of this system is that

because most of the laser energy is absorbed by the membrane, the absolute maximum temperature reached by the tissue is 90°C for approximately a millisecond, thus RNA degradation is limited. Captured material can be clearly visualised on the cap following lifting, allowing direct observation of the specific cell types from which the genetic or protein material is to be isolated. Specialist slides are not required and material can be stained and processed through a variety of RNase free steps, as long as the final step involves complete dehydration of the slide, as water interferes with composite formation. Disadvantages include the long duration of the procedure and lack of specificity as loose adjacent material can occasionally lift with the cap.

LASER PRESSURE CATAPULTING

In this procedure sections can be mounted on a selection of slides ranging from plain or charged to specialist membrane coated slides. The choice of slides is determined by tissue type, fixative and staining regime. The membrane coating most commonly utilised is polyethylene naphthalene. At 1.35μm thick this does not interfere with visualisation and prevents non-specific dusting of slides prior to section mounting, as only following UV exposure for 30 minutes at 254nm do they become receptive for mounting. Full dehydration is not essential for membrane mounted sections, indeed live cells grown on these membranes can also be catapulted.

In this procedure, slides are visualised on an inverted microscope with a computer controlled motorised stage. Areas of interest for cutting are drawn around and highlighted using an outlining tool in the PALM™ imaging software, not unlike the freehand tool in paint or similar software program (Figure 5.2). These regions are displayed as "elements", where the computer software remembers the location of each element on the stage, allowing the user to review an entire slide before collecting the material.

Rather than melting a membrane as in the LPC procedure, this system isolates the material contained within element areas by cutting the membrane and overlying tissue section along the element line with a highly focused 337nm pulsed nitrogen UV laser beam, rather than the infra-red used in

LCM. At the point of completing the element, near origin, an automatic pulse is fired, where the photonic force catapults the desired material into a receptacle above the slide; most frequently the cap of a standard Eppendorf tube, filled with a capture buffer of choice. Material entering the cap is held in place by the surface tension of the buffer in the cap.

The main advantages of this procedure are speed and accuracy, but at a cost of good visualisation of captured material and more restrictive slide preparatory techniques. The membranes are susceptible to lifting with some solvents and normal positively charged slides, if fixed excessively or prematurely, will exhibit reduced catapulting efficiency. However a recent publication[198] would suggest that visualisation can be improved with the addition of an aqueous gum medium of Pinpoint™ solution and a dark blue ink stain.

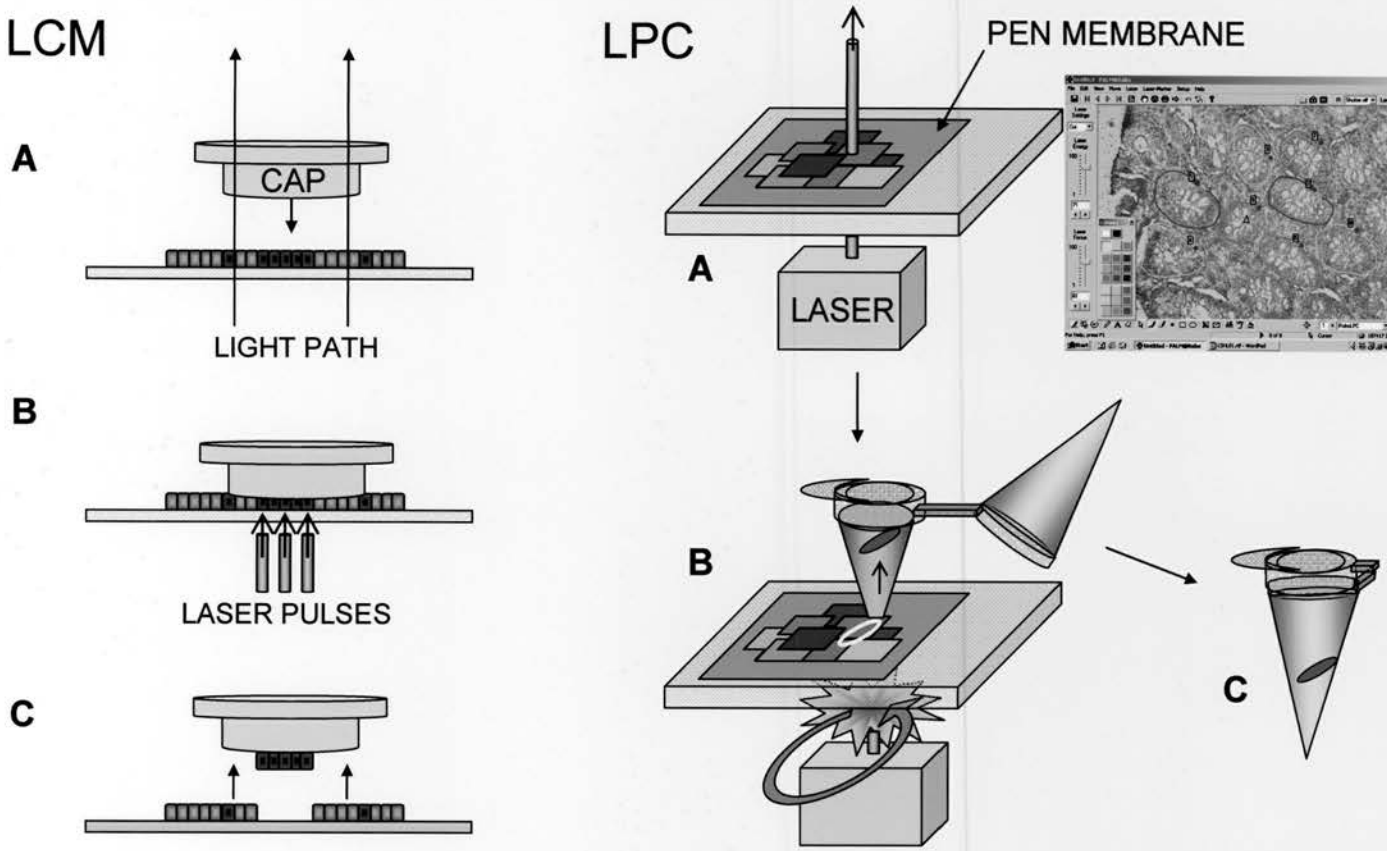

Figure 5.1: Schematic of Two Laser Dissection Methods

LCM: [A] The section is visualized on an inverted microscope where the section is viewed through the optically clear cap. [B] lasers fired at sites of interest melt the cap membrane causing fusion with the underlying material. [C] When lifted the cap takes the fused material with it. The cap then fits into the lid of an Eppendorf tube for inverted digestion in a buffer.

LPC: [A] Material visualised on an inverted microscope through the cap of a buffer filled Eppendorf tube lid. Areas of interest are circled as shown on insert screenshot and [B] upon completing the element a strong pulse is fired, literally flicking the material within the element into the Eppendorf tube lid.

LASER PRESURE CATAPULT MICRO-DISSECTION

LASER CAPTURE MICRO-DISSECTION

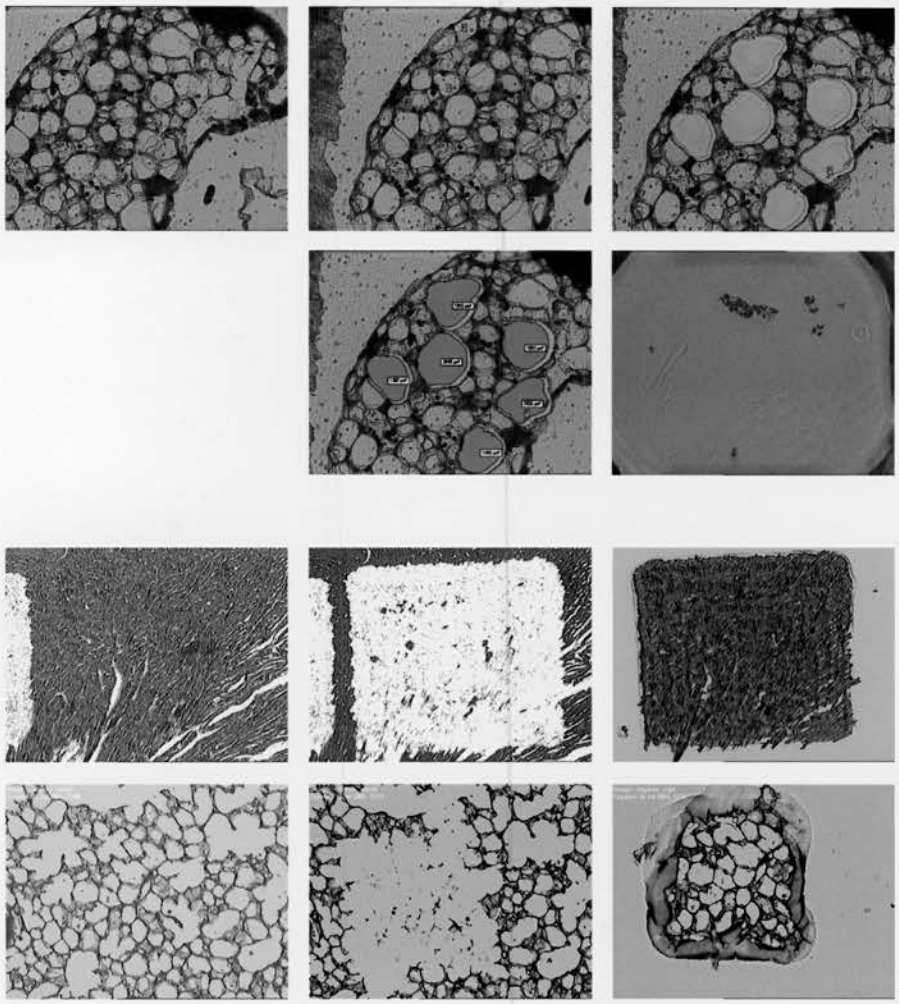

Figure 5.2: Photos from Laser Micro-dissection

[Top]: 12μm mouse lung sections, stained with H&E. red colouration of background due to H&E in Eppendorf tube cap through which the camera light path travels. Lines are drawn around areas of interest and cut / catapulted. The area catapulted can be calculated, although this is of limited use in an aerated tissue such as lung. Material can then be visualised in the Eppendorf tube cap. Performed on the PALM system

[Bottom]: Top row images are from 12μm mouse heart, the lower from 12μm mouse lung, where the first column is preview, second - post capture, third - material lifted onto the cap. Performed on the Pixcell II system.

5.1.3 TISSUE PREPARATION

There have been a great number of studies performed to ascertain how tissues should be preserved, processed and visualised for efficient laser micro-dissection. In general precipitating fixatives such as acetone or ethanol have been found to give better results than cross linking agents such as formalin. The fixation process is particularly important in relation to mRNA isolation, as in contrast to DNA, mRNA is more sensitive to fixation, is quickly degraded by ubiquitous RNases, and requires stringent RNase free conditions during specimen handling and preparation. To avoid these complications a number of recent studies have investigated the use of easily reversible cross linkers instead of formalin, notably dithio-bis(succinimidyl propionate) (DSP), also known as Lomant's reagent[199]. DSP links primary amino groups via an –S–S– bridge that can be cleaved by reducing agents such as DTT, producing unmodified RNA which exhibits less fragmentation than comparable formalin fixed tissues. However, for practical use with archival material, techniques based on formalin fixation are necessary.

5.1.4 IMMUNOHISTOCHEMISTRY

Identification of cell subtypes for laser assisted extraction from complex heterogeneous tissues can be difficult and time consuming in the absence of sufficient sub-type specific discriminating features. Standard staining procedures such as Mayer's haematoxylin and methyl green appear to be compatible with laser capture micro-dissection[200] for DNA extraction. More complex immunohistochemical techniques require more prolonged periods of aqueous contact which is deleterious to RNA preservation, and a number of harsh unmasking procedures, which reduce RNA yield[200]. However, a number of studies have now highlighted specific protocols for immunohistochemistry applicable to laser microdissection[201-203].

5.1.5 REAL TIME PCR

The majority of studies in laser micro-dissection involve analysis of the extracted RNA by quantitative real time RT-PCR. This technique is described briefly below and in Figure 5.3.

THE RT STEP

Reverse transcription for the generation of cDNA for real time PCR can be performed using any standard RT protocol, using either oligo-dt primers or random decomers/hexomers, with various salt concentrations. However, use of differing mastermixes requires re-optimisation of the subsequent PCR. Our lab uses Applied Biosystems default reagents/recipe. Here, oligo dTs can be used to copy mRNA or random hexomers can be applied, to copy total RNA including rRNA. The full reaction recipe is supplied in Chapter 2.

THE PCR REACTION

The PCR reaction exploits the 5' nuclease activity of AmpliTaq gold™ DNA polymerase to cleave a Taqman™ probe during PCR. The Taqman™ probe contains a 5' reporter dye, typically FAM (6-carboxy-fluorescein) or VIC™ (Applied Biosystems) and a 3' TAMRA (6-carboxy tetramethyl rhodamine) quencher dye. During the PCR, cleavage of the probe separates the reporter and quencher dyes, resulting in increased fluorescence of the reporter dye and reduced quencher fluorescence. Thus the accumulation of PCR products can be quantitatively defined by measuring the increase in fluorescence of the reporter dye. This is summarised in Figure 5.3.

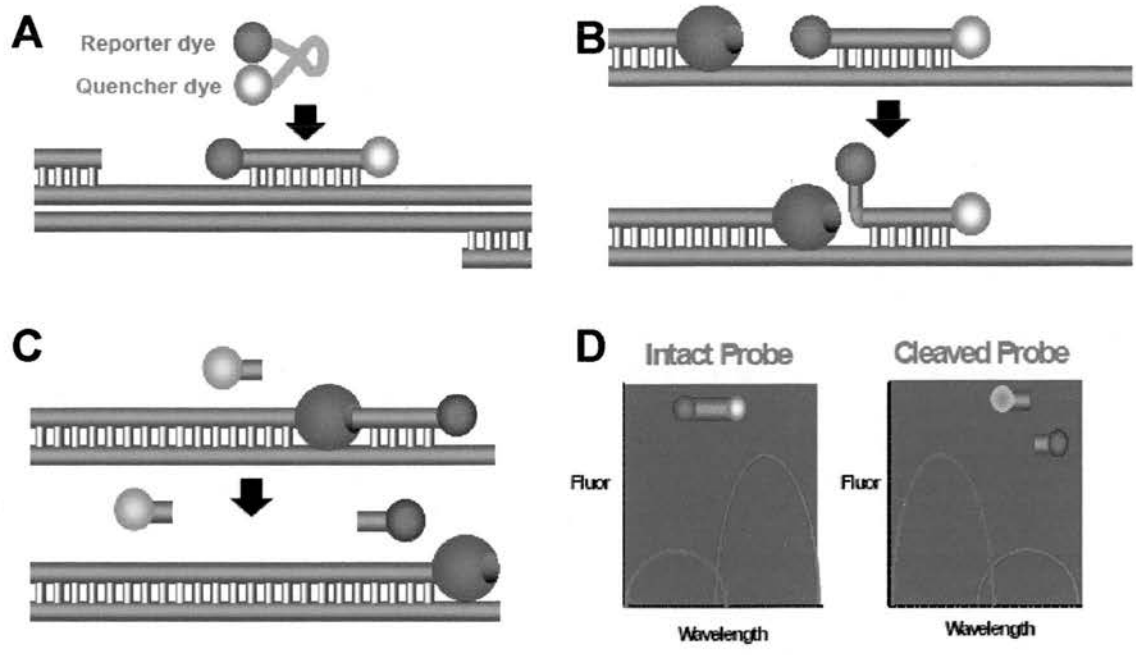

Figure 5.3: Real Time RT-PCR
(A) The Taqman probe binds to a sequence between the primer sets, recommended by Applied Biosystems to be no greater than 150bp in length. (B) Taq polymerase (purple) associates with the primers and transcribes complementary template where its exonuclease activity results separation of first reporter (C) then quencher from the probe. Such spatial separation results in increased detectable florescence from the reporter construct upon stimulation (D). Pictures modified from Applied Biosystems promotional and technical materials (www.appliedbiosystems.com).

CONTROL OPTIONS

The Taqman mastermix contains a passive reference to which reporter dye signal can be normalised during data analysis. However the majority of investigators utilise multiplex PCR to give optimal normalisation. Two primer probe sets with differing fluorescent labels are included in each reaction. One probe, conventionally labelled with VIC™ is specific for a housekeeping gene, highly expressed and unchanged by the experimental or condition analysed. The other probe, labelled with FAM, is specific for a gene of interest. A threshold is set against baseline fluorescence detection and the number of polymerase cycles at which each sample becomes positive on this baseline is denoted as a cycle threshold (ct) value. Thus house keeping genes generally have a low ct, in the range of 17-21 cycles if using approx 32ng of cDNA (16ng RNA), whilst lesser expressed genes of interest have higher ct values ranging from 22-35. Values above 35 can be difficult to interpret and highly influenced by minute contaminants or machine

fluctuations. FAM and VIC™ data can be presented as a direct comparison, however, Ct values are more commonly normalised and linearised for presentation, such that only the FAM values are supplied as a fold increase or decrease of FAM vs. VIC™ ratio, over a chosen negative sample i.e. untreated.

In our laboratory we utilise ribosomal *18S* as the house keeping gene, necessitating the use of random hexomers in the production of cDNA as oligos do not prime for ribosomal RNA. Primer probe sets for genes of interest are designed in house according to Applied Biosystems specifications, whilst *18S* sets are bought as pre-prepared stocks.

5.1.6 FRESH AND FROZEN TISSUES

Most studies have used fresh or frozen tissues for laser micro-dissection as the mRNA obtained from this material is of high quality, and a number of investigators have successfully isolated RNA from these tissues without the need for pre-PCR amplification.

One relevant recent study performed by Betsuyaku et al[204] used frozen mouse lungs to analyse pulmonary epithelial mRNA profiles. Mice were killed by CO_2 narcosis and lungs immediately inflated with Tissue-Tek™ OCT 50:50 with RNase free PBS/10%sucrose. The total time from death of the mouse to frozen tissue was 10 minutes to avoid post mortem changes in gene expression. Sections were prepared for LCM on glass slides, fixed in 100% ethanol, stained with 0.5% (w/v) Nissl (cresyl violet acetate) and dehydrated to xylene. The authors used the same PixCell II Laser Capture Micro-dissection system, which I used for my studies. Typically, 20 sections were used, where each tissue section contained 5–10 usable airways. 50 laser pulses were applied per airway in a procedure taking 4–5 hours per mouse.

RNA was extracted with a High Pure RNA Isolation Kit by Boehringer Mannheim™ and genomic DNA digested by incubation with DNase. They reported that the LCM isolated RNA was of excellent quality, where

approximately, 2–6 pg of total RNA was recovered from a captured 7-μm thick bronchiolar epithelial cell, so that a typical complete dissection yielded 600–900ng of total RNA. For subsequent real time RT-PCR the RNA isolated was sufficient for direct use, however, for oligonucleotide arrays, amplification was required.

cDNA was generated utilising random hexomers with half of the total RNA isolated used in the RT reaction (15μl RNA + 15μl Mastermix). 1μl of this reaction was then added into each real time PCR reaction mix, composed of TaqMan™ reagents, for PCR in an ABI Prism 7700 Sequence Detector. Applied Biosystems™ designed *GAPDH* was used as the internal standard (house keeping) gene. Other housekeeping genes were also utilised, Hypoxanthine Guanine Phosphor-RibosylTransferase (*HPRT1*) for low levels of the target or *18S* rRNA for high levels. The PCR reactions for the target gene and *GAPDH* were performed in separate tubes to avoid possible competition and/or interference.

Another study by the same group used LCM to harvest terminal bronchiolar epithelium for quantification of mRNAs by real time RT-PCR. Specifically, they examined the response of *CC10, TGF-β, Epidermal Growth Factor (EGF) receptor*, and *KGF receptor* mRNAs to intratracheal administration of bleomycin[205]. They identified reductions in *CC10* and *KGF receptor* mRNAs in both terminal bronchiolar epithelium and whole-lung homogenates 7 days after bleomycin. In contrast, terminal bronchiolar epithelial *TGF-β* mRNA was reduced, but whole-lung *TGF-β* mRNA remained unchanged. Findings with *EGF* were the reverse, where terminal bronchiolar *EGF* receptor mRNA was not changed but whole-lung *EGF* receptor was reduced. This illustrates the limitations of relying on whole lung homogenates as a means of analyzing cell specific RNA modulations in complex tissues.

5.1.7 FORMALIN FIXATION

Histological examination of sections from fresh or frozen material usually shows poor morphology, making distinct cell types difficult to identify, even with the development of rapid IHC staining techniques[203].

For this reason human biopsy material exists almost exclusively as fixed and embedded samples, where the most widely used fixative in pathology remains formalin. It is comparably cheap, easy to handle, gives good morphological quality and is compatible with a wide variety of antibodies. The aim is thus to achieve viable mRNA extraction from formalin fixed paraffin embedded tissue as this would allow retrospective analysis of large volumes of archival tissue.

Initial attempts to extract RNA identified reduced yield from formalin fixed material compared with frozen samples. This was initially attributed to cross linking induced fragmentation of RNA[206, 207]. But, a study by Masuda and colleagues[208] suggested that chemical modification is just as important as fragmentation. Formalin fixation was found to modify all four bases through the addition of mono-methylol (-CH(2)OH) groups at various levels, varying from 40% for adenine to 4% for uracil. In addition, some adenines underwent dimerisation through methylene bridging. This could be resolved to give approximately 50% of the yield from unfixed material by an increase in temperature of the formalin free buffer following extraction.

Some studies had suggested that RNase activity prior to fixation of tissue, such as prolonged post mortem periods could also play a role in reduced yield[209]. Equally, some had suggested that the size of a biopsy might influence RNA integrity, due to internal variation in fixation speed. However, Specht and colleagues[210], taking serial sections every 1 cm through a 7cm solid biopsy, where central fixation would be expected to be slower or incomplete, found that degradation during the fixation process was not a factor in reduced RNA yield, although observations made by Lehmann et al and discussed in a methods review[211], would suggest that fixation for greater than a week in standard formalin completely destroys nucleic acids.

Thus in conclusion, current literature suggests that LCM suitable samples are those which have a short post mortem storage time prior to fixation and are fixed for not more than a few days. Observations made by Mizano[209] would also suggest that when dealing with samples embedded decades apart, time and preservation matched controls should be included, to track post

embedding degradation of RNA sequences and ensure that this does not bias the RNA profile of the samples.

One of the first papers to utilise real time RT-PCR with laser micro-dissected material was that of Specht and colleagues[210]. Samples of oesophageal adenocarcinoma fixed in 10% formalin overnight were cut to 5μM, H&E stained for 45 seconds and dissected using the LPC system to collect approx 1,000 cells. In this early version of the current equipment adjacent areas of tissue to the area of interest were ablated and the area of interest transferred to a vessel via mechanically aided sterile needles. RNA was isolated via a phenol chloroform method and *Phosphoglycerate Kinase 1* and *HPRT* were used as internal controls for real time RT-PCR. Importantly this study highlighted that real time amplicon sizes up to 122bp had no affect on amplification yield, but values from real time RT-PCR were reduced above this size, and no product could be obtained with amplicons greater than 374 bases apart, where frozen samples were unaffected. This suggested that formalin fixed material contained only short sequences of material viable for transcription. Others have suggested that 200bp is the average size fragment available[211].

Subsequent studies have also reported good success using real time RT-PCR and nested RT-PCR on laser dissected cells from paraffin wax embedded archival tissue, fixed in either methacarn or formalin[212 213 214]. A number of interesting gene expression profiles have also been demonstrated through the use of microarrays in some studies[215, 216], although this has necessitated amplification of RNA prior to PCR, due to the poor quality of the isolated RNA. Such amplification raises a number of procedural bias issues, such as transcript stability and size, which although also an issue in normal RT-PCR, is more notable in amplified microarray applications.

5.1.8 THE FUTURE

Establishment of a reliable, high-throughput method of RNA/DNA recovery from formalin fixed tissue, has the potential to unlock a huge archive of material for retrospective analysis of case studies[209]. This would enable a

rapid advancement in understanding of disease initiation and progression, and the elucidation of differentially expressed genes as novel therapeutic targets or prognostic indicators.

Genotyping for hereditary conditions such as breast cancer, cystic fibrosis and Down's syndrome has revolutionised the preventative and ameliorative treatments available to patients and has facilitated a greater understanding of many of these conditions. Laser micro-dissection also offers the opportunity to perform similar prognostic testing, but with the advantageous ability to perform cell specific diagnostic screening. This could be used to identify locally induced cancerous mutations and erroneous signalling, such as the identification of loss of heterozygosity in neoplasias/cancers[217-219], mutations of *p53* & *K-ras* in colorectal carcinomas[220] or differential mRNA expression in biopsies of renal transplant rejection[221]. Recent developments utilising reverse phase protein microarray analysis may also allow the application of the laser micro-dissection technique to protein signalling[222]. Combined, these techniques will generate a greater understanding of the cell specific signalling interactions which occur in both healthy and diseased tissue, allowing more specific targeting of future therapies.

5.1.9 HYPOTHESIS AND AIMS

The aim of the work presented in this Chapter was to develop the laser micro-dissection technique and apply it to the study of developmental genes in pulmonary fibrosis.

The following hypotheses were addressed:

— Formalin fixed material contains viable RNA that is suitable for RT-PCR and real time RT-PCR

— Formalin fixed human and mouse adult lung contains detectable Shh and Ptc mRNA sequence

— Epithelial cells represent a putative producer & responder population for Shh, whilst mesenchyme is primarily responder in profile

5.2 RESULTS

5.2.1 PRELIMINARY STUDIES

At the time of initial investigation kits for use with laser micro-dissection were emerging from Ambion™, (Paraffin Block RNA isolation Kit, Cells to cDNA II kit) designed specifically for the extraction of RNA from very small numbers of cells obtained from frozen or formalin fixed, wax embedded, tissue sections.

For this investigation both of these kits were utilised, with a number of variations to the standardised protocols. Initial trials used solid tissue such as mouse kidney, heart and spleen fixed in formalin and paraffin embedded in conjunction with the LCM technique. Sections were prepared as for immunohistochemistry, i.e. 10 minutes in xylene to dewax, an alcohol rehydration, standard haematoxylin staining, alcohol dehydration to xylene, all with RNase free reagents. Section thicknesses ranging from 5-12μm were cut onto standard superfrost slides and remained adherent to the slide despite a range of treatments. Complete dehydration of the sections was found to be crucial, as the presence of water inhibited the binding of tissue to the cap membrane.

No positive RT-PCR data were obtained with laser micro-dissected and isolated RNA with mouse *β-Actin* RT primers (Table 2.5), nor real time RT-PCR data with commercially prepared *18S* primers. The Ambion™ kit controls were also notably inconsistent. These controls consisted of RNA template enveloped in a protein coat, supplied with specific RT primers. The protein coat acted as a measure of the proteinase efficiency in the RNA isolation process. Repetition of the suggested protocol produced differing yields of control with each experiment (n=5), where cell line RT and PCR controls of known cell number or cDNA concentration with our usual *β-Actin* primers were consistent. This would suggest that some variation occurred with the supplied controls, rather than the extraction method, a conclusion confirmed by personal communication with Ambion™.

Addition of supplementary proteinase K to the extraction buffer (original concentrations are patent protected), extending 55°C incubation times from the suggested 10 minutes to 2 hours and use of water baths and PCR blocks, rather than incubators, for high ramp temperature, also failed to produce detectable RT-PCR products.

Despite its advertised application, a number of workers have reported problems using these kits in combination with formalin fixed paraffin embedded material (Ambion™ technical services, personal communication). This would suggest that the observed difficulties may represent a general procedural limitation.

5.2.2 WHOLE SECTION FROZEN MATERIAL

To address the problems encountered with the kits for RNA extraction from formalin fixed biopsy sections, another approach was undertaken. This initially used frozen sections with the intention of defining an extraction protocol, before attempting the more complex isolation of RNA from formalin fixed paraffin embedded material. This new approach utilised a micro column system (Qiagen), which enables the on-column isolation of RNA and elution in a small water volume. These experiments were performed with the assistance of Ms Su Haley, a technician in our lab.

For these studies initial optimisation was performed in a manner similar to that performed by Rupp and Locker using frozen sections[206], where 1-3 whole sections of frozen mouse lung tissue were placed in an Eppendorf tube. RNA was isolated from sections via the Qiagen™ column method. This was first run in a standard *β-Actin* PCR from RNA to check for genomic contamination (Figure 5.4). Negative samples were then reverse transcribed using Applied Biosystems™ reverse transcription reagents with oligo dTs, then a PCR performed with an Access PCR kit (Promega). Eluted column material (approx 12-14μl) was sufficient for 1 *β-Actin* check gel and 1 reverse transcription (see Chapter 2). The cDNA mix was then sufficient for 4 wells of a realtime plate (5μl each) or 2 RT-PCR reactions (10μl each), where the total volume was 25μl.

RNA could be reverse transcribed and entered into a 40 cycle PCR to produce a viable 2% agarose gel band from both freshly cut sections and those stored at -70°C. This is important as the laser micro-dissection process is very time consuming, thus it is likely that at some stage of the procedure samples would have to be stored. Given the small volume / concentrations of the samples, data may be more consistent if all material is processed together. Thus preservation following isolation is perhaps the best time for storage without a detrimental affect on mRNA isolation.

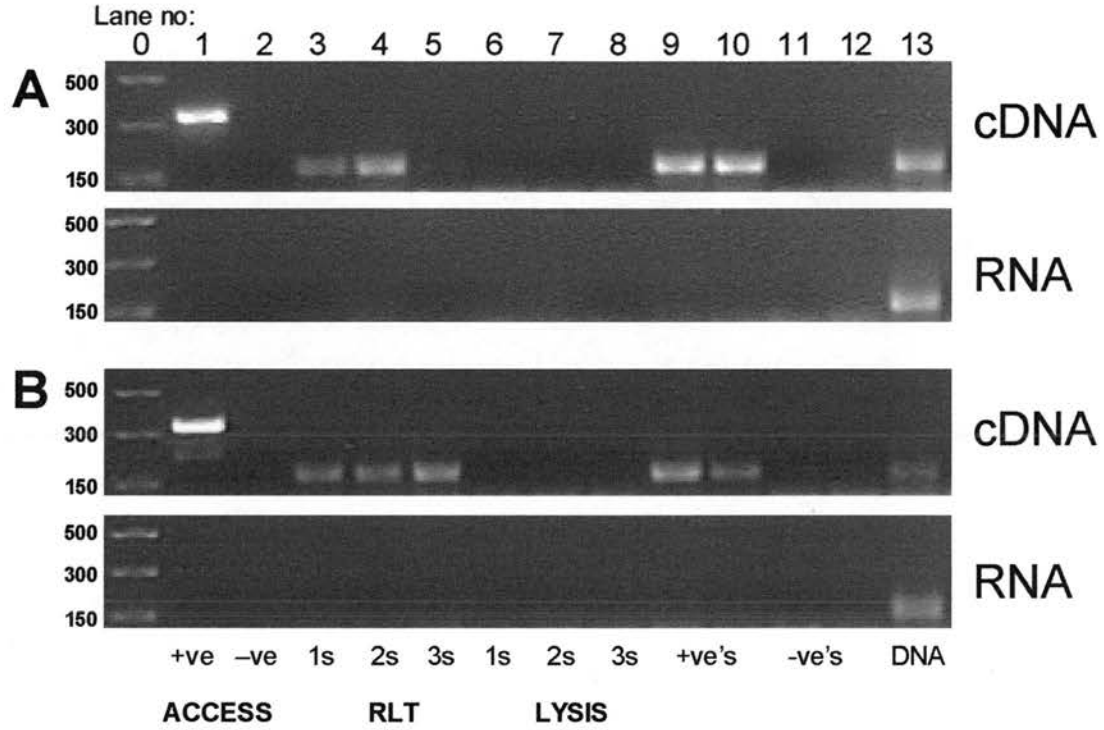

Figure 5.4: Frozen Sections Yield Viable RNA
Frozen sections taken directly to Eppendorf tubes following cutting. RNA was isolated using RNeasy micro columns and reverse transcribed and PCR amplified using the Access RT-PCR system and *β-Actin* primers (153bp). [A] Fresh sections [B] Sections stored for 7 days at -70°C. Upper gel PCR products, Lower gel identical PCR using RNA to check for DNA contamination. Lane **0:** ladder. Lane **1:** Access kit positive control (323bp). Lane **2:** a negative control. Lanes **3-5:** 1, 2 & 3 sections per Eppendorf tube in RLT lysis buffer (Qiagen). Lanes: **6-8:** 1, 2 & 3 sections per Eppendorf tube in a PALM™ recommended lysis buffer. Lane **9:** Mouse epithelial cell line lysis control, Lane **10:** Mouse epithelial cDNA control. Lanes **11 & 12:** Negative controls. **13:** DNA positive control. A band in Lane 5 of [A] upper is absent due to loss of a pellet during a wash step. Future studies could incorporate molecular grade glycogen to secure material during wash steps. The second band in Lane 1 [B] upper, is genetic material from an *E. coli* carrier used in the production of control RNA (Promega technical services).

5.2.3 WHOLE SECTION FORMALIN FIXED MATERIAL

Having established viable RNA extraction from frozen sections, the same approach was utilised for formalin fixed, paraffin wax embedded material. Sections were cut at 10μm and either, one, two or three sections placed in an Eppendorf tube. These samples included the complication of paraffin wax, which is normally removed via a 10 minute submersion in xylene when mounted on a slide. This was completed within the Eppendorf tube by addition of 1ml of xylene for 10 minutes, followed by centrifugation steps associated with 100% alcohol and rehydration procedures as discussed in Chapter 2. Once ultrafuged from water, the resulting pellet was re-suspended in RLT buffer containing βME and proteinase K. The proteinase K is necessary for protein degradation, and specifically the removal of the formalin cross links generated during fixation. This enzyme is ideal as it operates in conditions inhibitory for nucleases. RT-PCR was performed using the real time reagents as this is the intended final investigative tool, but PCR was performed in a standard PCR block.

Various proteinase K digestion buffer incubation times were tested from 1hr to 5 days. Data presented in Figure 5.5[A] would suggest that the 24 & 48hr periods were sufficient to obtain RNA from tissues. Real time RT-PCR primers for *CC10* were used in these studies to demonstrate that a gene other than *β-Actin* could be detected, and that the biochemistry of real time RT-PCR primers was compatible with transcripts isolated from formalin fixed material.

Increased RT-PCR yield of *β-Actin* signal was obtained when oligo dT was substituted with random hexomers (Figure 5.5[B]), and also allowed for the use of *18S* as an internal control in subsequent real time RT-PCR. In these studies 24hrs was sufficient to obtain RNA. The signal reduction in Lane 6 of [B] in Figure 5.5 is attributable to a partial loss through processing, as section material was easily lost with viscous wax removal. Although a problem here, loss of material with wax was not an immediate concern, as these steps would not be necessary in the final laser micro-dissection technique.

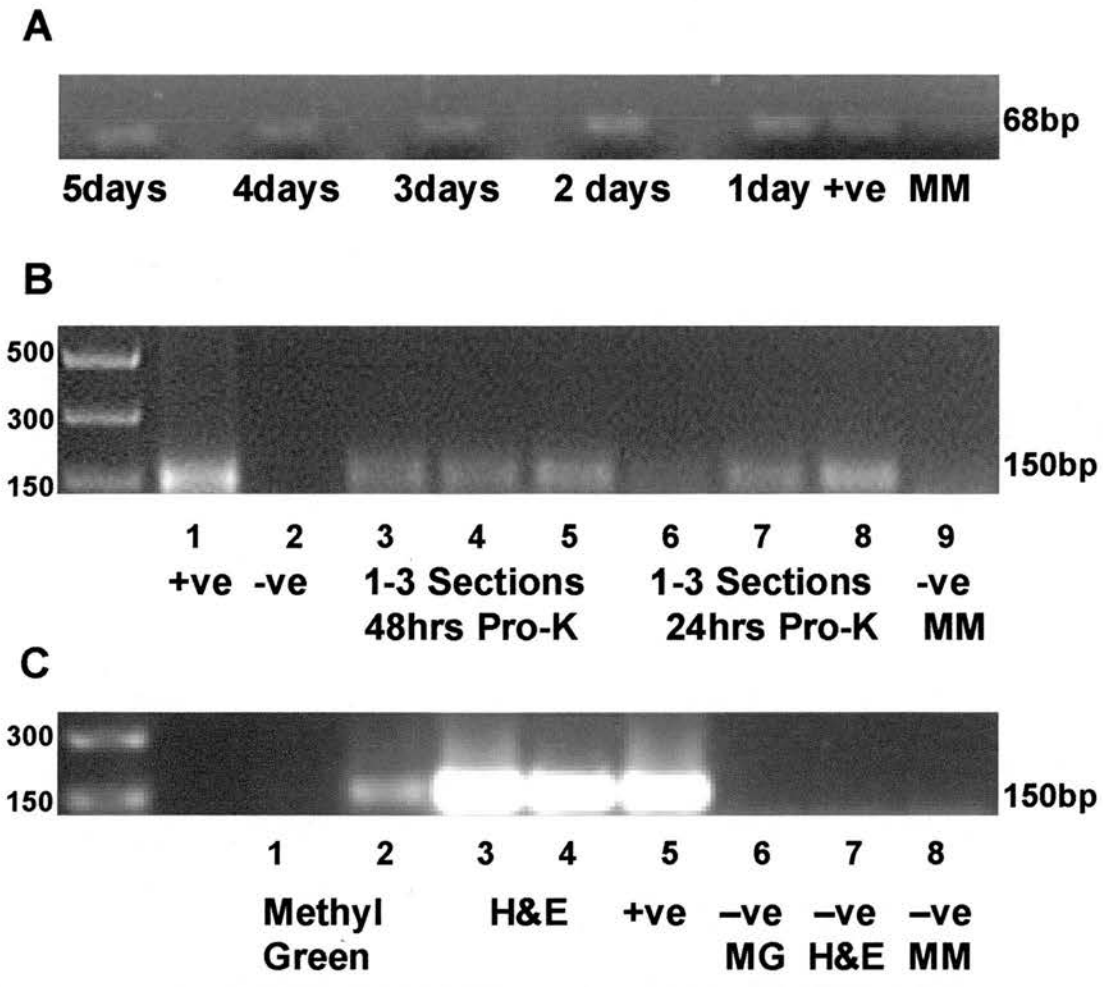

Figure 5.5: RT-PCR Optimisation For Formalin Fixed Material
[A] One Mouse lung section per Eppendorf tube, incubated for up to 5 days in proteinase K supplemented RLT buffer. The positive control is mouse epithelial cDNA (CMT). MM refers to PCR mastermix, containing negative RT fraction as a negative control. *CC10* real time primers used in an Access kit, product size 68bp.

[B] Material titration of 1, 2 & 3 sections per Eppendorf tube, incubated at 55°C overnight for either 24 or 48 hours. –ve, as above. Random hexomers and real time reagents used with *β-Actin* primers, product size 150bp.

[C] CMT cell line lysate spiked with acidified H&E or methyl green to an equal OD of overnight digestion of one section. Extracted and processed as above. *β-Actin* primers were used, product (150bp), in an Access kit reaction, performed in duplicate. Controls are single replicates, positive control (5) is unspiked. Negatives are MM plus stain in the absence of cell line lysate.

To ascertain whether genes of interest were highly expressed or stable enough to be suitable for analysis in dissected samples of human lung biopsies, and as proof of concept, whole sections were analysed with primers for genes of interest in RT-PCR using real time reagents in standard PCR blocks (Figure 5.6). Biopsy sections were classified as b1, 2, 3, 4 according

to the number of biopsy pieces visible on each block face. Thus b1-b4 can be considered an increasing gradient of biopsy material per section.

This study demonstrated that whilst transcripts such as TGF-β1 and 3, MMP-7, GAPDH, Ptc and Smo could be detected, others such as TGF-β-2, Gli-1-3, Shh, BMP-4 and FGF-10 could not. This was interesting as immunohistochemistry in the lab has identified Gli1-3 and Shh protein in these sections. This could represent an absence of mRNA, indicating slow turnover protein, or incorrect antibody / primer function. Alternatively, it could be postulated that these sequences were not detected as they were more susceptible to formalin fixation related degradation. These hypotheses could be confirmed through the use of frozen material taken from similar biopsies. This comparison remains to be performed.

Once effective retrieval of viable RNA from formalin fixed material had been established it was necessary to identify the optimum method for mounting and staining of sections to enable specific laser micro-dissection of cells. The gel in Figure 5.5 illustrates the affect of spiking PCR reactions with quantities of stain equal to that obtained from the lysis of a whole section overnight. Methyl green was found to inhibit the PCR, where as the addition of acidified H&E had no affect on the PCR versus the control in lane 5. H&E was therefore selected as the preferred stain, but was not required in these preliminary studies as specific cell types were not selected in either whole section or LCM studies.

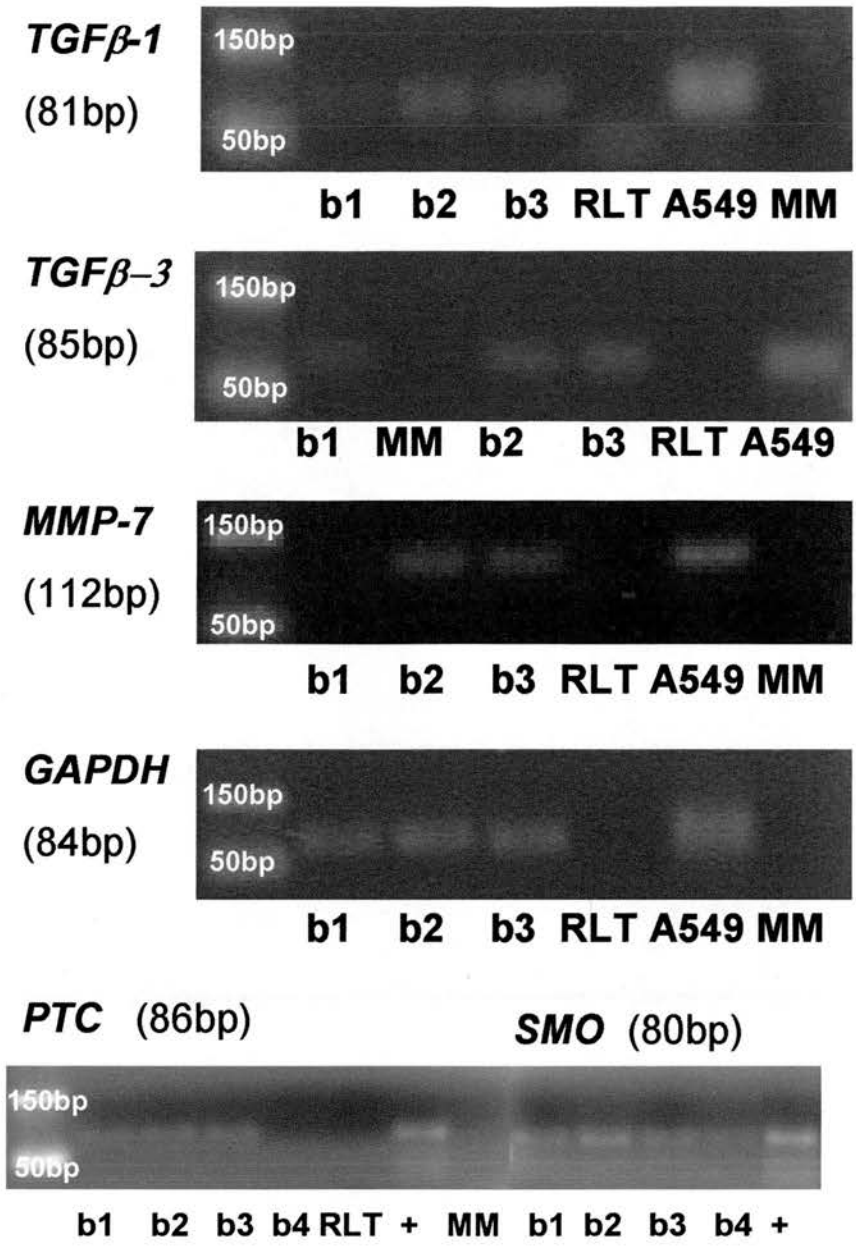

Figure 5.6: Whole Sections of Human Archive Lung Biopsy Yield Viable RNA
A single section of a block containing one (b1), two (b2) three (b3) or four (b4) lung biopsy pieces were placed in an Eppendorf tube and processed as previously described, except in that the proteinase K digestion concentration was doubled and the digestion performed at 24hrs. Real time reagents were used as described in Chapter 2. Primer probe sets that failed on sections but were successful with control human cDNA include: *TGFβ-2, Gli1-3, Shh, BMP-4, FGF-10.*

Whilst cutting and slide mounting of solid tissues such as kidney and spleen had been relatively straight forward in preliminary kit studies, use of a more aerated tissue, such as lung, necessitated titration of conditions to enable optimum lifting. The most important steps were identified as dehydration

(Figure 5.7), particularly the duration of xylene exposure (Figure 5.8), and the temperature used to mount the section onto the slide (Figure 5.9).

Dehydration was likely essential to prevent water in the section interfering with the formation of a composite with the overlying cap membrane. The temperature of incubation altered the lifting efficiency of the cap, presumably by increasing the adhesion of the section to the superfrost slide. Room temperature incubation resulted in some non-specific lifting, whilst lifting following 37°C resulted in highly specific lifting, but leaving some material behind. 52°C incubation resulted in a highly reduced lifting efficiency. Thus the preparatory steps for superfrost slide mounted, formalin fixed, paraffin embedded lung sections, for use with laser capture micro-dissection are as follows:

Section cut at 10μm on DNase washed microtome
Floated on RNase free water at 42°C in a water bath for 2 minutes
Mounted on superfrost slide
Incubated at room temperature overnight in silica gel box
Dewaxed for 10 minutes in xylene
Rehydrated in alcohol series
Optional staining with counter stain
Dehydrated in alcohol series, 30 seconds in each
Xylene 15 minutes

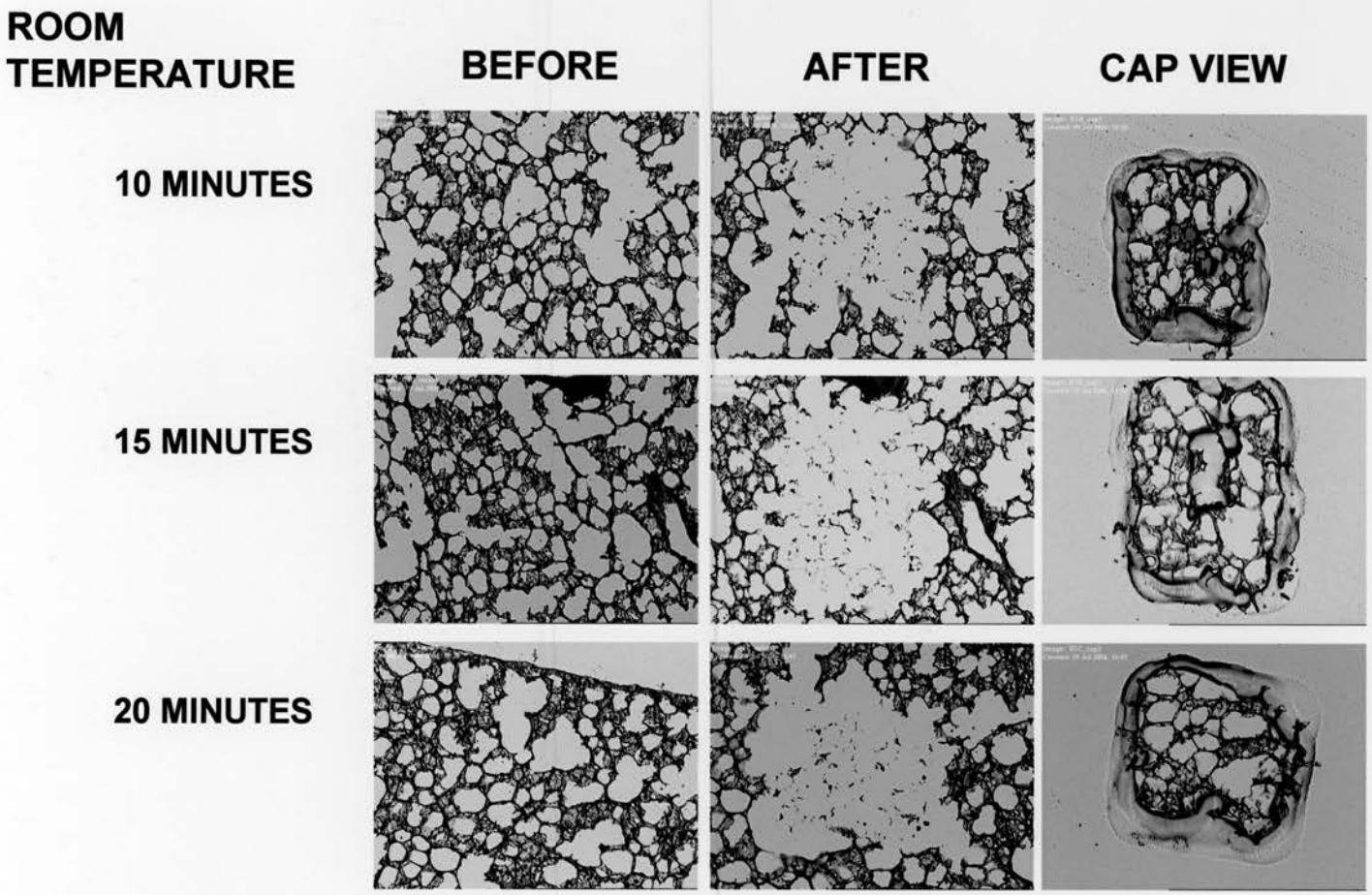

Figure 5.8: Prolonged Xylene Dehydration Improves Capture Quality
Slides stored at room temperature for 1 hour prior to dewaxing, rehydration, then dehydration through alcohol series, final period of xylene incubation given on the left of the Figure.

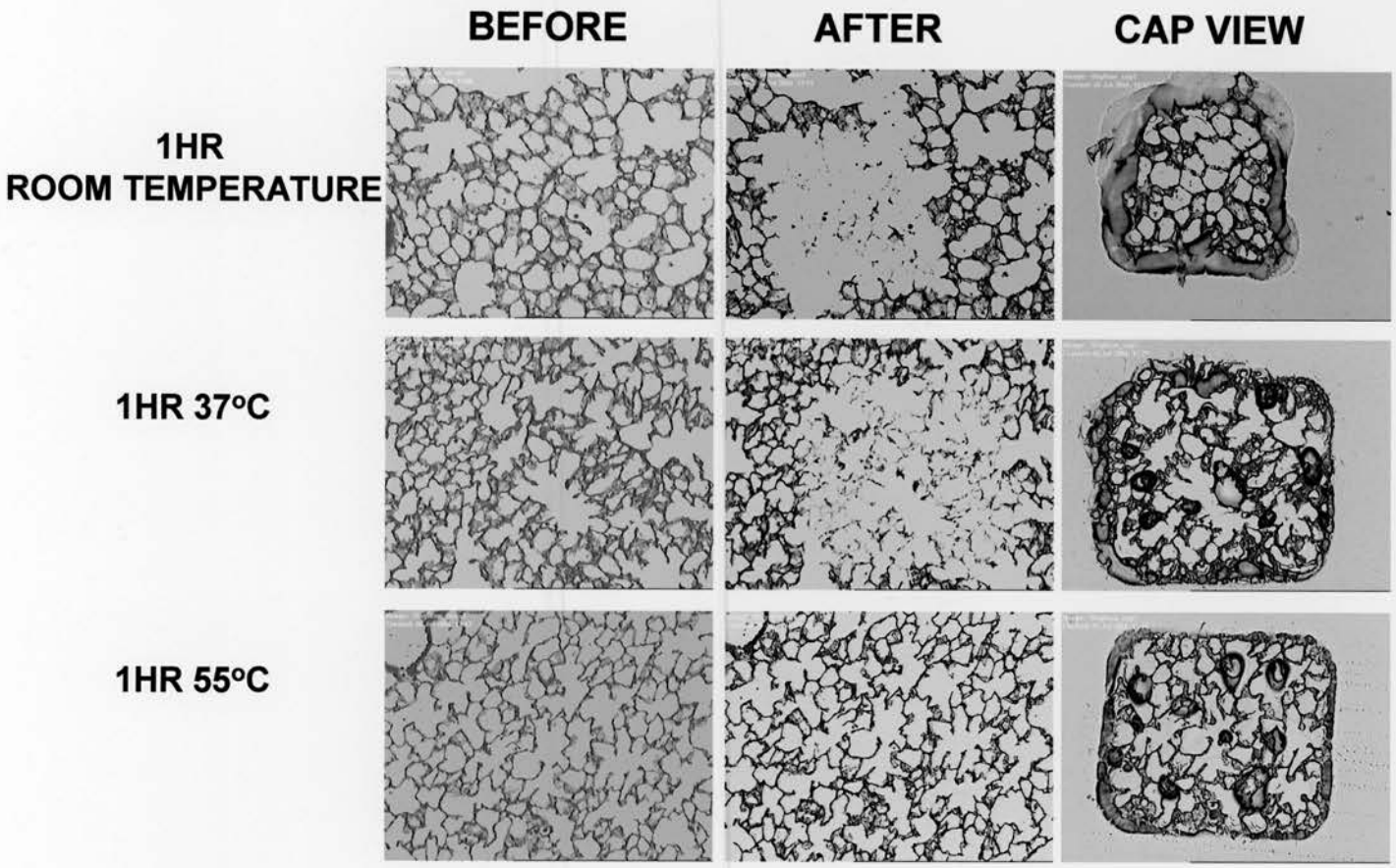

Figure 5.9: Temperature Used To Mount Slide Affects Cutting Efficiency
Sections stored for 1hr at room temperature, 37°C and 55°C in a silica gel box prior to dewaxing, rehydration, dehydration through alcohol series and xylene.

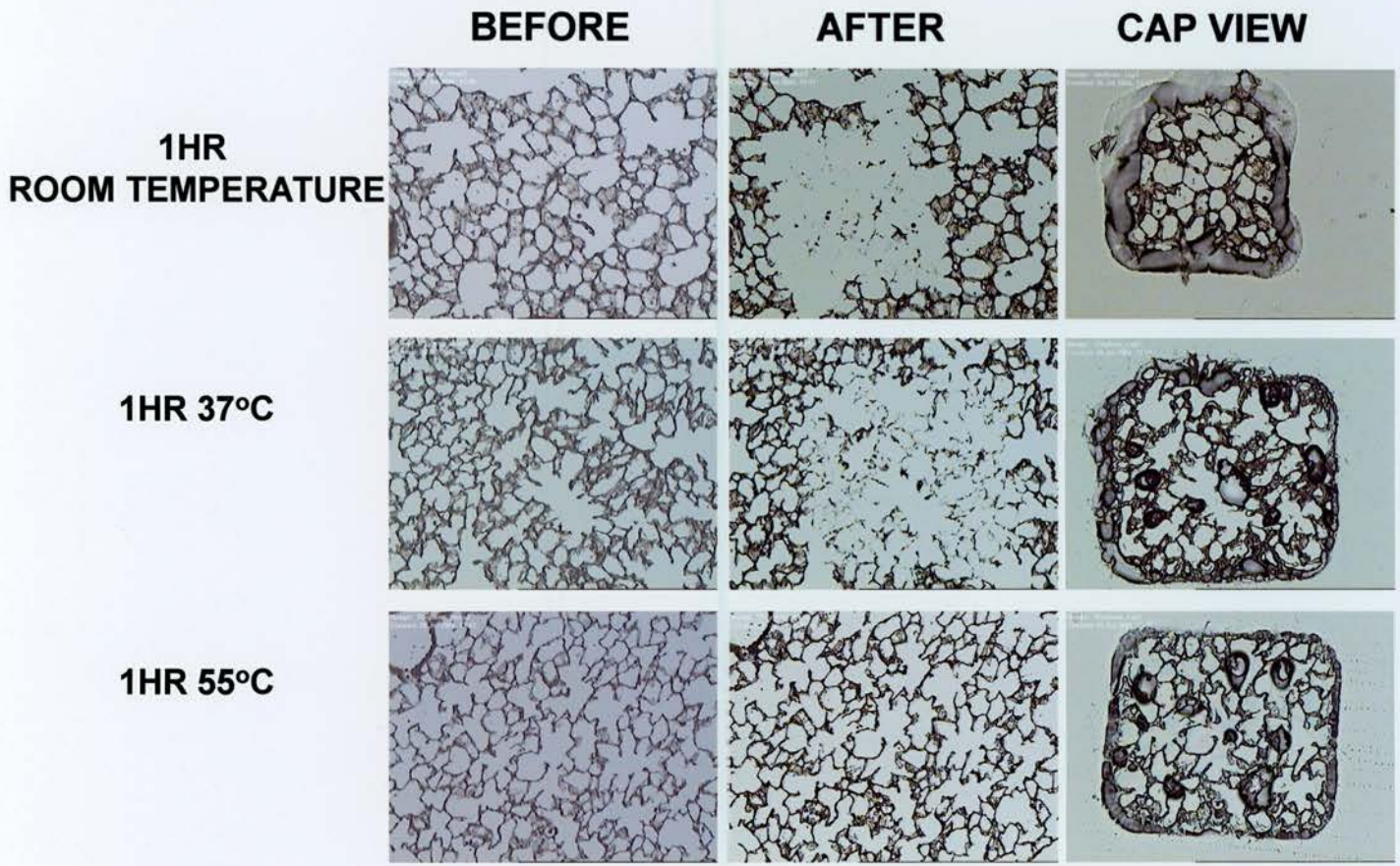

Figure 5.9: Temperature Used To Mount Slide Affects Cutting Efficiency
Sections stored for 1hr at room temperature, 37°C and 55°C in a silica gel box prior to dewaxing, rehydration, dehydration through alcohol series and xylene.

5.2.4 LASER CAPTURE MICRO-DISSECTION

Once the optimum conditions for section preparation had been established, laser capture micro-dissection was performed using the Pixcell II system, as used in the preceeding figures. Material fixed onto the cap following laser dissection was transferred to a 450μl solution of proteinase K digestion buffer in a 0.5ml Eppendorf tube and digested for 24hrs. The use of a shaker platform (see Chapter 2) was found to increase yield following this incubation. Real time RT-PCR reactions were prepared using standard 18S endogenous control and a gene of interest. These were then run on an ABI 7700 sequence detector in 96 well plates, Figure 5.10 shows results for *CC10* in mouse and *Ptc* in human.

What was notable from these experiments was that the *18S* amplicon detected by a VIC™ labelled probe, was only marginally more frequent than the mRNA of interest detected with a FAM labelled probe. As a housekeeping gene *18S* would normally be substantially higher in abundance, i.e. have a lower ct value. This is most striking when comparing the positive cell line control *CC10* values with those obtained from the LCM cap (Figure 5.10[A]). Given the findings of others concerning the importance of the size of the PCR amplicon in laser capture micro-dissection[210, 211], the products of the RNA positive reaction in Figure 5.10[A] were run out on a 2% agarose gel electrophoresis, and the size of the products confirmed (Figure 5.10[D]). The CC10 amplicon, generated from a primer probe set designed in the lab, was 68bp in size. Quite unexpectedly, given Applied Biosystems own guidelines on amplicon size (<150bp), the amplicon from the Applied Biosystems™ 18S primer probe set was 200bp in size.

Applied Biosystems do not routinely reveal the specifics of their pre-designed primer probe sets, thus it was assumed they conformed to their specifications. However upon communicating my problems and reservations concerning product size, another internal control primer probe set was suggested by Applied Biosystems technical services. This set, specific for *β-Actin* was also unsuitable as its amplicon was found to be 300bp in size. Further communication with Applied Biosystems technical services

concerning their endogenous control selection plate, (a pre-designed method of identifying appropriate experimental controls from samples added to a selection of differing house keeping genes), would suggest that the majority of their designed sets would be "unsuitable" for laser micro-dissection. The most recent real time RT-PCR experiments have utilised *GAPDH* primers with VIC™ labeled probes as a control (Figure 5.11), designed in house where all sets are now routinely below 100bp in size (Table 2.6 & Table 2.7).

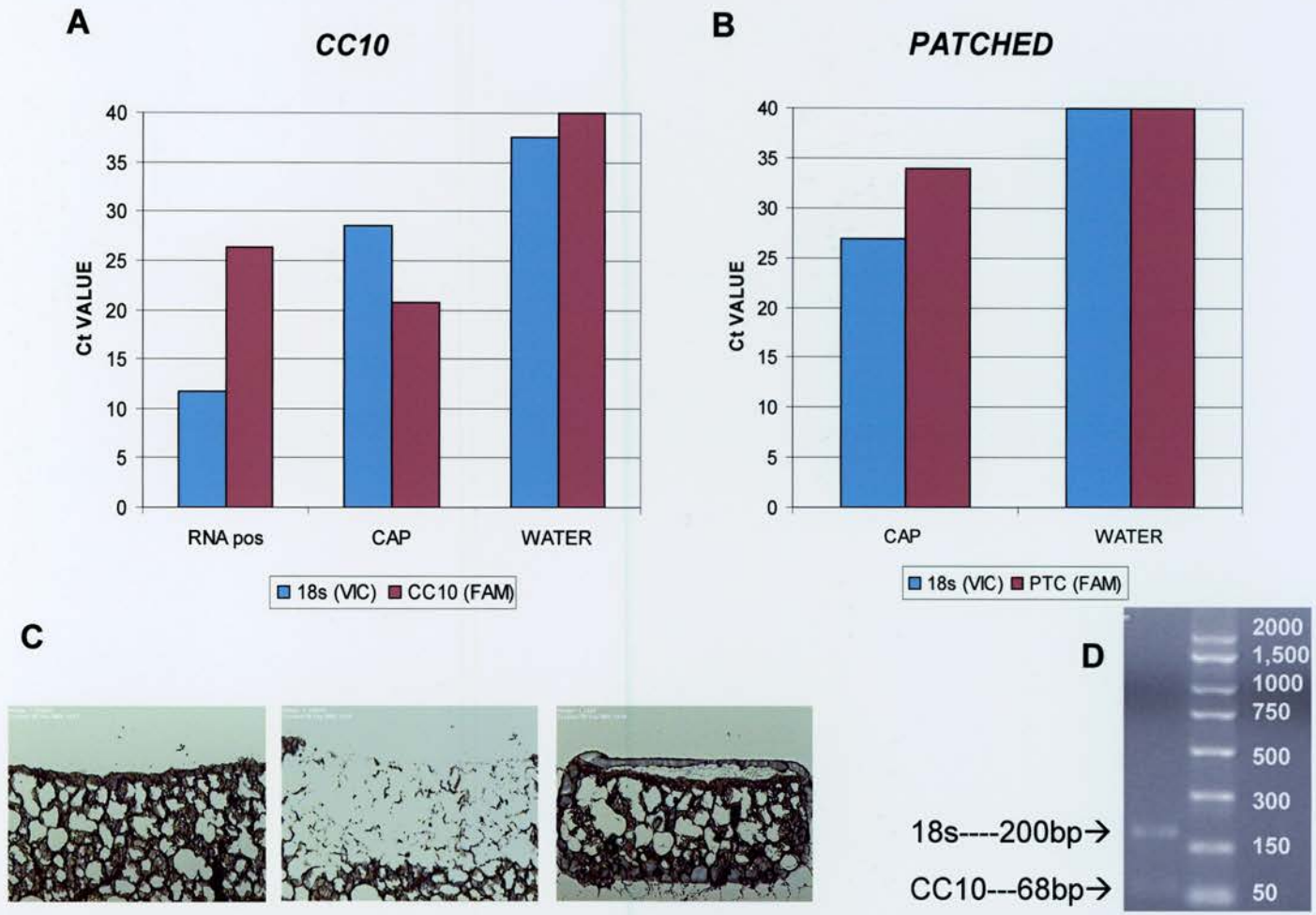

Figure 5.10: Laser Capture Micro-Dissected Material Yields Viable RNA
[A] Mouse *CC10* (68bp) on a control mouse section, note the reversal of ratio in VIC™ : FAM with RNA positive control (CMT) vs. CAP. [B] *Ptc* (86bp) in human lung biopsy. An example of the amount of material taken is shown in [C], where three amounts of this size were pooled. [D] Illustrates the size of the cDNA being produced.

5.2.5 LASER PRESSURE CATAPULT MICRO-DISSECTION

Due to a number of technical and mechanical failures with the laser capture micro-dissection system, Laser Pressure Catapult micro-dissection was then tried. These studies centred primarily on human tissues where, in collaboration with Dr William Wallace and Ms Su Haley, human lung biopsies with BOOP (Figure 1.6) and UIP (Figure 1.7) patterns of disease were dissected and extracted using the methods previously described in the introduction to this Chapter. It was hoped that by using two differing morphological patterns of fibrosis, it might be possible to identify differential gene expression in alternate patterns of fibroplasia.

This switch in technique necessitated an alteration in slide preparation. LPC membrane coated slides were utilised. One of the major problems with these slides is lifting in the presence of xylene, a necessary step to remove the paraffin wax component of the section. By reducing this step to two washes of two minutes it was possible to remove wax without lifting the section. To allow the visualisation of morphological features a wide range of stains were tested including H&E, Giemsa and acridine orange. Of these Giemsa was found to give the best visualisation with minimal detriment to incubation or processing steps. This stain was not applicable to previous LCM studies due to its solubility in alcohol, where dehydration was essential. Dehydration was not necessary in these studies, as the membrane acts as a support to dissected section material. Slides were prepared as follows:

Slide washed in DNase and RNase free water
Slide UV exposed to activate LPC membrane
Section cut at 5-10μm on DNase washed microtome
Floated on RNase free water at 42°C in a water bath for 2 minutes
Mounted on LPC membrane slide
Incubated at 37°C overnight in a silica gel box
Dewaxed for 2x2minutes in xylene
Rehydrated in alcohol series
Giemsa staining
Minimum of 30 minutes in a silica gel box

Recent studies in the laboratory have shown that use of Histoclear™ as a substitute for xylene increases micro-dissection efficiency and reduces the lifting phenomenon, but comes too late for inclusion in this thesis (data not shown).

In order to evaluate the catapulting technique as a means of concentrating RNA, whole biopsy sections of either UIP or BOOP were mounted onto membrane slides, and the areas of active fibroplasia present in one 5μm section dissected out and catapulted into lysis buffer by an experienced pathologist (Dr WAH Wallace). This material was then processed as a pair; catapulted material, which can be considered as "fibrotic enriched" (Figure 5.11[E] lane 2), and the remainder of the section placed in an Eppendorf tube, considered "fibrotic depleted" (Figure 5.11[E] lane 3). A mounted but un-dissected section from the same block was also processed (Figure 5.11[E] lane 1), as was a cut but un-mounted section (Figure 5.11[E] lane 4), to ascertain the affect of the attached membrane on down stream applications.

No interference from the membrane on RNA digestion and isolation was identified and a viable signal could be obtained from the enriched and depleted material using *GAPDH* primers. Giemsa staining was also shown to have no affect on processing through the analysis of unstained membrane mounted sections vs. stained (data not shown).

BOOP studies are illustrated in Figure 5.11 as the most complete data set at the time of thesis submission. Subsequent collaborative work with others in the lab has demonstrated similar data for UIP sections where the intention is to compare the relative expression of signalling pathways such as Shh in BOOP vs. UIP as a means to elucidate the mechanisms which lead to luminal vs. sub epithelial fibrosis.

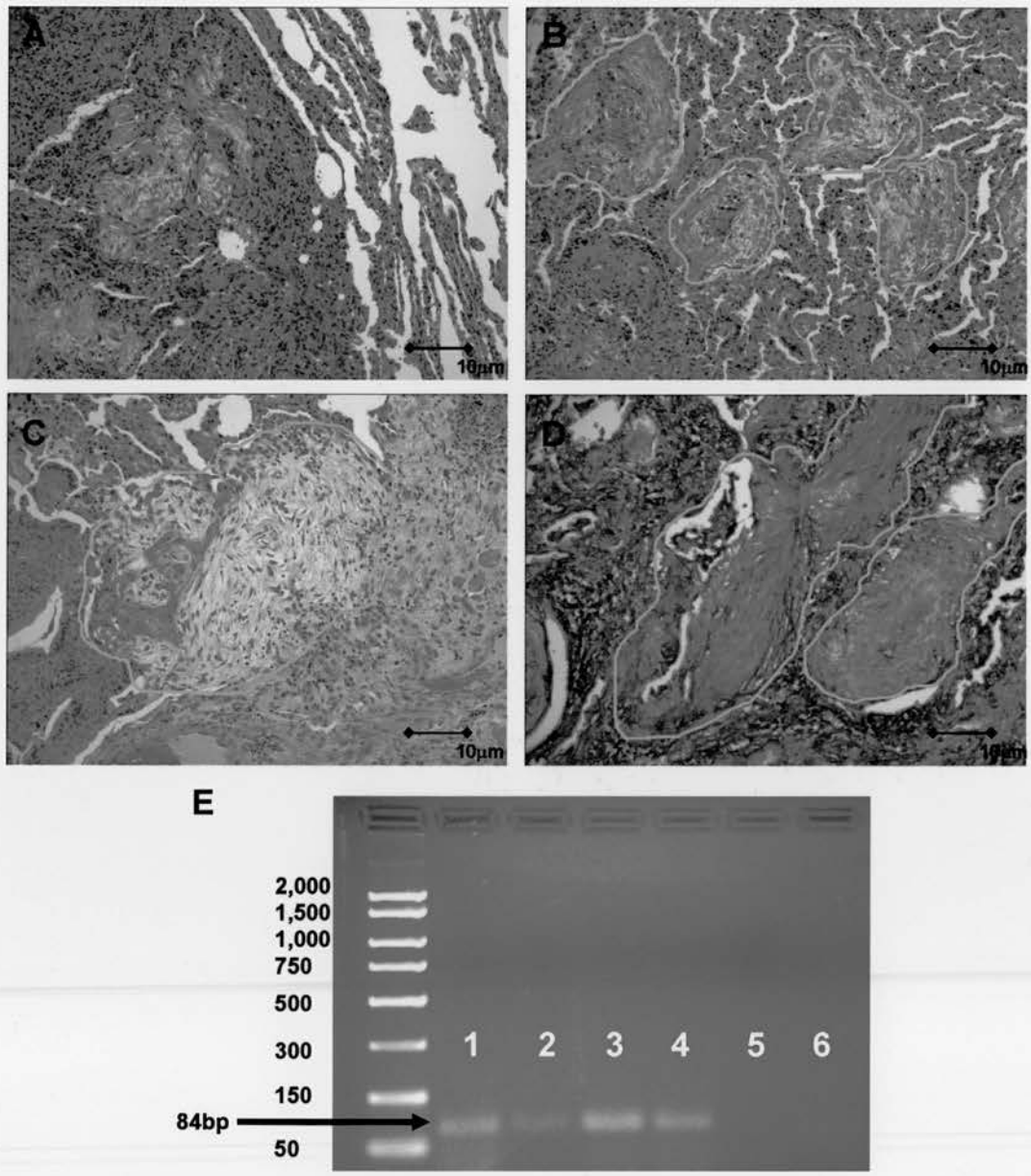

Figure 5.11: *GAPDH* RT-PCR from Micro-Dissected Formalin Fixed Human Tissues

[A]&[B] BOOP biopsies, where the * in [A] denotes an area of deregulated fibroblast proliferation and collagen deposition, compared with a relatively normal area of neighbouring lung, denoted **. [B] Yellow areas are catapulted to form a fibrotic enriched sample, whilst remaining tissue makes up a fibrotic depleted sample, the area denoted by a * is not catapulted as this is fibrosed blood vessel unlike the fibroblastic foci circled. [C]&[D] UIP Biopsies, where the * in [C] denotes an area of deregulated fibroblastic proliferation and collagen deposition. [D] is a 10µm giesma stained section. Catapulted areas marked in yellow. [E] A 2% gel electrophoresis of *GAPDH* real time primer use in standard PCR of Giemsa stained, formalin fixed BOOP biopsies; 1: Whole section taken immediately after staining. 2: BOOP fibrotic enriched catapulted material, 3: Fibrotic depleted section, 4: Un stained un-mounted section, 5: mastermix control, 6: RLT neg.

5.3 DISCUSSION

5.3.1 INTRODUCTION

Viable RNA has been isolated from single sections of frozen mouse lung without DNA contamination, both from freshly cut and -70°C stored sections. Viable RNA has also been obtained from freshly cut and room temperature stored, single sections of formalin fixed, paraffin embedded human and mouse lung. Processing of this material incorporated proteinase K supplemented lysis buffers, Qiagen™ RNA isolation columns, and real time RT-PCR reagent mediated amplification step. Preparatory techniques for sections destined for LCM and LPC were developed here and used in the LPC isolation of active fibroplasias in BOOP biopsies. Viable RNA could be isolated from this fibrotic enriched material and from the remaining, fibrotic depleted section. This establishes this technique as a means of mRNA expression profiling diseased and non diseased areas of patient biopsies.

5.3.2 MICRO-DISSECTION KITS

Initial experiments were conducted primarily with the Ambion™ cells to cDNA kit supplemented with highly sensitive supertaq for PCR, as per manufacturers recommendation. Failure to detect message in dissected material, and inconsistent recovery of the protein encapsulated control, suggests that the limitations experienced with these kits reside in the digestion process. The RT and PCR steps themselves were correct as they generated products from cell line control RNA of comparable, if not greater amplification, than in standard RT-PCR using the Promega™ Access RT-PCR system. This conclusion would appear vindicated by subsequent work with RLT digestion buffers in the Qiagen column system where the active ingredient, as with the Ambion™ kit, is proteinase K. Using this buffer no mRNA could be recovered from 3hr incubations (data not shown), such as those used in the longest digestion periods with the Ambion™ kit. The discovery that correct protein digestion requires up to 24hrs with the Qiagen™ RLT proteinase buffer would suggest that the problems encountered with the kit, and indeed the protein encapsulated control, were attributable to an insufficient digestion period.

It would be interesting to see whether products could indeed be acquired from these Ambion™ kits with longer digestion steps, as the kits are very quick, and it would be expected that less material would be "lost" during the procedure as no on column isolation step is involved, i.e. the lysis and RT-steps are all performed on un-purified RNA.

Early studies were also likely inhibited by use of the *β-Actin* RT primers as the product is greater than 150bp in length, where work here with *18S* and *β-Actin* controls on VIC™ primer probe sets with amplicons in the range of 200 and 300bp respectively would suggest that the greater amplicon size, the lower the PCR yield.

5.3.3 HISTOCHEMISTRY

A further complication in RNA isolation was histochemistry. Contrary to published reports[200], I found the presence of methyl green to be seriously detrimental to PCR yield, whilst H&E and Giemsa had no affect. Although Giemsa was found to be the best and most convenient stain for differentiating between fibrotic and non-fibrotic areas in sections ranging in thickness from 5-12μm, H&E would likely be a better stain for routine dissection on material <5μm as it also gives more precise definition to the immunological cell types present than Giemsa. Picrosirius red and trichrome would ultimately be preferable, for collagen/fibroblast immunohistochemical imaging, as they would clearly mark fibrotic foci rather than atelectasis. However this would likely necessitate too many potentially RNA degrading steps.

5.3.4 PROTOCOL DEVELOPMENT

By beginning with whole sections of frozen lung, then moving on to formalin fixed material and finally dissected material, it was possible to optimize the protocols in a logical stepwise fashion, facilitating the optimization of RT and PCR steps without time consuming and costly micro-dissection. Thus when dissection was undertaken, a clear protocol had been established and suitable targets had already been identified. Any future substantial alterations to these protocols, principally the incorporation of rapid immunohistochemical

treatment, should also utilise this approach. New genes of interest, or primer probe sets should first be analysed on whole sections. This will limit the time, cost and material wasted on unsuitable targets with laser micro-dissection.

Lack of detection with a primer probe set does not of course guarantee the absence of mRNA from lung as the sequence may have a short half life or be primarily composed of those bases most susceptible to formalin induced chemical modification. Also the sections used in this study were mainly from BOOP biopsies. Normal or otherwise diseased lung may present with a substantially different profile.

5.3.5 APPLICATION OF THE MICRO-DISSECTION TECHNIQUES

How feasible is laser micro-dissection as a medical tool? The dissection of relevant material requires a practiced and trained eye and whatever method of dissection is used, remains relatively time consuming. Implementation of laser dissection as a diagnostic or prognostic tool would also require that strict controls were placed on the variables discussed in Section 5.1.7 concerning biopsy preparation. Such requirements would likely make this procedure too expensive to become a routine NHS tool. What is more likely is that this technique will be used to identify a gold standard of candidate disease associated factors for further investigation at the genetic and molecular level and for the identification of potential drug targets. Once established more routine methods might then be used to aid the pathologist in diagnosis, such as *in situ* PCR or immunohistochemistry.

The development of the protocols shown here confirmed the original hypothesis that viable RNA could be obtained from formalin fixed paraffin embedded material. However, the development of the protocols presented in this Chapter was more complicated than originally anticipated and thus there was insufficient time to apply it to the study of disease and address the hypotheses concerning the involvement of Shh in human fibrotic disease recapped below:

"Formalin fixed human and mouse adult lung contains *Shh* and *Ptc* sequence"

"Epithelial cells represent a putative producer/responder population of Shh signalling whilst mesenchyme is primarily responder in profile"

However these studies are ongoing in the laboratory, and it is hoped that by pooling large numbers of microdissected fibrotic foci versus normal morphology, with new more efficient human Shh primer probe sets, it may be possible to detect Shh mRNA in those cell populations where new immunohistochemical data would suggest that Shh protein is highly expressed.

5.4 CONCLUSIONS

Work presented within this Chapter has highlighted both the benefits and restrictions of the laser micro-dissection technique and has defined novel protocols for section preparation for two dissecting techniques, clearly demonstrating that viable RNA can be obtained from less than one section of formalin fixed, paraffin embedded human lung biopsy.

Whilst the technique of RNA extraction from formalin fixed, paraffin embedded, laser micro-dissected material has been developed and perfected here, there was insufficient time to investigate disease specific RNA expression. Furthermore, several validating and optimising experiments may be required before this technique can be applied specifically to the *Shh* signalling pathway to address the hypotheses set out at the start of this thesis.

The value of this procedure as a potential diagnostic or prognostic tool in the treatment of lung disease is currently limited, given the number of issues which remain to be resolved concerning transcript stability and the vast array of clinical and histochemical analytical tools already available. Where its value lies is as a research tool, allowing a greater understanding of the cell

specific signaling interactions which occur in fibrosis and responses to treatment. This knowledge may lead to better prognostic staining and *in situ* hybridization techniques, allowing the identification of patients with expression profiles more likely to worsen, exacerbate or be more responsive to treatments such as corticosteroids.

5.5 FUTURE WORK

5.5.1 REAL TIME RT-PCR STANDARD CURVE

Use of a standard curve of RNA derived from normal formalin fixed lung material in real time RT-PCR studies could partially address potential mRNA bias issues, and would allow the pooling of separate real time RT-PCR plate data.

5.5.2 NEW TARGETS

Although this technique has been validated through the work presented in this Chapter, there was insufficient opportunity to apply this technique to a given question. Thus future work should concentrate on applying the protocols developed here, to the hypotheses stated at the start of this Chapter concerning the role of Shh in human pulmonary fibrotic disorders.

One attractive experimental approach would have been to compare diseased and non-diseased whole lung sections, however such an approach suffers from all the drawbacks of whole lung homogenates of fresh tissue, as the section will inevitably contain some non diseased areas, and "contaminating" cell populations not involved in disease. Thus the studies here with whole lung sections can be considered as a proof of technique and a control for subsequent experiments. Only by using enriched and depleted isolates from the same section can a true picture of mRNA expression be elucidated from a defined cell population.

GENERAL DISCUSSION

6.1 GENERAL DISCUSSION

Through *in vitro* and *in situ* analysis, in conjunction with a mouse model of inflammatory lung fibrosis, this thesis sought to further the previous immunohistochemical evidence for Shh expression in the adult lung, previously identified by this lab[1]. This approach facilitated the development of three novel experimental systems; a Shh ELISA system, for quantitative analysis of culture supernatants; a methodology for RNA isolation and purification from formalin fixed laser micro-dissected material; and characterisation of the FITC instillation model of inflammatory fibrosis.

Using these systems the following hypotheses were addressed:

- Shh expression is an indicator of acute or chronic epithelial cell injury.

- Shh up regulation initiates defensive functions independent of systemic immunity, i.e. the activation of epithelial cytokine production, maintenance of stem cell function and effects on alveolar macrophage and fibroblast function.

- Shh expression in UIP and the FITC lung model indicates an active association of Shh signalling with the development of fibroblastic foci

- Disease progression in the FITC instillation mouse model is potentiated by Th2 anti-FITC antibody

With reference to the first three hypotheses above, *in vitro* data clearly indicated a correlation between reduced viability, increased membrane permeability and soluble Shh release in a mouse type II epithelial cell line in response to H_2O_2 exposure. This suggested that Shh release might occur as a response to oxidant exposure or as a more generalised response to injury. However, Shh was not evident in immunohistochemistry of healthy lung, nor in FITC instilled mice at 1-14 days post instillation[184] or the 6, 12 and 18 week time points illustrated in Chapter 4.

Despite the observation of some studies that Shh signalling can occur in the absence of positive IHC Shh detection[178], it is my conclusion that the absence of Shh expression in both healthy and diseased sites indicates that Shh is not a prominent *in vivo* signal in FITC induced lung fibrosis, and that previous IHC detection was attributable to largely non-specific staining. Moreover, that the absence of prominent Ptc staining on fibroblasts (Figure 4.4[D] & Figure 4.5[F]) indicates that direct epithelial to fibroblast Shh signalling is also unlikely in this context.

Studies here with r-Shh and mouse epithelium derived Shh, within the parameters measured, have not shown any physiologically relevant effects in epithelium, AM or fibroblasts *in vitro*. It is possible that Shh modulates responses in cells not characterised here, that it requires the presence of an intermediate cell type or secondary signal, or that the cells used in these studies may require other stimuli to induce responsiveness. However, the general conclusion that can be drawn from murine studies alone, is that whilst Shh release can be considered as a cellular response to oxidative damage *in vitro*, its absence in normal and diseased tissues and its failure to induce proliferative or cytokine responses in a range of cell types, would suggest that Shh release *in vitro* could be an artefact derived from *in vitro* culture, and the use of carcinoma derived cell lines.

In contrast, human fibrotic lung conditions such as UIP and BOOP do demonstrate an up regulation of Shh expression in areas of disease, absent in normal alveolar tissue. Thus, given the release of Shh identified in human epithelial cell lines in response to H_2O_2, Shh up-regulation could be considered a fibrosis associated signal in humans, perhaps associated with persistent injury or oxidant exposure. This difference in mouse and human could represent a difference in immunohistochemical sensitivity for species specific Shh or a difference in disease mechanism, between the FITC mouse model and human UIP. Therefore, it may be that IHC analysis of different models of mouse lung disease, perhaps including incidences of oxidative damage, may elucidate Shh signalling, such that *in vitro* murine data may indeed be representative of a disease associated signal.

The lack of functional Shh signalling data with epithelium discussed in Chapter 3 (p139), could be attributable to the use of cell lines. Certainly the expression of Ptc by pulmonary epithelium would suggest that autocrine and paracrine signalling is at least possible, and given data derived from other cellular systems, the function of such a signalling interaction can be hypothesised (Figure 6.1).

An oxidative or injurious stimulus might induce Shh release from type II epithelium, to act as an auto and paracrine proliferative factor for epithelium[139], allowing those cells spreading to fill denuded surfaces, to replicate and resume their normal physiology and cuboidal morphology (Figure 6.1[A]). Alternately, Shh could play a role in the maintenance of epithelial stem cell populations, as suggested in a recent review[178]. For example, injurious stimuli or oxidative damage leads to the shedding of type I epithelium and the spreading and differentiation of Type II cells into type I cells to cover denuded areas. Shh expressed by these differentiating cells in periods of excessive denudement, could act to maintain the type II stem cell population, as in haematopoiesis[127](Figure 6.1[B]).

However, it could also be hypothesised that the observed lack of functional data for Shh *in vitro* may be that Shh up regulation occurs as a *response* to the development of the underlying fibrotic foci, and that it performs no active signalling function in the adult lung. This is unlikely as a role for Shh in the maintenance of T-lymphocyte responses has already been identified[2, 3], thus interactions with other cells of the immune system, such as B cells and APC are possible, although the role of Shh in T-lymphocyte signalling has only been confirmed *in vitro* and awaits validation *in vivo*.

Shh up regulation could result from a range of factors associated with the development of underlying fibrotic foci, such as increased ECM interactions, distension of the epithelium and increased myofibroblast derived signals (Figure 6.1[C]).

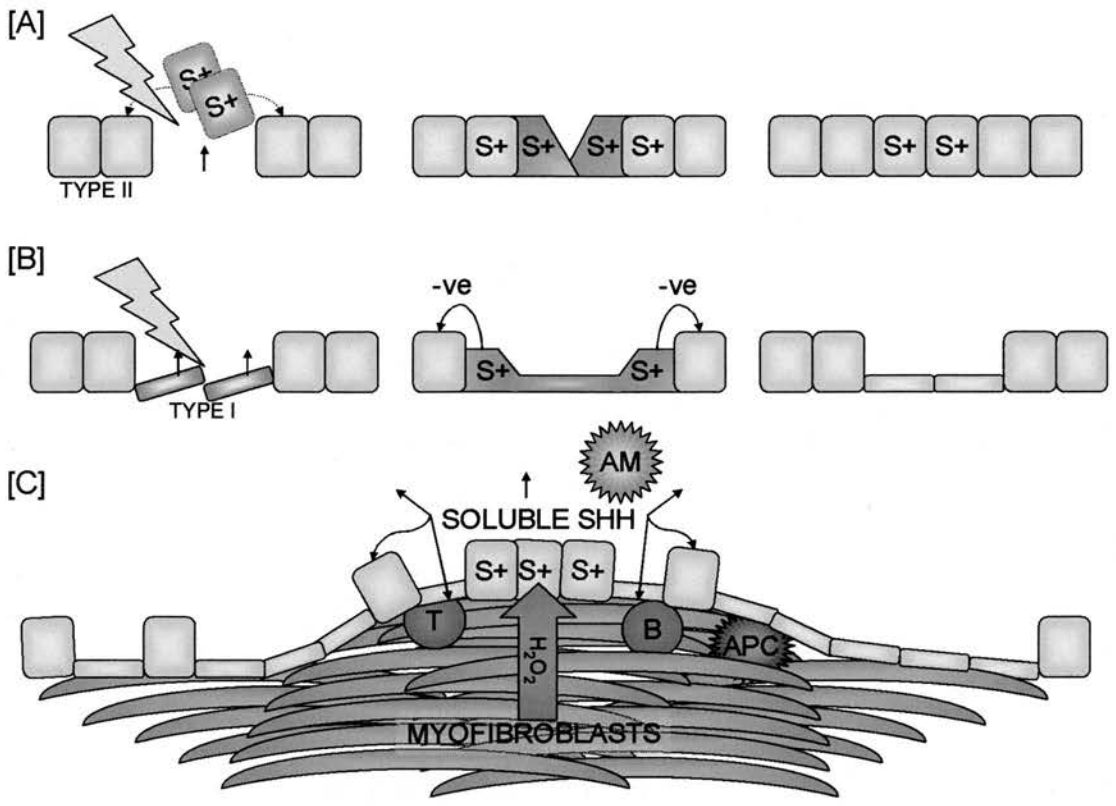

Figure 6.1: Hypothetical Roles for Shh at the Pulmonary Surface
[A] Shh upregulation in injured and differentiating (orange) epithelium as a response to oxidative injury, acting in an auto/paracrine fashion to induce epithelial activation and proliferation to recover denuded areas. [B] Shh upregulation by proliferating and differentiating type II cells (orange) following oxidative injury, in the maintenance of type II stem cell populations. [C] Myofibroblast derived H_2O_2 upregulates Shh in epithelium overlying fibrotic areas. Shh expression in all three hypothetical molecules has the potential to act with cells of the immune system such as T and B lymphocytes (T) & (B), Antigen presenting cells (APC) and alveolar macrophage (AM),

One way in which Shh up regulation might be induced by fibrotic foci can be extrapolated from studies conducted by Waghray *et al* at the University of Michigan[223]. This paper presents evidence to suggest that myofibroblasts, when stimulated with TGF-β, produce H_2O_2 which induces epithelial cell death. Given the data presented here concerning the effect of H_2O_2 on Shh expression, it is possible that the expression observed in UIP biopsies represents a response to myofibroblast derived H_2O_2 (Figure 6.1[C]).

However, if a closer analysis of immunohistochemical expression of Shh in human biopsies is made, another hypothesis can be put forward to explain the differences in immunohistochemistry between mouse and human. Shh expression is not observed in *all* areas of UIP, negating a continuing role in

fibrotic progression and Shh expression is observed in the epithelium of the *normal* upper airways in the *absence* of fibrotic foci, thus it is not a definitive fibrosis associated signal. It could be hypothesised that the induced expression of Shh in the lower airways versus constitutive expression of Shh in the upper airway cells represents an adoption of an upper airway phenotype by alveolar epithelial cells, or transmigration of upper airway epithelium into the terminal bronchioles and acini. This process is already known to occur in these conditions, and is referred to as "bronchiolisation". The absence of this phenomenon in mouse may be a consequence of an absence of constitutive Shh expression in upper airway epithelium in mice.

Replicating the *in vivo* effect of FITC addition to epithelium *in vitro,* as a comparable measurement to H_2O_2 addition, was one method employed to distinguish whether Shh up regulation and release was specific for a H_2O_2 response. This proved most problematic, the basis of which lies in our lack of understanding as to how the delivery of FITC *in vivo* actually induces inflammation. It is possible that FITC induces the observed epithelial shedding and activation in mouse lung[184] through direct physical injury, following the formation of colloidal aggregates, or through its alkaline pH. Equally, the hyperactivation of alveolar or interstitial macrophages, as an indirect cause, is also a possibility. However, literature sources would indicate that the major cause of FITC toxicity could be derived from its ability to conjugate to proteins, crucial to the functionality and survival of the cell[224, 225]. This activity is linked to the isothiocyanate structure of the fluorescein molecule. Studies, reviewed in a recent article by Zhang et al[226], have demonstrated that whilst chronic exposure to some ITC containing proteins can prevent cancer development and increase cellular tolerance to oxidant exposure, the acute (1-3hr) response to similar concentrations[227] can be highly injurious itself, causing genetic damage inducing a transitory drop in glutathione levels (an antioxidant), rendering cells more susceptible to oxidative damage.

It could be hypothesised that, if cells respond similarly to FITC as to other ITC containing compounds, responses induced in the epithelial and mesenchymal cells exposed to FITC might go beyond anti-oxidant activities,

perhaps including the up regulation of inflammatory pathways, both acutely and chronically, and that this might be involved in the maintenance of the chronic inflammatory infiltrate observed in these mice.

Alternatively, as suggested in the fourth hypothesis listed at the start of this discussion, the acute inflammation induced by FITC initiates an immune reaction which potentiates the chronicity of the inflammation through the generation of an antibody response. Chapter 4 demonstrated that there is a clear association between anti FITC IgG1 antibody titre and fibrotic score in the FITC model. However, this is far from conclusive, as the nature of this association, be it ameliorative, pathological or inconsequential, was not determined. To fully address this observation and the hypothesis posited above, sera or purified IgG1 antibody transfers between FITC instilled mice could be performed and the affects on pathology analysed, using the inflammatory and fibrotic scoring systems described in this thesis.

Furthermore, it could be hypothesised that the continued presence of FITC in the lung, associated with a persistent inflammatory infiltrate, contributes to chronic inflammation and fibrosis by facilitating the development of an autoimmune response. Such a hypothesis could be addressed with sera or antibody transfers into naïve mice or through *in vitro* co culture of sera with pulmonary cell types, similar to those conducted by Wallace et al[113], where antibodies against an epithelial antigen stimulated TGF-β and tenascin production; both profibrotic factors.

Whilst the level of anti-FITC antibody participation in disease awaits further investigation the elucidation of the IgG1 class of this antibody, in the absence of FITC specific IgE or eosinophils infiltration, has firmly established that FITC instillation initiates a Th2 dominant, non allergic inflammatory fibrotic response. This information along with the predominance of mononuclear foci has confirmed an immuno-modulatory role in this mouse model, which when altered, perhaps through the use of T regulatory cell studies, may elucidate the role played by the immune system in inflammatory lung fibrosis.

Thus in conclusion, it is my belief that the development of fibrosis in the FITC instillation model is initiated through a combination of factors. Acutely, the delivery of FITC causes cellular death and the initiation of oxidative damage. This leads to an inflammatory response and the adoption of new, potentially proinflammatory characteristics in surviving cells, located in areas of FITC deposition. This along with the persistence of FITC, maintains a Th2 polarised inflammatory infiltrate, incorporating anti-FITC antibody producing cells. These may aid in the clearance of FITC, but this very process could maintain the infiltrate, through complement deposition, until the majority of FITC has been removed from the lung. Any fibrosis that develops in areas of FITC deposition is attributable to cytokine signalling associated with this inflammatory process and does not involve the Shh signalling pathway in any way. The expression of this pathway in human fibrotic conditions is representative of an adoption of a larger airway phenotype by lower airway epithelial cells and this is not a prognostic factor in the development of fibrosis. The potential recipients of this Shh signal in UIP and BOOP biopsies may be identifiable in future through the use of the laser catapult and RNA isolation techniques developed here.

APPENDICES

7.1 SANDWICH SHH ELISA STANDARD CURVE

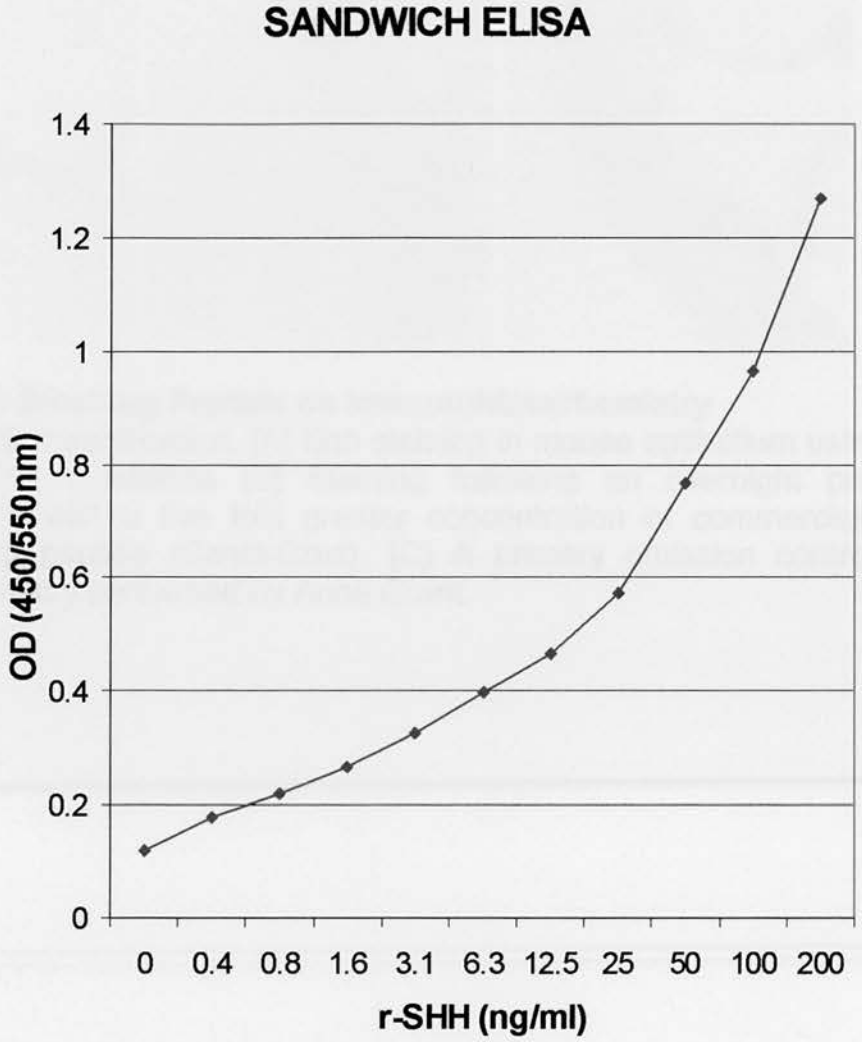

Figure 7.1: Sandwich ELISA Standard Curve
Curve generated with N19 capture (2μg/ml) on high binding EIA plates (Corning-Costar) in Carbonate-Bicarbonate buffer, 50μl per well. Left overnight at 4°C. All subsequent steps separated by wash steps with wash buffer (Tween20/PBS). Blocked for 2hrs at RT with standard blocking solution. Triplicate standard curve of recombinant Shh prepared in diluent with a top standard of 200ng/ml, loaded in 50μl volumes per well and incubated overnight at 4°C. 5E1 was added at 700ng/ml in diluting fluid (50μl/well) RT 2 hours. Biotinylated anti-mouse (R&D) was then added at 250ng/ml in diluting fluid (50μl/well). Developed using Streptavidin/substrate system using 50μl of Streptavidin (R&D) for 20 minutes RT, followed by 3,3,5 TMB for 25 minutes, stopped with $2NH_2SO_4$.

7.2 SHH IMMUNOHISTOCHEMISTRY BLOCKING

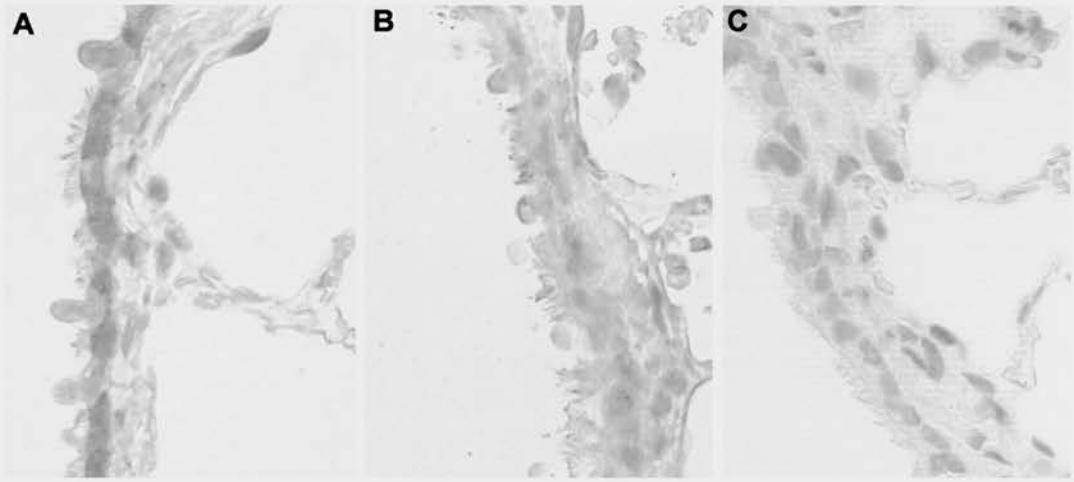

Figure 7.2: N19 Blocking Peptide on Immunohistochemistry
All images at x400 magnification. [A] Shh staining in mouse epithelium using standard N19 IHC conditions [B] Staining following an overnight pre-incubation of N19 with a five fold greater concentration of commercially available blocking peptide (Santa-Cruz). [C] A primary omission control. Immunohistochemistry performed by Anne Grant.

7.3 CD3 AND B220 IMMUNOHISTOCHEMISTRY

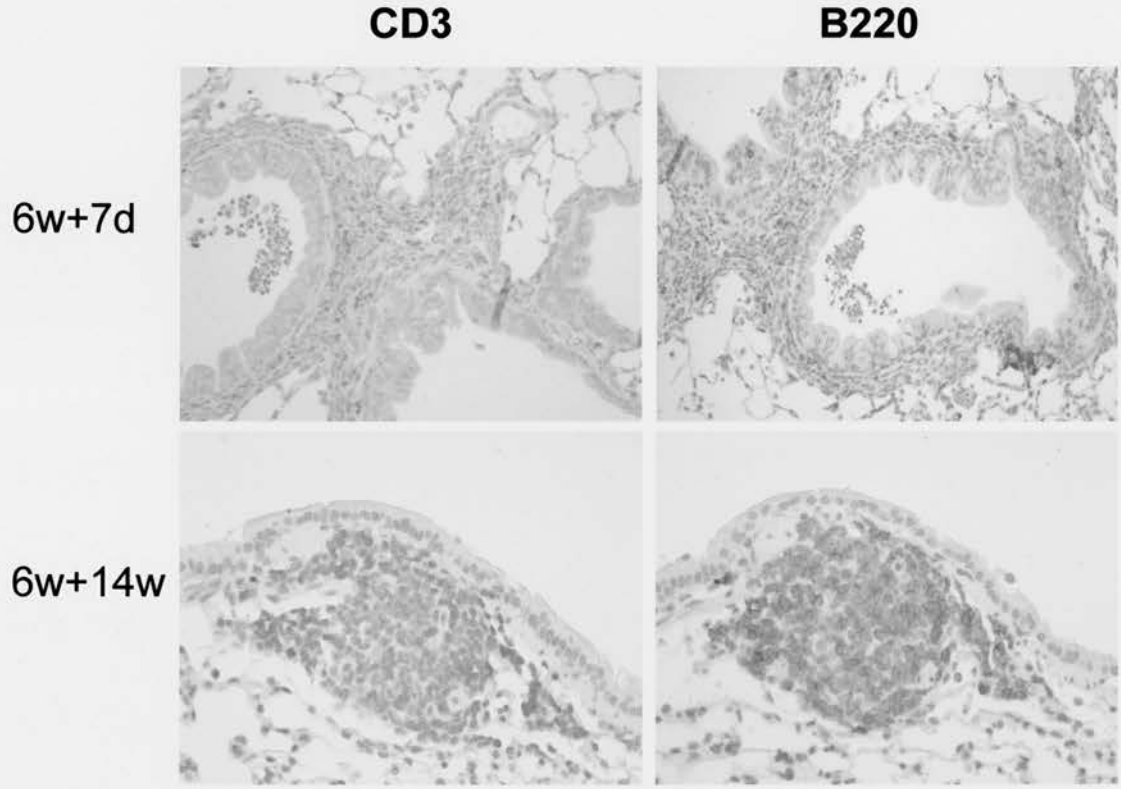

Figure 7.3: CD3 & B220 Immunohistochemistry
Photos from the thesis of Dr S.A Ahmad. [Top] x200, Illustrating the presence of both B-cells (B220) and T-cells (CD3) in mononuclear infiltrates in FITC positive areas. [Bottom] x 800, Later time points (14 weeks post second instillation (2mg/ml)) saw the occurrence of mononuclear foci containing both B & T cells.

7.4 PUBLICATIONS ARISING FROM THIS THESIS

Fisher CE, Ahmad SA, Fitch PM, Lamb JR, Howie SE. FITC-induced murine pulmonary inflammation: CC10 up-regulation and concurrent Shh expression. Cell Biol Int, 2005, Oct, 29(10):868-76.

Fitch P.M, Wakelin J.W, Lowrey J.A, Wallace W.A.H, Howie S.E.M. Shh expression in pulmonary injury and disease Published in *Hedgehog-gli signalling and human disease*, 2005, Altaba RI (ed). Eurekah Publishing.

Lowrey JA, Fitch PM, Stewart JA, Lamb JR & Howie SEM. Investigation of the mechanism by which sonic hedgehog enhances proliferation of activated $CD4^{+}$T cells. *Immunology* 2004, December; 113(supp): 112-113. [Abstract]

Fitch PM, Lamb JR, Wallace WAH, Howie SEM. The developmental signalling molecule sonic hedgehog is released by damage to pulmonary epithelial cells. AJRCCM 2004, April; 169 (7): A676 [Abstract]

Fitch PM, Wallace W, Howie SEM. Oxidising damage results in the release of Shh and the up regulation of GM-CSF from pulmonary epithelial cells. *Immunology* 2003, December, 110(supp) 54 [Abstract]

Stewart GA, Lowrey JA, Wakelin SJ, Fitch PM, Lindey S, Dallman MJ, Lamb JR, Howie SE. Sonic hedgehog signalling modulates activation of and cytokine production by human peripheral CD4+ T cells. *J Immunol* 2002 November 15;169(10):5451-7.

7.5 CONFERENCE POSTGRAD COURSE ATTENDANCE

The cutting edge of lung fibrosis: how our current understanding of pathogenesis is leading to new therapeutic approaches. American Thoracic Society (ATS) postgraduate course 21. ATS annual congress, Florida, 2004.

Host defence mechanisms in pulmonary infection ATS postgraduate course 8. ATS annual congress, Florida 2004.

Recent advances in understanding pulmonary fibrogenesis. European Respiratory Society (ERS) school postgraduate course. ERS annual congress, Vienna, 2003

British society for immunology summer school, Bristol, 2003.

REFERENCE LIST

Reference List

(1) Stewart GA, Hoyne GF, Ahmad SA et al. Expression of the developmental Sonic hedgehog (Shh) signalling pathway is up-regulated in chronic lung fibrosis and the Shh receptor patched 1 is present in circulating T lymphocytes. *J Pathol* 2003 April;199(4):488-95.

(2) Lowrey JA, Stewart GA, Lindey S et al. Sonic hedgehog promotes cell cycle progression in activated peripheral CD4(+) T lymphocytes. *J Immunol* 2002 August 15;169(4):1869-75.

(3) Stewart GA, Lowrey JA, Wakelin SJ et al. Sonic hedgehog signaling modulates activation of and cytokine production by human peripheral CD4+ T cells. *J Immunol* 2002 November 15;169(10):5451-7.

(4) Mohler J. Requirements for hedgehog, a Segmental Polarity Gene, in Patterning Larval and Adult Cuticle of Drosophila. *Genetics* 1988 December 1;120(4):1061-72.

(5) McMahon AP. More surprises in the Hedgehog signaling pathway. *Cell* 2000 January 21;100(2):185-8.

(6) McMahon AP, Ingham PW, Tabin CJ. Developmental roles and clinical significance of hedgehog signaling. *Curr Top Dev Biol* 2003;53:1-114.

(7) Marigo V, Roberts DJ, Lee SM et al. Cloning, expression, and chromosomal location of SHH and IHH: two human homologues of the Drosophila segment polarity gene hedgehog. *Genomics* 1995 July 1;28(1):44-51.

(8) Sukegawa A, Narita T, Kameda T et al. The concentric structure of the developing gut is regulated by Sonic hedgehog derived from endodermal epithelium. *Development* 2000 May;127(9):1971-80.

(9) Lee JJ, Ekker SC, von Kessler DP, Porter JA, Sun BI, Beachy PA. Autoproteolysis in hedgehog protein biogenesis. *Science* 1994 December 2;266(5190):1528-37.

(10) Hall TM, Porter JA, Young KE, Koonin EV, Beachy PA, Leahy DJ. Crystal structure of a Hedgehog autoprocessing domain: homology between Hedgehog and self-splicing proteins. *Cell* 1997 October 3;91(1):85-97.

(11) Porter JA, von Kessler DP, Ekker SC et al. The product of hedgehog autoproteolytic cleavage active in local and long-range signalling. *Nature* 1995 March 23;374(6520):363-6.

(12) Fietz MJ, Jacinto A, Taylor AM, Alexandre C, Ingham PW. Secretion of the amino-terminal fragment of the hedgehog protein is necessary

and sufficient for hedgehog signalling in Drosophila. *Curr Biol* 1995 June 1;5(6):643-50.

(13) Guy RK. Inhibition of sonic hedgehog autoprocessing in cultured mammalian cells by sterol deprivation. *Proc Natl Acad Sci U S A* 2000 June 20;97(13):7307-12.

(14) Lee JD, Kraus P, Gaiano N et al. An acylatable residue of Hedgehog is differentially required in Drosophila and mouse limb development. *Dev Biol* 2001 May 1;233(1):122-36.

(15) Feng J, White B, Tyurina OV et al. Synergistic and antagonistic roles of the Sonic hedgehog N- and C-terminal lipids. *Development* 2004 September;131(17):4357-70.

(16) Pepinsky RB, Zeng C, Wen D et al. Identification of a palmitic acid-modified form of human Sonic hedgehog. *J Biol Chem* 1998 May 29;273(22):14037-45.

(17) Taylor FR, Wen D, Garber EA et al. Enhanced potency of human Sonic hedgehog by hydrophobic modification. *Biochemistry* 2001 April 10;40(14):4359-71.

(18) Kohtz JD, Lee HY, Gaiano N et al. N-terminal fatty-acylation of sonic hedgehog enhances the induction of rodent ventral forebrain neurons. *Development* 2001 June;128(12):2351-63.

(19) Ma Y, Erkner A, Gong R et al. Hedgehog-mediated patterning of the mammalian embryo requires transporter-like function of dispatched. *Cell* 2002 October 4;111(1):63-75.

(20) Zeng X, Goetz JA, Suber LM, Scott WJ, Jr., Schreiner CM, Robbins DJ. A freely diffusible form of Sonic hedgehog mediates long-range signalling. *Nature* 2001 June 7;411(6838):716-20.

(21) Peters C, Wolf A, Wagner M, Kuhlmann J, Waldmann H. The cholesterol membrane anchor of the Hedgehog protein confers stable membrane association to lipid-modified proteins. *Proc Natl Acad Sci U S A* 2004 June 8;101(23):8531-6.

(22) Chuang PT, McMahon AP. Vertebrate Hedgehog signalling modulated by induction of a Hedgehog- binding protein. *Nature* 1999 February 18;397(6720):617-21.

(23) The I, Bellaiche Y, Perrimon N. Hedgehog movement is regulated through tout velu-dependent synthesis of a heparan sulfate proteoglycan. *Mol Cell* 1999 October;4(4):633-9.

(24) Lind T, Tufaro F, McCormick C, Lindahl U, Lidholt K. The putative tumor suppressors EXT1 and EXT2 are glycosyltransferases required for the biosynthesis of heparan sulfate. *J Biol Chem* 1998 October 9;273(41):26265-8.

(25) Stickens D, Clines G, Burbee D et al. The EXT2 multiple exostoses gene defines a family of putative tumour suppressor genes. *Nat Genet* 1996 September;14(1):25-32.

(26) Bellaiche Y, The I, Perrimon N. Tout-velu is a Drosophila homologue of the putative tumour suppressor EXT-1 and is needed for Hh diffusion. *Nature* 1998 July 2;394(6688):85-8.

(27) Ingham PW, McMahon AP. Hedgehog signaling in animal development: paradigms and principles. *Genes Dev* 2001 December 1;15(23):3059-87.

(28) Perrimon N, Hacker U. Wingless, hedgehog and heparan sulfate proteoglycans. *Development* 2004 June;131(11):2509-11.

(29) Marigo V, Davey RA, Zuo Y, Cunningham JM, Tabin CJ. Biochemical evidence that patched is the Hedgehog receptor. *Nature* 1996 November 14;384(6605):176-9.

(30) Stone DM, Hynes M, Armanini M et al. The tumour-suppressor gene patched encodes a candidate receptor for Sonic hedgehog. *Nature* 1996 November 14;384(6605):129-34.

(31) Denef N, Neubuser D, Perez L, Cohen SM. Hedgehog induces opposite changes in turnover and subcellular localization of patched and smoothened. *Cell* 2000 August 18;102(4):521-31.

(32) Capdevila J, Pariente F, Sampedro J, Alonso JL, Guerrero I. Subcellular localization of the segment polarity protein patched suggests an interaction with the wingless reception complex in Drosophila embryos. *Development* 1994 April;120(4):987-98.

(33) McCarthy RA, Barth JL, Chintalapudi MR, Knaak C, Argraves WS. Megalin functions as an endocytic sonic hedgehog receptor. *J Biol Chem* 2002 July 12;277(28):25660-7.

(34) Barth JL, Argraves WS. Cubilin and megalin: partners in lipoprotein and vitamin metabolism. *Trends Cardiovasc Med* 2001 January;11(1):26-31.

(35) McCarthy RA, Argraves WS. Megalin and the neurodevelopmental biology of sonic hedgehog and retinol. *J Cell Sci* 2003 March 15;116(Pt 6):955-60.

(36) Kounnas MZ, Chappell DA, Wong H, Argraves WS, Strickland DK. The cellular internalization and degradation of hepatic lipase is mediated by low density lipoprotein receptor-related protein and requires cell surface proteoglycans. *J Biol Chem* 1995 April 21;270(16):9307-12.

(37) Shakibaei M, Frevert U. Dual interaction of the malaria circumsporozoite protein with the low density lipoprotein receptor-related protein (LRP) and heparan sulfate proteoglycans. *J Exp Med* 1996 November 1;184(5):1699-711.

(38) Carpenter D, Stone DM, Brush J et al. Characterization of two patched receptors for the vertebrate hedgehog protein family. *Proc Natl Acad Sci U S A* 1998 November 10;95(23):13630-4.

(39) Karpen HE, Bukowski JT, Hughes T, Gratton JP, Sessa WC, Gailani MR. The sonic hedgehog receptor patched associates with caveolin-1 in cholesterol-rich microdomains of the plasma membrane. *J Biol Chem* 2001 June 1;276(22):19503-11.

(40) Rietveld A, Neutz S, Simons K, Eaton S. Association of sterol- and glycosylphosphatidylinositol-linked proteins with Drosophila raft lipid microdomains. *J Biol Chem* 1999 April 23;274(17):12049-54.

(41) Jeong J, McMahon AP. Cholesterol modification of Hedgehog family proteins. *J Clin Invest* 2002 September;110(5):591-6.

(42) Wang TY, Leventis R, Silvius JR. Partitioning of lipidated peptide sequences into liquid-ordered lipid domains in model and biological membranes. *Biochemistry* 2001 October 30;40(43):13031-40.

(43) De Lean A, Stadel JM, Lefkowitz RJ. A ternary complex model explains the agonist-specific binding properties of the adenylate cyclase-coupled beta-adrenergic receptor. *J Biol Chem* 1980 August 10;255(15):7108-17.

(44) Chen Y, Struhl G. Dual roles for patched in sequestering and transducing Hedgehog. *Cell* 1996 November 1;87(3):553-63.

(45) DeCamp DL, Thompson TM, de Sauvage FJ, Lerner MR. Smoothened activates Galphai-mediated signaling in frog melanophores. *J Biol Chem* 2000 August 25;275(34):26322-7.

(46) Incardona JP, Gruenberg J, Roelink H. Sonic hedgehog induces the segregation of patched and smoothened in endosomes. *Curr Biol* 2002 June 25;12(12):983-95.

(47) Taipale J, Cooper MK, Maiti T, Beachy PA. Patched acts catalytically to suppress the activity of Smoothened. *Nature* 2002 August 22;418(6900):892-7.

(48) Davies JP, Chen FW, Ioannou YA. Transmembrane molecular pump activity of Niemann-Pick C1 protein. *Science* 2000 December 22;290(5500):2295-8.

(49) Chen JK, Taipale J, Cooper MK, Beachy PA. Inhibition of Hedgehog signaling by direct binding of cyclopamine to Smoothened. *Genes Dev* 2002 November 1;16(21):2743-8.

(50) Frank-Kamenetsky M, Zhang XM, Bottega S et al. Small-molecule modulators of Hedgehog signaling: identification and characterization of Smoothened agonists and antagonists. *J Biol* 2002 November 6;1(2):10.

(51) Williams JA, Guicherit OM, Zaharian BI et al. Identification of a small molecule inhibitor of the hedgehog signaling pathway: effects on basal cell carcinoma-like lesions. *Proc Natl Acad Sci U S A* 2003 April 15;100(8):4616-21.

(52) Sasaki H, Nishizaki Y, Hui C, Nakafuku M, Kondoh H. Regulation of Gli2 and Gli3 activities by an amino-terminal repression domain: implication of Gli2 and Gli3 as primary mediators of Shh signaling. *Development* 1999 September;126(17):3915-24.

(53) Lei Q, Zelman AK, Kuang E, Li S, Matise MP. Transduction of graded Hedgehog signaling by a combination of Gli2 and Gli3 activator functions in the developing spinal cord. *Development* 2004 August;131(15):3593-604.

(54) Park HL, Bai C, Platt KA et al. Mouse Gli1 mutants are viable but have defects in SHH signaling in combination with a Gli2 mutation. *Development* 2000 April;127(8):1593-605.

(55) Kogerman P, Krause D, Rahnama F et al. Alternative first exons of PTCH1 are differentially regulated in vivo and may confer different functions to the PTCH1 protein. *Oncogene* 2002 September 5;21(39):6007-16.

(56) Agren M, Kogerman P, Kleman MI, Wessling M, Toftgard R. Expression of the PTCH1 tumor suppressor gene is regulated by alternative promoters and a single functional Gli-binding site. *Gene* 2004 April 14;330:101-14.

(57) Lee J, Platt KA, Censullo P, Altaba A. Gli1 is a target of Sonic hedgehog that induces ventral neural tube development. *Development* 1997 July;124(13):2537-52.

(58) Sasaki H, Hui C, Nakafuku M, Kondoh H. A binding site for Gli proteins is essential for HNF-3beta floor plate enhancer activity in transgenics and can respond to Shh in vitro. *Development* 1997 April;124(7):1313-22.

(59) Ingram WJ, Wicking CA, Grimmond SM, Forrest AR, Wainwright BJ. Novel genes regulated by Sonic Hedgehog in pluripotent mesenchymal cells. *Oncogene* 2002 November 21;21(53):8196-205.

(60) Cardoso WV. Molecular regulation of lung development. *Annu Rev Physiol* 2001;63:471-94.

(61) Bellusci S, Furuta Y, Rush MG, Henderson R, Winnier G, Hogan BL. Involvement of Sonic hedgehog (Shh) in mouse embryonic lung growth and morphogenesis. *Development* 1997 January;124(1):53-63.

(62) Grindley JC, Bellusci S, Perkins D, Hogan BL. Evidence for the involvement of the Gli gene family in embryonic mouse lung development. *Dev Biol* 1997 August 15;188(2):337-48.

(63) Lebeche D, Malpel S, Cardoso WV. Fibroblast growth factor interactions in the developing lung. *Mech Dev* 1999 August;86(1-2):125-36.

(64) Outram SV, Varas A, Pepicelli CV, Crompton T. Hedgehog signaling regulates differentiation from double-negative to double-positive thymocyte. *Immunity* 2000 August;13(2):187-97.

(65) Marshall LJ, Perks B, Ferkol T, Shute JK. IL-8 released constitutively by primary bronchial epithelial cells in culture forms an inactive complex with secretory component. *J Immunol* 2001 September 1;167(5):2816-23.

(66) Singh G, Singh J, Katyal SL et al. Identification, cellular localization, isolation, and characterization of human Clara cell-specific 10 KD protein. *J Histochem Cytochem* 1988 January;36(1):73-80.

(67) Reynolds SD, Hong KU, Giangreco A et al. Conditional clara cell ablation reveals a self-renewing progenitor function of pulmonary neuroendocrine cells. *Am J Physiol Lung Cell Mol Physiol* 2000 June;278(6):L1256-L1263.

(68) Reynolds SD, Giangreco A, Power JH, Stripp BR. Neuroepithelial bodies of pulmonary airways serve as a reservoir of progenitor cells capable of epithelial regeneration. *Am J Pathol* 2000 January;156(1):269-78.

(69) Giangreco A, Shen H, Reynolds SD, Stripp BR. Molecular phenotype of airway side population cells. *Am J Physiol Lung Cell Mol Physiol* 2004 April;286(4):L624-L630.

(70) Hong KU, Reynolds SD, Giangreco A, Hurley CM, Stripp BR. Clara cell secretory protein-expressing cells of the airway neuroepithelial body microenvironment include a label-retaining subset and are critical for epithelial renewal after progenitor cell depletion. *Am J Respir Cell Mol Biol* 2001 June;24(6):671-81.

(71) Borthwick DW, Shahbazian M, Krantz QT, Dorin JR, Randell SH. Evidence for stem-cell niches in the tracheal epithelium. *Am J Respir Cell Mol Biol* 2001 June;24(6):662-70.

(72) Hong KU, Reynolds SD, Watkins S, Fuchs E, Stripp BR. Basal cells are a multipotent progenitor capable of renewing the bronchial epithelium. *Am J Pathol* 2004 February;164(2):577-88.

(73) Watkins DN, Berman DM, Burkholder SG, Wang B, Beachy PA, Baylin SB. Hedgehog signalling within airway epithelial progenitors and in small-cell lung cancer. *Nature* 2003 March 20;422(6929):313-7.

(74) Watkins DN, Berman DM, Baylin SB. Hedgehog signaling: progenitor phenotype in small-cell lung cancer. *Cell Cycle* 2003 May;2(3):196-8.

(75) Persson CG, Erjefalt JS, Greiff L et al. Plasma-derived proteins in airway defence, disease and repair of epithelial injury. *Eur Respir J* 1998 April;11(4):958-70.

(76) Erjefalt JS, Persson CG. Airway epithelial repair: breathtakingly quick and multipotentially pathogenic. *Thorax* 1997 November;52(11):1010-2.

(77) Adamson IY, Hedgecock C, Bowden DH. Epithelial cell-fibroblast interactions in lung injury and repair. *Am J Pathol* 1990 August;137(2):385-92.

(78) Toews GB, Vial WC, Dunn MM et al. The accessory cell function of human alveolar macrophages in specific T cell proliferation. *J Immunol* 1984 January;132(1):181-6.

(79) Adler KB, Fischer BM, Wright DT, Cohn LA, Becker S. Interactions between respiratory epithelial cells and cytokines: relationships to lung inflammation. *Ann N Y Acad Sci* 1994 May 28;725:128-45.

(80) Martin LD, Rochelle LG, Fischer BM, Krunkosky TM, Adler KB. Airway epithelium as an effector of inflammation: molecular regulation of secondary mediators. *Eur Respir J* 1997 September;10(9):2139-46.

(81) Finkelstein JN, Johnston C, Barrett T, Oberdorster G. Particulate-cell interactions and pulmonary cytokine expression. *Environ Health Perspect* 1997 September;105 Suppl 5:1179-82.

(82) Maus U, Huwe J, Maus R, Seeger W, Lohmeyer J. Alveolar JE/MCP-1 and endotoxin synergize to provoke lung cytokine upregulation, sequential neutrophil and monocyte influx, and vascular leakage in mice. *Am J Respir Crit Care Med* 2001 August 1;164(3):406-11.

(83) Holt PG, Oliver J, Bilyk N et al. Downregulation of the antigen presenting cell function(s) of pulmonary dendritic cells in vivo by resident alveolar macrophages. *J Exp Med* 1993 February 1;177(2):397-407.

(84) Bilyk N, Holt PG. Cytokine modulation of the immunosuppressive phenotype of pulmonary alveolar macrophage populations. *Immunology* 1995 October;86(2):231-7.

(85) Bilyk N, Holt PG. Inhibition of the immunosuppressive activity of resident pulmonary alveolar macrophages by granulocyte/macrophage colony-stimulating factor. *J Exp Med* 1993 June 1;177(6):1773-7.

(86) Janeway CA, Travers P, Walport M, Shlomchik MJ. *IMMUNOBIOLOGY the immune system in health and disease*. Sixth ed. Garland Science Publishing; 2005.

(87) Rabu C, Quemener A, Jacques Y, Echasserieau K, Vusio P, Lang F. Production of recombinant human trimeric CD137L(4-1BBL): Crosslinking is essential to its T cell co-stimulation activity. *J Biol Chem* 2005 October 4.

(88) Lee BO, Moyron-Quiroz J, Rangel-Moreno J et al. CD40, but not CD154, expression on B cells is necessary for optimal primary B cell responses. *J Immunol* 2003 December 1;171(11):5707-17.

(89) Moyron-Quiroz JE, Rangel-Moreno J, Kusser K et al. Role of inducible bronchus associated lymphoid tissue (iBALT) in respiratory immunity. *Nat Med* 2004 September;10(9):927-34.

(90) Selman M, Pardo A. The epithelial/fibroblastic pathway in the pathogenesis of idiopathic pulmonary fibrosis. *Am J Respir Cell Mol Biol* 2003 September;29(3 Suppl):S93-S97.

(91) Adamson IY, Bakowska J, Prieditis H. Proliferation of rat pleural mesothelial cells in response to hepatocyte and keratinocyte growth factors. *Am J Respir Cell Mol Biol* 2000 September;23(3):345-9.

(92) Nunes H, Soler P, Valeyre D. Pulmonary sarcoidosis. *Allergy* 2005 May;60(5):565-82.

(93) Kolodsick JE, Toews GB, Jakubzick C et al. Protection from fluorescein isothiocyanate-induced fibrosis in IL-13-deficient, but not IL-4-deficient, mice results from impaired collagen synthesis by fibroblasts. *J Immunol* 2004 April 1;172(7):4068-76.

(94) Bergeron C, Page N, Joubert P, Barbeau B, Hamid Q, Chakir J. Regulation of procollagen I (alpha1) by interleukin-4 in human bronchial fibroblasts: a possible role in airway remodelling in asthma. *Clin Exp Allergy* 2003 October;33(10):1389-97.

(95) Lordan JL, Bucchieri F, Richter A et al. Cooperative effects of Th2 cytokines and allergen on normal and asthmatic bronchial epithelial cells. *J Immunol* 2002 July 1;169(1):407-14.

(96) Jakubzick C, Choi ES, Kunkel SL et al. Augmented pulmonary IL-4 and IL-13 receptor subunit expression in idiopathic interstitial pneumonia. *J Clin Pathol* 2004 May;57(5):477-86.

(97) Jakubzick C, Kunkel SL, Puri RK, Hogaboam CM. Therapeutic Targeting of IL-4- and IL-13-Responsive Cells in Pulmonary Fibrosis. *Immunol Res* 2004;30(3):339-50.

(98) Jakubzick C, Choi ES, Carpenter KJ et al. Human pulmonary fibroblasts exhibit altered interleukin-4 and interleukin-13 receptor subunit expression in idiopathic interstitial pneumonia. *Am J Pathol* 2004 June;164(6):1989-2001.

(99) Riha RL, Yang IA, Rabnott GC, Tunnicliffe AM, Fong KM, Zimmerman PV. Cytokine gene polymorphisms in idiopathic pulmonary fibrosis. *Intern Med J* 2004 March;34(3):126-9.

(100) Knight DA, Ernst M, Anderson GP, Moodley YP, Mutsaers SE. The role of gp130/IL-6 cytokines in the development of pulmonary fibrosis: critical determinants of disease susceptibility and progression? *Pharmacol Ther* 2003 September;99(3):327-38.

(101) Moodley YP, Scaffidi AK, Misso NL et al. Fibroblasts isolated from normal lungs and those with idiopathic pulmonary fibrosis differ in interleukin-6/gp130-mediated cell signaling and proliferation. *Am J Pathol* 2003 July;163(1):345-54.

(102) Moodley YP, Misso NL, Scaffidi AK et al. Inverse effects of interleukin-6 on apoptosis of fibroblasts from pulmonary fibrosis and normal lungs. *Am J Respir Cell Mol Biol* 2003 October;29(4):490-8.

(103) Charbeneau RP, Christensen PJ, Chrisman CJ et al. Impaired synthesis of prostaglandin E2 by lung fibroblasts and alveolar epithelial cells from GM-CSF-/- mice: implications for fibroproliferation. *Am J Physiol Lung Cell Mol Physiol* 2003 June;284(6):L1103-L1111.

(104) Ikegami M, Jobe AH, Huffman Reed JA, Whitsett JA. Surfactant metabolic consequences of overexpression of GM-CSF in the epithelium of GM-CSF-deficient mice. *Am J Physiol* 1997 October;273(4 Pt 1):L709-L714.

(105) Xing Z, Tremblay GM, Sime PJ, Gauldie J. Overexpression of granulocyte-macrophage colony-stimulating factor induces pulmonary granulation tissue formation and fibrosis by induction of transforming growth factor-beta 1 and myofibroblast accumulation. *Am J Pathol* 1997 January;150(1):59-66.

(106) Akagawa KS, Kamoshita K, Tokunaga T. Effects of granulocyte-macrophage colony-stimulating factor and colony-stimulating factor-1 on the proliferation and differentiation of murine alveolar macrophages. *J Immunol* 1988 November 15;141(10):3383-90.

(107) Epler GR. Bronchiolitis obliterans organizing pneumonia. *Arch Intern Med* 2001 January 22;161(2):158-64.

(108) Epler GR, Colby TV, McLoud TC, Carrington CB, Gaensler EA. Bronchiolitis obliterans organizing pneumonia. *N Engl J Med* 1985 January 17;312(3):152-8.

(109) American Thoracic Society/European Respiratory Society International Multidisciplinary Consensus Classification of the Idiopathic Interstitial Pneumonias. This joint statement of the American Thoracic Society (ATS), and the European Respiratory Society (ERS) was adopted by the ATS board of directors, June 2001 and by the ERS Executive Committee, June 2001. *Am J Respir Crit Care Med* 2002 January 15;165(2):277-304.

(110) Thannickal VJ, Toews GB, White ES, Lynch JP, III, Martinez FJ. Mechanisms of pulmonary fibrosis. *Annu Rev Med* 2004;55:395-417.

(111) Wallace WA, Roberts SN, Caldwell H et al. Circulating antibodies to lung protein(s) in patients with cryptogenic fibrosing alveolitis. *Thorax* 1994 March;49(3):218-22.

(112) Wallace WA, Schofield JA, Lamb D, Howie SE. Localisation of a pulmonary autoantigen in cryptogenic fibrosing alveolitis. *Thorax* 1994 November;49(11):1139-45.

(113) Wallace WA, Howie SE. Upregulation of tenascin and TGFbeta production in a type II alveolar epithelial cell line by antibody against a pulmonary auto-antigen. *J Pathol* 2001 September;195(2):251-6.

(114) Wallace WA, Ramage EA, Lamb D, Howie SE. A type 2 (Th2-like) pattern of immune response predominates in the pulmonary interstitium of patients with cryptogenic fibrosing alveolitis (CFA). *Clin Exp Immunol* 1995 September;101(3):436-41.

(115) Wallace WA, Howie SE, Lamb D, Salter DM. Tenascin immunoreactivity in cryptogenic fibrosing alveolitis. *J Pathol* 1995 April;175(4):415-20.

(116) Khalil N, O'Connor RN, Unruh HW et al. Increased production and immunohistochemical localization of transforming growth factor-beta in idiopathic pulmonary fibrosis. *Am J Respir Cell Mol Biol* 1991 August;5(2):155-62.

(117) Chua F, Gauldie J, Laurent GJ. Pulmonary fibrosis: searching for model answers. *Am J Respir Cell Mol Biol* 2005 July;33(1):9-13.

(118) Hu H, Stein-Streilein J. Hapten-immune pulmonary interstitial fibrosis (HIPIF) in mice requires both CD4+ and CD8+ T lymphocytes. *J Leukoc Biol* 1993 November;54(5):414-22.

(119) Zhang-Hoover J, Sutton A, van RN, Stein-Streilein J. A critical role for alveolar macrophages in elicitation of pulmonary immune fibrosis. *Immunology* 2000 December;101(4):501-11.

(120) Zhang-Hoover J, Sutton A, Stein-Streilein J. CD40/CD40 ligand interactions are critical for elicitation of autoimmune-mediated fibrosis in the lung. *J Immunol* 2001 March 1;166(5):3556-63.

(121) Moore BB, Paine R, III, Christensen PJ et al. Protection from pulmonary fibrosis in the absence of ccr2 signaling. *J Immunol* 2001 October 15;167(8):4368-77.

(122) Moore BB, Coffey MJ, Christensen P et al. GM-CSF regulates bleomycin-induced pulmonary fibrosis via a prostaglandin-dependent mechanism. *J Immunol* 2000 October 1;165(7):4032-9.

(123) Roberts SN, Howie SE, Wallace WA et al. A novel model for human interstitial lung disease: hapten-driven lung fibrosis in rodents. *J Pathol* 1995 July;176(3):309-18.

(124) Charytoniuk D, Porcel B, Rodriguez GJ, Faure H, Ruat M, Traiffort E. Sonic Hedgehog signalling in the developing and adult brain. *J Physiol Paris* 2002 January;96(1-2):9-16.

(125) Taipale J, Beachy PA. The Hedgehog and Wnt signalling pathways in cancer. *Nature* 2001 May 17;411(6835):349-54.

(126) Taipale J, Chen JK, Cooper MK et al. Effects of oncogenic mutations in Smoothened and Patched can be reversed by cyclopamine. *Nature* 2000 August 31;406(6799):1005-9.

(127) Bhardwaj G, Murdoch B, Wu D et al. Sonic hedgehog induces the proliferation of primitive human hematopoietic cells via BMP regulation. *Nat Immunol* 2001 February;2(2):172-80.

(128) Weaver M, Yingling JM, Dunn NR, Bellusci S, Hogan BL. Bmp signaling regulates proximal-distal differentiation of endoderm in mouse lung development. *Development* 1999 September;126(18):4005-15.

(129) Bellusci S, Henderson R, Winnier G, Oikawa T, Hogan BL. Evidence from normal expression and targeted misexpression that bone morphogenetic protein (Bmp-4) plays a role in mouse embryonic lung morphogenesis. *Development* 1996 June;122(6):1693-702.

(130) Pepinsky RB, Shapiro RI, Wang S et al. Long-acting forms of Sonic hedgehog with improved pharmacokinetic and pharmacodynamic properties are efficacious in a nerve injury model. *J Pharm Sci* 2002 February;91(2):371-87.

(131) Bambakidis NC, Wang RZ, Franic L, Miller RH. Sonic hedgehog-induced neural precursor proliferation after adult rodent spinal cord injury. *J Neurosurg* 2003 July;99(1 Suppl):70-5.

(132) Zhao Y, Young SL, McIntosh JC. Induction of tenascin in rat lungs undergoing bleomycin-induced pulmonary fibrosis. *Am J Physiol* 1998 June;274(6 Pt 1):L1049-L1057.

(133) Kaarteenaho-Wiik R, Kinnula V, Herva R, Paakko P, Pollanen R, Soini Y. Distribution and mRNA expression of tenascin-C in developing human lung. *Am J Respir Cell Mol Biol* 2001 September;25(3):341-6.

(134) Chuang PT, Kawcak T, McMahon AP. Feedback control of mammalian Hedgehog signaling by the Hedgehog-binding protein, Hip1, modulates Fgf signaling during branching morphogenesis of the lung. *Genes Dev* 2003 February 1;17(3):342-7.

(135) Wechsler-Reya RJ, Scott MP. Control of neuronal precursor proliferation in the cerebellum by Sonic Hedgehog. *Neuron* 1999 January;22(1):103-14.

(136) Ruiz IA, Palma V, Dahmane N. Hedgehog-Gli signalling and the growth of the brain. *Nat Rev Neurosci* 2002 January;3(1):24-33.

(137) Brewster R, Mullor JL, Altaba A. Gli2 functions in FGF signaling during antero-posterior patterning. *Development* 2000 October;127(20):4395-405.

(138) Parmantier E, Lynn B, Lawson D et al. Schwann cell-derived Desert hedgehog controls the development of peripheral nerve sheaths. *Neuron* 1999 August;23(4):713-24.

(139) Fan H, Khavari PA. Sonic hedgehog opposes epithelial cell cycle arrest. *J Cell Biol* 1999 October 4;147(1):71-6.

(140) Sherr CJ, Roberts JM. CDK inhibitors: positive and negative regulators of G1-phase progression. *Genes Dev* 1999 June 15;13(12):1501-12.

(141) Ware LB, Matthay MA. Keratinocyte and hepatocyte growth factors in the lung: roles in lung development, inflammation, and repair. *Am J Physiol Lung Cell Mol Physiol* 2002 May;282(5):L924-L940.

(142) Rice R, Spencer-Dene B, Connor EC et al. Disruption of Fgf10/Fgfr2b-coordinated epithelial-mesenchymal interactions causes cleft palate. *J Clin Invest* 2004 June;113(12):1692-700.

(143) Upadhyay D, Bundesmann M, Panduri V, Correa-Meyer E, Kamp DW. Fibroblast Growth Factor-10 Attenuates H2O2-Induced Alveolar Epithelial Cell DNA Damage: Role of MAPK Activation and DNA Repair. *Am J Respir Cell Mol Biol* 2004 July;31(1):107-13.

(144) Oswari J, Matthay MA, Margulies SS. Keratinocyte growth factor reduces alveolar epithelial susceptibility to in vitro mechanical deformation. *Am J Physiol Lung Cell Mol Physiol* 2001 November;281(5):L1068-L1077.

(145) Thibert C, Teillet MA, Lapointe F, Mazelin L, Le Douarin NM, Mehlen P. Inhibition of neuroepithelial patched-induced apoptosis by sonic hedgehog. *Science* 2003 August 8;301(5634):843-6.

(146) Miao N, Wang M, Ott JA et al. Sonic hedgehog promotes the survival of specific CNS neuron populations and protects these cells from toxic insult In vitro. *J Neurosci* 1997 August 1;17(15):5891-9.

(147) Dass B, Iravani MM, Jackson MJ, Engber TM, Galdes A, Jenner P. Behavioural and immunohistochemical changes following supranigral administration of sonic hedgehog in 1-methyl-4-phenyl-1,2,3,6-tetrahydropyridine-treated common marmosets. *Neuroscience* 2002;114(1):99-109.

(148) Tsuboi K, Shults CW. Intrastriatal injection of sonic hedgehog reduces behavioral impairment in a rat model of Parkinson's disease. *Exp Neurol* 2002 January;173(1):95-104.

(149) Pola R, Ling LE, Silver M et al. The morphogen Sonic hedgehog is an indirect angiogenic agent upregulating two families of angiogenic growth factors. *Nat Med* 2001 June;7(6):706-11.

(150) Pola R, Ling LE, Aprahamian TR et al. Postnatal recapitulation of embryonic hedgehog pathway in response to skeletal muscle ischemia. *Circulation* 2003 July 29;108(4):479-85.

(151) Lawson ND, Vogel AM, Weinstein BM. sonic hedgehog and vascular endothelial growth factor act upstream of the Notch pathway during arterial endothelial differentiation. *Dev Cell* 2002 July;3(1):127-36.

(152) Kanda S, Mochizuki Y, Suematsu T, Miyata Y, Nomata K, Kanetake H. Sonic hedgehog induces capillary morphogenesis by endothelial cells through phosphoinositide 3-kinase. *J Biol Chem* 2003 March 7;278(10):8244-9.

(153) Lieber M, Smith B, Szakal A, Nelson-Rees W, Todaro G. A continuous tumor-cell line from a human lung carcinoma with properties of type II alveolar epithelial cells. *Int J Cancer* 1976 January 15;17(1):62-70.

(154) Buckley S, Shi W, Driscoll B, Ferrario A, Anderson K, Warburton D. BMP4 signaling induces senescence and modulates the oncogenic phenotype of A549 lung adenocarcinoma cells. *Am J Physiol Lung Cell Mol Physiol* 2004 January;286(1):L81-L86.

(155) Christian-Ritter KK, Hill LD, Hoie EB, Zach TL. Effect of interleukin-4 on the synthesis of the third component of complement by pulmonary epithelial cells. *Am J Pathol* 1994 January;144(1):171-6.

(156) Franks LM, Carbonell AW, Hemmings VJ, Riddle PN. Metastasizing tumors from serum-supplemented and serum-free cell lines from a C57BL mouse lung tumor. *Cancer Res* 1976 March;36(3):1049-55.

(157) Kim JI, Chung DI, Choi DW. Egg production of Clonorchis sinensis in different strains of inbred mice. *Kisaengchunghak Chapchi* 1992 September;30(3):169-75.

(158) Yoshikura H, Hirokawa Y. Endogenous C-type virus of a mouse cell line and its defectiveness. *J Virol* 1974 June;13(6):1319-25.

(159) Cerwenka A, Bakker AB, McClanahan T et al. Retinoic acid early inducible genes define a ligand family for the activating NKG2D receptor in mice. *Immunity* 2000 June;12(6):721-7.

(160) Tong L, Smyth D, Kerr C, Catterall J, Richards CD. Mitogen-activated protein kinases Erk1/2 and p38 are required for maximal regulation of TIMP-1 by oncostatin M in murine fibroblasts. *Cell Signal* 2004 October;16(10):1123-32.

(161) Ericson J, Morton S, Kawakami A, Roelink H, Jessell TM. Two critical periods of Sonic Hedgehog signaling required for the specification of motor neuron identity. *Cell* 1996 November 15;87(4):661-73.

(162) Pepinsky RB, Rayhorn P, Day ES et al. Mapping sonic hedgehog-receptor interactions by steric interference. *J Biol Chem* 2000 April 14;275(15):10995-1001.

(163) Scott MG, Vreugdenhil AC, Buurman WA, Hancock RE, Gold MR. Cutting edge: cationic antimicrobial peptides block the binding of lipopolysaccharide (LPS) to LPS binding protein. *J Immunol* 2000 January 15;164(2):549-53.

(164) Ashcroft T, Simpson JM, Timbrell V. Simple method of estimating severity of pulmonary fibrosis on a numerical scale. *J Clin Pathol* 1988 April;41(4):467-70.

(165) Yasui H, Gabazza EC, Tamaki S et al. Intratracheal administration of activated protein C inhibits bleomycin-induced lung fibrosis in the mouse. *Am J Respir Crit Care Med* 2001 June;163(7):1660-8.

(166) Oury TD, Thakker K, Menache M, Chang LY, Crapo JD, Day BJ. Attenuation of bleomycin-induced pulmonary fibrosis by a catalytic antioxidant metalloporphyrin. *Am J Respir Cell Mol Biol* 2001 August;25(2):164-9.

(167) Tojo M, Mori T, Kiyosawa H et al. Expression of sonic hedgehog signal transducers, patched and smoothened, in human basal cell carcinoma. *Pathol Int* 1999 August;49(8):687-94.

(168) Regl G, Neill GW, Eichberger T et al. Human GLI2 and GLI1 are part of a positive feedback mechanism in Basal Cell Carcinoma. *Oncogene* 2002 August 15;21(36):5529-39.

(169) Sacedon R, Diez B, Nunez V et al. Sonic hedgehog is produced by follicular dendritic cells and protects germinal center B cells from apoptosis. *J Immunol* 2005 February 1;174(3):1456-61.

(170) Standiford TJ, Kunkel SL, Basha MA et al. Interleukin-8 gene expression by a pulmonary epithelial cell line. A model for cytokine networks in the lung. *J Clin Invest* 1990 December;86(6):1945-53.

(171) Standiford TJ, Kunkel SL, Phan SH, Rollins BJ, Strieter RM. Alveolar macrophage-derived cytokines induce monocyte chemoattractant protein-1 expression from human pulmonary type II-like epithelial cells. *J Biol Chem* 1991 May 25;266(15):9912-8.

(172) Sato N, Leopold PL, Crystal RG. Induction of the hair growth phase in postnatal mice by localized transient expression of Sonic hedgehog. *J Clin Invest* 1999 October;104(7):855-64.

(173) Spinella-Jaegle S, Rawadi G, Kawai S et al. Sonic hedgehog increases the commitment of pluripotent mesenchymal cells into the osteoblastic lineage and abolishes adipocytic differentiation. *J Cell Sci* 2001 June;114(Pt 11):2085-94.

(174) Nakamura T, Aikawa T, Iwamoto-Enomoto M et al. Induction of osteogenic differentiation by hedgehog proteins. *Biochem Biophys Res Commun* 1997 August 18;237(2):465-9.

(175) Paine R, III, Morris SB, Jin H et al. Impaired functional activity of alveolar macrophages from GM-CSF-deficient mice. *Am J Physiol Lung Cell Mol Physiol* 2001 November;281(5):L1210-L1218.

(176) Gudmundsson G, Hunninghake GW. Respiratory epithelial cells release interleukin-8 in response to a thermophilic bacteria that causes hypersensitivity pneumonitis. *Exp Lung Res* 1999 April;25(3):217-28.

(177) Moore BB, Moore TA, Toews GB. Role of T- and B-lymphocytes in pulmonary host defences. *Eur Respir J* 2001 November;18(5):846-56.

(178) Fitch PM, Wakelin SJ, Lowrey JA, Wallace WA, Howie SE. Shh expression in pulmonary injury and disease. In: Ruiz IA, Ruiz, editors. *Hedgehog-Gli signalling in human disease*. Eurekah; 2005.

(179) Corrin B, Dewar A, Rodriguez-Roisin R, Turner-Warwick M. Fine structural changes in cryptogenic fibrosing alveolitis and asbestosis. *J Pathol* 1985 October;147(2):107-19.

(180) Myers JL, Katzenstein AL. Epithelial necrosis and alveolar collapse in the pathogenesis of usual interstitial pneumonia. *Chest* 1988 December;94(6):1309-11.

(181) Barbas-Filho JV, Ferreira MA, Sesso A, Kairalla RA, Carvalho CR, Capelozzi VL. Evidence of type II pneumocyte apoptosis in the pathogenesis of idiopathic pulmonary fibrosis (IFP)/usual interstitial pneumonia (UIP). *J Clin Pathol* 2001 February;54(2):132-8.

(182) Nielsen CM, Williams J, van den Brink GR, Lauwers GY, Roberts DJ. Hh pathway expression in human gut tissues and in inflammatory gut diseases. *Lab Invest* 2004 December;84(12):1631-42.

(183) Stewart GA. The sonic hedgehog and wnt signalling pathways in interstitial lung disease and CD4+ T cell activation University of Edinburgh; 2003.

(184) Ahmad SA. in vitro and in vivo characterisation of a murine model of pulmonary fibrosis University of Edinburgh; 2002.

(185) Christensen PJ, Goodman RE, Pastoriza L, Moore B, Toews GB. Induction of lung fibrosis in the mouse by intratracheal instillation of fluorescein isothiocyanate is not T-cell-dependent. *Am J Pathol* 1999 November;155(5):1773-9.

(186) Takeshita K, Yamasaki T, Akira S, Gantner F, Bacon KB. Essential role of MHC II-independent CD4+ T cells, IL-4 and STAT6 in contact

hypersensitivity induced by fluorescein isothiocyanate in the mouse. *Int Immunol* 2004 May;16(5):685-95.

(187) Goodman RB, Strieter RM, Martin DP et al. Inflammatory cytokines in patients with persistence of the acute respiratory distress syndrome. *Am J Respir Crit Care Med* 1996 September;154(3 Pt 1):602-11.

(188) Cockrill BA, Hales CA. Allergic bronchopulmonary aspergillosis. *Annu Rev Med* 1999;50:303-16.

(189) Huaux F, Liu T, McGarry B, Ullenbruch M, Xing Z, Phan SH. Eosinophils and T lymphocytes possess distinct roles in bleomycin-induced lung injury and fibrosis. *J Immunol* 2003 November 15;171(10):5470-81.

(190) Moore BB, Kolodsick JE, Thannickal VJ et al. CCR2-mediated recruitment of fibrocytes to the alveolar space after fibrotic injury. *Am J Pathol* 2005 March;166(3):675-84.

(191) Singh S, du BR. Autoantibodies in cryptogenic fibrosing alveolitis. *Respir Res* 2001;2(2):61-3.

(192) Torroja C, Gorfinkiel N, Guerrero I. Patched controls the Hedgehog gradient by endocytosis in a dynamin-dependent manner, but this internalization does not play a major role in signal transduction. *Development* 2004 May;131(10):2395-408.

(193) van den Brink GR, Hardwick JC, Nielsen C et al. Sonic hedgehog expression correlates with fundic gland differentiation in the adult gastrointestinal tract. *Gut* 2002 November;51(5):628-33.

(194) van den Brink GR, Hardwick JC, Tytgat GN et al. Sonic hedgehog regulates gastric gland morphogenesis in man and mouse. *Gastroenterology* 2001 August;121(2):317-28.

(195) Dimmler A, Brabletz T, Hlubek F et al. Transcription of sonic hedgehog, a potential factor for gastric morphogenesis and gastric mucosa maintenance, is up-regulated in acidic conditions. *Lab Invest* 2003 December;83(12):1829-37.

(196) Ishizuya-Oka A, Ueda S, Inokuchi T et al. Thyroid hormone-induced expression of sonic hedgehog correlates with adult epithelial development during remodeling of the Xenopus stomach and intestine. *Differentiation* 2001 December;69(1):27-37.

(197) Cho-Vega JH, Troncoso P, Do KA et al. Combined laser capture microdissection and serial analysis of gene expression from human tissue samples. *Mod Pathol* 2004 October 29.

(198) van Dijk MC, Rombout PD, Dijkman HB, Ruiter DJ, Bernsen MR. Improved resolution by mounting of tissue sections for laser microdissection. *Mol Pathol* 2003 August;56(4):240-3.

(199) Xiang CC, Mezey E, Chen M, Key S, Ma L, Brownstein MJ. Using DSP, a reversible cross-linker, to fix tissue sections for immunostaining, microdissection and expression profiling. *Nucleic Acids Res* 2004;32(22):e185.

(200) Tanji N, Ross MD, Cara A, Markowitz GS, Klotman PE, D'agati VD. Effect of tissue processing on the ability to recover nucleic acid from specific renal tissue compartments by laser capture microdissection. *Exp Nephrol* 2001;9(3):229-34.

(201) Fink L, Kinfe T, Stein MM et al. Immunostaining and laser-assisted cell picking for mRNA analysis. *Lab Invest* 2000 March;80(3):327-33.

(202) Fink L, Kinfe T, Seeger W, Ermert L, Kummer W, Bohle RM. Immunostaining for cell picking and real-time mRNA quantitation. *Am J Pathol* 2000 November;157(5):1459-66.

(203) Fend F, Emmert-Buck MR, Chuaqui R et al. Immuno-LCM: laser capture microdissection of immunostained frozen sections for mRNA analysis. *Am J Pathol* 1999 January;154(1):61-6.

(204) Betsuyaku T, Senior RM. Laser capture microdissection and mRNA characterization of mouse airway epithelium: methodological considerations. *Micron* 2004;35(4):229-34.

(205) Betsuyaku T, Griffin GL, Watson MA, Senior RM. Laser capture microdissection and real-time reverse transcriptase/ polymerase chain reaction of bronchiolar epithelium after bleomycin. *Am J Respir Cell Mol Biol* 2001 September;25(3):278-84.

(206) Rupp GM, Locker J. Purification and analysis of RNA from paraffin-embedded tissues. *Biotechniques* 1988 January;6(1):56-60.

(207) Su JM, Perlaky L, Li XN et al. Comparison of ethanol versus formalin fixation on preservation of histology and RNA in laser capture microdissected brain tissues. *Brain Pathol* 2004 April;14(2):175-82.

(208) Masuda N, Ohnishi T, Kawamoto S, Monden M, Okubo K. Analysis of chemical modification of RNA from formalin-fixed samples and optimization of molecular biology applications for such samples. *Nucleic Acids Res* 1999 November 15;27(22):4436-43.

(209) Mizuno T, Nagamura H, Iwamoto KS et al. RNA from decades-old archival tissue blocks for retrospective studies. *Diagn Mol Pathol* 1998 August;7(4):202-8.

(210) Specht K, Richter T, Muller U, Walch A, Werner M, Hofler H. Quantitative gene expression analysis in microdissected archival formalin-fixed and paraffin-embedded tumor tissue. *Am J Pathol* 2001 February;158(2):419-29.

(211) Lehmann U, Kreipe H. Real-time PCR analysis of DNA and RNA extracted from formalin-fixed and paraffin-embedded biopsies. *Methods* 2001 December;25(4):409-18.

(212) Finke J, Fritzen R, Ternes P, Lange W, Dolken G. An improved strategy and a useful housekeeping gene for RNA analysis from formalin-fixed, paraffin-embedded tissues by PCR. *Biotechniques* 1993 March;14(3):448-53.

(213) Stanta G, Schneider C. RNA extracted from paraffin-embedded human tissues is amenable to analysis by PCR amplification. *Biotechniques* 1991 September;11(3):304, 306, 308.

(214) Shibutani M, Uneyama C, Miyazaki K, Toyoda K, Hirose M. Methacarn fixation: a novel tool for analysis of gene expressions in paraffin-embedded tissue specimens. *Lab Invest* 2000 February;80(2):199-208.

(215) Luo L, Salunga RC, Guo H et al. Gene expression profiles of laser-captured adjacent neuronal subtypes. *Nat Med* 1999 January;5(1):117-22.

(216) Singh R, Maganti RJ, Jabba SV et al. Microarray based comparison of three amplification methods for nanogram amounts of total RNA. *Am J Physiol Cell Physiol* 2004 December 21.

(217) Zhuang Z, Vortmeyer AO, Mark EJ et al. Barrett's esophagus: metaplastic cells with loss of heterozygosity at the APC gene locus are clonal precursors to invasive adenocarcinoma. *Cancer Res* 1996 May 1;56(9):1961-4.

(218) Bianchi AB, Navone NM, Conti CJ. Detection of loss of heterozygosity in formalin-fixed paraffin-embedded tumor specimens by the polymerase chain reaction. *Am J Pathol* 1991 February;138(2):279-84.

(219) Deng G, Lu Y, Zlotnikov G, Thor AD, Smith HS. Loss of heterozygosity in normal tissue adjacent to breast carcinomas. *Science* 1996 December 20;274(5295):2057-9.

(220) Bazan V, La Rocca G, Corsale S et al. Laser pressure catapulting (LPC): optimization LPC-system and genotyping of colorectal carcinomas. *J Cell Physiol* 2005 February;202(2):503-9.

(221) Cohen CD, Grone HJ, Grone EF, Nelson PJ, Schlondorff D, Kretzler M. Laser microdissection and gene expression analysis on formaldehyde-fixed archival tissue. *Kidney Int* 2002 January;61(1):125-32.

(222) Cowherd SM, Espina VA, Petricoin EF, III, Liotta LA. Proteomic analysis of human breast cancer tissue with laser-capture microdissection and reverse-phase protein microarrays. *Clin Breast Cancer* 2004 December;5(5):385-92.

(223) Waghray M, Cui Z, Horowitz JC et al. Hydrogen peroxide is a diffusible paracrine signal for the induction of epithelial cell death by activated myofibroblasts. *FASEB J* 2005 May;19(7):854-6.

(224) Breier A, Ziegelhoffer A, Famulsky K, Michalak M, Slezak J. Is cysteine residue important in FITC-sensitive ATP-binding site of P-type ATPases? A commentary to the state of the art. *Mol Cell Biochem* 1996 July;160-161:89-93.

(225) Champeil P, Riollet S, Orlowski S, Guillain F, Seebregts CJ, McIntosh DB. ATP regulation of sarcoplasmic reticulum Ca2+-ATPase. Metal-free ATP and 8-bromo-ATP bind with high affinity to the catalytic site of phosphorylated ATPase and accelerate dephosphorylation. *J Biol Chem* 1988 September 5;263(25):12288-94.

(226) Zhang Y, Li J, Tang L. Cancer-preventive isothiocyanates: dichotomous modulators of oxidative stress. *Free Radic Biol Med* 2005 January 1;38(1):70-7.

(227) Zhang Y, Tang L, Gonzalez V. Selected isothiocyanates rapidly induce growth inhibition of cancer cells. *Mol Cancer Ther* 2003 October;2(10):1045-52.